

Source rock evaluation and predicted petroleum compositions related to samples from the Adavale, Bowen, Cooper and Eromanga Basins, Queensland

GEOS4 Report 20161216

Nicolaj Mahlstedt, Brian Horsfield

GEOS4 GmbH

Peter-Huchel-Chaussee 88
14552 Michendorf · Germany

Phone +49 (0)331.2 88 17 80
Fax +49 (0)331.2 88 17 82

info@geos4.com
www.geos4.com

Address:	GEOS4 GmbH Peter-Huchel-Chaussee 88 14552 Michendorf Germany
Telephone:	+49 3312881780
Telefax:	+49 3312881782
e-mail:	info@geos4.com
Report Title:	Source rock evaluation and predicted petroleum compositions related to samples from the Adavale, Bowen, Cooper and Eromanga Basins, Queensland FINAL REPORT GEOS4 Report 20161216
Authors:	N. Mahlstedt, B. Horsfield
Classification:	Confidential
Client:	Geological Survey of Queensland
Client reference:	
Distribution:	Electronic files: Report (.pdf) PetroMod® geo-files


N. Mahlstedt
B. Horsfield

Summary

Adavale Basin

Screening - The two samples from the Bury Limestone and Log Creek Formation are at an advanced maturity level. Current organic richness is fair to good. Only the Bury Limestone was examined further.

Source quality - The Bury Limestone sample had an inherent potential for generating mixed base crude oil, but due to its advanced maturity level its potential is bordering on gas/condensate. The original organic matter was likely of algal origin, possibly deposited in a marine environment.

Thermal lability - bulk kinetics predict that remaining generation can occur where $T > 140^\circ\text{C}$ and will extend beyond 200°C (geological heating rate of 3K/Ma).

Retention properties - The sample's high PI value of 0.27 points to an abundance of retained hydrocarbons. Yet, thermovaporisation yields were low, pointing to the original presence and subsequent loss (during sample prep) of mainly gaseous hydrocarbons.

Late gas potential - Late gas generation takes place between 2.5 and 3.5% R_0 . At its current maturity level the Bury Limestone sample has only a low late gas potential, but this is expected to develop during the remainder of catagenesis.

Cooper Basin

Screening - The coals and carbonaceous shales of the Patchawarra, Toolachee and Epsilon Formations fall into two groups based on TOC, with the coals having the higher values. Maximum Hydrogen Index values for the Toolachee and Patchawarra coals are 225 and 233 mgHC/g TOC, respectively. Mudstones from these formations have values in the range 90-212 mgHC/g TOC, and predominantly at the low end. The Epsilon Formation has the lowest quality of all (64 mgHC/g TOC).

Source quality and thermal maturity - The relatively mature coals and one carbonaceous shale of the Patchawarra and Toolachee Formations generate pyrolysates whose chain length distributions and the presence of phenols, point to inherent gas/condensate generation potential. Vitrinite macerals are in strong abundance. The pyrolysate of the least mature Toolachee Formation sample is slightly more liquid-prone, though this is not readily relatable to increased proportions of liptinite macerals. Biomarkers point to strong bacterial reworking during diagenesis. Patchawarra Formation sample G016496 has a mean $\text{R}_0 = 0.88\%$; the Toolachee Formation sample G016500 has a mean $\text{R}_0 = 0.72\%$.

Thermal lability - Bulk kinetics measured on Toolachee Formation sample G016500 are in line with the presence of mature organic matter, and remaining generation predicted to begin where $T > 140^\circ\text{C}$ at a generalised heating rate of 3K/Ma .

Retention properties - The Patchawarra Formation mudstone G016494 has a high Production Index (PI = 0.39), pointing to enhanced hydrocarbon retention. Importantly, the retained hydrocarbon composition is consistent with a very high quality light oil signature. *These attributes might be highly significant as far as unconventional shale plays are concerned.*

Late gas potential - The late gas generating potential of the Patchawarra and Toolachee Formations increases during catagenesis up to values of ~40 mg/g TOC at the onset of metagenesis ($\text{R}_0 = 2.0\%$), this constituting a high proportion of total generative potential.

Eromanga Basin

Screening - All of the three Birkhead Formation and one Poolowana Formation samples analysed are of low maturity. The two carbonaceous mudstones of the Birkhead Fm are of likely anoxic lacustrine origin as they contain Type I kerogen, displaying a high Tmax due to a stable kerogen structure rather than because of an advanced level of maturity. The coals contain kerogen Type III (Poolowanna Fm) and II/III (Birkhead Formation). Only the Birkhead Formation was examined further.

Source quality and thermal maturity - Pyrolysates of the two low maturity carbonaceous mudstones of the Birkhead Fm. (G016504 and G016506) plot in the Paraffinic Oil High Wax Petroleum Type Organofacies field, typical for Type I kerogen-containing source rocks deposited in an anoxic lacustrine

environment. Nevertheless, low amounts of woody organic matter are also indicated. The sample has a mean $Ro = 0.53\%$. By contrast, the coal sample (G016505) exhibits a strong woody character, yet is still capable of generating Paraffinic-Naphthenic-Aromatic high wax crude oil. The sample has a mean $Ro = 0.48\%$. Biomarkers (retene and tetracyclic diterpanes) show that gymnosperms (fruiting plants) are the main terrigenous source components in both coals and mudstones. Organic petrology reveals that the mudstone (G016504) contains alginite, sporinite and vitrinite, whereas the coal (G016505) is comprised of vitrinite and subordinate liptinite (resinite, sporinite).

Thermal lability and compositional evolution (PhaseKinetics) - The Birkhead Formation sample G016504 exhibits one dominant energy at 51 kcal/mol and four main energies between 50 and 53 kcal/mol accounting for >90% of the total kerogen to petroleum conversion reaction. The coal G016505 has a broader range of energies. Nevertheless, their generation characteristics are broadly similar, with a narrow generation range ($T = 120-170^\circ\text{C}$ for 3K/Ma heating rate). Fluids generated from the predominantly algal Type I mudstone sample G016504 exhibit more or less uniformly low saturation pressures between 120 and 150 bar, and the gas-oil ratio GOR values increase only slightly from 80 to $120 \text{ Sm}^3/\text{Sm}^3$ with maturity. By stark contrast, the fluids generated from the heterogeneous Type II/III coal sample G016505 exhibit saturation pressures of >200 bars (approximating to volatile oil) already at lowest maturity levels (10% Transformation Ratio (TR)) and increase to >300 bar at highest maturity levels (90% TR). GOR values also strongly increase from $160 \text{ Sm}^3/\text{Sm}^3$ to $200 \text{ Sm}^3/\text{Sm}^3$ at 70% TR and to $425 \text{ Sm}^3/\text{Sm}^3$ at 90% TR.

Bowen Basin

Screening - Seven formations and members were evaluated from the GSQ Springsure 19 well. The Bandanna Formation contained one low maturity coal sample with an enhanced Hydrogen Index (HI) (274 mgHC/g TOC). Argillaceous samples from the Black Alley Shale, Peawaddy Formation, Catherine Sandstone, Ingelara Formation, Freitag Formation, and Aldebaran Sandstone all displayed quite good organic richness but their kerogens are of low quality. The Aldebaran Sandstone towards the base of that well contained one low maturity coal sample with a rather high HI of 308 mgHC/g TOC.

The Snake Creek Mudstone Member sample from the APN Snake Creek 1 well is immature, with modest TOC and low Hydrogen Index. Samples from the The Blackwater Group and Back Creek Group samples in the AAO Meeleebee 1 well are all of peak maturity ($T_{\max} = 449^\circ\text{C}$), but are organic lean and contain poor quality organic matter. Coals from the Tinowon Sandstone represent the richer (TOC range 53.1-57.4%) and higher quality (Hydrogen Index range 176-232 mgHC/g TOC) units analysed from the OCA Myall Creek 3 well. The Wallabella Coal Member samples was relatively high in ash (TOC = 36%), and its organic matter was of poor quality (Hydrogen Index 133 mgHC/g TOC). The Cattle Creek Fm in the GSQ Eddystone 4 well contains mudstones with low maturity and whose source quality is poor (Hydrogen Index <100 mgHC/g TOC); only the two coal samples display promising signs of source rock potential (high TOC, fair Hydrogen Index of ca. 180-200 mgHC/g TOC; Type II/III kerogen). The coals and organic-rich mudstones of the Reids Dome Beds have fair Hydrogen Indices (177-254 mgHC/g TOC).

Source quality and thermal maturity - The inferred petroleum type for the Bowen Basin shales and coals from Reids Dome beds, Cattle Creek Formation and Bandanna Formation is mainly Paraffinic-Naphthenic-Aromatic High Wax Oil, this usually equating to lower delta plain environments. On the other hand, the Tinowon Sandstone coal sample has gas and condensate potential, whereas the Snake Creek Mudstone Member has Paraffinic-Naphthenic-Aromatic low wax oil potential. A mixing of aquatic organic matter with terrestrial organic matter (sporinite, cutinite, vitrinite) can explain all the observed variability in the chain length distributions of the kerogens. Petrographically, vitrinite and inertinite are dominant, with sporinite as the main subsidiary liptinite maceral. The samples have a range in mean $Ro = 0.40-0.63\%$. Sterane distributions have deltaic-terrigenous character. The presence of diterpanes points to a gymnosperm flora, especially pronounced in the Aldebaran Sandstone and Cattle Creek Formation.

Retention properties - Rather high Production Indices (PI)(0.08-0.27) signify that hydrocarbons have been retained by the sampled shales at the base Aldebaran Sandstone of the Springsure 19 well, in the topmost sample in the OCA Myall Creek 3 well, in the APN Snake Creek 1 well and especially in the AAO Meeleebie 1 well. These high PIs probably reflect the presence of gas-condensate range components; differences in aromatic versus saturate content were recorded for liquids by thermovaporisation, whereas gases were lost.

Thermal lability and compositional evolution (PhaseKinetics) - A broad activation energy distribution was observed for all samples, this being consistent with the heterogeneous, terrestrial-aquatic organic matter mix. There is significant variability in the thermal stress required to bring about generation, with the Tinowon Sandstone coal (G016531) being most stable and the Bandanna Fm shale (G016511) most labile. Fluids generated from sample G016531 exhibit saturation pressures (Psat) which increase from >200 bars at low maturity levels to ~450 bar at highest maturity levels, falling within the volatile oil class. The Cattle Creek Fm. sample G016535 and Reids Dome Beds sample G016539 generate volatile oil from 50% TR onward, whereas the Bandanna Formation. sample G0165311 and Aldebaran Sandstone sample G0165322 generate fluids with Psat values exceeding 200 bar only at highest maturity levels (90% TR). At lower transformation ratios Psat values range between 150 and 200 bar indicating generation of black oil.

Contents

Introduction.....	1
Experimental details	4
Results.....	7
1 Screening Analyses	7
2 Analytical pyrolysis and thermovaporisation	34
3 Organic petrology.....	59
4 Biomarkers & isotopes (maltenes)	75
5 Late Gas Potential	110
6 PhaseKinetics.....	121

Introduction

The Geological Survey of Queensland (GSQ) of the Department of Natural Resources and Mines (DNRM) contracted GEOS4 to evaluate the petroleum geochemical characteristics of 48 samples from the Cooper, Eromanga, Bowen and Adavale basins of Queensland. GSQ provided the following background information:

Adavale Basin

The Adavale Basin is an under-explored basin in southern-central Queensland. Exploration in the 1960s resulted in the discovery of the Gilmore gas field, though no other commercial discoveries have been made. There is a need to better understand the petroleum system, particularly helping to better define understanding of source rocks for Gilmore field as well as identify new potential source rocks. In addition to this, these sources may also be of interest as constituting shale oil or shale gas plays,

Cooper Basin

The Cooper Basin forms part of one of Queensland's major petroleum provinces, and hosts several conventional oil and gas fields. There has also been recent exploration for unconventional gas resources in the deeper troughs of the basin with several discoveries made to date, including commercial production in the South Australian side of the basin. There is a need to further refine known source rock characteristics and to add to the spatial coverage of results, as well as identifying new potential source rocks for improving our understanding of the petroleum system. Identifying and characterising potential unconventional plays are also needed.

Eromanga Basin

The Eromanga Basin overlies the Cooper Basin and is the other component of the Cooper-Eromanga petroleum province in south-west Queensland. Discoveries in the Eromanga Basin have been predominantly oil, and include the Jackson field, which is Australia's largest onshore oil field. There exists a need to help better characterise potential source rocks in the Eromanga sequence, identify new source rocks, and potential unconventional resource plays.

Bowen Basin

The Bowen Basin forms part of the other major petroleum province in Queensland and is believed to host the principal source rocks for the Bowen and Surat basins conventional accumulations. Conventional reserves were first discovered in the basin in the 1960s, though recent development in the area has focussed on coal seam gas resources underpinning the world class CSG to LNG industry. Recent exploration has targeted deeper sections of the Taroom Trough for tight gas resources with a significant potential for additional unconventional resources

such as deep shales and coals yet to be discovered. There exists a need to refine the characterisation of known source rocks as well as to identify new potential source rocks in order to improve our understanding of the conventional petroleum system. Characterising potential unconventional plays such as shale gas, shale oil, or deep coal source reservoirs is also needed.

Overall objectives

Our objective is to provide the GSQ and the petroleum industry with a better understanding of the petroleum systems and the petroleum resource potential within these basins through provision of pre-competitive data. There are two principal foci: compositional kinetics for potential sources in the Bowen and Eromanga Basins, and deep gas generation in the Cooper and Adavale Basins.

Samples under analysis

The samples, all provided by GSQ, are listed in Table 1-1. One carbonate (Bury Limestone) and one siltstone (Log Creek Fornation), are the Adavale Basin. One coal and two carbonaceous mudstones from the Birkhead Formation and one coal from the Poolowanna Formation are from the Eromanga Basin. Three carbonaceous mudstones and two coals from the Patchawarra Formation, four coals from the Toolachee Formation and one carbonaceous mudstone from the Epsilon Formation constitute the Cooper Basin sample set. In all, thirty-two samples are from the Bowen Basin. Fourteen of these, consisting of shales and coals are from the Bandanna Formation, Black Alley Shale, Peawaddy Formation, Catherine Sandstone, Ingelara Formation, Freitag Formation and Aldebaran Sandstone, and came from the Springsure-19 well. Nine shales and coals from the Cattle Creek Formation, and Reids Dome Beds came from the Eddystone-4 well. Three coals and one shale from the Tinowon Formation taken from the Myall Creek 3 well, and four shales from the Blackwater and Back Creek Groups taken from the Meeleebie-1 and Snake Creek-1 wells .

Analytical scheme

Analyses undertaken in the course of the whole project included Rock-Eval, TOC, pyrolysis gas chromatography, photomicrograph preparation and reflectance measurement, solvent extraction MPLC, gas chromatography-mass spectroscopy of saturates and gas chromatography-mass spectroscopy of aromatics, delta ^{13}C saturates and aromatics, bulk kinetics, late gas analysis, and compositional kinetics.

Step 1.

All 48 samples were analysed using Rock-Eval and Leco in order to enable screening based on organic richness, elementally based kerogen type (I, II, III) and approximate thermal maturity.

Step 2.

Based on the results of step 1, fifteen samples that had been selected according to consideration of lithofacies, thermal maturity and/or geographic regions were analysed by pyrolysis gas chromatography. This was undertaken to determine the bulk chemical signature of the kerogen in terms of how paraffinic, aromatic, waxy or sulphur-rich the generated petroleum from these source rocks are likely to be. Additionally, eight samples were analysed by thermovaporisation gas chromatography in order to provide compositional information on the free hydrocarbons occurring in those samples whose Production Index (PI) was anomalously high.

Step 3.

Upon review of results in Steps 1 and 2, nine selected samples underwent extraction using organic solvents. After removal of asphaltenes, the remaining maltenes were fractionated into saturates, aromatics and resins using Medium Pressure Liquid Chromatography (MPLC). Gas chromatography-mass spectroscopy (GC-MS) of the saturates and aromatics fractions was then used to identify facies and maturity signatures based on *inter alia* biomarkers. Stable carbon isotopes of the saturates and aromatics fractions supplemented this. Using bulk pyrolysis data, bulk kinetic parameters for ten selected immature samples were calculated to demonstrate the stability/lability of the kerogen, and these form the basis for predicting when petroleum generation would occur under given temperature exposure over geological time. These results were directly incorporated into the PhaseKinetics model, completed in Step 4.

Step 4.

Following the results of Steps 1 and 2, six key samples were selected and analysed for their Late Gas potential ($R_r > 2\%$). Eleven samples were also examined using organic petrography to document the nature of the particulate organic matter (macerals in coals, phytoclasts in shales), illustrate textural relationships, and measure vitrinite reflectance.

For seven key representative samples, compositional kinetics (PhaseKinetics) parameters were calculated so that the gas to oil ratio (GOR) and Saturation Pressure can be predicted as a function of transformation ratio in petroleum system models. 2-, 4- and 14- compound compositional kinetics are here provided both in tabulated and digital format for direct incorporation into the Geological Survey of Queensland's in-house software (ie. PetroMod).

An overview of the analyses conducted on the samples is given in Table 1-2.

Experimental details

Leco and Rock Eval analyses – classical screening

A Leco SC-632 instrument was used for TOC determination. Diluted hydrochloric acid (HCl) was added to the crushed rock sample to remove carbonate. The sample was then introduced into the Leco combustion oven (1,300°C, pure O₂ flow), and the amount of carbon in the sample measured as carbon dioxide using an IR-detector.

Rock Eval style analysis was performed using a Hawk instrument. Jet Rock 1 was run as a standard and checked against the acceptable range given in the Norwegian Industry Guide to Organic Geochemical Analysis (NIGOGA). Original data traces are given in the Appendix.

Temperature programme:

- Pyrolysis: 300°C for 3 minutes then 25°C/min. to 650°C (0 min.)

Thermovaporisation – free hydrocarbons

Thermovaporisation was used to analyse the free hydrocarbons (C₅+) contained in the original samples, and performed using the Quantum MSSV-2 Thermal Analysis System©. Milligram quantities of sample material were sealed in a glass capillary tube and heated to 300°C in the injector unit for 5 minutes to purge external surface contaminants . The tube was then cracked open using a piston device coupled with the injector, and the released volatile hydrocarbons analysed by gas chromatography (conditions given in next sub-chapter).

Pyrolysis gas chromatography – petroleum types

Pyrolysis gas chromatography was performed using the Quantum Microscale Sealed Vessel (MSSV-2) Thermal Analysis System®. The samples were heated in a flow of helium, and products released over the temperature range 300-600°C (temperature increased at 40K/min) were focussed using a cryogenic trap, and then analysed using a 50m x 0.32mm HP-1 capillary column equipped with a flame ionisation detector. The gas chromatography (GC) oven temperature was programmed from 40°C to 320°C at a heating rate of 8°C/minute. Boiling ranges (C₁, C₂-C₅, C₆-C₁₄, C₁₅+) and individual compounds (*n*-alkenes, *n*-alkanes, alkylaromatic hydrocarbons and alkylthiophenes) were quantified by external standardisation using *n*-butane. Response factors for all compounds were considered the same (1.0), except for methane whose response factor was 1.1.

Organic petrography

For optical microscopy on coal and shale samples, blocks (ca. 1cm³) were cut, embedded in epoxy resin and polished to obtain a smooth surface. Mean random reflectance (%R_r, oil immersion) was determined using a Leica MPV microscope equipped with 50x and 100x objectives at a wavelength of 546 nm. The 50x magnification was used for coals, while shale samples were investigated using the 100x magnification. Maceral composition was assessed qualitatively and semi-quantitatively using

white-light and blue-light irradiation. The fluorescence color of liptinite macerals was used as a quality parameter for reassurance of measured vitrinite reflectance values.

Solvent Extraction

A Soxtec Tecator instrument was used. Thimbles were pre-extracted in dichloromethane with 7% (vol/vol) methanol, 10 minutes boiling and 20 minutes rinsing. The crushed sample was weighed accurately in the pre-extracted thimbles and boiled for 1 hour and rinsed for 2 hours in approximately 80 cc of dichloromethane with 7% (vol/vol) methanol. Copper blades activated in concentrated hydrochloric acid were added to the extraction cups to cause free sulphur to react with the copper. An aliquot of 10% of the extract was transferred to a pre-weighed bottle and evaporated to dryness. The amount of extractable organic matter was calculated from the weight of this 10% aliquot.

Quantitative MPLC fractions

Asphaltene precipitation was first performed on the solvent extracts using the methodology described by Theuerkorn et al. (2008). The de-asphaltened extract, termed maltenes, was then fractionated using MPLC.

The MPLC system includes two HPLC pumps, sample injector, sample collector and two packed columns. The pre-column was filled with Kieselgel 100, which was heated at 600 °C for 2 hours to deactivate it. The main column, a LiChroprep Si60 column, was heated at 120 °C for 2 hours with a helium flow to make it water free. Approximately 30 mg of maltenes diluted in 1 ml hexane was injected into a sample loop. The solvents used were hexane and dichloromethane.

Stable carbon isotope analysis of fractions

The saturates and aromatics fractions were dissolved in a known amount of dichloromethane, and 0.2 mg of each sample (or as much as possible) was transferred to a 6x8mm tin capsule. The solvent was evaporated in an oven at 50 °C. The samples were then combusted in a EuroVector Elemental Analyser EA3028-IRMS at 1700 °C. The produced water was trapped on Mg(ClO₄)₂ and the CO₂ flushed into a Horizon, isotope ratio mass spectrometer (IRMS) from NU-Instruments. A standard (NGS NSO-1, topped oil) was analysed after each 10th sample. The $\delta^{13}\text{C}$ value obtained for this standard is -28.61‰ VPDB. The variation in the isotopic values for the standard by repeated analysis over a period of three years is $\pm 0.09\text{\textperthousand}$.

Gas chromatography-mass spectrometry (GC-MS) of saturates and aromatics

A Micromass ProSpec high resolution instrument was used. The instrument was tuned to a resolution of 3000 and data was acquired in Selected Ion Recording (SIR) mode. The column used was a 60 m CP-Sil-5 CB-MS with an internal diameter of 0.25 mm and a film thickness 0.25 µm. D₄-27 $\alpha\alpha$ R was used as an

internal standard when quantitative results are requested for the saturated compounds. D₈-Naphthalene, D₁₀-Phenanthrene and D₁₂-Chrysene are used as internal standards when quantitative results are required for the aromatic compounds.

Temperature programme: 50 °C (1 min.) - 20 °C/min. - 120 °C - 2 °C/min - 320 °C (20 min.)

Kinetics determination – thermal response

Rock samples were analysed by non-isothermal open system pyrolysis at four different laboratory heating rates (0.7, 2.0, 5.0 and 15K/min) using a Source Rock Analyzer®. The generated bulk petroleum formation curves serve as input for the bulk kinetic model consisting of an activation energy distribution and a single frequency factor.

MSSV Pyrolysis – data for PhaseKinetics and Late Gas Potential

Microscale sealed vessel (MSSV) pyrolysis (Horsfield et al., 1989) was performed using the Quantum MSSV-2 Thermal Analysis System®. For generating raw data for PhaseKinetics (method given in Chapter 6), milligram quantities of solvent-extracted samples were sealed in glass capillaries and artificially matured at 0.7K/min using a special MSSV prep-oven. The tubes were then cracked open using a piston device coupled with the injector, and the released products were swept into the GC using a flow of helium. A HP5890 II instrument was used for GC analysis (column: HP-1, 50 m length0.32 mm internal diameter, film thickness 0.52 µm) with flame ionisation detection. Individual compounds in the gas range (C₁-C₅), coarse boiling ranges (C₁, C₂-C₅, C₆-C₁₄, C₁₅₊) and 25 pseudo-boiling ranges for each carbon number at and above C₆ were quantified for the PhaseKinetics approach. Quantification was performed by external standardisation using *n*-butane. Response factors for all compounds were assumed the same, except for methane whose response factor was 1.1.

For the determination of Late Gas potential, milligram quantities of each sample were sealed in glass capillaries and artificially matured at 2.0K/min to two end temperatures, 560°C and 700°C, using a special MSSV prep-oven. Analytical procedures were as described above

Results

1 Screening Analyses

The results of Rock-Eval and TOC analyses are presented in Table 1-3 and Figures 1-1 to 1-10.

All basins (see Figure 1-1 and 1-2)

The range in TOC for the entire sample set is broad. Though two samples have values <1% (one from the Adavale Basin and one from the Bowen Basin), the remainder fall into two groups; one whose TOC is between 1-40%, consisting of mudstones, carbonaceous shales and high ash coals, and the other whose TOC is between 50-90%, these being low ash coals.

The range in Tmax is extremely wide, extending from 426°C to 480°C and covering immature through extremely overmature maturation stages. The least mature overall is the Eromanga Basin sample suite followed by Bowen Basin with an abundance of samples within the oil maturity window. Adavale Basin samples are in the late oil window, while the Cooper Basin sample suite has mainly late oil/gas condensate to dry gas maturity.

Hydrogen Indices are generally rather low, with the vast majority of samples having values <300 mgHC/gTOC. The Eromanga Basin sample suite is the main exception, having two samples with very high values typical of lacustrine source rocks. Bowen Basin samples fall into two groups, one apparently more liquid-prone than the other. The Cooper Basin sample suite constitutes a maturity series, as seen in the Hydrogen Index-Tmax plot.

Adavale Basin (see Figure 1-3 and 1-4)

The two samples from the Bury Limestone and Log Creek Formation are at an advanced maturity level (Tmax = 455°C, 458°C), and have low Hydrogen Index values. Organic richness is currently fair to good; it should be kept in mind that extensive TOC loss has already taken place, and that original richness may have been substantially higher. The more organic-rich sample (Bury Limestone) was later evaluated as regards its potential as a late gas source, beginning with characterisation using pyrolysis gas chromatography. It is noteworthy that the Bury Limestone sample has a high PI, indicating the strong retention of free hydrocarbons within the rock matrix, and therefore pointing to enhanced unconventional hydrocarbon potential.

Cooper Basin (see Figure 1-5 and 1-6)

The coals and carbonaceous shales of the Patchawarra, Toolachee and Epsilon formations fall into two groups based on TOC, with the coals having the higher values. Some of the samples described by GSQ as coal actually fall in the carbonaceous shale lithofacies as their TOC values range between 2 and 29%. Hydrogen Indices for the lowest maturity samples (Tmax = 441°C) centre around 200-230 mgHC/g TOC, this being an assessment of total generative yield. Pyrolysis gas chromatography was later run to examine whether this represented oil or gas potential. The sample suite constitutes a maturity series and is therefore ideally suited for examining late gas generation, as presented later. It

is noteworthy that very high concentrations of gas, evidenced by a high Production Index (0.39), have been retained by shales in the uppermost Patchawarra Formation sample. The composition of the free hydrocarbons was therefore measured using thermovaporisation, as outlined later.

Eromanga Basin (see Figure 1-7 and 1-8)

All of the three Birkhead Formation samples and the single Poolawanna Formation sample analysed are of low maturity. The two carbonaceous mudstone samples from the Birkhead Formation are of likely anoxic lacustrine origin as they contain Type I kerogen, displaying a high Tmax due to having an inherently stable kerogen structure with strong C-C bonds inherited from aliphatic biopolymers in algal cell walls; advanced maturity is not the cause of the high Tmax. The coals have lower Hydrogen Indices (HI), and are classed as containing kerogen Type III (Poolawanna Formation) and II/III (Birkhead Formation). Pyrolysis gas chromatography was later used to assess the Petroleum Type Organofacies of the lacustrine shales and the liptinitic coal of the Birkhead Formation. The same samples were also studied by advanced methods to ascertain compositional kinetic behaviour.

Bowen Basin (see Figure 1-9 and 1-10)

Seven formations and members were evaluated in the Springsure 19 well. Two of the three analysed coals from the Bandanna Formation had very low hydrocarbon potential, and Tmax was in the range 426-441°C. One of the low maturity coals had a relatively high Hydrogen Index of 274 mgHC/g TOC, and was therefore analysed in more detail (Table 1-2) beginning with pyrolysis gas chromatography. Argillaceous samples from the Black Alley Shale, Peawaddy Formation, Catherine Sandstone, Ingelara Formation, Freitag Formation, and Aldebaran Sandstone all displayed quite good organic richness but their kerogens are of low quality with limited petroleum potential, as seen in their low Hydrogen Index values. However, one sample of the Aldebaran Sandstone towards the base of the well was a low maturity coal sample that had a relatively high Hydrogen Index of 308 mgHC/g TOC. Clearly, this sample was worthy of further detailed investigation beginning with pyrolysis gas chromatography. Tmax values in the well show a large spread that is not depth related. Production Indices (PI) are uniformly low. Higher values of around 440°C might reflect that the kerogens were deposited under oxidising redox conditions, whereas low values around 430°C might reflect more reducing conditions.

Samples from the Snake Creek 1, Meeleebie 1, and Myall Creek 3 wells all display high Tmax values consistent in this case with the late oil window/early gas window. It is noteworthy that very high concentrations of petroleum (the technique does not discriminate gas from oil), evidenced by high Production Indices (0.08-0.27), have been retained by shales in the topmost sample of the Myall Creek 3 well, (Tinowon Formation), Snake Creek 1 (Snake Creek Mudstone Member) and especially Meeleebie 1 (Blackwater Group and Back Creek Group). These samples were chosen for further analysis. (Table 1-2).

The top four samples of the Cattle Creek Fm in the Eddystone 4 well are immature, and only the two coal samples display promising signs of source rock potential (high TOC, fair Hydrogen Index of ca. 180-200 mgHC/g TOC; Type II/III kerogen). One Cattle Creek Formation sample was chosen for further analysis to document its petroleum generating properties. The same is true of one coal sample in the

deeper Reids Dome Beds of the same well which exhibits a rather high Hydrogen Index (254 mgHC/g TOC).

References

Horsfield, B., Disko, U., Leistner, F., 1989. The micro-scale simulation of maturation: outline of a new technique and its potential applications. *Geologische Rundschau* 78, 361-374.

Theuerkorn, K., Horsfield, B., Wilkes, H., di Primio, R., Lehne, E., 2008. A reproducible and linear method for separating asphaltenes from crude oil. *Organic Geochemistry* 39, 929-934.

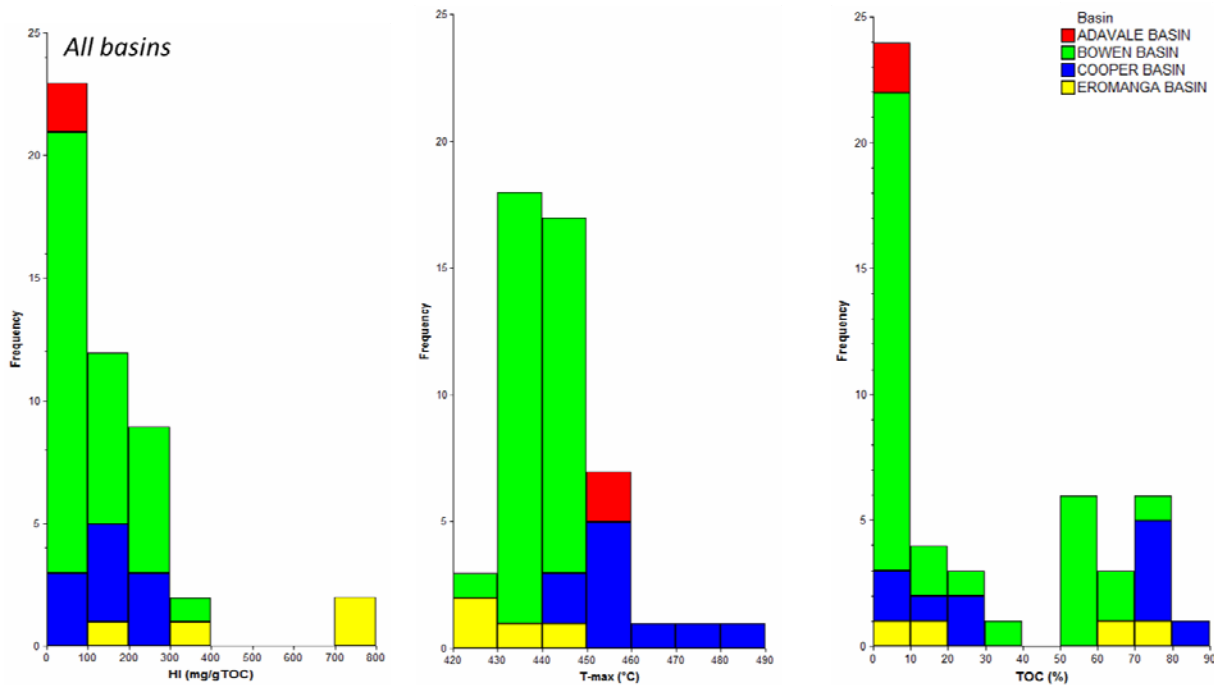


Figure 1-1: All basins. Histograms of Hydrogen Index, Tmax and TOC.

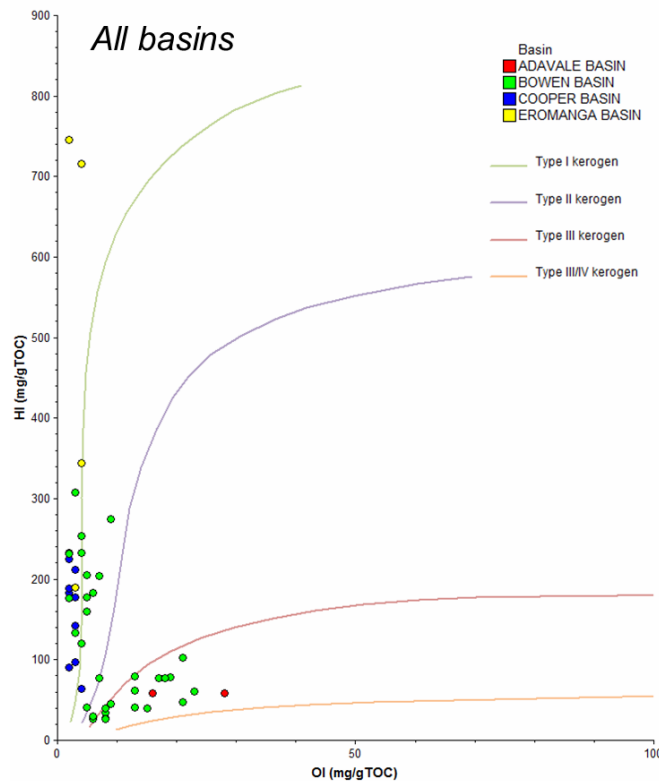


Figure 1-2a: All basins. Hydrogen Index – Oxygen Index kerogen classification (the pseudo-Van Krevelen diagram).

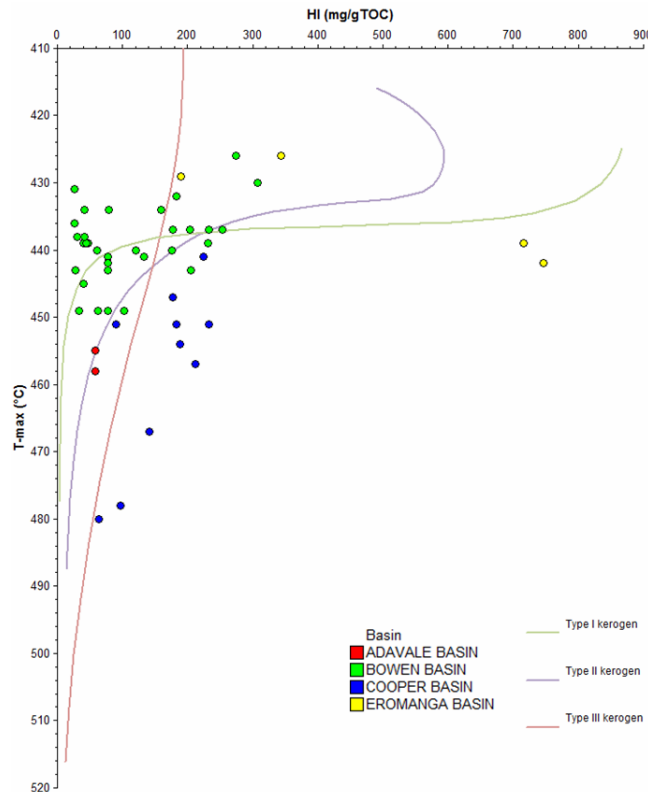


Figure 1-2b: All basins. Hydrogen Index – Tmax reveals changing petroleum potential with maturation.

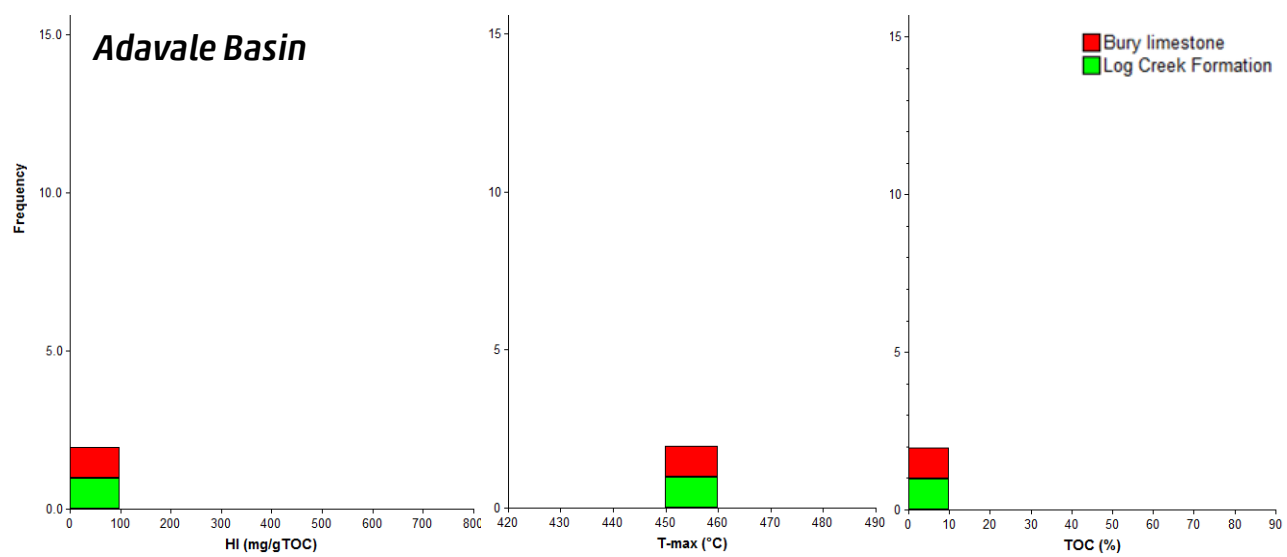


Figure 1-3: Adavale Basin. Histograms of Hydrogen Index, Tmax and TOC.

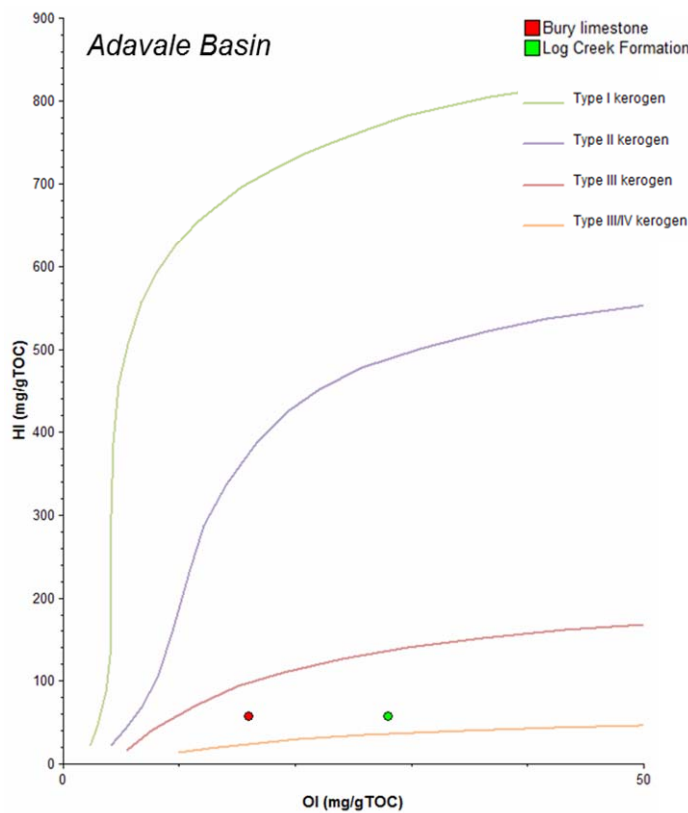


Figure 1-4a: Adavale Basin. Hydrogen Index - Oxygen Index kerogen classification.

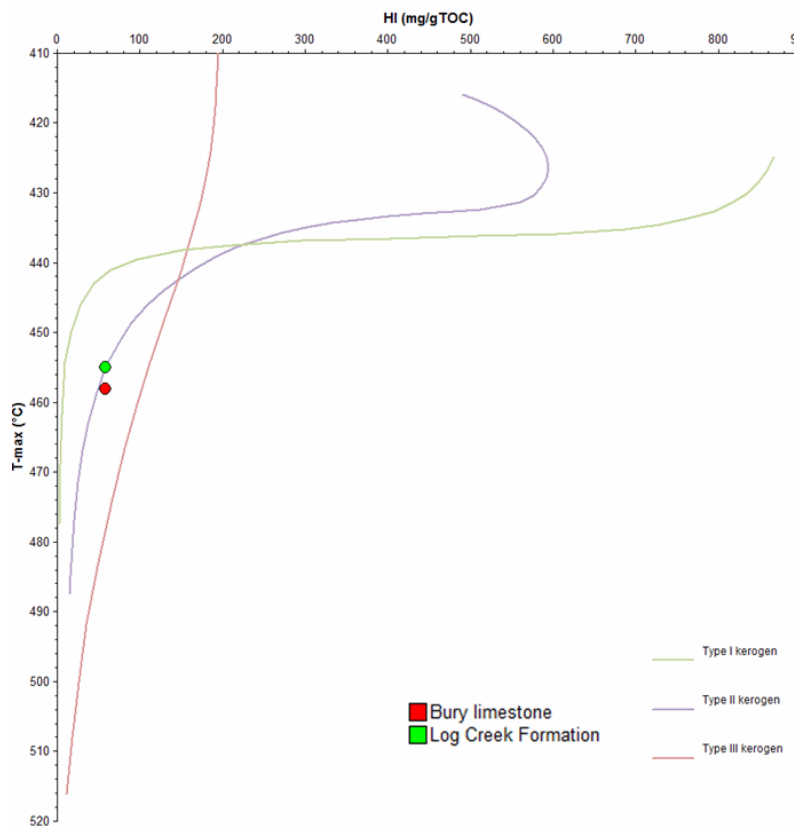


Figure 1-4b: Adavale Basin. Hydrogen Index - Tmax reveals changing petroleum potential with maturation.

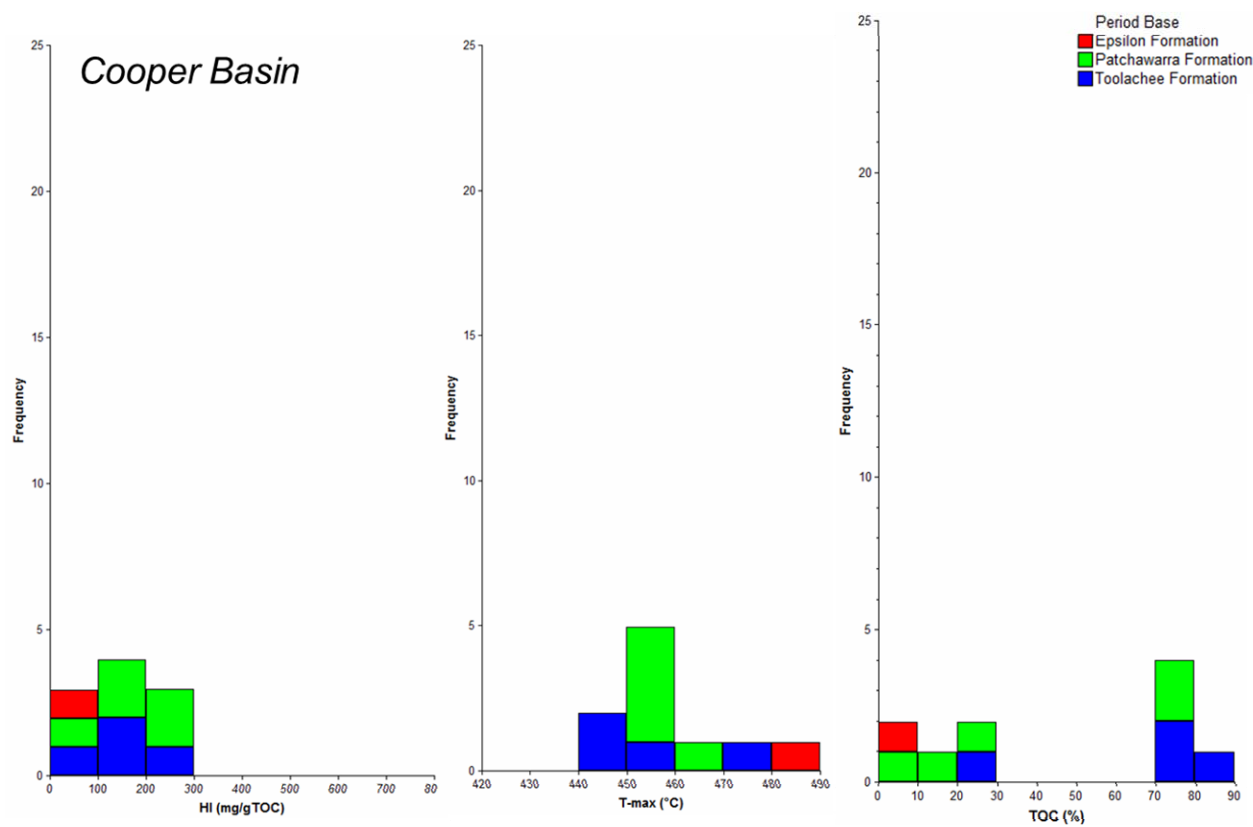


Figure 1-5: Cooper Basin. Histograms of Hydrogen Index, Tmax and TOC.

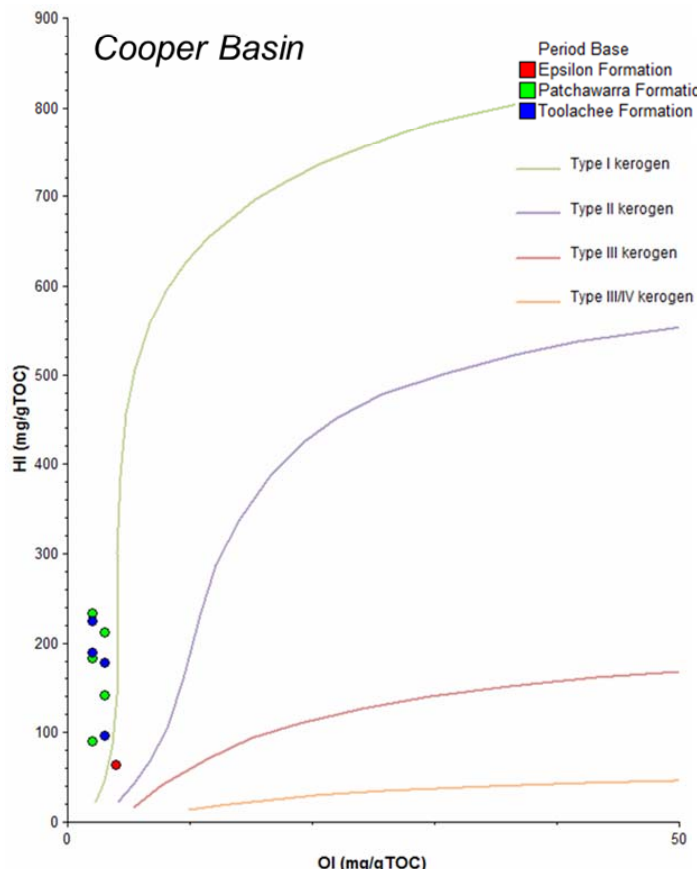


Figure 1-6a: Cooper Basin. Hydrogen Index - Oxygen Index kerogen classification.

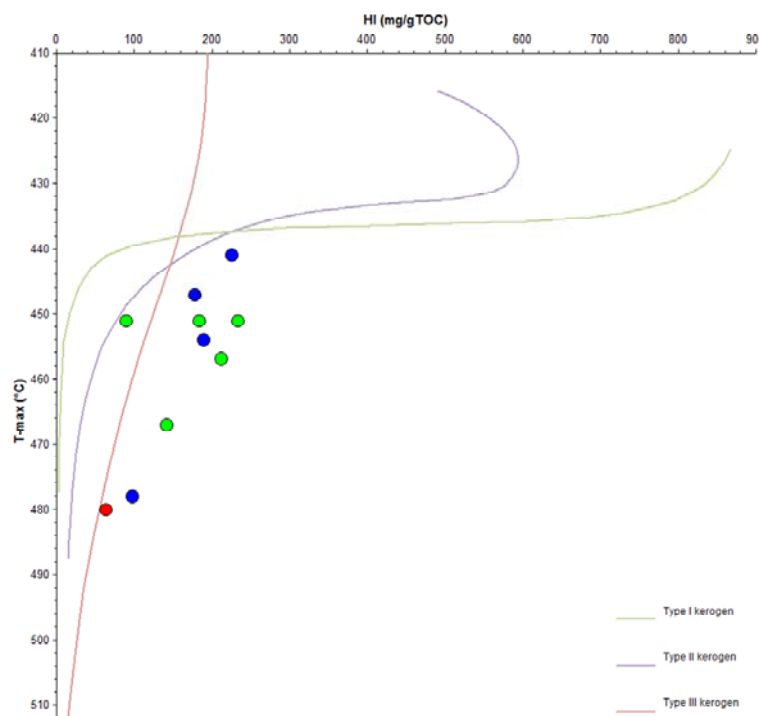


Figure 1-6b: Cooper Basin. Hydrogen Index - Tmax reveals changing petroleum potential with maturation.

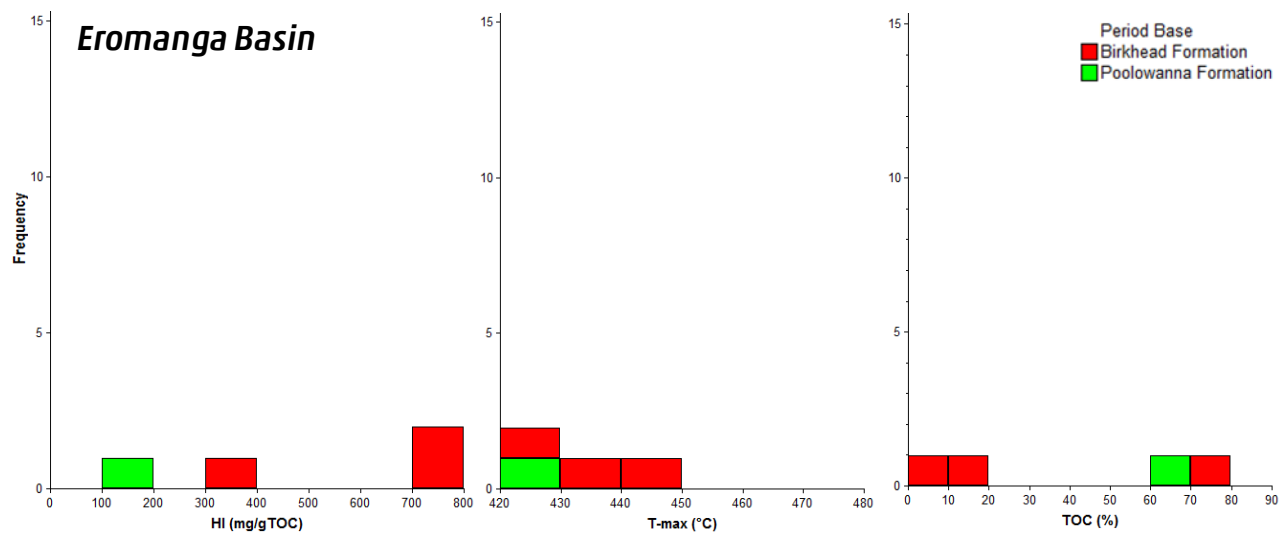


Figure 1-7: Eromanga Basin. Histograms of Hydrogen Index, Tmax and TOC.

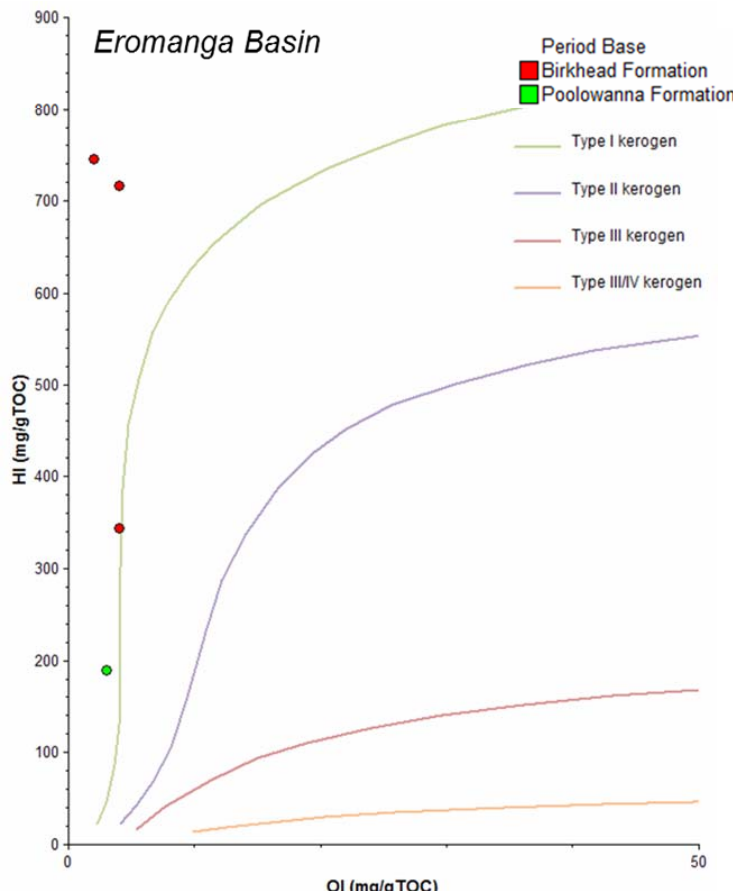


Figure 1-8a: Eromanga Basin. Hydrogen Index - Oxygen Index kerogen classification.

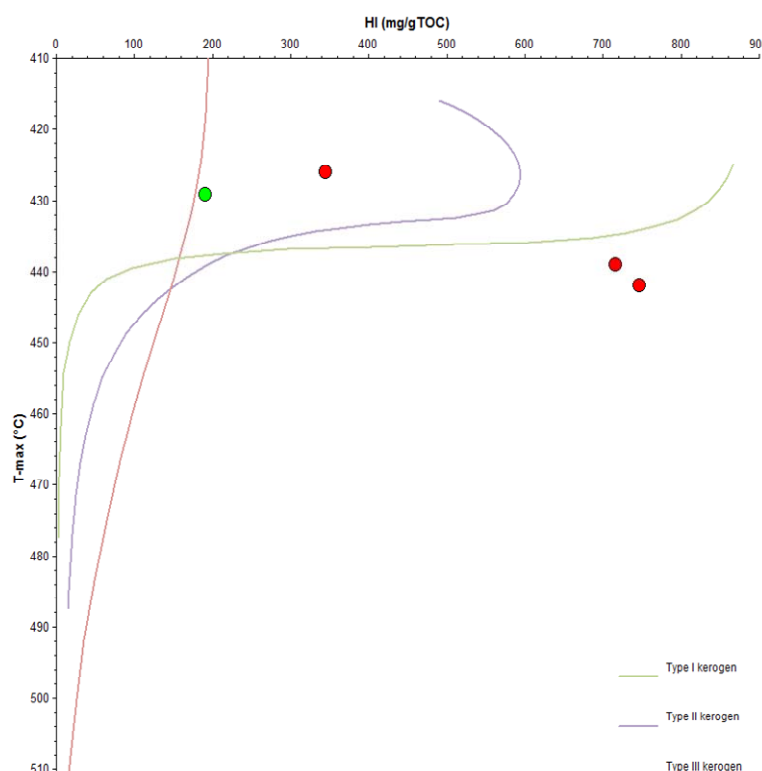


Figure 1-8b: Eromanga Basin. Hydrogen Index - Tmax reveals changing petroleum potential with maturation.

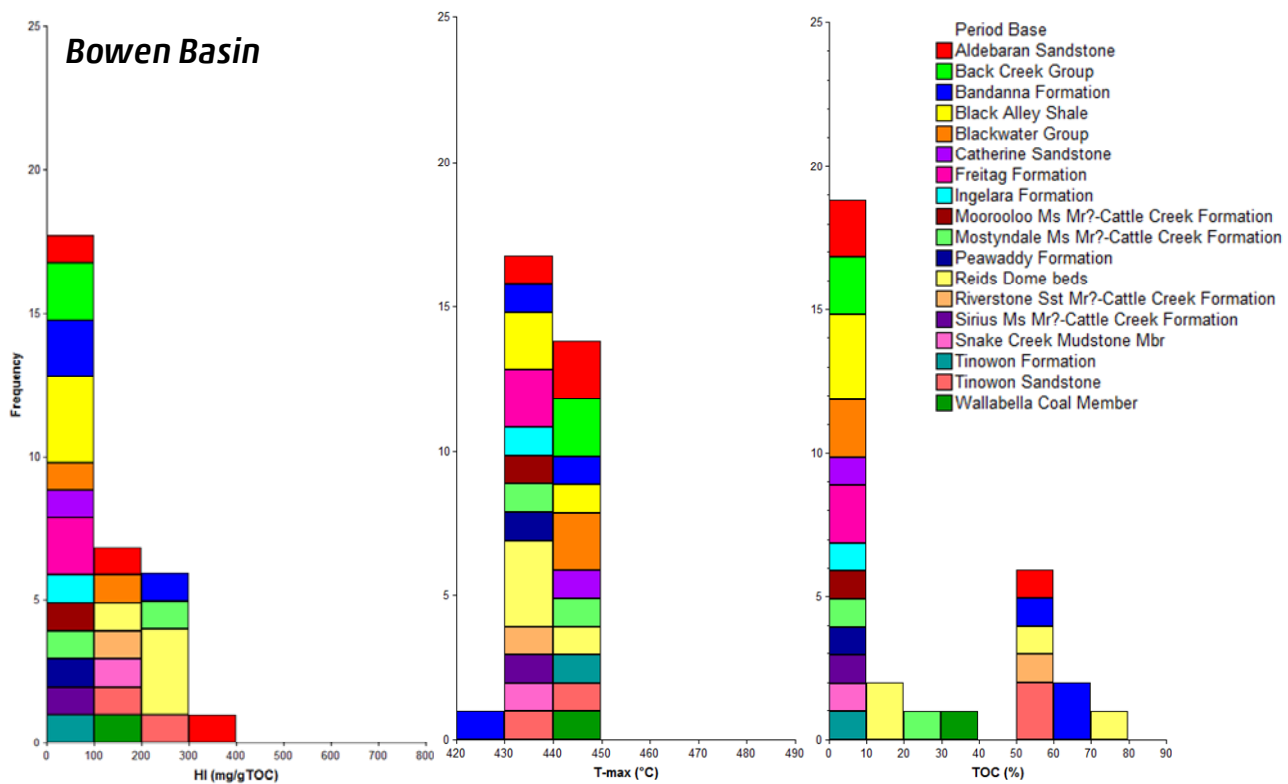


Figure 1-9: Bowen Basin. Histograms of Hydrogen Index, Tmax and TOC.

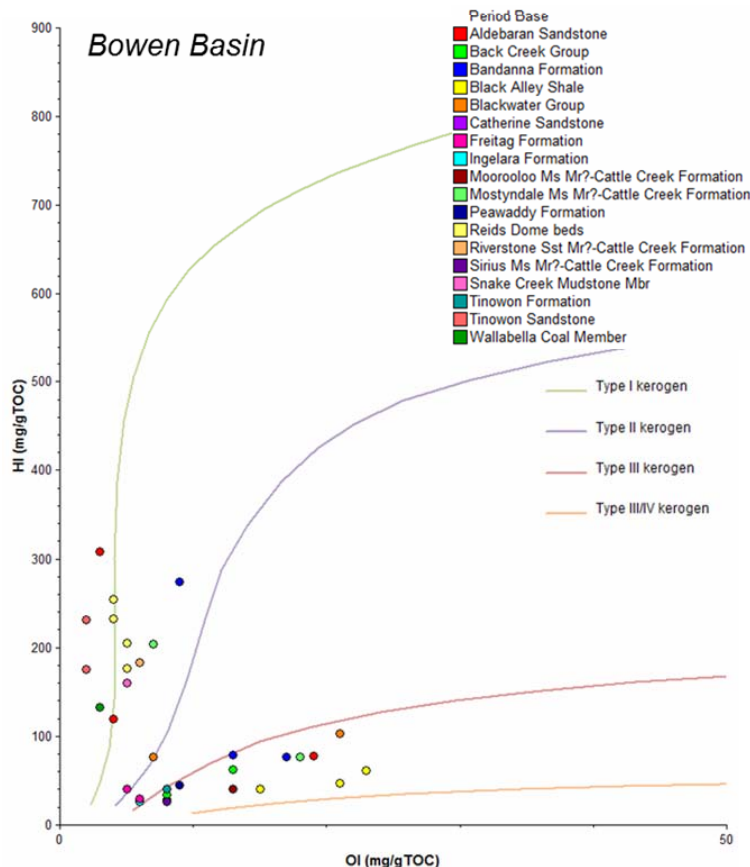


Figure 1-10a: Bowen Basin. Hydrogen Index – Oxygen Index kerogen classification.

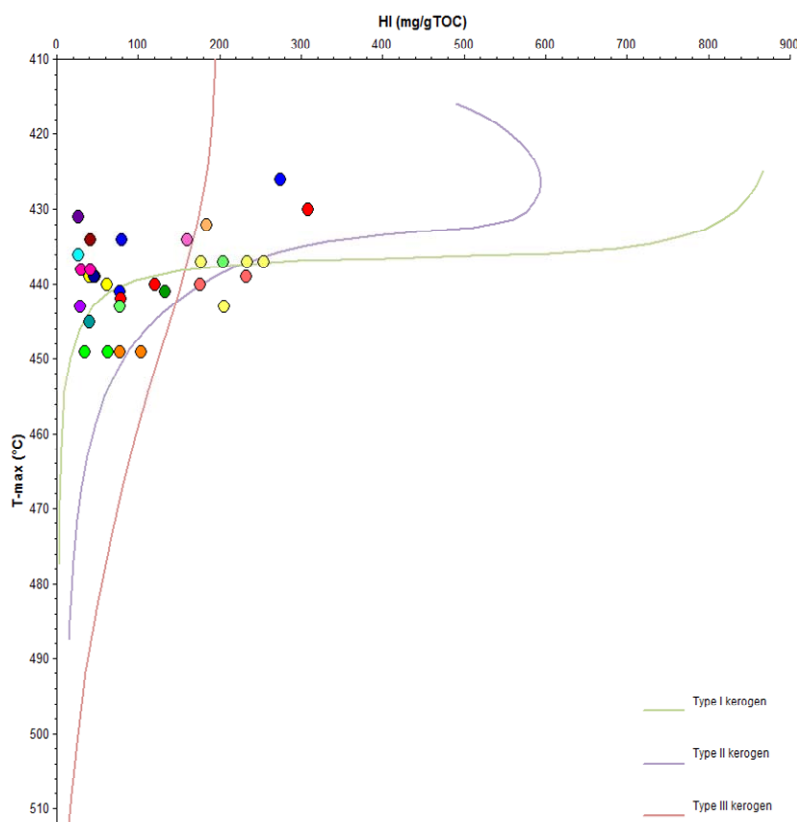


Figure 1-10b: Bowen Basin. Hydrogen Index – Tmax reveals changing petroleum potential with maturation.

Tab.1-1: Sample set

Basin	Code	GSQ i.d.	Rock Type	Description	Well Name	Rock Unit Name	Depth (m)	Rv Estimates
COOPER BASIN	G016494	GSV01	Carb'ceous mst	dull	CHANDOS 1	Patchawarra Formation	2427.94	0.9
COOPER BASIN	G016495	GSV02	Carb'ceous mst	bright	CHANDOS 1	Patchawarra Formation	2430.76	0.9
COOPER BASIN	G016496	GSV03	Coal	bright	YANDA 1	Patchawarra Formation	2265.34	0.9
COOPER BASIN	G016497	GSV04	Carb'ceous mst	black	YANDA 1	Patchawarra Formation	2270.43	0.9
COOPER BASIN	G016498	GSV05	Coal		ASHBY 1	Patchawarra Formation	2068.27	1
COOPER BASIN	G016499	GSV06	Coal	bright + dull	THUNDA 1	Toolachee Formation	2337.89	0.95
COOPER BASIN	G016500	GSV07	Coal	bright	NACCOWLAH 1	Toolachee Formation	1861.11	0.8
COOPER BASIN	G016501	GSV08	Coal	bright	COCOS 2	Toolachee Formation	2361.74	1.3
COOPER BASIN	G016502	GSV09	Coal	bright	ORIENTOS NORTH 1	Toolachee Formation	1957.88	0.9
COOPER BASIN	G016503	GSV10	Carb'ceous mst	black	ORIENTOS NORTH 1	Epsilon Formation	2152.28	1
EROMANGA BASIN	G016504	GSV11	Carb'ceous mst	dark grey	EROMANGA 1	Birkhead Formation	1054.75	0.5
EROMANGA BASIN	G016505	GSV12	Coal	bright	EROMANGA 1	Birkhead Formation	1064.37	0.5
EROMANGA BASIN	G016506	GSV13	Carb'ceous mst	black	EROMANGA 1	Birkhead Formation	1100.12	0.5
EROMANGA BASIN	G016507	GSV14	Coal	bright (2m thick)	EROMANGA 1	Poolowanna Formation	1222.66	0.7
ADAVALE BASIN	G016508	GSV15	carbonate	brown	BURY 1	Bury limestone	2631.34	1.2
ADAVALE BASIN	G016509	GSV16	Siltstone	grey (fragmented core)	ETONVALE 1	Log Creek Formation	2672.18	1
BOWEN BASIN	G016510	GSV17	Coal	bright	SPRINGSURE 19	Bandanna Formation	378.41	0.5
BOWEN BASIN	G016511	GSV18	shale	black, carbonaceous	SPRINGSURE 19	Bandanna Formation	385.02	0.5
BOWEN BASIN	G016512	GSV19	Coal	bright	SPRINGSURE 19	Bandanna Formation	399.72	0.5
BOWEN BASIN	G016513	GSV20	shale	dark grey, carbonaceous	SPRINGSURE 19	Black Alley Shale	453.33	0.6
BOWEN BASIN	G016514	GSV21	shale	dark grey, carbonaceous	SPRINGSURE 19	Black Alley Shale	470.67	0.6
BOWEN BASIN	G016515	GSV22	shale	dark grey, carbonaceous	SPRINGSURE 19	Black Alley Shale	488.7	0.6
BOWEN BASIN	G016516	GSV23	shale	dark grey, carbonaceous	SPRINGSURE 19	Peawaddy Formation	601.52	0.54

BOWEN BASIN	G016517	GSV24	shale	dark grey, silty carbonaceous	SPRINGSURE 19	Catherine Sandstone	652.75	0.52
BOWEN BASIN	G016518	GSV25	shale	black, carbonaceous	SPRINGSURE 19	Ingelara Formation	736.72	0.5
BOWEN BASIN	G016519	GSV26	shale	black, carbonaceous	SPRINGSURE 19	Freitag Formation	784.3	0.45
BOWEN BASIN	G016520	GSV27	shale	black, carbonaceous	SPRINGSURE 19	Freitag Formation	816.26	0.45
BOWEN BASIN	G016521	GSV28	shale	black, carbonaceous	SPRINGSURE 19	Aldebaran Sandstone	898.97	0.5
BOWEN BASIN	G016522	GSV29	Coal	dull	SPRINGSURE 19	Aldebaran Sandstone	966.62	0.5
BOWEN BASIN	G016523	GSV30	shale	dark grey, carbonaceous	SPRINGSURE 19	Aldebaran Sandstone	1058	0.5
BOWEN BASIN	G016524	GSV34	shale	black, carbonaceous	SNAKE CREEK 1	Snake Creek Mudstone Member	1534.39	0.8
BOWEN BASIN	G016525	GSV35	shale	dark grey carb. shale & thin coal interbedding	MEELEEBEE 1	Blackwater Group	1141.6	0.8
BOWEN BASIN	G016526	GSV36	shale	dark & light grey carb. shales interbedding	MEELEEBEE 1	Blackwater Group	1247.24	0.9
BOWEN BASIN	G016527	GSV37	shale	black, carbonaceous	MEELEEBEE 1	Back Creek Group	1360.75	1
BOWEN BASIN	G016528	GSV38	shale	black, carbonaceous	MEELEEBEE 1	Back Creek Group	1482.78	1
BOWEN BASIN	G016529	GSV39	shale	dark grey, carbonaceous	MYALL CREEK 3	Tinowon Formation	2034.9	0.8
BOWEN BASIN	G016530	GSV42	Coal	dull	MYALL CREEK 3	Tinowon Sandstone	2112.89	0.8
BOWEN BASIN	G016531	GSV40	Coal	bright	MYALL CREEK 3	Tinowon Sandstone	2067.1	0.8
BOWEN BASIN	G016532	GSV41	Coal	bright	MYALL CREEK 3	Wallabella Coal Member	2081.14	0.8
BOWEN BASIN	G016533	GSV43	shale	black, silty carbonaceous	EDDYSTONE 4	Sirius Ms Mr?-Cattle Creek Formation	454.62	0.72
BOWEN BASIN	G016534	GSV44	shale	black, carbonaceous	EDDYSTONE 4	Moorooloo Ms Mr?-Cattle Creek Formation	667.37	0.72
BOWEN BASIN	G016535	GSV45	Coal	bright	EDDYSTONE 4	Riverstone Sst Mr?-Cattle Creek Formation	837.67	0.72
BOWEN BASIN	G016536	GSV46	Coal	bright	EDDYSTONE 4	Mostyndale Ms Mr?-Cattle Creek Formation	898.99	0.72
BOWEN BASIN	G016537	GSV47	shale	dark grey, carbonaceous	EDDYSTONE 4	Mostyndale Ms Mr?-Cattle Creek Formation	935.54	0.72
BOWEN BASIN	G016538	GSV48	Coal	bright	EDDYSTONE 4	Reids Dome beds	970.05	0.75
BOWEN BASIN	G016539	GSV49	Coal	bright	EDDYSTONE 4	Reids Dome beds	1076.19	0.75
BOWEN BASIN	G016540	GSV50	Coal	bright	EDDYSTONE 4	Reids Dome beds	1146.94	0.75
BOWEN BASIN	G016541	GSV51	Shale	black, carbonaceous (or dull coal?)	EDDYSTONE 4	Reids Dome beds	1214.25	0.75

Table 1-2: Analytical plan

Code	QLD i.d.	Rock Unit Name	RE TOC	PyGC	Tvap	BulkKin	Late Gas	Petrology	PhaseKin	Maltenes
G016494	GSV01	Patchawarra Formation	1	1	1		1			1
G016495	GSV02	Patchawarra Formation	1							
G016496	GSV03	Patchawarra Formation	1	1			1	1		
G016497	GSV04	Patchawarra Formation	1							
G016498	GSV05	Patchawarra Formation	1							
G016499	GSV06	Toolachee Formation	1	1			1			
G016500	GSV07	Toolachee Formation	1	1		1	1	1		
G016501	GSV08	Toolachee Formation	1	1			1			
G016502	GSV09	Toolachee Formation	1							
G016503	GSV10	Epsilon Formation	1							
G016504	GSV11	Birkhead Formation	1	1		1		1	1	1
G016505	GSV12	Birkhead Formation	1	1		1		1	1	1
G016506	GSV13	Birkhead Formation	1	1						
G016507	GSV14	Poolowanna Formation	1							
G016508	GSV15	Bury limestone	1	1	1	1	1			1
G016509	GSV16	Log Creek Formation	1							
G016510	GSV17	Bandanna Formation	1							
G016511	GSV18	Bandanna Formation	1	1		1		1	1	1
G016512	GSV19	Bandanna Formation	1							
G016513	GSV20	Black Alley Shale	1					1		
G016514	GSV21	Black Alley Shale	1							
G016515	GSV22	Black Alley Shale	1							
G016516	GSV23	Peawaddy Formation	1							
G016517	GSV24	Catherine Sandstone	1							
G016518	GSV25	Ingelara Formation	1							
G016519	GSV26	Freitag Formation	1							
G016520	GSV27	Freitag Formation	1							
G016521	GSV28	Aldebaran Sandstone	1							

G016522	GSV29	Aldebaran Sandstone	1	1	1			1	1	1	1
G016523	GSV30	Aldebaran Sandstone	1		1						
G016524	GSV34	Snake Creek Mudstone Mbr	1	1	1	1			1		
G016525	GSV35	Blackwater Group	1								
G016526	GSV36	Blackwater Group	1		1						
G016527	GSV37	Back Creek Group	1		1						
G016528	GSV38	Back Creek Group	1		1						
G016529	GSV39	Tinowon Formation	1		1						1
G016530	GSV42	Tinowon Sandstone	1								
G016531	GSV40	Tinowon Sandstone	1	1		1		1	1	1	
G016532	GSV41	Wallabella Coal Member	1								
G016533	GSV43	Sirius Ms Mr?-Cattle Creek Formation	1								
G016534	GSV44	Moorooloo Ms Mr?-Cattle Creek Formation	1								
G016535	GSV45	Riverstone Sst Mr?-Cattle Creek Formation	1	1		1		1	1	1	
G016536	GSV46	Mostyndale Ms Mr?-Cattle Creek Formation	1								
G016537	GSV47	Mostyndale Ms Mr?-Cattle Creek Formation	1								
G016538	GSV48	Reids Dome beds	1								
G016539	GSV49	Reids Dome beds	1	1		1		1	1		
G016540	GSV50	Reids Dome beds	1								
G016541	GSV51	Reids Dome beds	1								

48 15 8 10 6 11 7 9

Table 1-3: Rock-Eval data

Basin	Code	GSQ i.d.	Rock Unit Name	Depth (m)	ca. Ro (%)	S1 (mg/g)	S2 (mg/g)	S3 (mg/g)	T _{max} °C	PP (mg/g)	PI (ratio)	OSI (mgS1/gTOC)	HI (mgS2/gTOC)	OI (mgS3/gTOC)	TOC (%)
COOPER BASIN	G016494	GSV01	Patchawarra Formation	2427.94	0.9	1.87	2.93	0.06	467	4.8	0.39	90.34	142	3	2.07
COOPER BASIN	G016495	GSV02	Patchawarra Formation	2430.76	0.9	2.67	24.56	0.38	457	27.23	0.1	23.02	212	3	11.6
COOPER BASIN	G016496	GSV03	Patchawarra Formation	2265.34	0.9	10.55	182.49	1.43	451	193.04	0.05	13.46	233	2	78.4
COOPER BASIN	G016497	GSV04	Patchawarra Formation	2270.43	0.9	3.7	52.78	0.64	451	56.48	0.07	12.85	183	2	28.8
COOPER BASIN	G016498	GSV05	Patchawarra Formation	2068.27	1	6.73	68.98	1.28	451	75.71	0.09	8.79	90	2	76.6
COOPER BASIN	G016499	GSV06	Toolachee Formation	2337.89	0.95	7.36	143.08	2.27	447	150.44	0.05	9.18	178	3	80.2
COOPER BASIN	G016500	GSV07	Toolachee Formation	1861.11	0.8	21.27	179.45	1.87	441	200.72	0.11	26.69	225	2	79.7
COOPER BASIN	G016501	GSV08	Toolachee Formation	2361.74	1.3	1.14	25.39	0.71	478	26.53	0.04	4.35	97	3	26.2
COOPER BASIN	G016502	GSV09	Toolachee Formation	1957.88	0.9	8.03	146.8	1.85	454	154.83	0.05	10.36	189	2	77.5
COOPER BASIN	G016503	GSV10	Epsilon Formation	2152.28	1	0.24	3.77	0.23	480	4.01	0.06	4.07	64	4	5.89
EROMANGA BASIN	G016504	GSV11	Birkhead Formation	1054.75	0.5	0.88	32.16	0.18	439	33.04	0.03	19.60	716	4	4.49
EROMANGA BASIN	G016505	GSV12	Birkhead Formation	1064.37	0.5	20.62	259.38	3.33	426	280	0.07	27.38	344	4	75.3
EROMANGA BASIN	G016506	GSV13	Birkhead Formation	1100.12	0.5	2.39	89.54	0.27	442	91.93	0.03	19.92	746	2	12
EROMANGA BASIN	G016507	GSV14	Poolowanna Formation	1222.66	0.7	5.96	124.91	2.17	429	130.87	0.05	9.09	190	3	65.6
ADAVALE	G016508	GSV15	Bury	2631.34	1.2	0.24	0.66	0.18	458	0.9	0.27	21.05	58	16	1.14

BASIN			limestone																
ADAVALE BASIN	G016509	GSV16	Log Creek Formation	2672.18	1	0.04	0.31	0.15	455	0.35	0.11	7.55	58	28	0.53				
BOWEN BASIN	G016510	GSV17	Bandanna Formation	378.41	0.5	1	48.28	10.53	441	49.28	0.02	1.59	77	17	62.8				
BOWEN BASIN	G016511	GSV18	Bandanna Formation	385.02	0.5	4.2	138.42	4.6	426	142.62	0.03	8.32	274	9	50.5				
BOWEN BASIN	G016512	GSV19	Bandanna Formation	399.72	0.5	1.59	50.3	8.22	434	51.89	0.03	2.51	79	13	63.3				
BOWEN BASIN	G016513	GSV20	Black Alley Shale	453.33	0.6	0.04	1.01	0.44	439	1.05	0.04	1.87	47	21	2.14				
BOWEN BASIN	G016514	GSV21	Black Alley Shale	470.67	0.6	0.07	0.78	0.29	440	0.85	0.08	5.47	61	23	1.28				
BOWEN BASIN	G016515	GSV22	Black Alley Shale	488.7	0.6	0.03	0.57	0.21	439	0.6	0.05	2.11	40	15	1.42				
BOWEN BASIN	G016516	GSV23	Peawaddy Formation	601.52	0.54	0.04	0.85	0.16	439	0.89	0.04	2.13	45	9	1.88				
BOWEN BASIN	G016517	GSV24	Catherine Sandstone	652.75	0.52	0.05	0.8	0.22	443	0.85	0.06	1.74	28	8	2.87				
BOWEN BASIN	G016518	GSV25	Ingelara Formation	736.72	0.5	0.04	0.6	0.15	436	0.64	0.06	1.73	26	6	2.31				
BOWEN BASIN	G016519	GSV26	Freitag Formation	784.3	0.45	0.05	1.07	0.2	438	1.12	0.04	1.42	30	6	3.51				
BOWEN BASIN	G016520	GSV27	Freitag Formation	816.26	0.45	0.07	1.74	0.2	438	1.81	0.04	1.65	41	5	4.23				
BOWEN BASIN	G016521	GSV28	Aldebaran Sandstone	898.97	0.5	0.16	5.05	0.17	440	5.21	0.03	3.80	120	4	4.21				
BOWEN BASIN	G016522	GSV29	Aldebaran Sandstone	966.62	0.5	6.42	163.4	1.55	430	169.82	0.04	12.11	308	3	53				
BOWEN BASIN	G016523	GSV30	Aldebaran Sandstone	1058	0.5	0.08	0.54	0.13	442	0.62	0.13	11.59	78	19	0.69				
BOWEN BASIN	G016524	GSV34	Snake Creek Mudstone Mbr	1534.39	0.8	0.5	5.24	0.16	434	5.74	0.09	15.29	160	5	3.27				
BOWEN BASIN	G016525	GSV35	Blackwater Group	1141.6	0.8	0.13	1.5	0.13	449	1.63	0.08	6.70	77	7	1.94				
BOWEN BASIN	G016526	GSV36	Blackwater Group	1247.24	0.9	0.28	1.81	0.36	449	2.09	0.13	16.00	103	21	1.75				
BOWEN BASIN	G016527	GSV37	Back Creek Group	1360.75	1	0.12	0.52	0.13	449	0.64	0.19	7.79	34	8	1.54				
BOWEN BASIN	G016528	GSV38	Back Creek Group	1482.78	1	0.2	0.77	0.16	449	0.97	0.21	16.13	62	13	1.24				

Source Evaluation and Predicted Petroleum Compositions



BOWEN BASIN	G016529	GSV39	Tinowon Formation	2034.9	0.8	0.2	0.53	0.11	445	0.73	0.27	15.27	40	8	1.31
BOWEN BASIN	G016530	GSV42	Tinowon Sandstone	2112.89	0.8	6.24	101.03	1.17	440	107.27	0.06	10.87	176	2	57.4
BOWEN BASIN	G016531	GSV40	Tinowon Sandstone	2067.1	0.8	5.59	123.07	1.26	439	128.66	0.04	10.53	232	2	53.1
BOWEN BASIN	G016532	GSV41	Wallabella Coal Member	2081.14	0.8	4.09	47.96	1.19	441	52.05	0.08	11.36	133	3	36
BOWEN BASIN	G016533	GSV43	Sirius Ms Mr?-Cattle Creek Formation	454.62	0.72	0.07	0.75	0.22	431	0.82	0.09	2.46	26	8	2.85
BOWEN BASIN	G016534	GSV44	Moorooloo Ms Mr?-Cattle Creek Formation	667.37	0.72	0.08	0.67	0.21	434	0.75	0.11	4.91	41	13	1.63
BOWEN BASIN	G016535	GSV45	Riverstone Sst Mr?-Cattle Creek Formation	837.67	0.72	6.18	106.97	3.68	432	113.15	0.05	10.58	183	6	58.4
BOWEN BASIN	G016536	GSV46	Mostyndale Ms Mr?-Cattle Creek Formation	898.99	0.72	1.81	60.69	2.16	437	62.5	0.03	6.09	204	7	29.7
BOWEN BASIN	G016537	GSV47	Mostyndale Ms Mr?-Cattle Creek Formation	935.54	0.72	0.12	1.29	0.3	443	1.41	0.09	7.19	77	18	1.67
BOWEN BASIN	G016538	GSV48	Reids Dome beds	970.05	0.75	6.37	134.33	4.03	437	140.7	0.05	8.40	177	5	75.8
BOWEN BASIN	G016539	GSV49	Reids Dome beds	1076.19	0.75	1.4	29.99	0.52	437	31.39	0.04	11.86	254	4	11.8
BOWEN BASIN	G016540	GSV50	Reids Dome beds	1146.94	0.75	7.86	132.5	2.35	437	140.36	0.06	13.84	233	4	56.8
BOWEN BASIN	G016541	GSV51	Reids Dome beds	1214.25	0.75	1.61	25.23	0.63	443	26.84	0.06	13.09	205	5	12.3

PP = Total Petroleum Potential=S1+S2

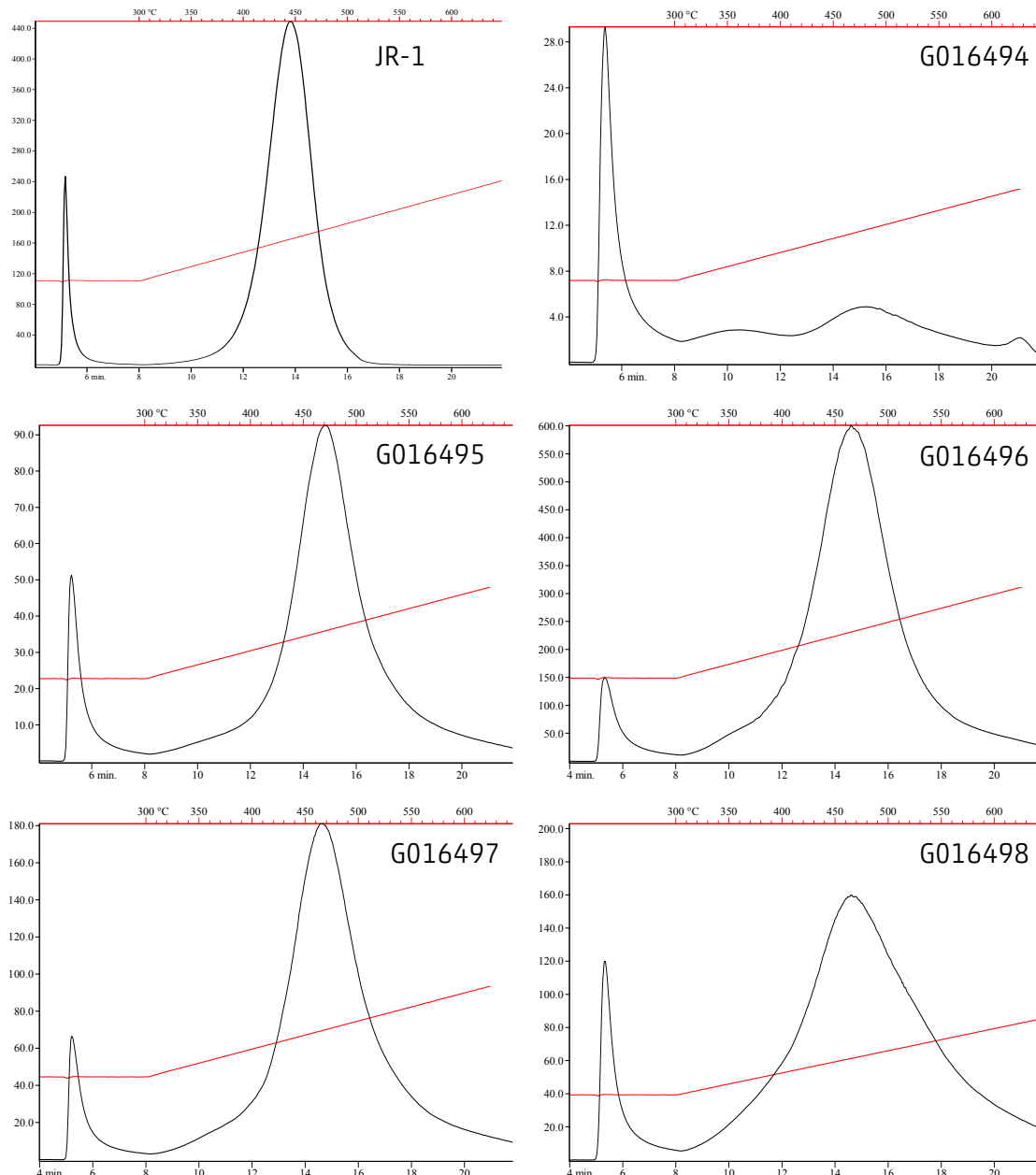
PI = Production Index

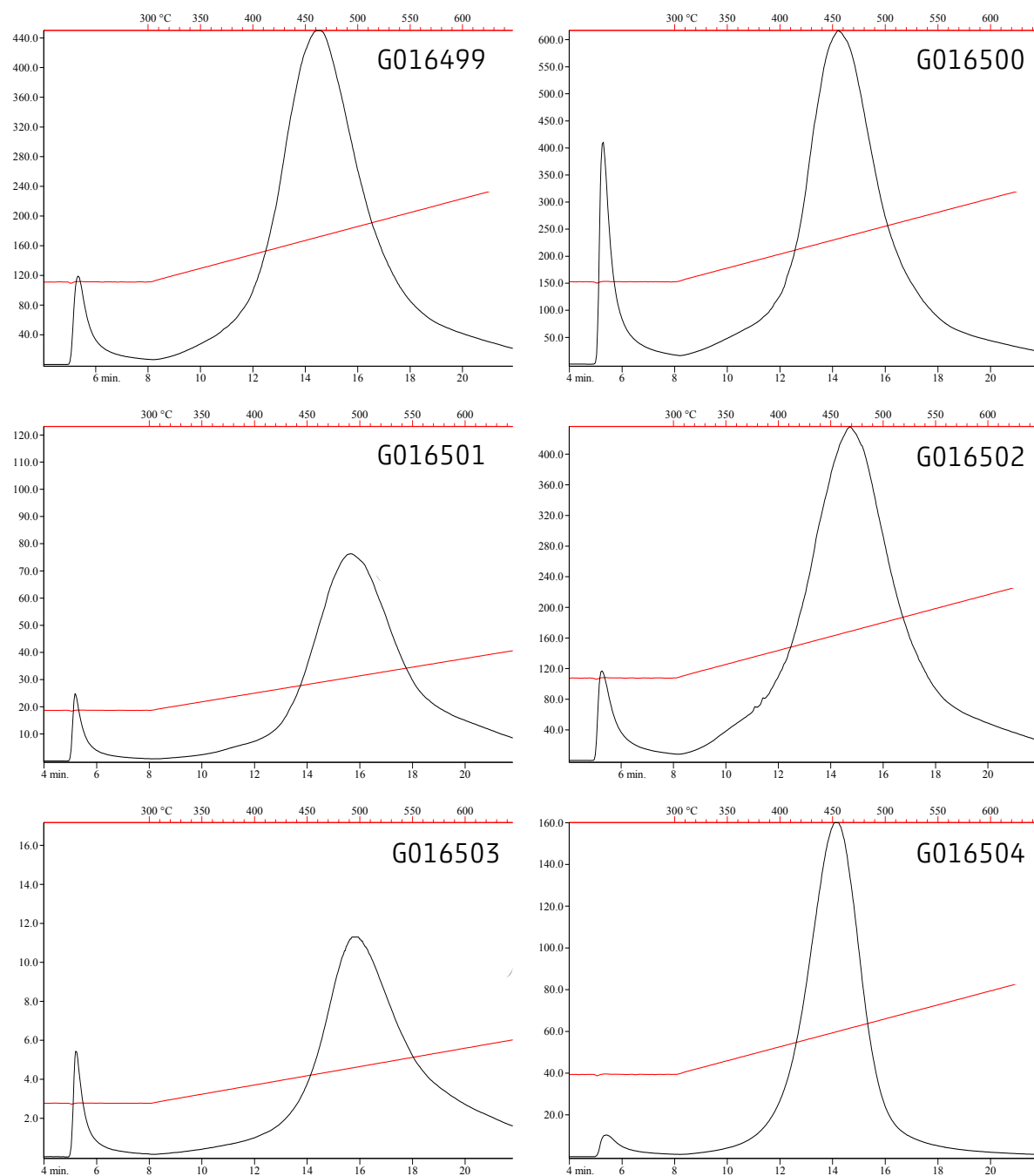
OSI = Oil Saturation Index

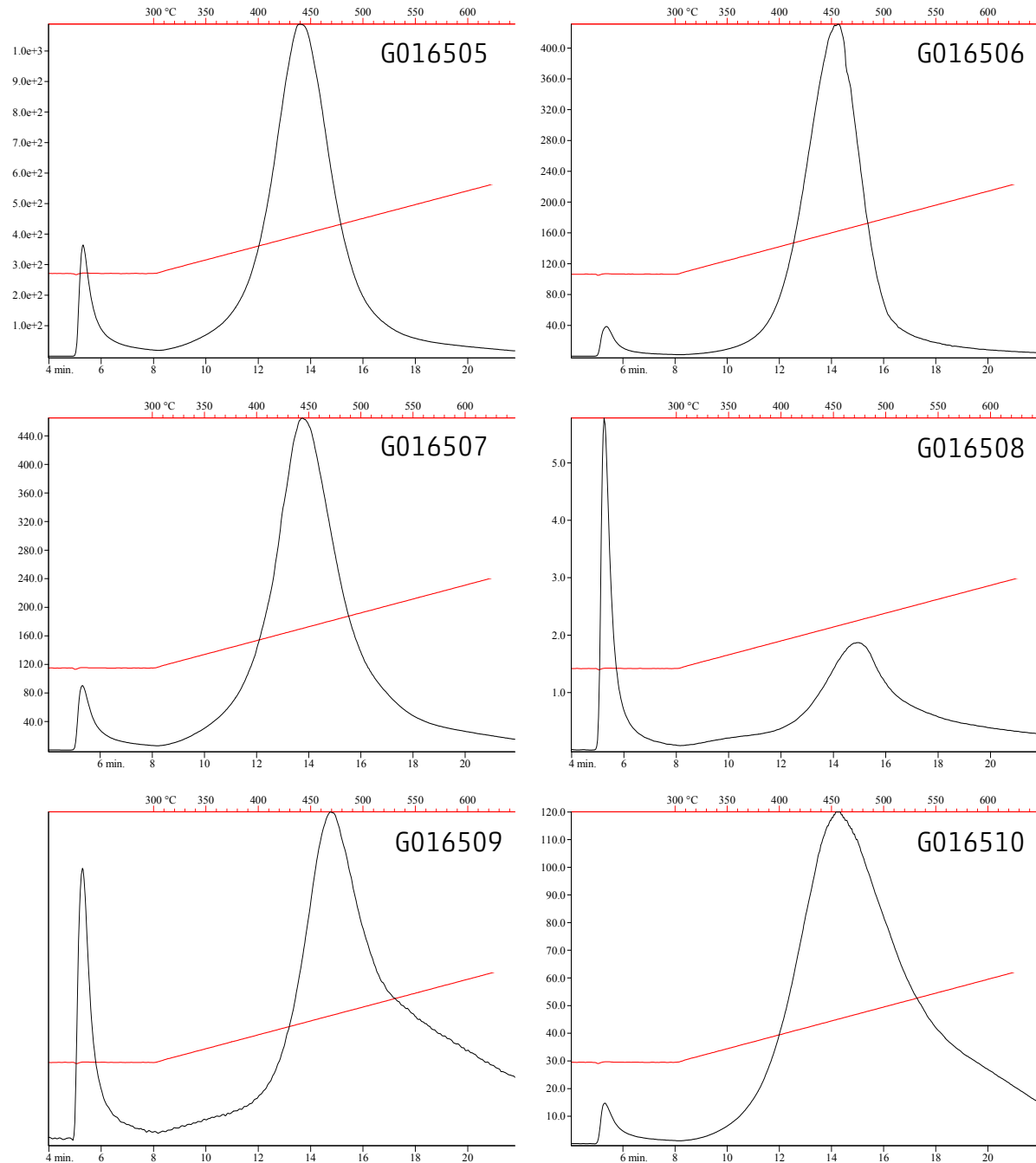
Appendix 1-1 – Figures

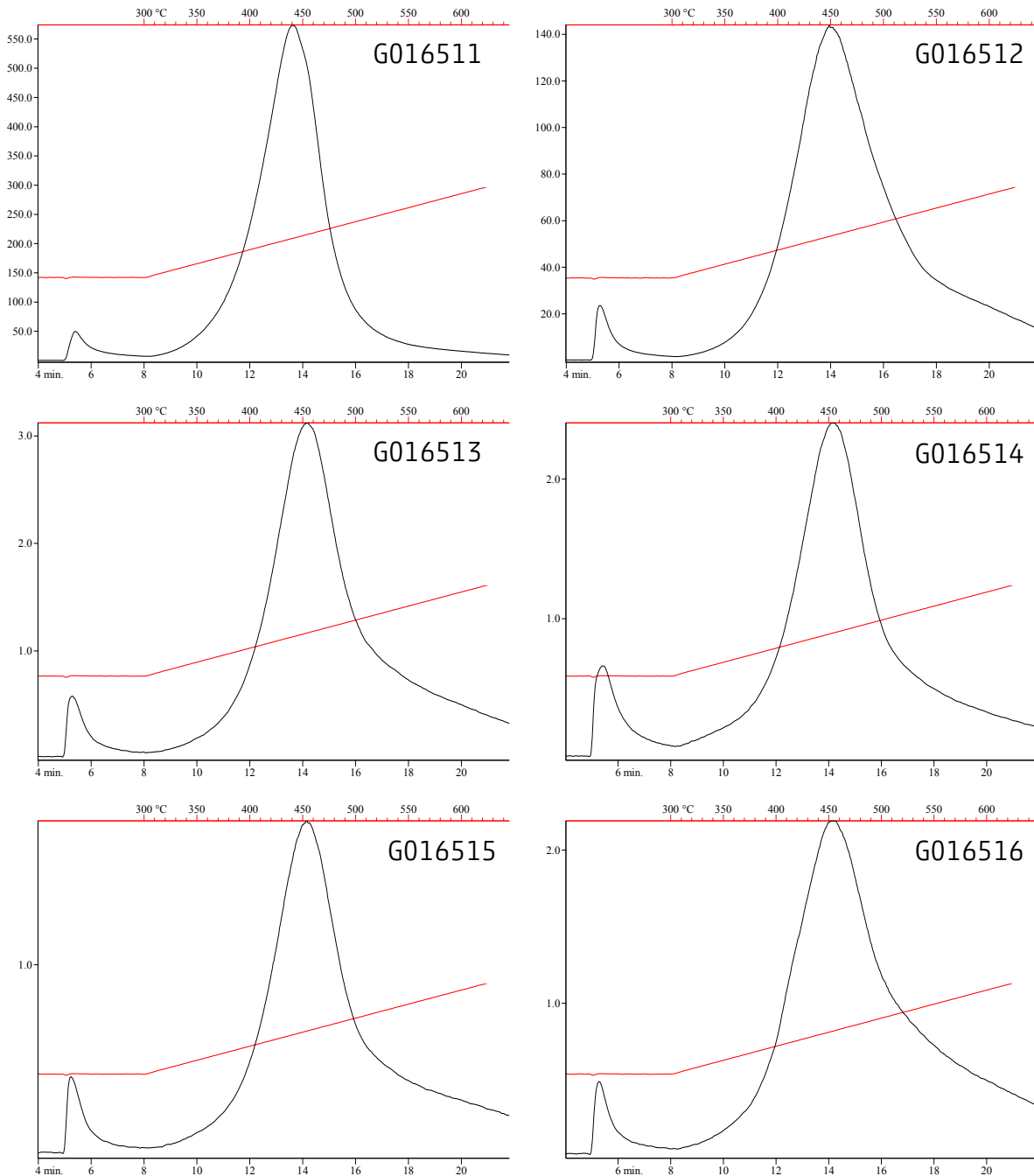
Rock-Eval programs

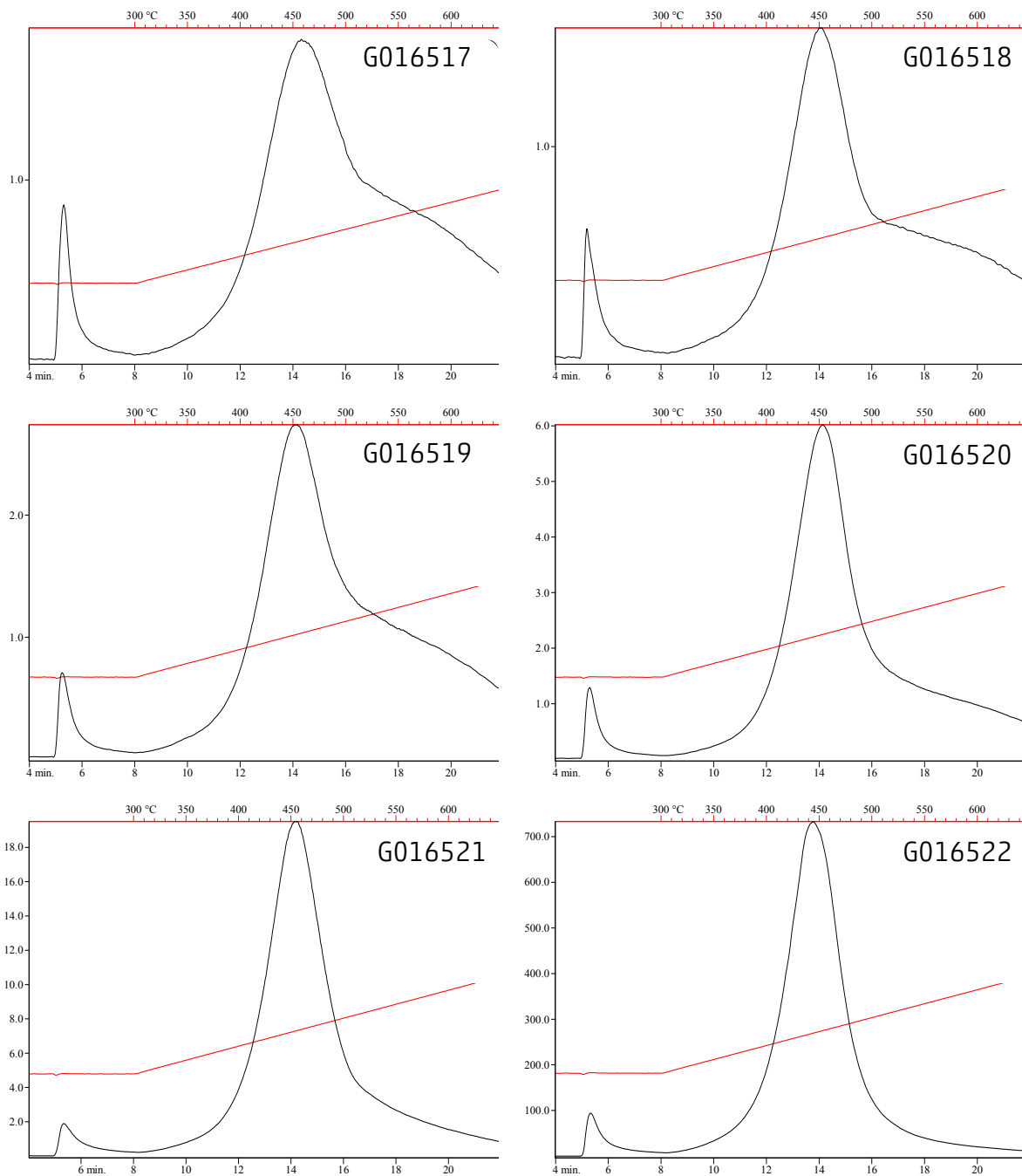
The FID trace shown for the standard Jet Rock (JR-1) displays the rate of HC evolution versus temperature. A sharp smaller peak, S1 (eluting at 300°C), and a broader bigger peak S2 eluting between 300 and 650°C on the x-axis are clear to see. Tmax is the temperature where S2 shows its maximum, and is measured automatically. These FID-traces from the Hawk instrument are presented to show the complexity and breadth that the S2 peak can have. The temperatures shown on the x-axes are measured in the analyzer. As is the case with modern Rock-Eval instruments too, these values are then adjusted down by 35°C to conform with published Rock-Eval Tmax temperatures which in truth are actually 35°C too low due to poor placement of the thermocouple in the original development work. The corrected data is presented in Table 1-3. S3 is not shown here as it is not used in the interpretation of hydrocarbon potential.

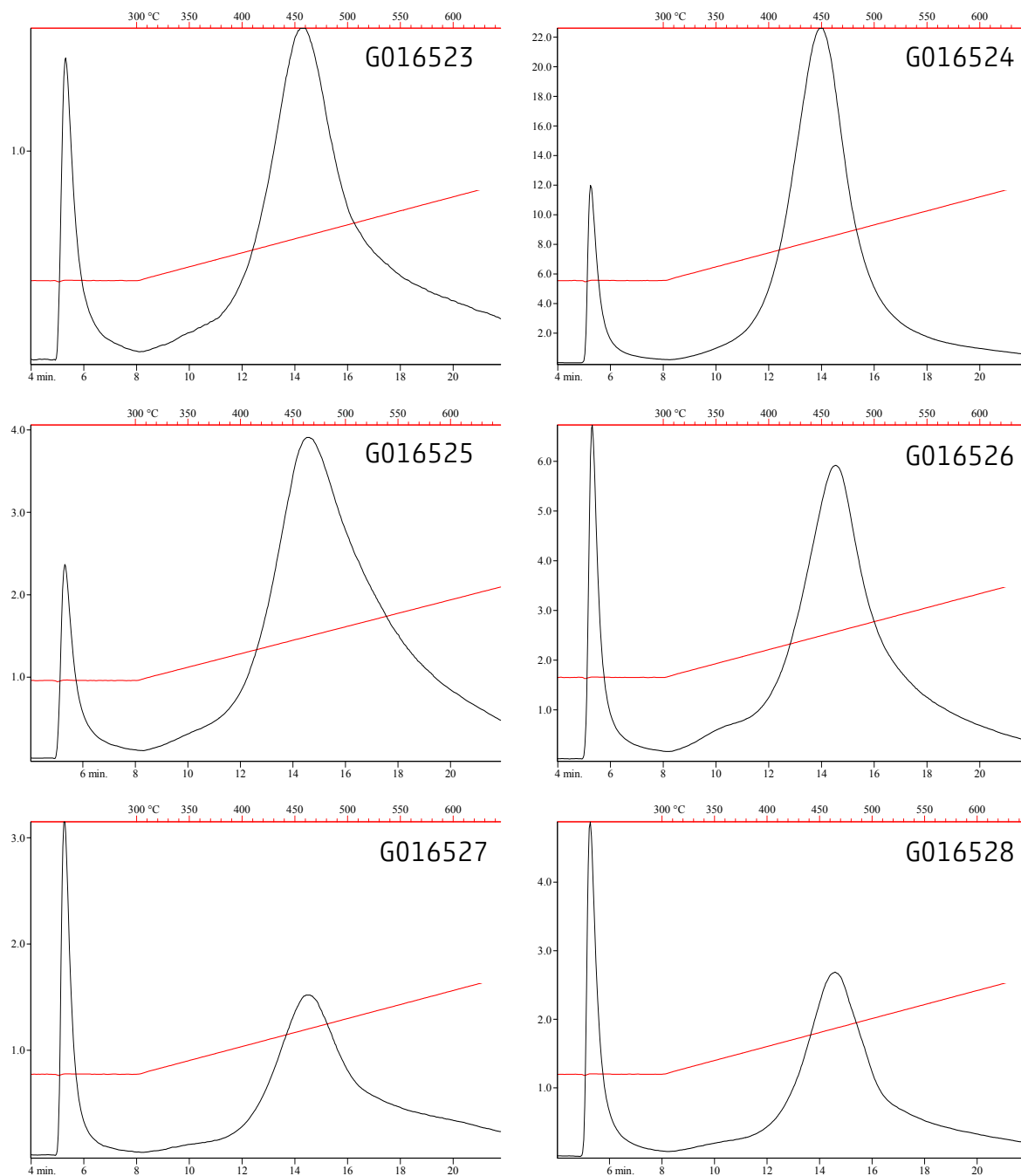


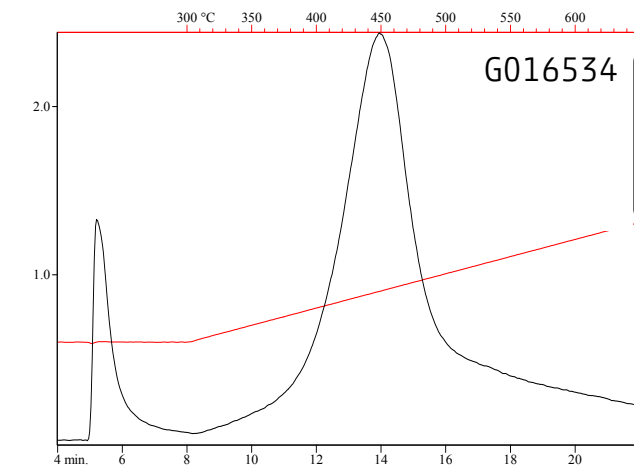
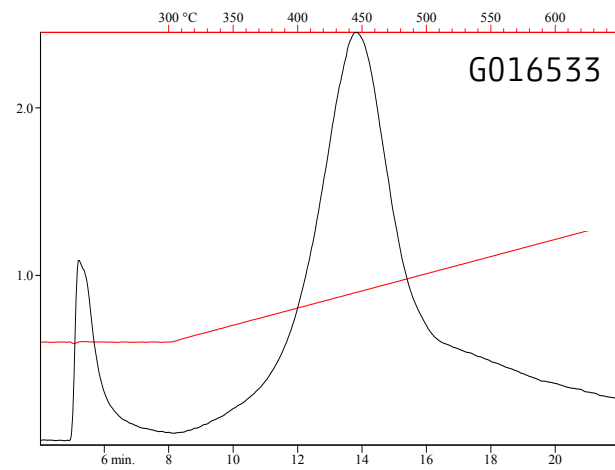
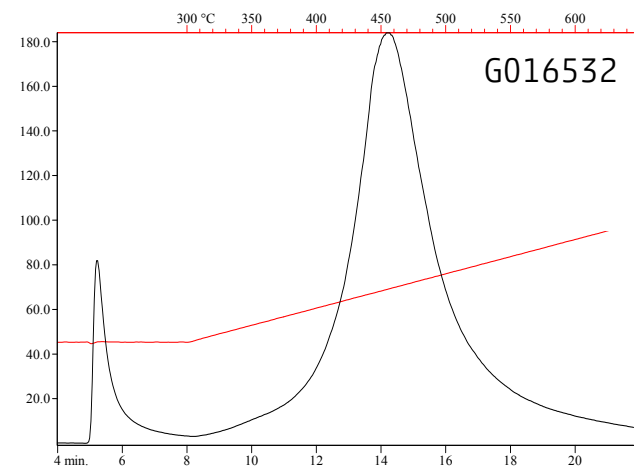
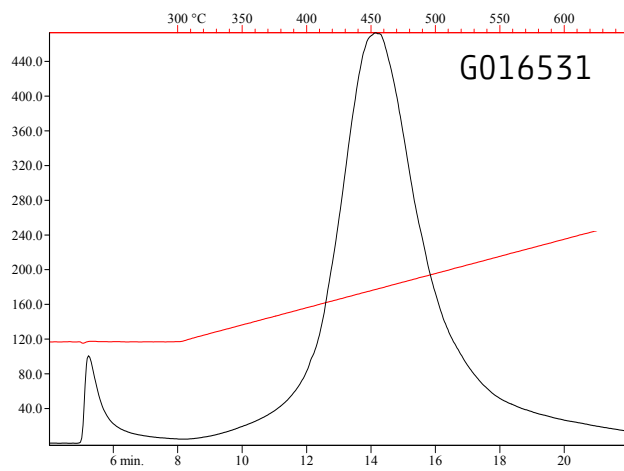
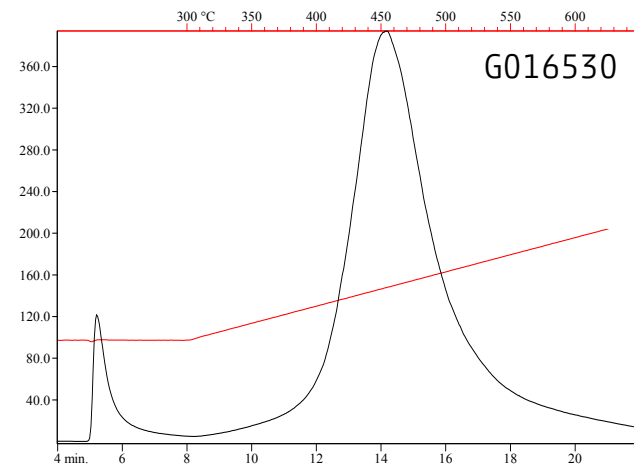
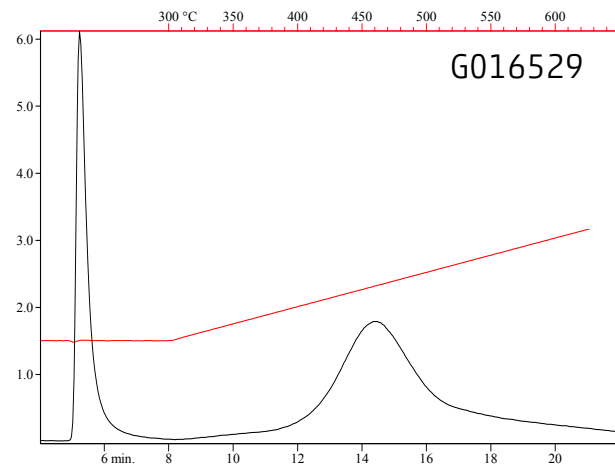


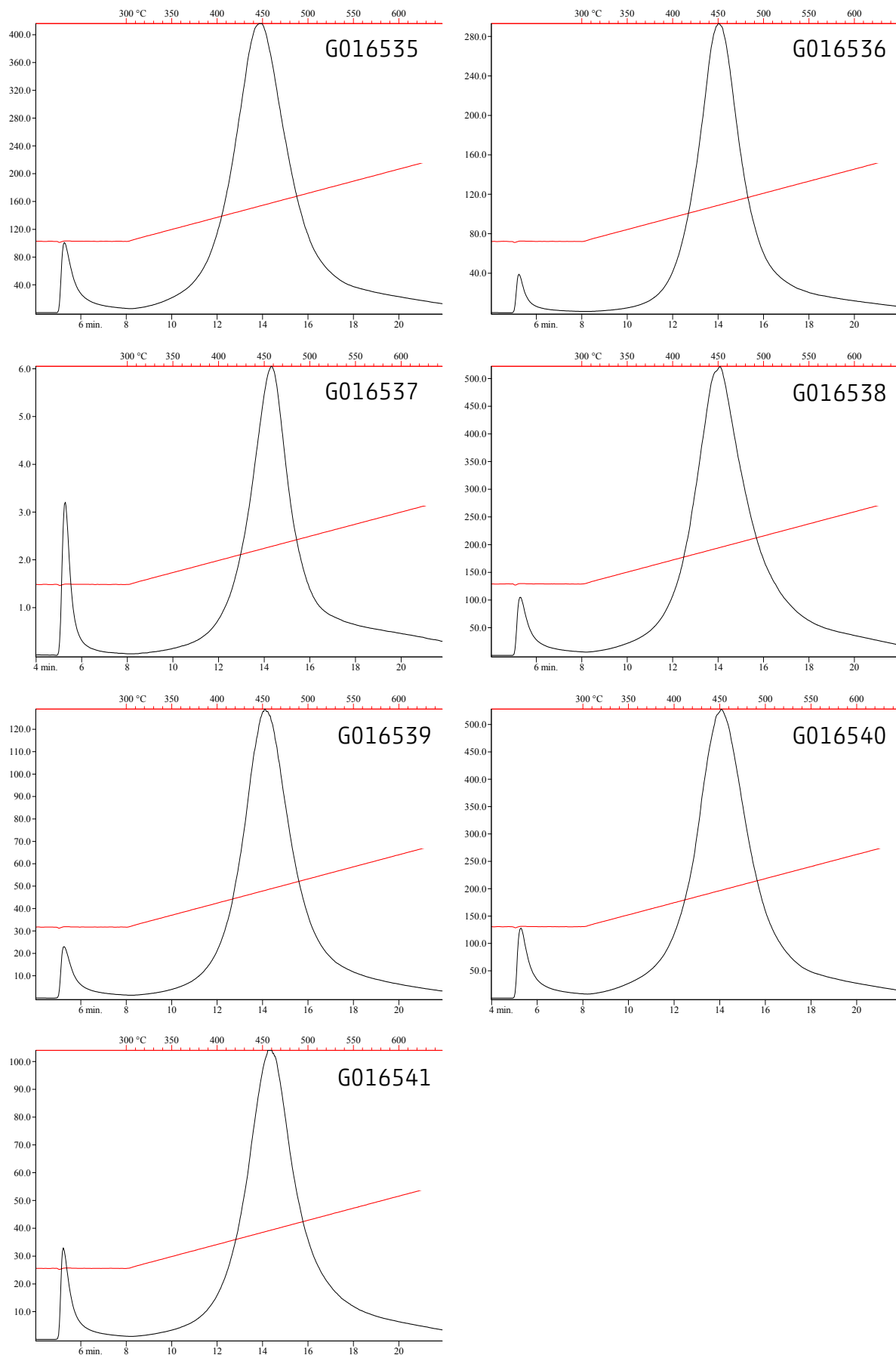












2 Analytical pyrolysis and thermovaporisation

Table 2-1: Analytical pyrolysis and thermovaporisation sample list

Basin	Code	QLD i.d.	Rock Type	Rock Unit Name	PyGC	Tvap
COOPER BASIN	G016494	GSV01	Carb'ceous mst	Patchawarra Formation	1	1
COOPER BASIN	G016496	GSV03	Coal	Patchawarra Formation	1	
COOPER BASIN	G016499	GSV06	Coal	Toolachee Formation	1	
COOPER BASIN	G016500	GSV07	Coal	Toolachee Formation	1	
COOPER BASIN	G016501	GSV08	Coal	Toolachee Formation	1	
EROMANGA BASIN	G016504	GSV11	Carb'ceous mst	Birkhead Formation	1	
EROMANGA BASIN	G016505	GSV12	Coal	Birkhead Formation	1	
EROMANGA BASIN	G016506	GSV13	Carb'ceous mst	Birkhead Formation	1	
ADAVALE BASIN	G016508	GSV15	carbonate	Bury limestone	1	1
BOWEN BASIN	G016511	GSV18	shale	Bandanna Formation	1	
BOWEN BASIN	G016522	GSV29	Coal	Aldebaran Sandstone	1	
BOWEN BASIN	G016523	GSV30	shale	Aldebaran Sandstone		1
BOWEN BASIN	G016524	GSV34	shale	Snake Creek Mudstone Mbr	1	1
BOWEN BASIN	G016526	GSV36	shale	Blackwater Group		1
BOWEN BASIN	G016527	GSV37	shale	Back Creek Group		1
BOWEN BASIN	G016528	GSV38	shale	Back Creek Group		1
BOWEN BASIN	G016529	GSV39	shale	Tinowon Formation		1
BOWEN BASIN	G016531	GSV40	Coal	Tinowon Sandstone	1	
BOWEN BASIN	G016535	GSV45	Coal	Riverstone Sst Mr?-Cattle Creek Formation	1	
BOWEN BASIN	G016539	GSV49	Coal	Reids Dome beds	1	

RUNNING TOTALS**15****8**

Petroleum Type Organofacies and Free Hydrocarbons

The pyrolysis gas chromatograms of fifteen selected samples are shown in Appendix Figure 2-A1; boiling range and individual compound yields are listed in Tables 2-A1a-c. Figure 2-1 in the main body of the report shows the carbon chain length distribution of the samples plotted in the Petroleum Type Organofacies triangle of Horsfield (1989). For further molecular description of the organic matter structure (phenol abundance, aromaticity, and sulphur content) the triangular plots of Larter (1984), and Eglinton et al. (1990) are used (Figures 2-3, respectively).

Thermovaporisation chromatograms/fingerprints of free hydrocarbons in eight selected samples are shown in Figure 2-A2.

Cooper Basin

The relatively mature coals (and one carbonaceous shale) of the Patchawarra and Toolachee formations generate pyrolysates that infer a remaining potential for gas/condensate generation (Figure 2-1). It should be noted that the gas and condensate field was originally defined for immature source rocks using pyrolysates of vitrinites and sporinites in accordance with the mainly Type III gas-prone nature of northwest European Carboniferous coals, which are rich in vitrinite and whose major liptinite maceral is sporinite (Horsfield, 1989; Stach et al., 1982). As pyrolysis products of those macerals are usually enriched in phenolic compounds, and pyrolysis products of the Patchawarra and Toolachee Formation coals are also enriched in phenolic compounds (Figure 2-2; Figure 2-A1), those samples can also be assumed to have been originally relatively gas-prone. The pyrolysate of the least mature Toolachee Fm. sample G0016500 ($T_{max} = 441^{\circ}\text{C}$) plots very close to the border of the Paraffinic-Naphthenic-Aromatic (P-N-A) Low Wax field and is characterised by slightly higher yields of long-chain aliphatic compounds up to $n\text{-C}_{27}$. This indicates that more hydrogen-rich precursor materials such as cutinite, liptodetrinite, or suberinite are also present in that sample.

Advanced maturity stages are also indicated by the overall very aromatic composition of the pyrolysates which plot in or very close to the Type IV kerogen field (Figure 2-2) and in the "aromatic" field (Figure 2-3). Low sulphur-contents are also in line with high maturities, as well as, in the case of the coals, with terrestrially land-plant dominated organic matter.

The uppermost Patchawarra Fm. mudstone sample G016494 (dark blue symbol in Figure 2-1) also exhibits a gas and condensate potential, but shows very few phenolic pyrolysis products (Figure 2-A1). Its pyrolysate is rather dominated by aromatic compounds and gradually decreasing aliphatic n -alkanes extending to $n\text{-C}_{27}$, indicating much lower abundance of higher land plant derived lignocellulosic material than observed for the coals. Because it had displayed a high Production Index ($PI = 0.39$), the latter sample was also analysed by thermovaporisation GC-FID in order to characterise the composition of its retained free hydrocarbons. Importantly, the T_{vap} fingerprint (Figure 2-A2) shows a domination of straight-chain paraffins gradually decreasing from $n\text{-C}_6$ to $n\text{-C}_{27}$, this being consistent with a *high quality light oil signature*. The high abundance of light hydrocarbons in particular implies that the mudstone is rather tight, i.e., capable of retaining large amounts of gas and oil. This finding is *highly significant* as far as unconventional shale plays are concerned.

Adavale Basin

The Petroleum Type Organofacies of the selected Bury Limestone sample G016508 is Paraffinic-Naphthenic-Aromatic Low Wax (Figure 2-1), albeit due to its advanced maturity level close to the border with the gas/condensate field. The pyrogram (Figure 2-A1) is dominated by gas range compounds, normal aliphatic hydrocarbons extending to $n\text{-C}_{15}$, and some aromatic compounds. The overall pyrolysate composition is, for this maturity stage, relatively aliphatic (Figures 2-2 and 2-3) indicating that the original organic matter was likely algae possibly deposited in a marine environment.

Interestingly and in contrast to the sample's high Production Index value of 0.27, thermovaporisation yields are low, and the chromatograms are dominated by aromatic compounds up to C18, as well as several major unidentified peaks. Gas loss is likely to have occurred, thus reducing the overall yield.

Eromanga Basin

Pyrolysates of the two low mature carbonaceous mudstones of the Birkhead Fm. plot, typical for Type I kerogen containing source rocks deposited in an anoxic lacustrine environment, in the Paraffinic Oil High Wax Petroleum Type Organofacies field (Figure 2-1). The chromatograms are strongly dominated by n -alkyl chains with maxima/plateaus at $n\text{-C}_{10-14}$ and $n\text{-C}_{22-26}$ (Figure 2-A1). Similar pyrolysis fingerprints are usually seen for structurally homogeneous Type I alginites formed either from the selective preservation of the outer cell walls of lacustrine microalgae, which are highly aliphatic (Berkaloff et al., 1983), e.g. remains of *Botryococcus braunii* in the case of Green River Shale (Horsfield et al., 1994), or of lipids grafted to the kerogen by neocondensation reactions (Larter and Douglas, 1980). Sulphur compounds are, as is typical for non-marine depositional environments, present in only very low amounts, whereas phenol and cresols, typical of land plant lignocellulosic pyrolysis products, can be readily discerned indicating the presence of low amounts of woody organic matter. This small land-plant derived organic matter fraction leads to pyrolysate compositions outside of the "aquatic" (Figure 2-2) and "aliphatic" (Figure 2-3) organofacies fields.

The Type II/III Birkhead Fm. coal sample exhibits very similar chain length compositions but there is a higher contribution of aromatic and phenolic compounds relative to aliphatic compounds (Figure 2-A1). This indicates a much higher contribution of terrestrial organic matter and explains pyrolysate compositions at the border of the Paraffinic-Naphthenic-Aromatic High Wax field in terms of chain length distribution (Figure 2-1), a position within the "terrestrial" field based on the relative abundance of lignocellulosic signals, namely phenol (Figure 2-2) and being near the "aromatic" field based on the relative abundance of sulphur compounds (Figure 2-3).

Bowen Basin

The inferred petroleum type for the early oil window mature Bowen Basin shales and coals is mainly P-N-A High Wax, for the Tinowon Sandstone coal sample Gas and Condensate, and for the Snake Creek Mudstone P-N-A Low Wax. Those pyrolysate positions within the ternary plot (Figure 2-1), together with the gas chromatographic fingerprints (Figure 2-A1) which are dominated by gas compounds, normal aliphatic hydrocarbons extending to long chain lengths, and by aromatic and especially phenolic compounds, are diagnostic of fluviodeltaic depositional environments with variable organic matter input leading to slightly differing maceral assemblages (e.g. vitrinite, cutinite, liptodetrinite, and resinite in variable proportions). An abundance of lignocellulosic material is reflected by pyrolysate compositions in the centre of the "terrestrial" organofacies field (Figure 2-2). Furthermore, and taking into account very low yields of sulphur compounds (Figure 2-A1; Figure 2-3), deposition in a marine environment is unlikely, whereas input of algal or bacterial organic matter into a lacustrine/brackish environment explains all observed compositional features.

Thermovaporisation was used to investigate those samples from the Bowen Basin that had a relatively high concentration of free hydrocarbons (PI 0.08-0.27). In the shale sample of the base Aldebaran Sandstone, (G016523) the chromatogram was completely dominated by aromatic hydrocarbons in low concentration, and not indicative of anything in particular. Thus, the hydrocarbons responsible for the high Production Index were absent. In the Snake Creek Mudstone Member sample (G016524), the dominant components were in the light hydrocarbon range (lighter than n-C12); the Back Creek Group sample (G016527) was closely similar in that respect, consistent with the presence of condensate range hydrocarbons. In contrast, the Blackwater Group sample (G016526) is dominated by saturated hydrocarbons with a bimodal distribution, suggestive of the expulsion of light hydrocarbons. The other Back Creek Group sample (G016528) is dominated by light hydrocarbons, suggestive of condensate potential, as is the Tinowon Formation sample (G016529). All in all, the high Production Indices reported earlier for these samples is consistent with the presence of condensate range components, ostensibly associated with gas that was lost during sample preparation.

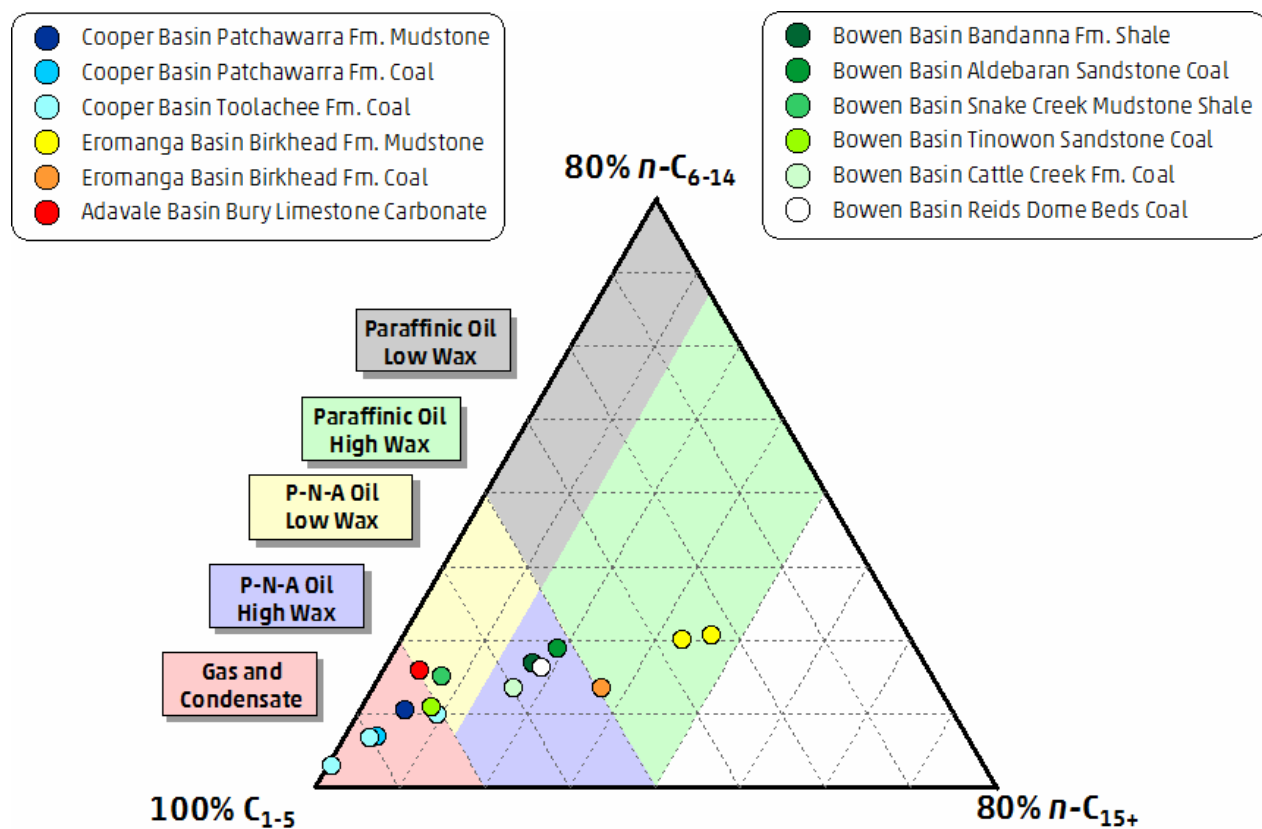


Figure 2-1: Petroleum Type Organofacies after Horsfield (1989).

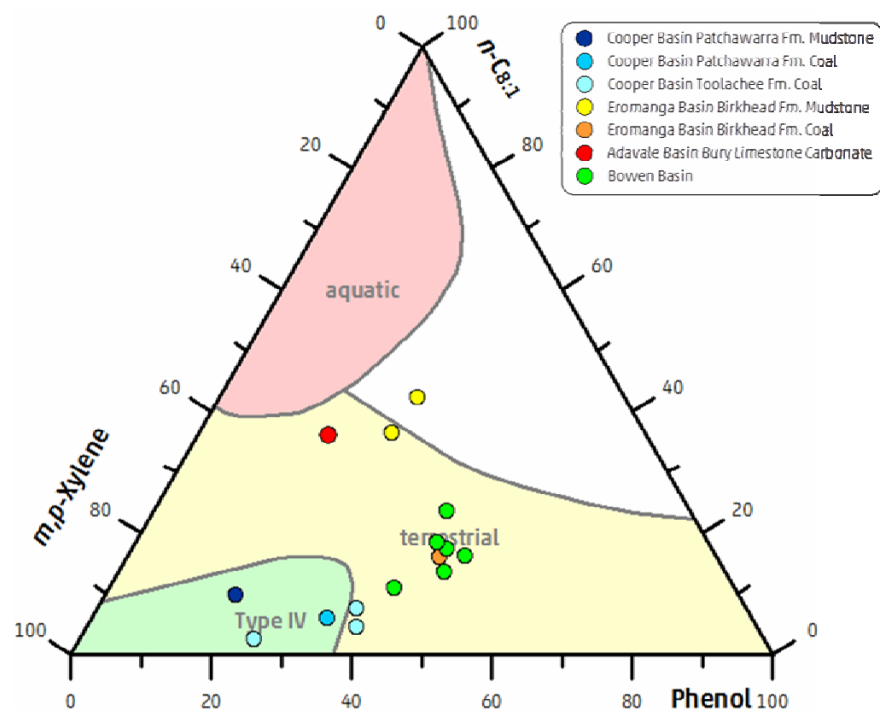


Figure 2-2: Phenol abundance (diagram after Larter, 1984).

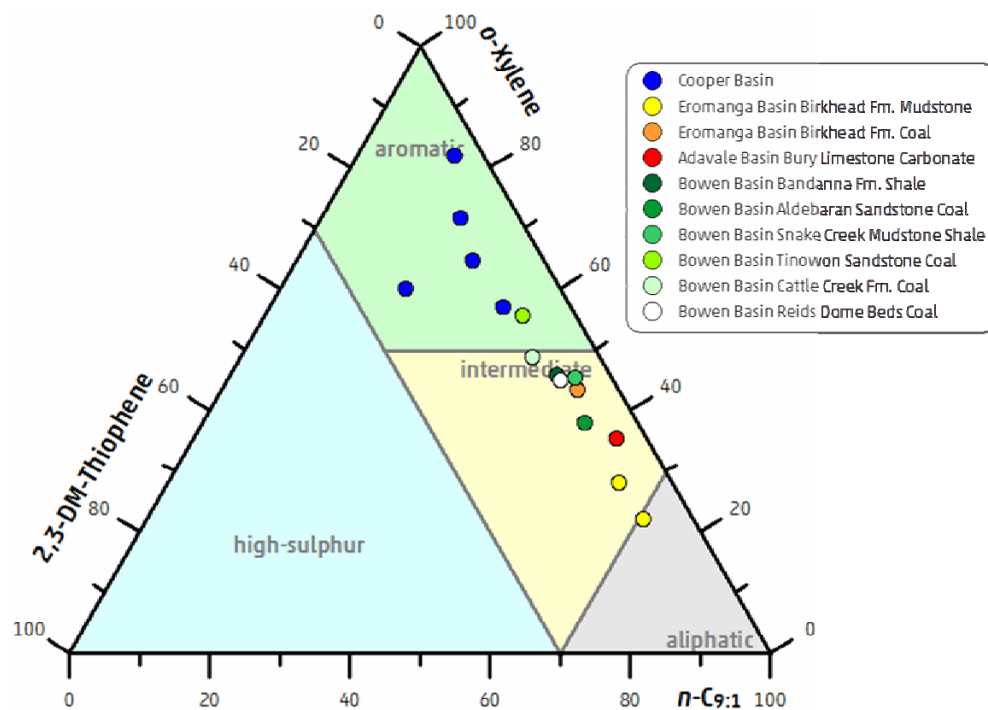


Figure 2-3: The kerogen type characterisation after Eglinton et al. (1990).

References

- Andresen, B., Thronsdæn, T., Barth, T., Bolstad, J., 1994. Thermal generation of carbon dioxide and organic acids from different source rocks. *Organic Geochemistry* 21, 1229-1242.
- Behar, F., Ungerer, P., Kressmann, S., Rudkiewicz, J.L., 1991. Thermal evolution of crude oils in sedimentary basins; experimental simulation in a confined system and kinetic modeling. *Revue de l'Institut Francais du Petrole* 46, 151-181.
- Berkaloff, C., Casadevall, E., Largeau, C., Peracca, M.S., Virlet, J., 1983. The resistant polymer of the walls of the hydrocarbon-rich alga *Botryococcus braunii*. *Phytochemistry* 22, 389-397.
- Berner, U., Faber, E., Scheeder, G., Panten, D., 1995. Primary cracking of algal and landplant kerogens; kinetic models of isotope variations in methane, ethane and propane, *Processes of natural gas formation*. Elsevier, Amsterdam, Netherlands, pp. 233-245.
- di Primio, R., Dieckmann, V., Mills, N., 1998. PVT and phase behaviour analysis in petroleum exploration. *Organic Geochemistry* 29, 207-222.
- di Primio, R., Horsfield, B., 2006. From petroleum-type organofacies to hydrocarbon phase prediction. *AAPG Bulletin* 90, 1031-1058.
- Dieckmann, V., Schenk, H.J., Horsfield, B., Welte, D.H., 1998. Kinetics of petroleum generation and cracking by programmed-temperature closed-system pyrolysis of Toarcian Shales. *Fuel* 77, 23-31.
- Eglinton, T.I., Sinninghe Damsté, J.S., Kohnen, M.E.L., de Leeuw, J.W., 1990. Rapid estimation of the organic sulphur content of kerogens, coals and asphaltenes by pyrolysis-gas chromatography. *Fuel* 69, 1394-1404.
- Erdmann, M., 1999. Gas generation from overmature Upper Jurassic source rocks, Northern Viking Graben. Report.
- Horsfield, B., 1989. Practical criteria for classifying kerogens: Some observations from pyrolysis-gas chromatography. *Geochimica et Cosmochimica Acta* 53, 891-901.
- Horsfield, B., Curry, D.J., Bohacs, K., Littke, R., Rullkötter, J., Schenk, H.J., Radke, M., Schaefer, R.G., Carroll, A.R., Isaksen, G., Witte, E.G., 1994. Organic geochemistry of freshwater and alkaline lacustrine sediments in the Green River Formation of the Washakie Basin, Wyoming, U.S.A. *Organic Geochemistry* 22, 415-440.
- Horsfield, B., Disko, U., Leistner, F., 1989. The micro-scale simulation of maturation: outline of a new technique and its potential applications. *Geologische Rundschau* 78, 361-374.
- Larter, S.R., 1984. Application of Analytical Pyrolysis Techniques to Kerogen Characterisation and Fossil Fuel Exploration/Exploitation, in: Voorhees, K. (Ed.), *Analytical pyrolysis, methods and applications*. Butterworth, London, pp. 212-275.
- Larter, S.R., Douglas, A.G., 1980. Melanoidins—kerogen precursors and geochemical lipid sinks: a study using pyrolysis gas chromatography (PGC). *Geochimica et Cosmochimica Acta* 44, 2087-2095.

Mahlstedt, N., 2012. Evaluating the late gas potential of source rocks stemming from different sedimentary environments. Dissertation. Technische Universität Berlin, Berlin, p. 342.

Mahlstedt, N., Horsfield, B., 2012a. Gas Generation at High Maturities ($> Ro = 2.0\%$) in Gas Shales. Search and Discovery Article #40873.

Mahlstedt, N., Horsfield, B., 2012b. Metagenetic methane generation in gas shales I. Screening protocols using immature samples. Marine and Petroleum Geology - Insights into Shale Gas Exploration and Exploitation 31, 27-42.

Mango, F.D., 1996. Transition metal catalysis in the generation of natural gas. Organic Geochemistry 24, 977-984.

Mango, F.D., 1997. The light hydrocarbons in petroleum: a critical review. Organic Geochemistry 26, 417-440.

Michels, R., Enjelvin-Raoult, N., Elie, M., Mansuy, L., Faure, P., Oudin, J.-L., 2002. Understanding of reservoir gas compositions in a natural case using stepwise semi-open artificial maturation. Marine and Petroleum Geology 19, 589-599.

Pedersen, K.S., Fredenslund, A., Thomassen, P., 1989. Properties of oils and natural gases. Gulf Publishing Company, Houston.

Pepper, A.S., Corvi, P.J., 1995a. Simple kinetic models of petroleum formation. Part I: oil and gas generation from kerogen. Marine and Petroleum Geology 12, 291-319.

Pepper, A.S., Corvi, P.J., 1995b. Simple kinetic models of petroleum formation. Part III: Modelling an open system. Marine and Petroleum Geology 12, 417-452.

Stach, E., Mackowsky, M.-T., Teichmüller, M., Taylor, G.H., Chandra, D., Teichmüller, R., 1982. Stach's Textbook of Coal Petrology, 3rd ed. Gebrüder Borntraeger, Stuttgart.

Appendix 2-1 – Tables

Tab. 2-A1a: Pyrolysis GC boiling ranges (μg/g sample). *GOR: C1 to C5/C6 to C30+

Sample	G016494	G016496	G016499	G016500	G016501	G016504	G016505	G016506
TOC (%)	2.07	78.40	80.20	79.70	26.20	4.49	75.30	12.00
Amount, mg	21.09	2.12	1.83	2.47	11.76	10.70	1.94	5.18
μg/g								
C1	646.9	27312.7	23390.0	22988.4	7115.8	1580.0	22116.6	3557.1
C2-C5 Total	1024.4	24719.7	19683.1	21694.8	4707.5	3978.1	28689.0	8678.0
C6-14 Total	1700.7	44789.3	37821.3	43818.3	7467.8	10117.4	63327.5	21432.1
C15_+ Total	1401.7	55509.8	62279.6	59792.1	8934.7	16604.9	133759.9	41483.0
C1-5 Total	1671.3	52032.3	43073.1	44683.2	11823.3	5558.2	50805.6	12235.1
C1-30+ Total	4773.7	152331.4	143174.0	148293.6	28225.7	32280.5	247893.0	75150.2
GOR Total	0.54	0.52	0.43	0.43	0.72	0.21	0.26	0.19
C6-C14 Resolved	1206.4	32751.0	27275.1	32668.8	4997.1	7277.2	45954.3	15201.9
C15+ Resolved	458.9	17531.7	17221.4	22753.4	4055.7	6563.2	44339.7	15776.0
C1-30 Resolved	3336.7	102315.0	87569.5	100105.5	20876.0	19398.5	141099.6	43213.0
GOR Resolved	1.00	1.03	0.97	0.81	1.31	0.40	0.56	0.39

Sample	G016508	G016511	G016522	G016524	G016531	G016535	G016539
TOC (%)	1.14	50.50	53.00	3.27	53.10	58.40	11.80
Amount, mg	23.26	2.68	2.21	20.56	2.46	3.13	10.95
μg/g							
C1	151.7	11172.3	12011.9	517.4	16100.4	14273.4	3796.3
C2-C5 Total	315.4	15339.7	18055.0	803.7	16620.6	16470.5	4718.7
C6-14 Total	510.6	39923.4	42837.2	1794.0	31792.9	35523.9	10082.3
C15_+ Total	95.5	63796.8	75980.6	2464.3	51355.0	46904.3	14666.9
C1-5 Total	467.1	26512.0	30066.9	1321.1	32721.1	30743.9	8515.0
C1-30+ Total	1073.2	130232.2	148884.7	5579.5	115869.0	113172.1	33264.2
GOR Total	0.77	0.26	0.25	0.31	0.39	0.37	0.34
C6-C14 Resolved	340.7	28543.6	31661.9	1206.2	23011.0	26546.6	7674.8
C15+ Resolved	95.5	17964.2	20435.9	520.7	13017.4	16306.3	4765.1
C1-30 Resolved	903.3	73019.8	82164.6	3048.1	68749.5	73596.8	20954.9
GOR Resolved	1.07	0.57	0.58	0.76	0.91	0.72	0.68

Tab. 2-A1b: Pyrolysis GC individual compounds amounts

Sample	G016494	G016496	G016499	G016500	G016501	G016504	G016505	G016506
TOC (%)	2.07	78.40	80.20	79.70	26.20	4.49	75.30	12.00
Amount, mg	21.09	2.12	1.83	2.47	11.76	10.70	1.94	5.18
<i>n</i> -Aliphatics μg/g								
C2:0	348.2	11898.7	9646.8	10592.6	2501.6	1191.5	11592.8	2904.3
C3:0	257.5	6390.7	5083.1	5833.2	1213.0	1087.8	8073.8	2388.1
C4:1	59.9	1071.1	1145.9	1399.7	214.9	476.0	2243.7	812.5
C4:0	75.1	1491.6	930.8	1100.2	217.3	237.9	1861.2	623.4
C5:1	15.3	380.3	311.7	476.6	49.5	200.1	848.5	438.8
C5:0	36.7	677.6	436.5	553.7	82.2	165.2	1081.0	464.8
C6:1	13.1	337.5	239.2	437.5	37.6	235.7	860.5	521.0
C6:0	28.2	495.3	298.0	423.0	50.1	154.0	910.5	406.2
C7:1	9.3	285.6	195.6	334.1	27.3	171.5	662.0	408.0
C7:0	22.6	514.8	350.8	486.8	50.6	155.8	913.6	421.3
C8:1	4.7	185.3	112.7	237.5	17.2	133.1	492.8	325.0
C8:0	18.5	332.4	198.9	333.2	26.2	133.3	662.7	339.5
C9:1	3.9	150.2	87.0	203.2	12.5	119.8	439.3	289.5
C9:0	13.4	254.7	158.1	291.8	19.0	108.6	579.4	292.3
C10:1	3.7	110.4	82.7	178.7	11.9	127.3	440.3	297.5
C10:0	12.8	234.3	152.9	310.9	15.6	105.4	587.2	282.9
C11:1	4.0	115.7	85.3	189.6	10.1	120.2	454.4	284.2
C11:0	14.5	201.4	134.1	301.2	13.1	105.7	565.4	282.2
C12:1	9.7	128.5	89.7	199.3	11.4	139.9	486.3	276.5
C12:0	14.3	317.3	219.5	424.1	14.6	119.0	864.6	329.1
C13:1	2.2	85.6	194.4	176.5	7.5	113.3	716.6	289.7
C13:0	12.8	221.5	190.8	375.5	12.5	117.6	791.0	314.9
C14:1	10.4	45.6	236.2	250.2	0.0	124.5	551.5	261.7
C14:0	11.9	43.6	171.4	347.2	10.4	116.3	665.3	295.0
C15:1	4.3	55.0	61.9	131.0	0.0	110.7	430.8	243.6
C15:0	11.7	210.4	165.8	406.9	18.4	121.1	663.1	296.0
C16:1	1.8	62.3	97.9	174.2	0.0	104.4	488.6	247.6
C16:0	8.9	134.6	94.0	297.6	4.0	118.8	663.2	299.1
C17:1	2.3	132.5	107.6	167.9	0.0	109.6	520.2	262.4
C17:0	13.4	233.6	134.6	392.4	0.0	143.5	790.0	339.2
C18:1	0.8	47.3	48.9	119.7	0.0	101.8	423.2	236.0
C18:0	8.0	132.4	76.9	324.0	0.0	139.9	792.9	354.5
C19:1	0.5	39.3	0.0	0.0	0.0	111.7	510.1	264.6
C19:0	7.4	106.0	0.0	410.2	0.0	160.6	917.9	395.8
C20:1	0.7	79.6	59.2	130.3	0.0	113.4	475.3	260.4
C20:0	6.1	82.2	77.3	345.9	0.0	175.4	965.7	435.2
C21:1	0.4	27.1	0.0	90.4	0.0	123.5	532.3	283.2
C21:0	6.6	127.0	35.1	297.5	0.0	195.1	1070.2	476.7
C22:1	0.0	11.4	0.0	97.7	0.0	123.8	512.4	279.7
C22:0	6.5	156.9	56.3	368.7	0.0	224.6	1216.9	562.1
C23:1	0.0	37.6	0.0	104.1	0.0	133.3	567.9	335.3
C23:0	4.8	100.8	69.0	279.8	0.0	216.6	1302.9	597.4
C24:1	0.0	0.0	0.0	77.6	0.0	110.2	544.7	288.3
C24:0	4.4	42.8	45.5	227.6	0.0	224.5	1345.5	668.1
C25:1	0.0	0.0	0.0	46.0	0.0	117.9	554.9	322.2
C25:0	3.4	54.8	47.3	170.7	0.0	198.9	1442.9	615.4
C26:1	0.0	0.0	0.0	24.5	0.0	76.0	406.6	199.5
C26:0	2.7	68.8	23.1	123.1	0.0	179.0	1226.2	547.8
C27:1	0.0	0.0	0.0	17.2	0.0	80.5	417.7	211.2
C27:0	1.9	42.0	47.1	112.7	0.0	143.1	1345.9	452.2
C28:1	0.0	0.0	0.0	10.7	0.0	39.9	230.9	105.6
C28:0	1.0	36.4	30.4	67.9	0.0	91.0	781.1	294.2
C29:1	0.0	0.0	0.0	5.2	0.0	25.2	171.2	66.4
C29:0	0.6	33.1	18.1	46.5	0.0	47.6	600.8	146.2
C30:1	0.0	0.0	0.0	0.0	0.0	12.9	86.5	33.4
C30:0	0.6	21.3	11.1	34.1	0.0	30.2	305.2	87.3
C31:1	0.0	0.0	0.0	0.0	0.0	18.2	162.0	44.2
C31:0	0.3	9.8	0.0	14.2	0.0	17.1	241.2	55.9
C32:1	0.0	0.0	0.0	0.0	0.0	4.1	16.7	7.7
C32:0	0.1	0.0	0.0	9.7	0.0	11.4	127.0	34.6
Sum nC6-14	210.0	4060.0	3197.2	5500.2	347.4	2401.0	11643.3	5916.5
Sum nC15+	99.4	2085.1	1307.2	5126.0	22.4	3955.5	22850.7	10348.9

Tab. 2-A1b (contd.): Pyrolysis GC individual compounds amounts

Sample	G016508	G016511	G016522	G016524	G016531	G016535	G016539
TOC (%)	1.14	50.50	53.00	3.27	53.10	58.40	11.80
Amount, mg	23.26	2.68	2.21	20.56	2.46	3.13	10.95
<i>n</i> -Aliphatics							
				μg/g			
C2:0	105.3	6191.9	7128.0	312.0	7531.5	7297.5	1930.5
C3:0	80.2	4018.5	4878.2	207.2	4486.3	4492.9	1266.0
C4:1	30.3	1182.4	1351.1	72.2	1028.0	1152.9	307.8
C4:0	18.3	1032.4	1334.5	44.8	987.0	970.9	351.6
C5:1	13.1	544.8	721.2	28.0	383.3	467.6	141.2
C5:0	6.1	642.6	852.0	22.0	554.8	588.0	229.4
C6:1	11.9	610.8	768.5	28.6	347.1	496.4	141.2
C6:0	4.5	579.0	741.6	18.0	426.9	494.8	196.4
C7:1	9.0	484.7	612.4	22.3	278.7	381.7	113.5
C7:0	4.5	563.5	750.3	18.7	450.4	494.3	191.9
C8:1	7.0	366.0	473.3	16.4	201.4	280.1	86.8
C8:0	3.8	464.0	583.2	14.1	306.0	375.3	153.8
C9:1	5.8	292.6	394.8	13.0	157.5	240.1	73.0
C9:0	3.0	368.8	482.4	11.2	246.1	314.2	130.2
C10:1	7.0	296.2	379.5	13.2	142.0	230.1	69.5
C10:0	2.9	331.9	456.4	10.2	221.1	310.1	125.3
C11:1	4.9	294.9	372.4	11.8	136.5	250.0	72.0
C11:0	2.5	315.5	446.1	9.2	202.1	289.6	120.6
C12:1	8.6	277.9	368.3	13.0	147.6	227.8	74.1
C12:0	2.8	395.8	605.1	14.2	273.7	378.9	163.5
C13:1	3.7	277.9	408.9	11.0	226.4	259.9	83.5
C13:0	2.3	373.9	532.9	11.2	267.5	377.3	138.5
C14:1	7.1	249.3	353.1	12.4	150.8	228.5	75.4
C14:0	2.3	308.9	458.7	8.9	237.5	337.4	130.6
C15:1	3.2	206.0	261.1	8.2	96.7	175.8	57.1
C15:0	2.4	322.4	442.4	8.4	214.5	354.7	130.3
C16:1	2.2	206.8	324.6	8.7	162.9	222.1	67.9
C16:0	1.2	291.5	408.6	6.1	169.9	312.3	122.4
C17:1	1.6	190.2	293.1	7.7	120.0	211.7	64.7
C17:0	1.1	293.3	440.3	6.9	196.3	363.7	135.5
C18:1	0.9	176.0	263.6	4.2	93.9	185.5	57.8
C18:0	0.9	298.7	434.4	6.2	178.9	389.2	148.8
C19:1	0.7	205.4	296.2	5.4	149.2	223.5	73.7
C19:0	0.8	334.5	504.0	6.8	218.4	455.7	169.6
C20:1	0.7	157.7	220.4	3.4	56.6	165.7	52.8
C20:0	0.6	272.7	478.5	5.0	175.1	458.3	169.6
C21:1	0.4	152.4	251.7	3.2	71.0	212.7	64.5
C21:0	0.6	280.4	489.5	4.1	153.8	482.3	176.8
C22:1	0.4	150.7	250.1	2.6	68.6	195.5	54.9
C22:0	1.2	282.0	531.5	4.2	153.6	512.1	170.0
C23:1	0.2	147.9	271.3	2.4	67.6	201.9	47.8
C23:0	0.6	283.7	537.6	3.2	141.4	567.3	185.9
C24:1	0.2	127.0	201.8	2.3	64.8	123.3	28.8
C24:0	0.5	255.0	452.7	3.0	122.8	385.0	102.2
C25:1	0.2	102.2	145.6	1.6	45.6	84.7	23.0
C25:0	0.5	229.9	342.6	2.7	99.4	354.2	102.8
C26:1	0.1	78.6	104.2	1.3	53.4	42.1	11.4
C26:0	0.5	142.4	212.2	2.3	79.9	137.4	41.1
C27:1	0.0	49.8	67.9	1.1	23.3	24.8	6.1
C27:0	0.5	139.2	185.5	2.3	70.2	142.6	36.6
C28:1	0.0	45.5	51.0	0.9	16.2	17.2	5.2
C28:0	0.3	112.0	120.0	1.9	43.7	59.0	16.0
C29:1	0.0	60.9	37.9	0.8	16.9	17.3	4.0
C29:0	0.2	80.1	81.3	1.3	34.3	49.2	11.9
C30:1	0.0	18.8	14.1	0.2	8.6	6.3	2.1
C30:0	0.2	259.0	74.9	1.4	24.2	36.0	7.7
C31:1	0.0	258.9	38.9	0.5	0.0	3.9	2.0
C31:0	0.1	346.8	173.0	0.3	16.5	65.6	16.2
C32:1	0.0	57.3	32.2	0.0	0.0	0.0	1.5
C32:0	0.0	155.2	98.4	0.0	0.0	0.0	7.2
Sum nC6-14	93.7	6851.6	9188.1	257.5	4419.1	5966.7	2139.6
Sum nC15+	23.2	6770.8	9133.3	120.5	3208.2	7238.5	2375.9

Tab. 2-A1c: Pyrolysis GC individual compounds amounts

Sample	G016494	G016496	G016499	G016500	G016501	G016504	G016505	G016506
TOC (%)	2.07	78.40	80.20	79.70	26.20	4.49	75.30	12.00
Amount, mg	21.09	2.12	1.83	2.47	11.76	10.70	1.94	5.18
Aliphatics - Isoprenoids μg/g								
iC18	0.8	33.0	12.5	27.9	0.0	4.1	49.0	9.5
Prist-1-ene	0.0	0.0	0.0	0.0	0.0	9.0	115.6	27.6
Prist-2-ene	0.0	0.0	0.0	0.0	0.0	14.1	118.5	31.1
Aromatics μg/g								
Benz	28.3	424.3	408.9	522.3	263.9	35.2	379.0	76.8
Toluene	45.7	1653.0	1350.8	1656.9	651.6	122.7	1238.5	242.2
et-Benz	9.3	298.7	222.9	278.4	67.7	38.3	297.0	74.1
m+p Xyl	34.8	1880.4	1382.1	1731.3	483.1	131.4	1212.4	226.3
Styr	4.5	39.9	56.1	65.5	10.3	21.4	97.1	33.4
o-Xyl	13.1	386.7	312.7	346.6	73.3	52.2	374.6	90.6
Phenol	9.0	1038.1	926.2	1142.9	163.6	99.4	1359.9	215.4
o-Cresol	1.2	808.5	779.4	683.8	60.5	60.4	1049.2	147.2
m+p Cresol	3.3	1245.9	1199.6	1297.0	105.6	85.5	1760.7	225.5
Napht	14.2	494.7	528.9	568.4	133.6	35.2	375.8	75.3
2meNapht	16.4	727.5	716.9	972.5	228.1	43.1	330.9	79.7
1meNapht	8.9	450.0	416.4	573.0	76.1	43.8	368.5	80.8
Sum dimeNapht	26.8	1529.8	1208.0	1547.5	280.5	119.9	1159.9	208.6
Tetra-meNapht	1.2	88.0	97.9	144.2	51.0	5.9	61.6	13.4
Sum monoaromatic HC	135.6	4683.1	3733.6	4601.1	1550.0	401.3	3598.6	743.3
Sum diaromatic HC	67.5	3290.0	2968.1	3805.5	769.3	247.9	2296.7	457.9
Sum phenols	13.5	3092.4	2905.2	3123.7	329.7	245.3	4169.8	588.1
Sulphur Compounds μg/g								
Thioph	5.0	388.5	316.7	304.8	29.0	87.2	587.5	197.5
2meThioph	0.0	0.0	0.0	0.0	0.0	0.0	0.0	19.3
3meThioph	2.7	100.0	76.6	103.6	15.1	34.7	164.3	79.8
2,5dimeThioph	0.0	0.0	0.0	0.0	0.0	0.0	0.0	0.0
2,3dimeThioph	4.8	61.1	37.1	59.4	3.8	14.2	51.3	29.3
Sum alkylthiophenes	7.5	161.1	113.6	163.0	18.9	48.9	215.6	128.4

Tab. 2-A1c (contd.): Pyrolysis GC individual compounds amounts

Sample	G016508	G016511	G016522	G016524	G016531	G016535	G016539
TOC (%)	1.14	50.50	53.00	3.27	53.10	58.40	11.80
Amount, mg	23.26	2.68	2.21	20.56	2.46	3.13	10.95
Aliphatics - Isoprenoids							
				µg/g			
iC18	0.1	36.7	27.6	0.4	12.5	20.8	4.5
Prist-1-ene	0.0	111.5	66.7	1.3	29.4	0.0	0.0
Prist-2-ene	0.0	48.8	47.6	2.6	59.8	48.8	16.8
Aromatics							
				µg/g			
Benz	20.6	366.0	324.9	21.9	292.6	485.6	84.3
Tol	21.8	1002.2	981.8	52.8	1040.4	1101.6	261.1
et-Benz	3.3	252.6	241.2	9.1	187.5	260.6	60.1
m+p Xyl	8.8	788.0	690.6	34.3	879.4	819.3	192.8
Styr	4.6	83.8	73.8	6.8	49.2	67.2	13.2
o-Xyl	3.4	287.5	274.5	11.9	237.7	280.8	68.9
Phenol	3.6	937.1	832.5	38.1	734.6	950.7	258.5
o-Cresol	1.0	532.4	648.7	22.7	645.8	579.7	191.1
m+p Cresol	1.1	895.8	994.6	38.4	919.2	1094.6	319.1
Napht	4.8	202.5	253.5	11.8	293.0	326.9	86.6
2meNapht	3.6	190.9	260.5	13.1	345.3	368.9	73.3
1meNapht	2.5	197.8	224.9	9.4	226.3	243.6	57.4
Sum dimeNapht	4.7	438.4	527.9	20.7	688.2	623.6	150.8
Tetra-meNapht	2.1	72.8	71.7	3.9	62.2	50.0	13.1
Sum monoaromatic HC	62.5	2780.0	2586.8	136.8	2686.7	3015.1	680.4
Sum diaromatic HC	17.8	1102.5	1338.5	59.0	1614.9	1613.0	381.3
Sum phenols	5.7	2365.3	2475.9	99.2	2299.6	2625.0	768.7
Sulphur Compounds							
				µg/g			
Thioph	1.1	216.4	348.8	10.5	282.1	256.3	64.1
2meThioph	0.0	71.1	51.2	0.0	16.9	56.5	7.2
3meThioph	1.3	97.8	125.1	5.4	63.2	69.6	19.0
2,5dimeThioph	0.0	0.0	0.0	0.0	0.0	0.0	0.0
2,3dimeThioph	0.4	47.3	53.9	1.4	32.1	55.4	11.7
Sum alkylthiophenes	1.7	216.2	230.2	6.8	112.3	181.5	37.9

Appendix 2-2 - Chromatograms

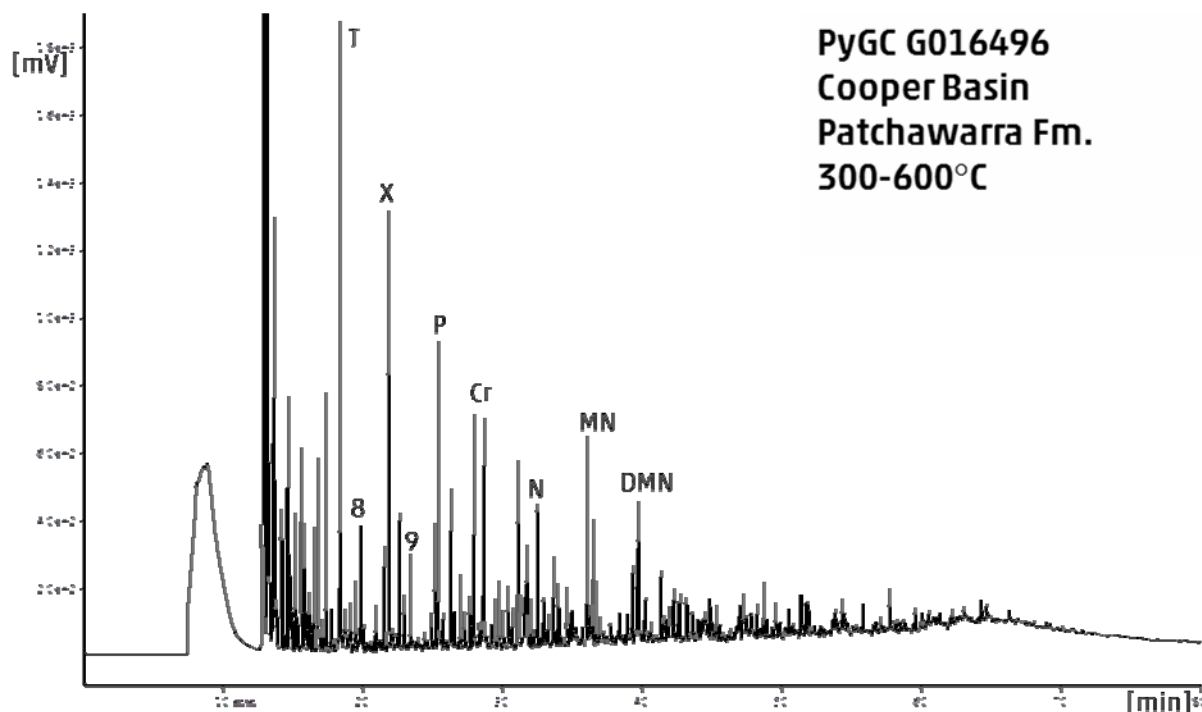
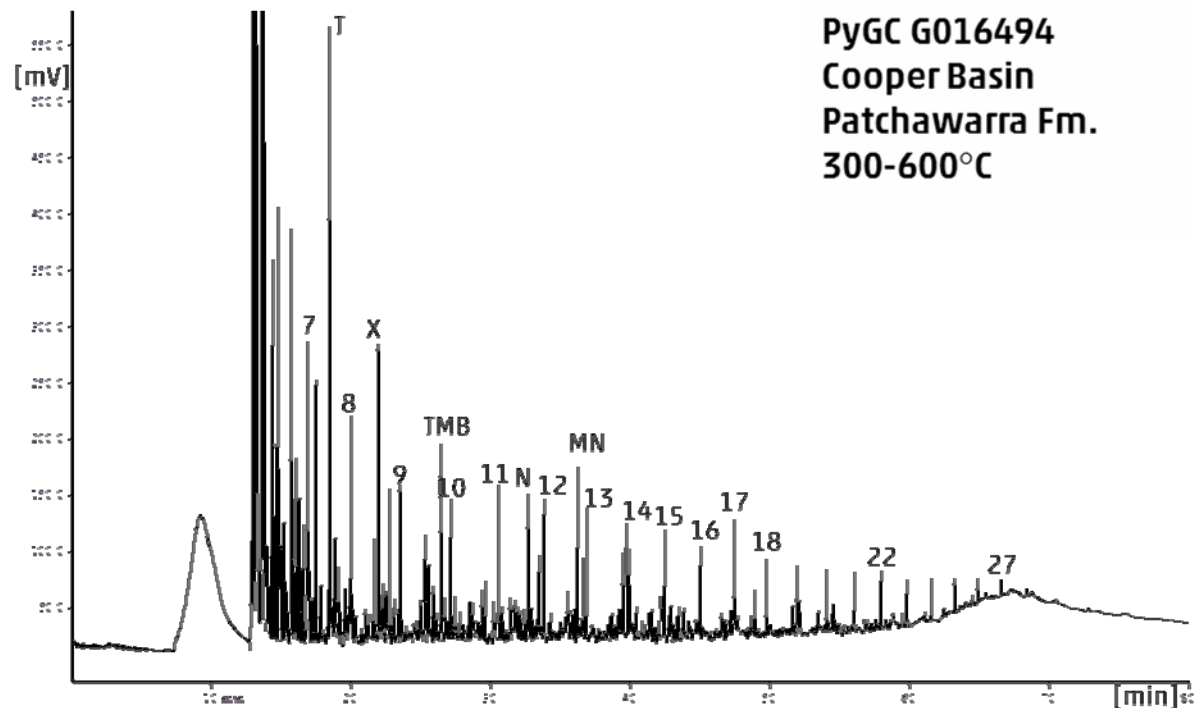


Figure 2-A1: Pyrolysis gas chromatograms. For reference, selected peaks are marked: numbers= *n*-alkane/alkene doublets, T = toluene, X = *meta/para*-xylene, P = phenol, Cr = cresol, TMB = trimethylbenzene, N = naphthalene, MN = methylnaphthalene, DMN = dimethylnaphthalene.

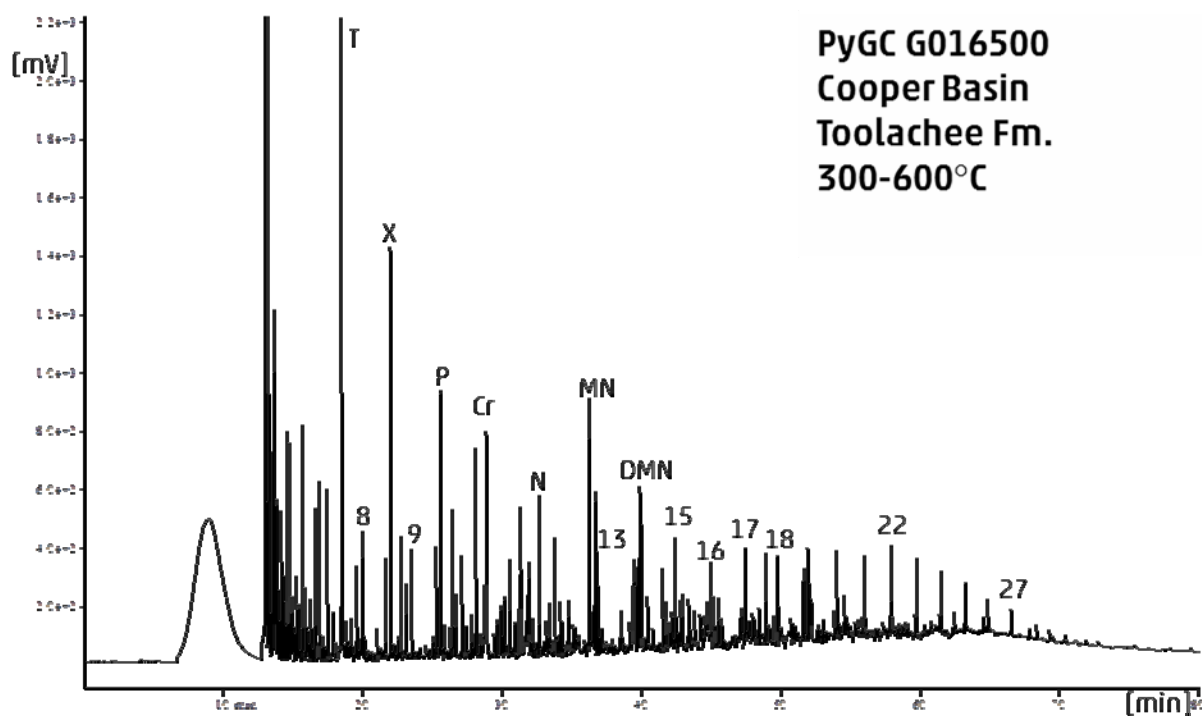
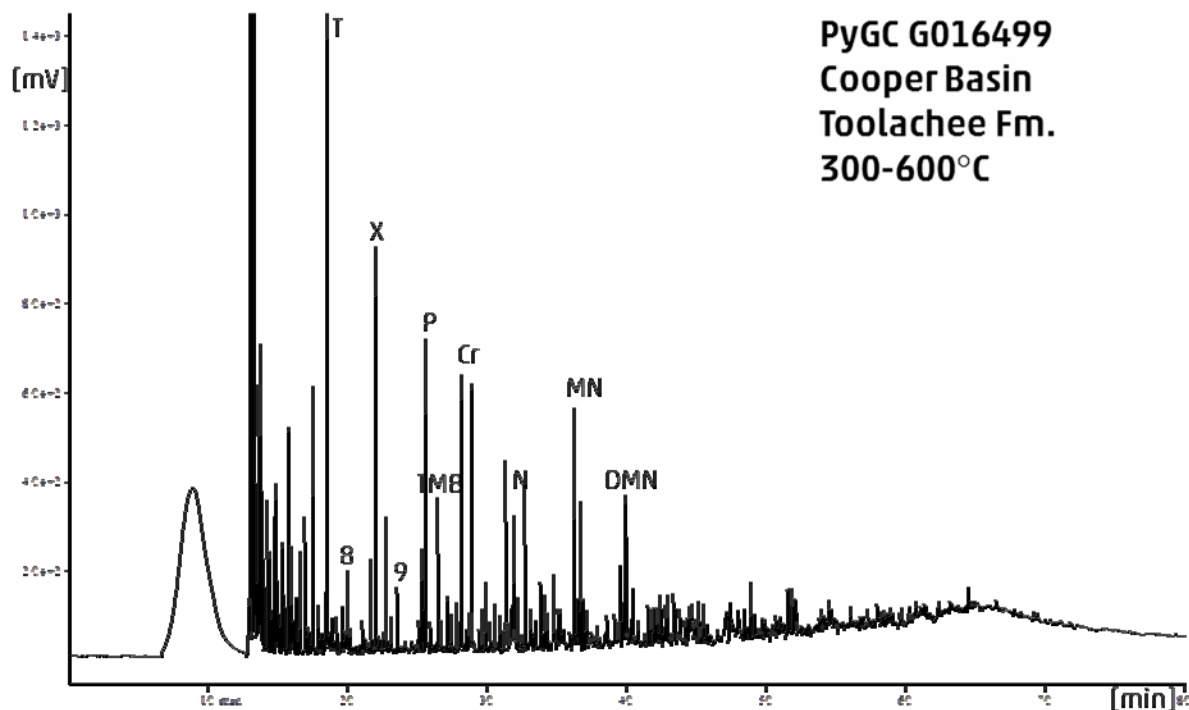


Figure 2-A1 (contd.): Pyrolysis gas chromatograms. For reference, selected peaks are marked: numbers= *n*-alkane/alkene doublets, T = toluene, X = meta/para-xylene, P = phenol, Cr = cresol, TMB = trimethylbenzene, N = naphthalene, MN = methylnaphthalene, DMN = dimethylnaphthalene.

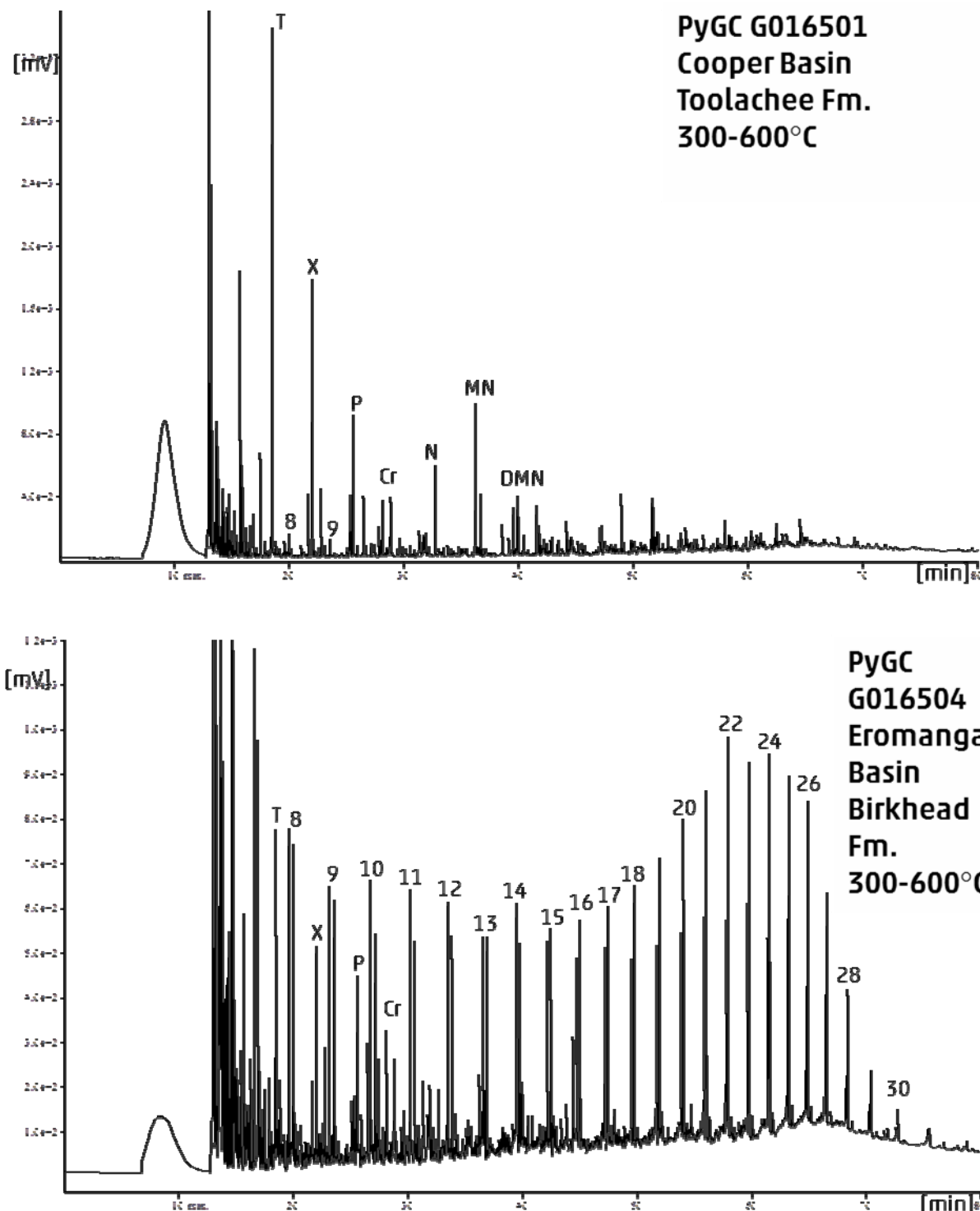


Figure 2-A1 (contd.): Pyrolysis gas chromatograms. For reference, selected peaks are marked: numbers = *n*-alkane/alkene doublets, T = toluene, X = meta/para-xylene, P = phenol, Cr = cresol, TMB = trimethylbenzene, N = naphthalene, MN = methylnaphthalene, DMN = dimethylnaphthalene.

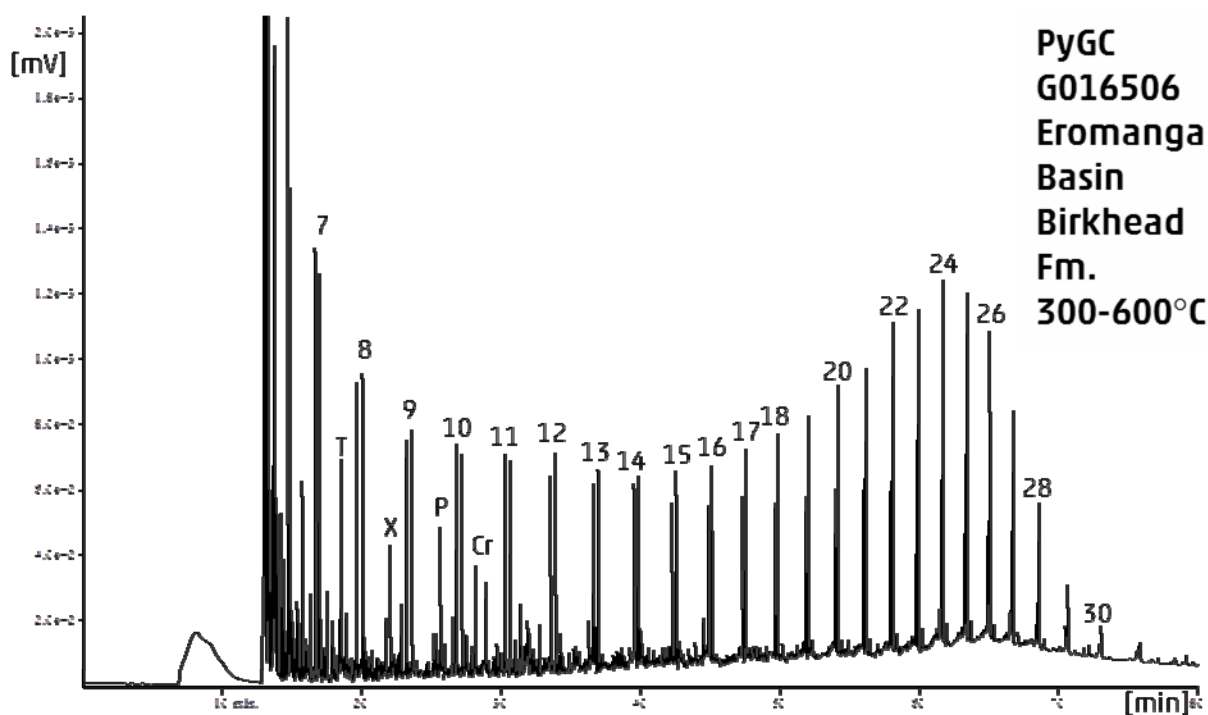
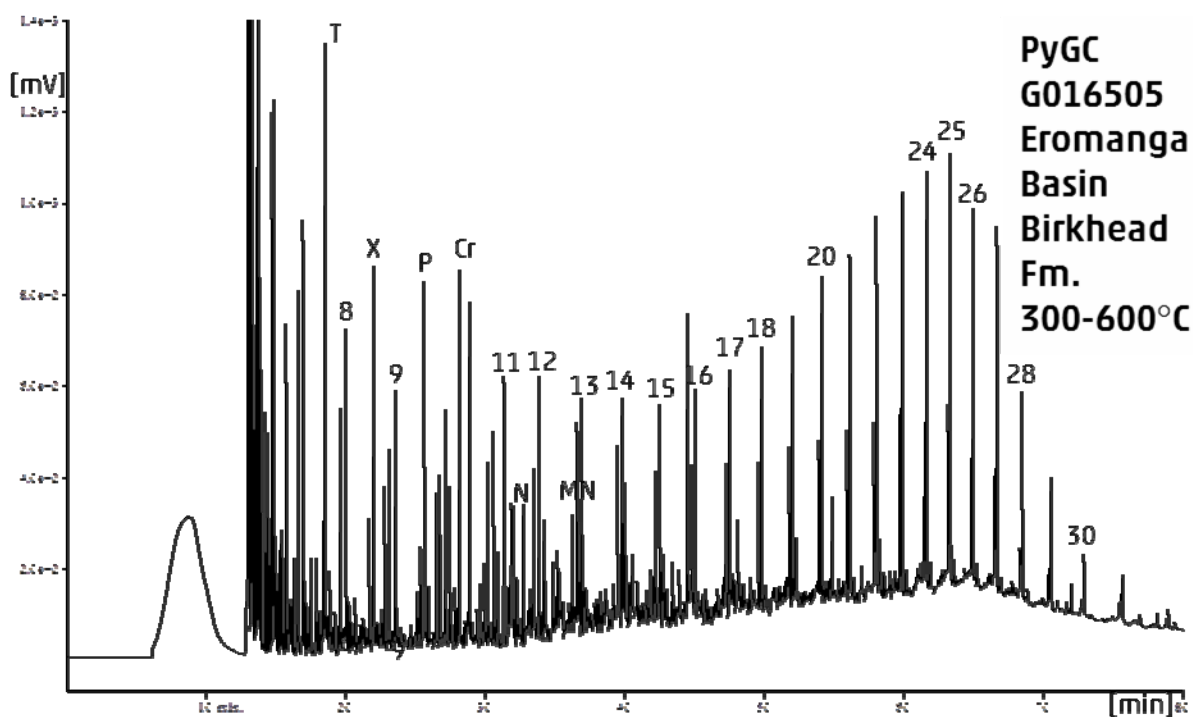


Figure 2-A1 (contd.): Pyrolysis gas chromatograms. For reference, selected peaks are marked: numbers= *n*-alkane/alkene doublets, T = toluene, X = meta/para-xylene, P = phenol, Cr = cresol, TMB = trimethylbenzene, N = naphthalene, MN = methylnaphthalene, DMN = dimethylnaphthalene.

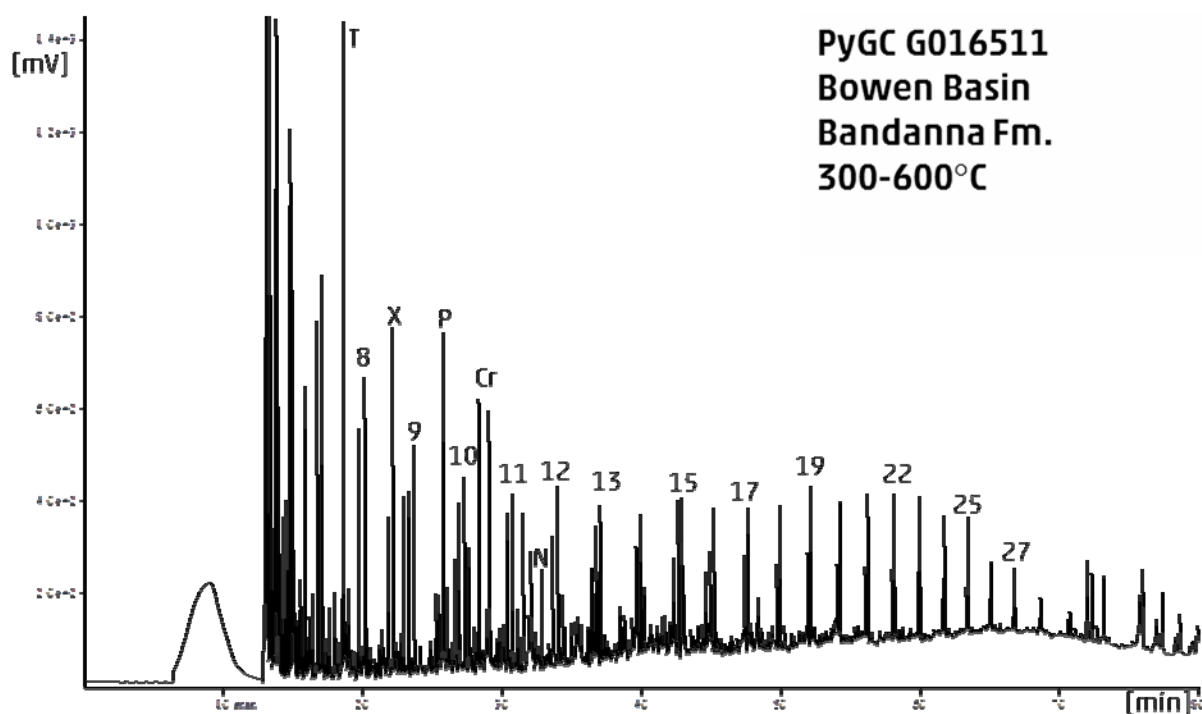
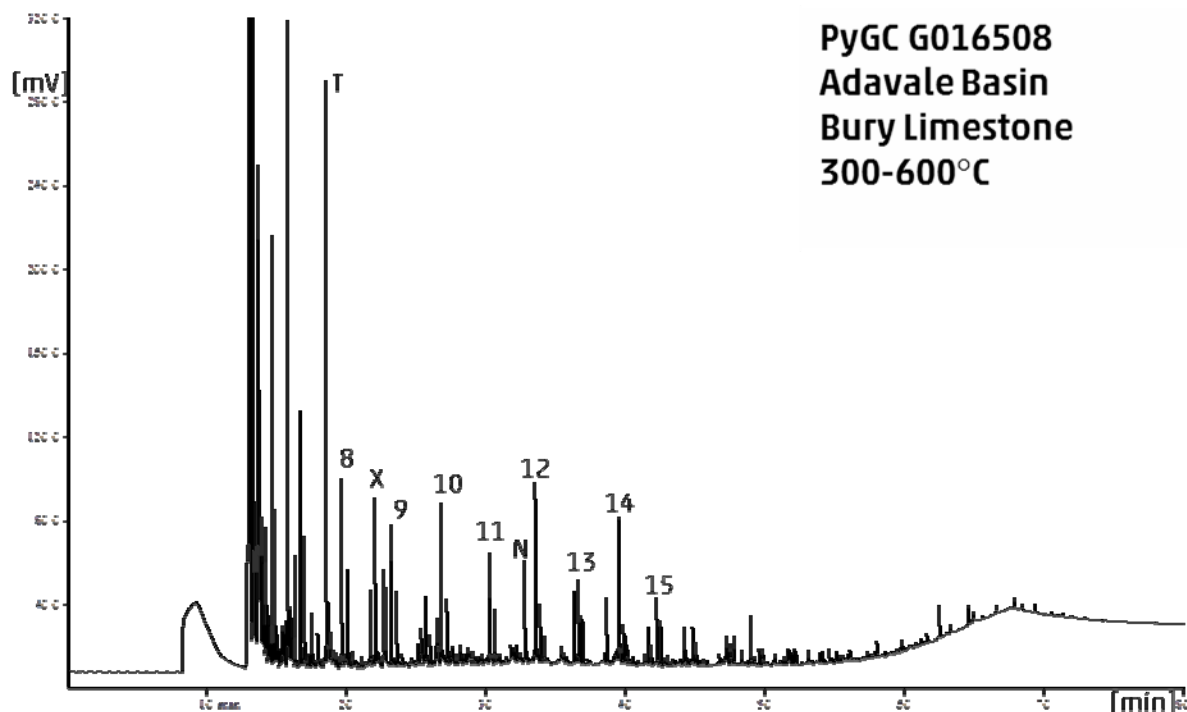


Figure 2-A1 (contd.): Pyrolysis gas chromatograms. For reference, selected peaks are marked: numbers = *n*-alkane/alkene doublets, T = toluene, X = meta/para-xylene, P = phenol, Cr = cresol, TMB = trimethylbenzene, N = naphthalene, MN = methylnaphthalene, DMN = dimethylnaphthalene.

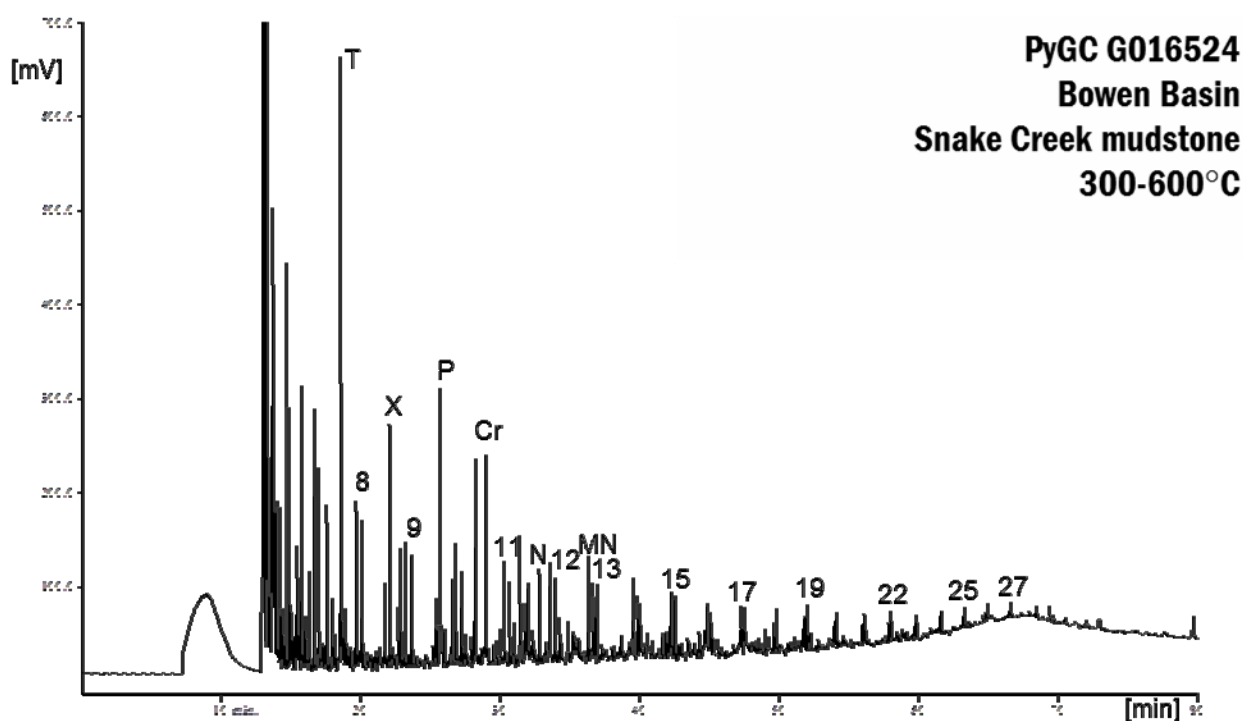
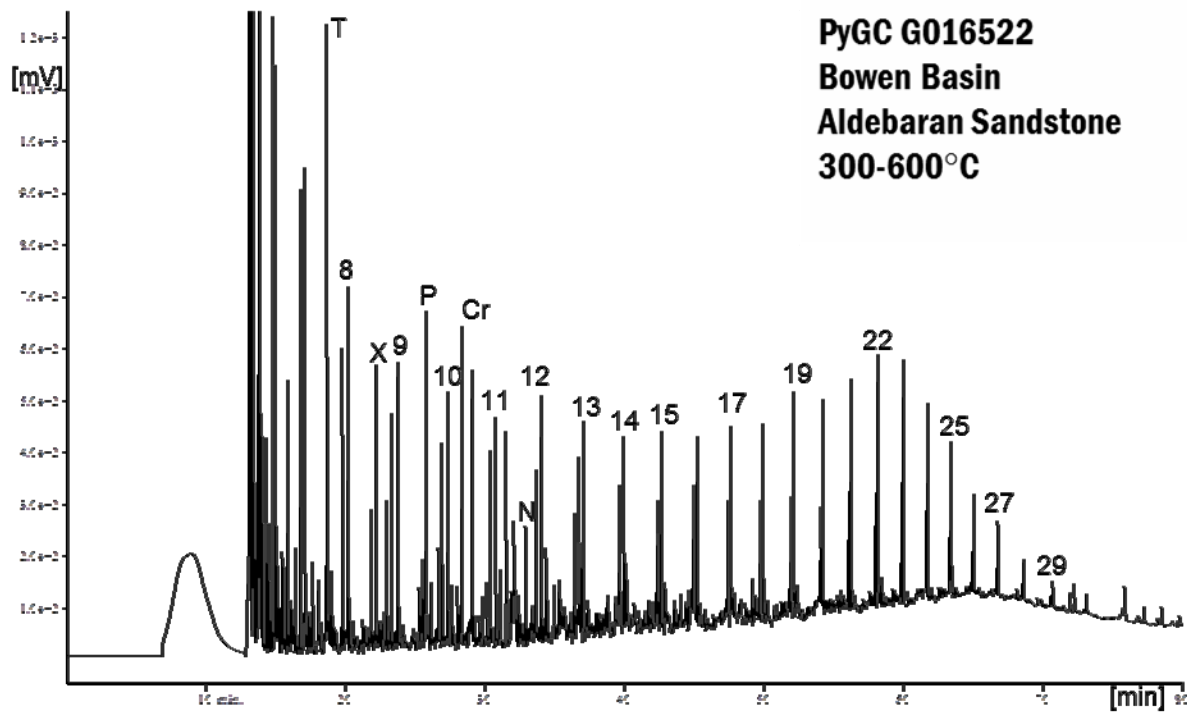


Figure 2-A1 (contd.): Pyrolysis gas chromatograms. For reference, selected peaks are marked: numbers = *n*-alkane/alkene doublets, T = toluene, X = meta/para-xylene, P = phenol, Cr = cresol, TMB = trimethylbenzene, N = naphthalene, MN = methylnaphthalene, DMN = dimethylnaphthalene.

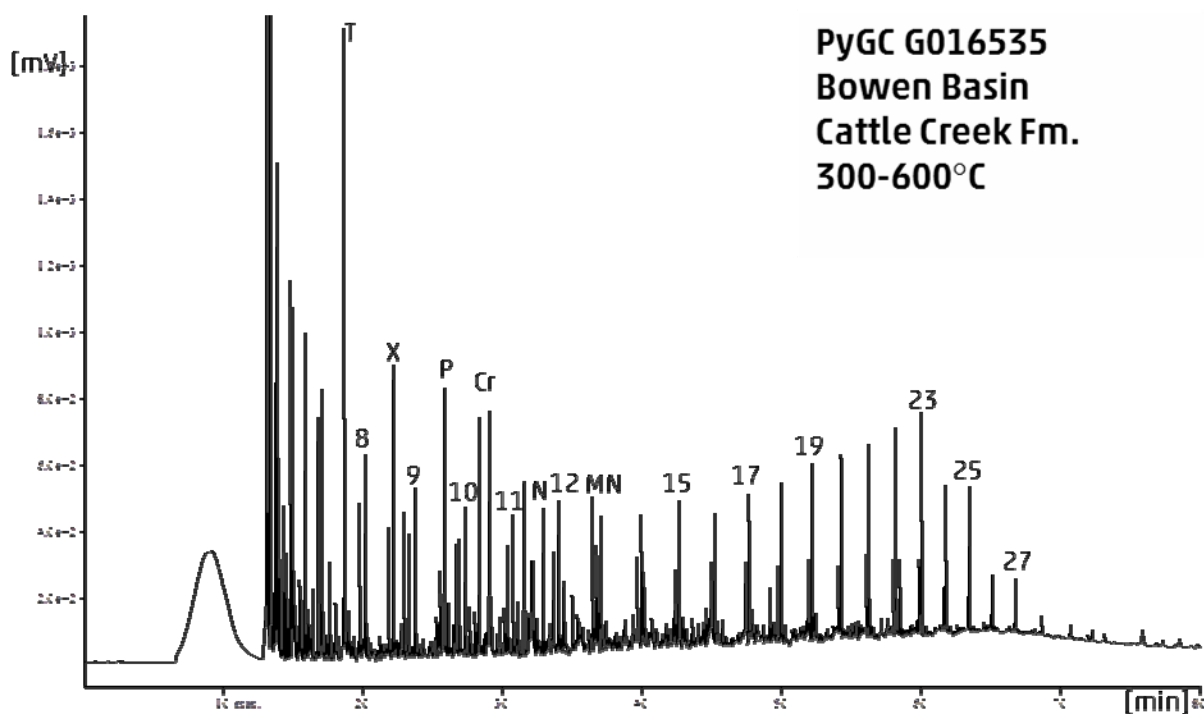
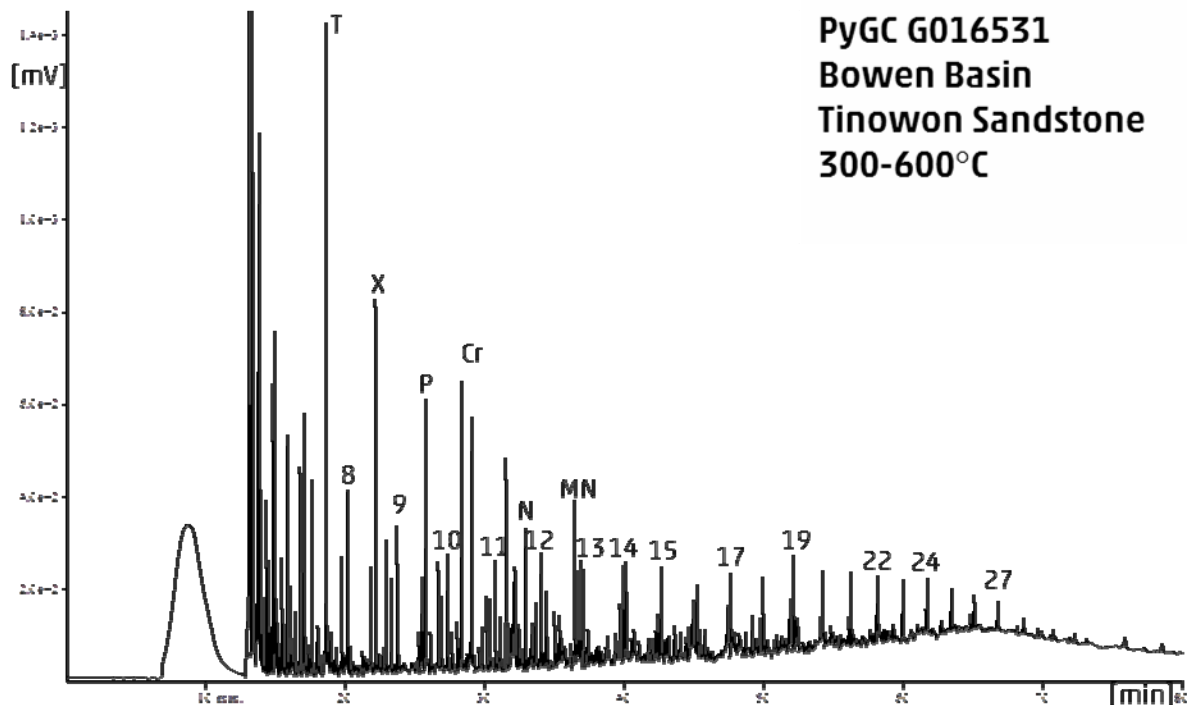


Figure 2-A1 (contd.): Pyrolysis gas chromatograms. For reference, selected peaks are marked: numbers = *n*-alkane/alkene doublets, T = toluene, X = meta/para-xylene, P = phenol, Cr = cresol, TMB = trimethylbenzene, N = naphthalene, MN = methylnaphthalene, DMN = dimethylnaphthalene.

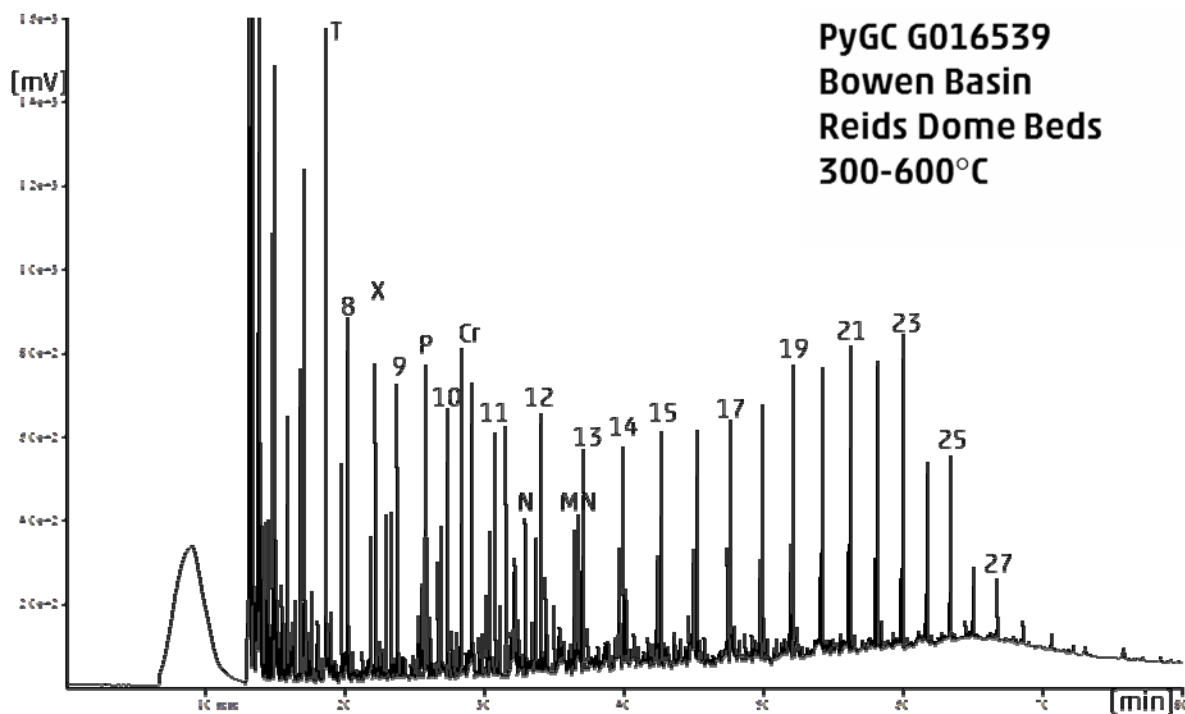


Figure 2-A1 (contd.): Pyrolysis gas chromatograms. For reference, selected peaks are marked: numbers = *n*-alkane/alkene doublets, T = toluene, X = *meta/para*-xylene, P = phenol, Cr = cresol, TMB = trimethylbenzene, N = naphthalene, MN = methylnaphthalene, DMN = dimethylnaphthalene.

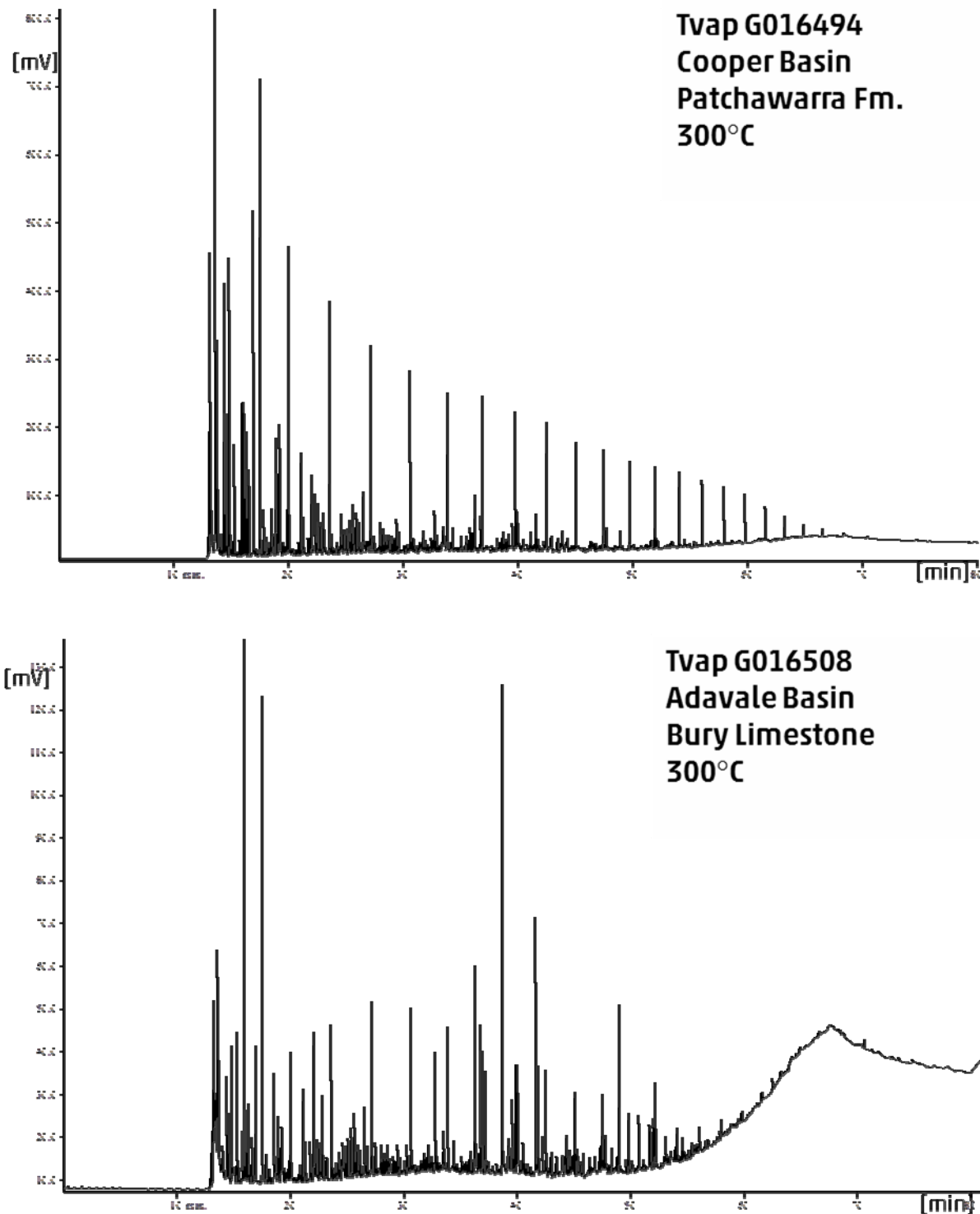


Figure 2-A2: Thermovaporisation gas chromatograms.

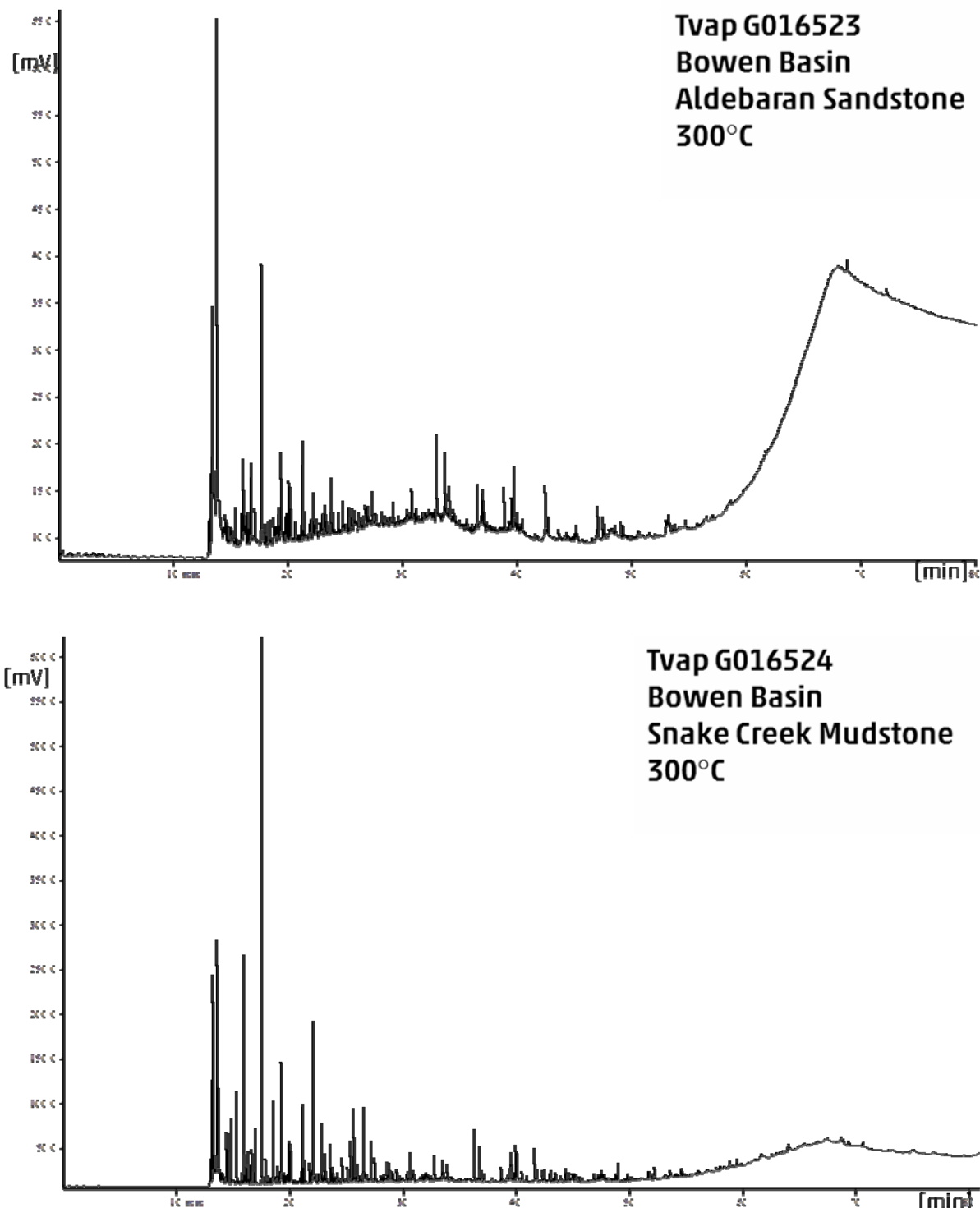


Figure 2-A2 (contd.): Thermovaporation gas chromatograms.

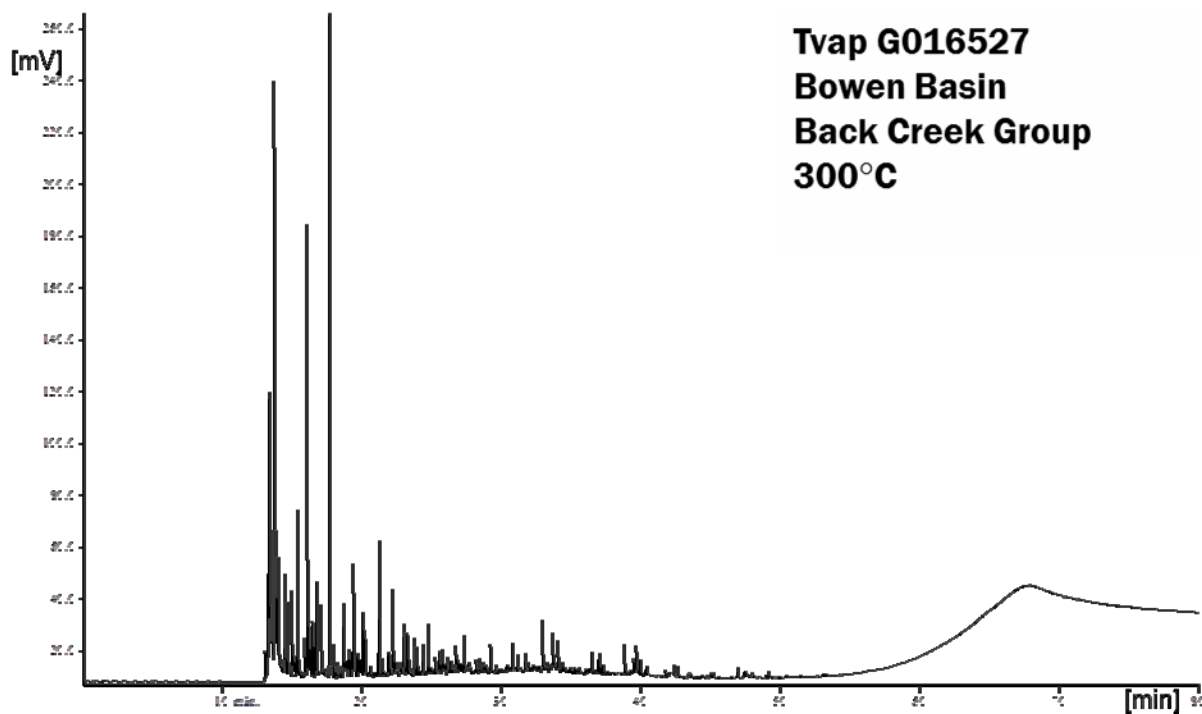
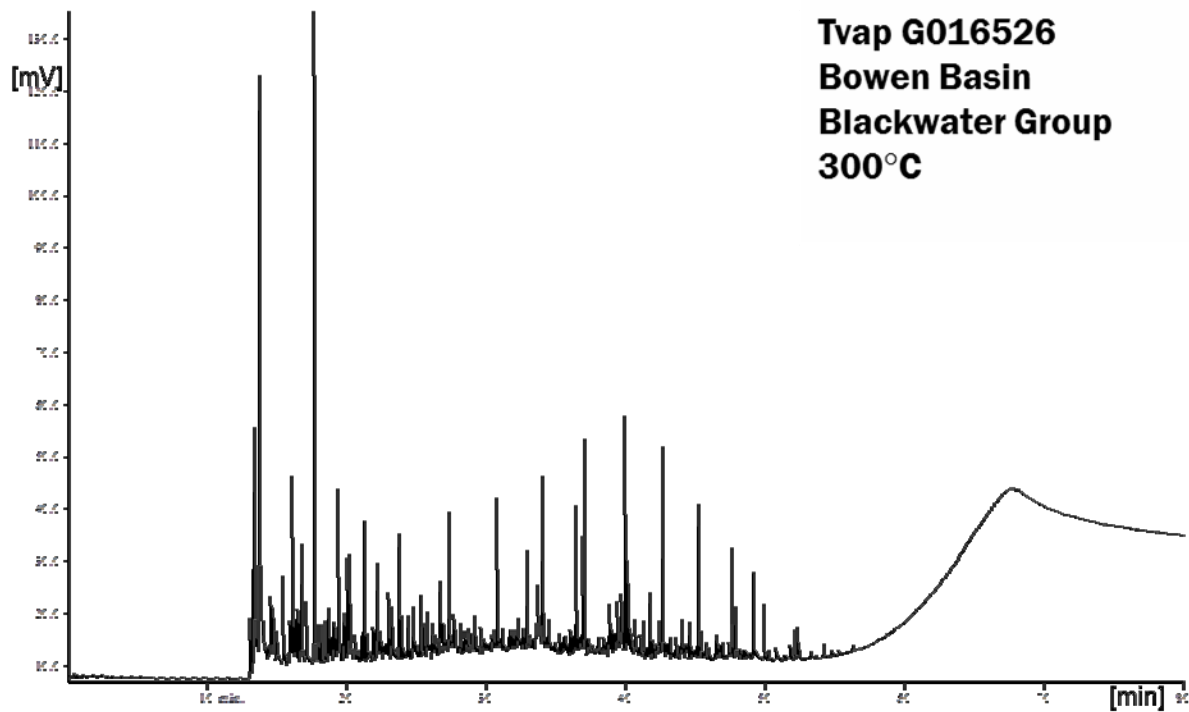


Figure 2-A2 (contd.): Thermovaporisation gas chromatograms.

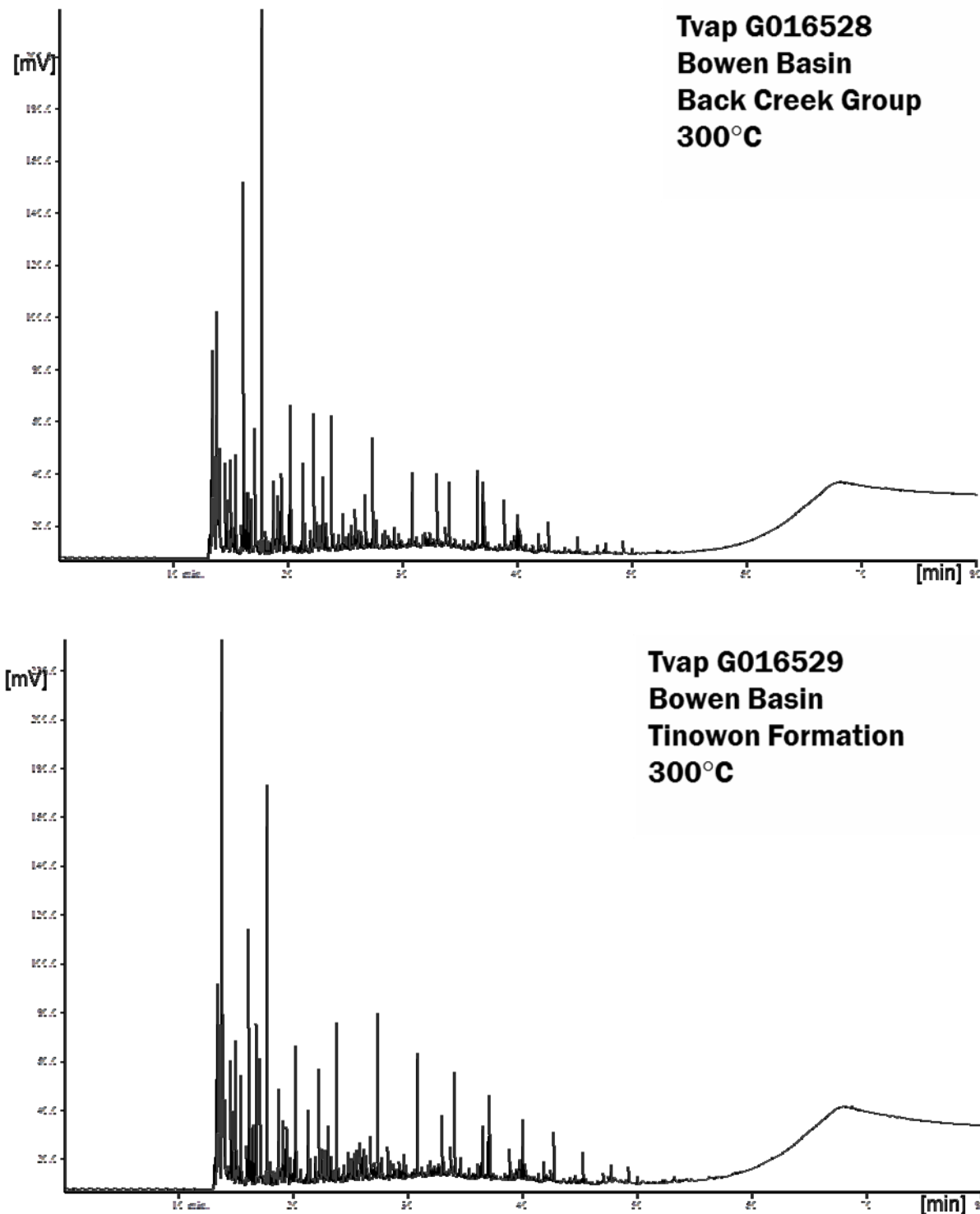


Figure 2-A2 (contd.); Thermovapourisation gas chromatograms.

3 Organic petrology

Organic petrology was conducted in close collaboration with Doris Gross (Montan University of Leoben, Austria).

Basin	Code	QLD i.d.	Rock Type	Rock Unit Name	Petrology
COOPER BASIN	G016496	GSV03	Coal	Patchawarra Formation	1
COOPER BASIN	G016500	GSV07	Coal	Toolachee Formation	1
EROMANGA BASIN	G016504	GSV11	Carb'ceous mst	Birkhead Formation	1
EROMANGA BASIN	G016505	GSV12	Coal	Birkhead Formation	1
BOWEN BASIN	G016511	GSV18	shale	Bandanna Formation	1
BOWEN BASIN	G016513	GSV20	shale	Black Alley Shale	1
BOWEN BASIN	G016522	GSV29	Coal	Aldebaran Sandstone	1
BOWEN BASIN	G016524	GSV34	shale	Snake Creek Mudstone Mbr	1
BOWEN BASIN	G016531	GSV40	Coal	Tinowon Sandstone	1
BOWEN BASIN	G016535	GSV45	Coal	Riverstone Sst Mr?-Cattle Creek Formation	1
BOWEN BASIN	G016539	GSV49	Coal	Reids Dome beds	1

RUNNING TOTALS

11

The maceral abundance and vitrinite reflectance data are found in Tables 3-1 and 3-2. The term average value as used in the report refers to arithmetic mean (sum of %R_r values divided by number of measurements. Photomicrographs are presented to illustrate maceral distributions and rock fabric. The white light and fluorescing light pictures usually show the same view, but in rare cases it could happen that they have a drift of a few micrometres.

G016496:

Organic matter (Figure G016496): The coal sample is dominated by vitrinite (mainly collodetrinite; 63 vol.%), followed by semi-inertinite (23 vol.%), which is part of the inertinite maceral group, and inertinite (mostly pyrofusinite; 6 vol.%). Liptinite (mainly sporinite) is less abundant. Mineral matter shows a weak fluorescence colour under blue light irradiation. Sporinite shows a very weak orange fluorescence colour under blue light irradiation. Cutinites mainly do not show fluorescence anymore.

Vitrinite reflectance: Vitrinite reflectance was measured on large, homogeneous and strongly gelified particles (collotelinite) and an average value of 0.88 %R_r was obtained. However, only weak to absent fluorescence of cutinite macerals might even point to a slightly higher maturity in the range of 0.90 - 0.95 %R_r.

G016500:

Organic matter (Figure G016500): This coal sample is dominated by vitrinite (83 vol.%). Vitrinite macerals consist mainly of collodetrinite and collotelinite in lower amounts. Semi-inertinite and inertinite occur in low amounts (14 vol.% in sum). Sporinite is the main liptinite maceral within this sample, while cutinite is very rare. Mineral matter is also very rare (very low ash content of the coal). A low amount of pyrite is visible in the polished block.

Vitrinite reflectance: An average vitrinite reflectance of 0.72 %Rr was obtained for this sample. The measured reflectance is in good agreement with the observed strong orange fluorescence of sporinite.

G016504:

Organic matter (Figure G016504): In total, 15 vol.% organic matter (OM) was counted within this sample. OM in the shale sample is dominated by vitrinite (35 vol.% of OM), alginite (35 vol.% of OM) and sporinite (27 vol.% of OM) in similar amounts. Inertinite is rare. Vitrinite and inertinite particles are often very small (~20-50 µm). Vitrinite is non-fluorescing, and therefore not perhydrous. Alginite often shows a bright orange-yellow fluorescence color under blue light irradiation whereas sporinite is characterized by a yellowish/orange fluorescence colour. Thin brown bands of OM occur within the sample. The relatively high counts for vitrinite and sporinite are not fully compatible with the high HI of ~700 mgHC/gTOC and the strongly alginitic fingerprint plus chain length distribution from pyrolysis gas chromatography (see earlier chapters). Sample heterogeneity is the only explanation we are aware of that can account for these discrepancies.

Vitrinite reflectance: Several populations of vitrinite with slightly differing reflectivity exist in this sample. Reflectance measurements were performed on isolated vitrinite particles and yielded an average value of 0.53 %Rr. This is in good agreement with the bright yellowish to orange fluorescence of sporinite, as well as a bright orange fluorescence of cutinite.

G016505:

Organic matter (Figure G016505): The coal sample is dominated by vitrinite (mainly collodetrinite; 89 vol.%). Phlobaphinite, which is also part of the vitrinite maceral group, occurs within the collodetrinite groundmass. Liptinite (11 vol.%) is visible in lower amounts. Sporinite is the most common maceral of the liptinite group. Rare cutinite occurs within the coal sample. Based on the shape and fluorescence colour under blue light irradiation, some liptinite particles were identified as resinite (see Figure G016505). Sporinite shows a yellowish-orange fluorescence colour under blue light irradiation.

Vitrinite reflectance: The yellowish to orange fluorescence of sporinite and a slight background reflectance indicate rather low (early oil window) maturity. The measured vitrinite reflectance, obtained mainly from phlobaphinite particles within larger collodetrinites, averages at 0.48 %Rr, which is in good agreement with the fluorescence of liptinites.

G016511:

Organic matter (Figure G016511): Vitrinite (collodetrinite) is the dominant maceral group (56 vol.%) followed by semi-inertinite (20 vol.%). Sporinite (5 vol.%) and alginite (4 vol.%) are the main macerals of the liptinite group. Inertinite is rare (4 vol.%). Mineral matter is in the range of 11 %. Alginite shows an orange fluorescence colour under blue light irradiation, sporinite exhibits a yellow fluorescence colour.

Vitrinite reflectance: The measured vitrinite reflectance in this sample averages at 0.40 %Rr. This is in good agreement with a yellow fluorescence of sporinite and generally strong background fluorescence.

G016513:

Organic matter (Figure G016513): In total, 7 vol.% OM was counted within this sample. OM in the shale sample is dominated by vitrinite (40 vol.% of OM), followed by semi-inertinite (40 vol.% of OM; mainly semi-fusinite). Inertinite is rare (12 vol.% of OM) but more abundant than sporinite (8 vol.% of OM), which is the dominant maceral of the liptinite group. Alginite is very rare (below 1

vol.% of OM). Particles of OM are usually small ($< 40 \mu\text{m}$) except some bigger, elongated vitrinite and semi-inertinite grains. Sporinite shows a yellowish/orange fluorescence colour. Pyrite within this sample sometimes shows an oxidation rim. The maceral counts are consistent with a Hydrogen Index of around 100 mgHC/g TOC; the fact that only 47 mgHC/g TOC was measured can be attributed to various factors such as mineral matrix effects during pyrolysis related to the presence of ferric iron, an underestimate of very finely divided inertinite and natural sample heterogeneity.

Vitrinite reflectance: Two populations of vitrinite with slightly differing reflectivity were found. Measurements were conducted on larger elongated vitrinite particles, rather than on isolated small grains. The measured reflectance averages at 0.63 %R_r, which agrees with a yellowish-orange fluorescence of sporinite and alginite. A possible explanation might be the presence of recycled/oxidized vitrinite particles.

G016522:

Organic matter (Figure G016522): The coal sample is dominated by vitrinite (42 vol.%). Semi-inertinite is abundant (22 vol.%). Sporinite is the main maceral of the liptinite group and occur frequently (13 vol.%). Inertinite and alginite are rare ($< 5 \text{ vol.}\%$). The mineral matter content is elevated (18 vol.%) in comparison to the other coal samples. Sporinite shows a yellowish/orange fluorescence colour under blue light irradiation.

Vitrinite reflectance: Two populations of vitrinites exist within this sample. The darker population has a reflectance $< 0.4 \text{ %R}_r$. However, a yellowish to orange fluorescence of spores supports a slightly higher vitrinite reflectance. Therefore, the average reflectance of the relatively brighter vitrinite population (0.41 %R_r) was adopted. This value is still slightly lower than expected, considering the given fluorescence colour.

G016524:

Organic matter (Figure G016524): In total, 10 vol.% OM was counted within this sample. OM in the shale sample is dominated by vitrinite (70 vol.% of OM), followed by semi-inertinite (13 vol.% of OM) and sporinite (10 vol.% of OM). Inertinite and cutinite are rare (3 vol.% of OM). Lamalginite occurs in very low amounts. Semi-inertinite particles are usually big ($> 100 \mu\text{m}$). Sporinite and cutinite show an orange fluorescence colour under blue light irradiation.

Vitrinite reflectance: Vitrinite macerals occur as relatively large bands, dominating over small, isolated particles. The reflectance along this layers is comparably uniform, an average random vitrinite reflectance of 0.59 %R_r was obtained, which is in good agreement with the orange fluorescence of sporinite, as well as a bright orange to slightly brownish fluorescence of (rare) lamalginite.

G016531:

Organic matter (Figure G016531): The coal sample is dominated by vitrinite (collodetrinite; 37 %). Semi-inertinite is abundant (29 vol.%) and inertinite is common (13 vol.%). Sporinite is the main maceral of the liptinite group and occur in low amounts (3 vol.%). Mineral matter content is elevated (14 vol.%). This mineral ground mass show a weak fluorescence colour under blue light irradiation. Sporinite shows an orange fluorescence colour under blue light irradiation.

Vitrinite reflectance: Vitrinite macerals within this sample show a relatively variable reflectivity with different sub-populations (partly $< 0.5 \text{ %R}_r$). A clear orange fluorescence of sporinite argues for a vitrinite reflectance higher than the values obtainable from the relatively darker vitrinite populations, therefore, the most frequently occurring, relatively brighter population of vitrinites was measured. An mean average vitrinite reflectance of 0.63 %R_r was obtained, which is

generally supported by the fluorescence colors of liptinites, although the orange fluorescence of sporinites (as well as the Tmax of 439 °C) might even point to a slightly higher maturity.

G016535:

Organic matter (Figure G016535): Vitrinite (collodetrinite; 67 vol.%) is the dominant maceral group in the coal. Phlobaphinite which is part of the vitrinite maceral group, occur within the collodetrinite groundmass. Semi-inertinite and inertinite occur in similar amounts (10 vol.%, 7 vol.%, respectively). Sporinite and cutinite is common. Based on the strong fluorescence colour and the shape several particles were identified as fluorinitite (see Figure G016535). Alginite, resinite and pyrite are very rare. Sporinite shows an orange fluorescence colour under blue light irradiation.

Vitrinite reflectance: An average vitrinite reflectance of 0.56 %R_r was obtained for this sample. This value is supported by the fluorescence colors of liptinites, as well as by the Tmax of 432 °C.

G016539:

Organic matter (Figure G016539): OM in the shale sample is dominated by bands of vitrinite (80 vol.% of OM). The sample is slightly laminated. Semi-inertinite, inertinite and sporinite occur in similar amounts (~6 vol.% of OM). The mineral ground mass show a weak fluorescence color under blue light irradiation. Sporinite shows a yellowish/orange fluorescence colour under blue light irradiation.

Vitrinite reflectance: An average vitrinite reflectance of 0.59 %R_r was determined for this sample, which is in good agreement with the yellowish to slightly orange fluorescence of sporinite macerals, a relatively strong background fluorescence, as well as a Tmax of 437 °C.

Table 3-1: Results of semi-quantitative maceral analysis (mmf: mineral matter free)

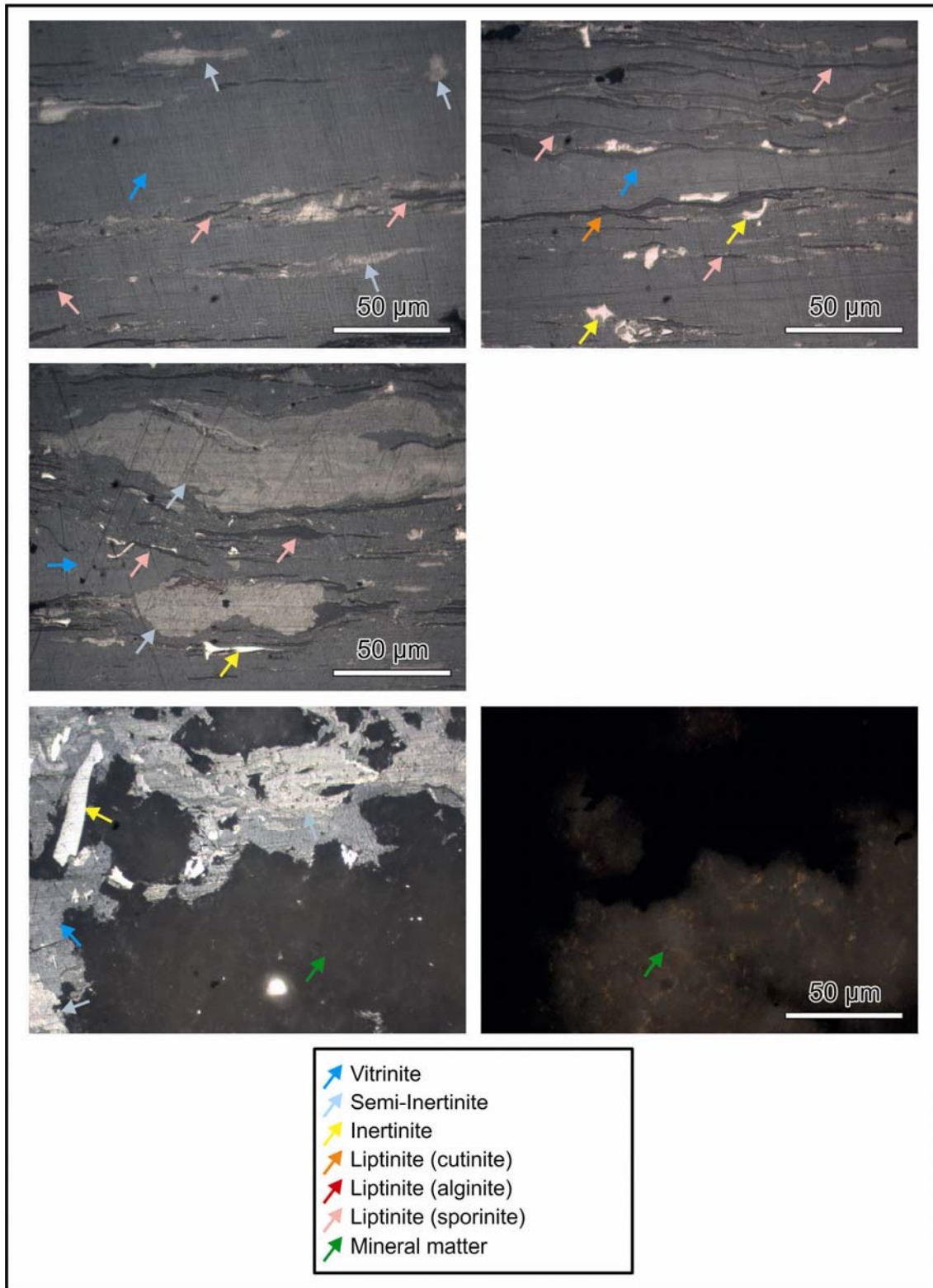
Coal samples	Vitrinite [vol.%]	Semi-Inertinite [vol.%]	Inertinite [vol.%]	Liptinite				Mineral matter [vol.%]	Comments
				Sporinite [vol.%]	Cutinite [vol.%]	Alginite [vol.%]	Fluorinite/ Resinite [vol.%]		
G016496	63	23	6	3	1			6	
G016500	83	8	6	4					Cutinite and pyrite are visible
G016505	89			8	2		1		6 % Phlobaphene within Vitrinite
G016511	56	20	4	5		4		11	
G016522	42	22	4	13		1		18	
G016531	37	29	16	3			1	14	fluorescing ground mass; Cutinite is visible
G016535	67	10	7	4	2	1	1	83	3 % Phlobaphene within Vitrinite; pyrite

Shale samples	Vitrinite [vol.% mmf]	Semi-Inertinite [vol.% mmf]	Inertinite [vol.% mmf]	Sporinite [vol.% mmf]	Cutinite [vol.% mmf]	Alginite [vol.% mmf]
G016504	35		3	27		35
G016513	40	40	12	8		
G016524	70	13	3	10	3	
G016539	80	8	6	6		

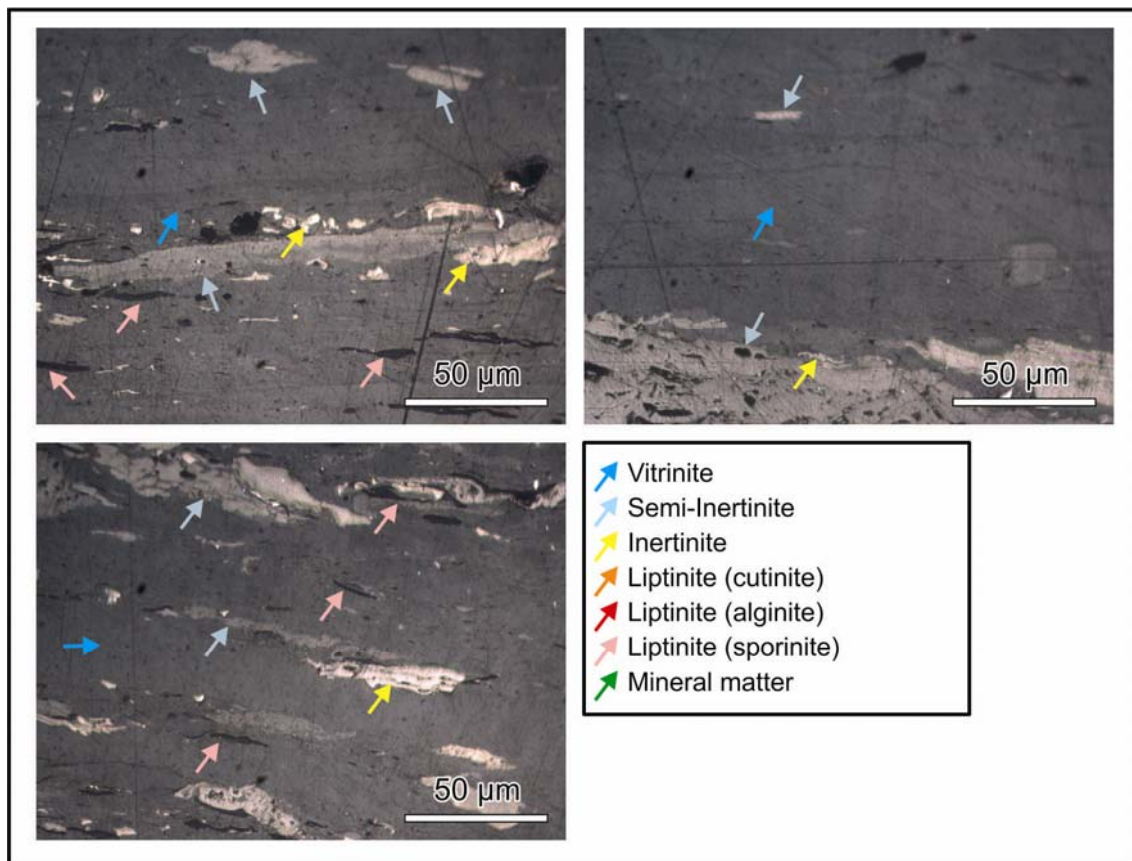
Table 3-2: Results of vitrinite reflectance measurements

Sample	Rr [%]			min.	max.
		s	n	Rr [%]	Rr [%]
<i>coals</i>					
G016496	0.88	0.02	30	0.84	0.92
G016500	0.72	0.02	30	0.69	0.75
G016505	0.48	0.02	30	0.43	0.51
G016511	0.40	0.01	30	0.38	0.43
G016522	0.41	0.02	30	0.38	0.45
G016531	0.63	0.02	20	0.60	0.67
G016535	0.56	0.03	30	0.53	0.62
<i>shales</i>					
G016504	0.53	0.02	20	0.49	0.57
G016513	0.63	0.02	30	0.60	0.68
G016524	0.59	0.02	30	0.54	0.61
G016539	0.59	0.03	30	0.54	0.64

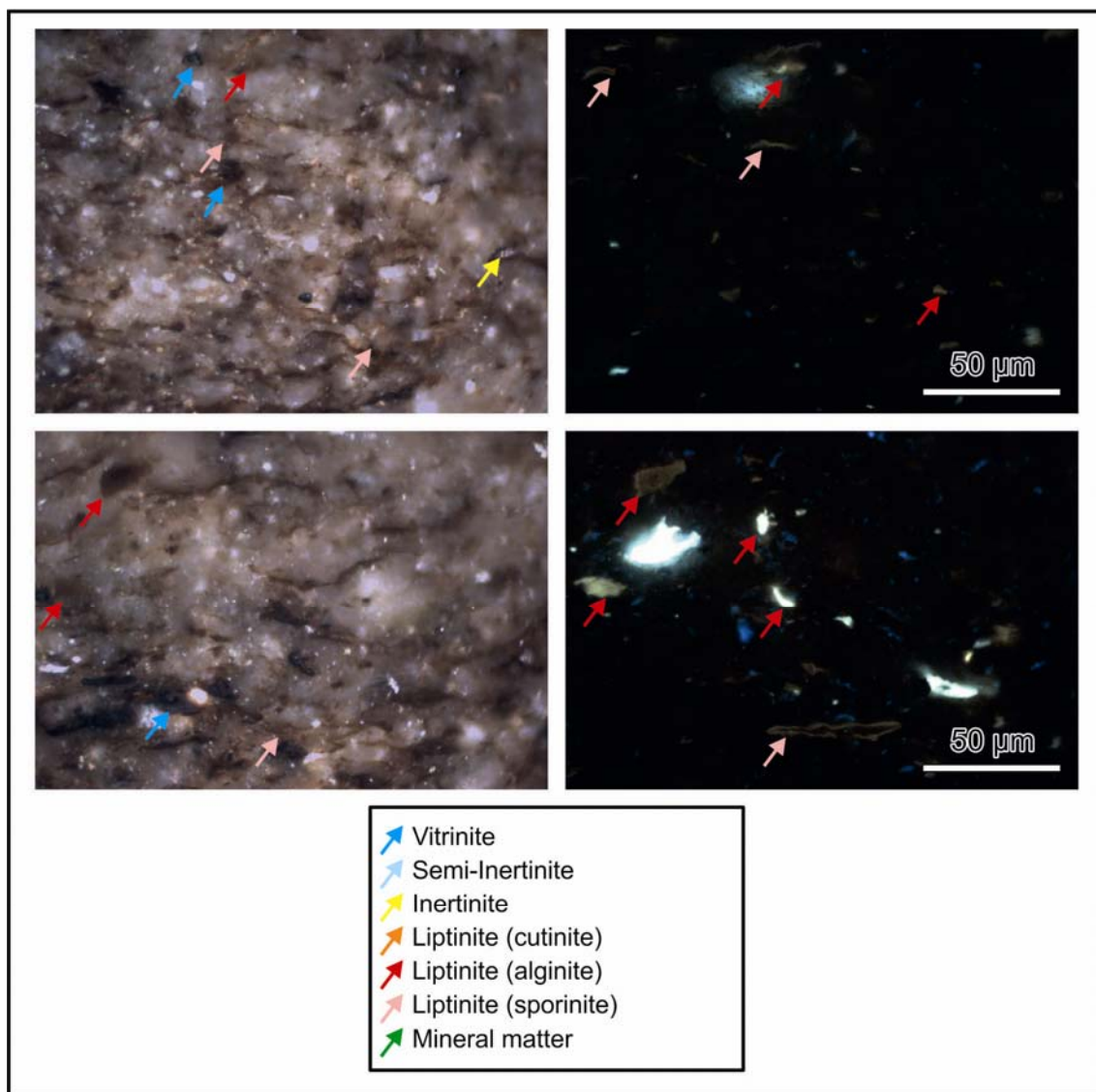
Rr [%]- random vitrinite reflectance, s-standard deviation, n-number of measurements



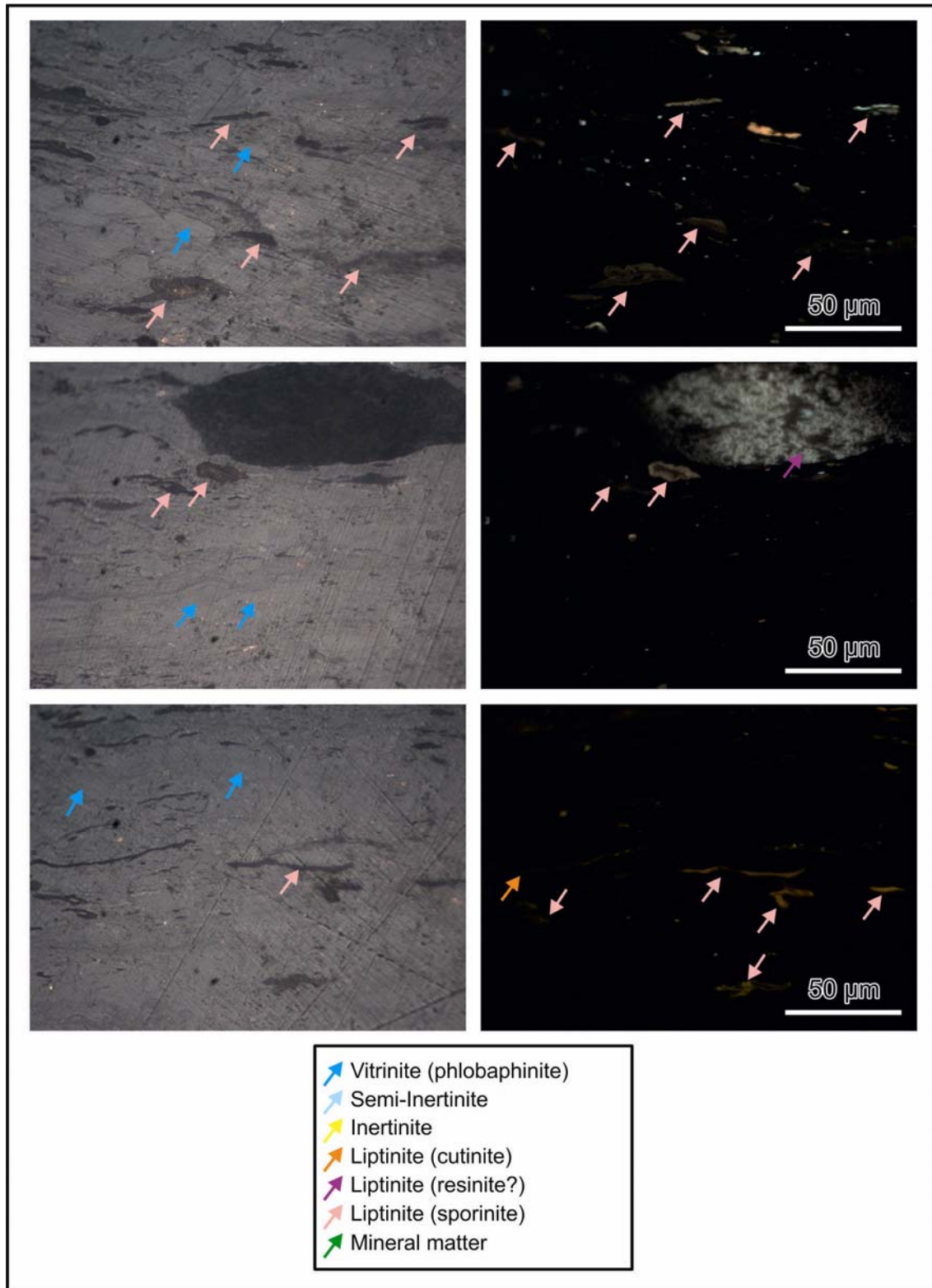
Photomicrographs (oil immersion) of sample G016496. Photographs are taken using incident white light and fluorescing light (lower right side).



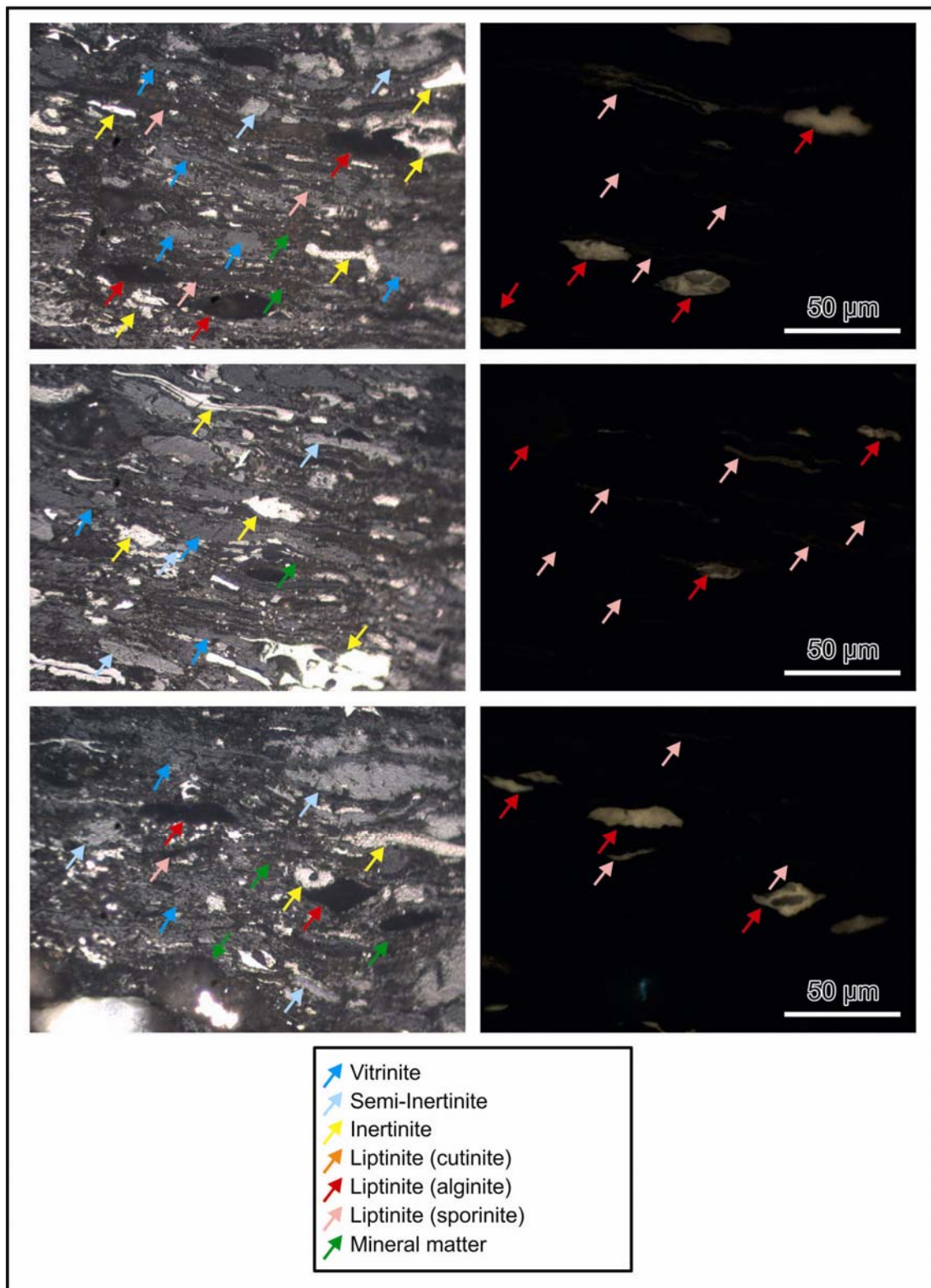
Photomicrographs (oil immersion) of sample G016500. Photographs are taken using incident white light.



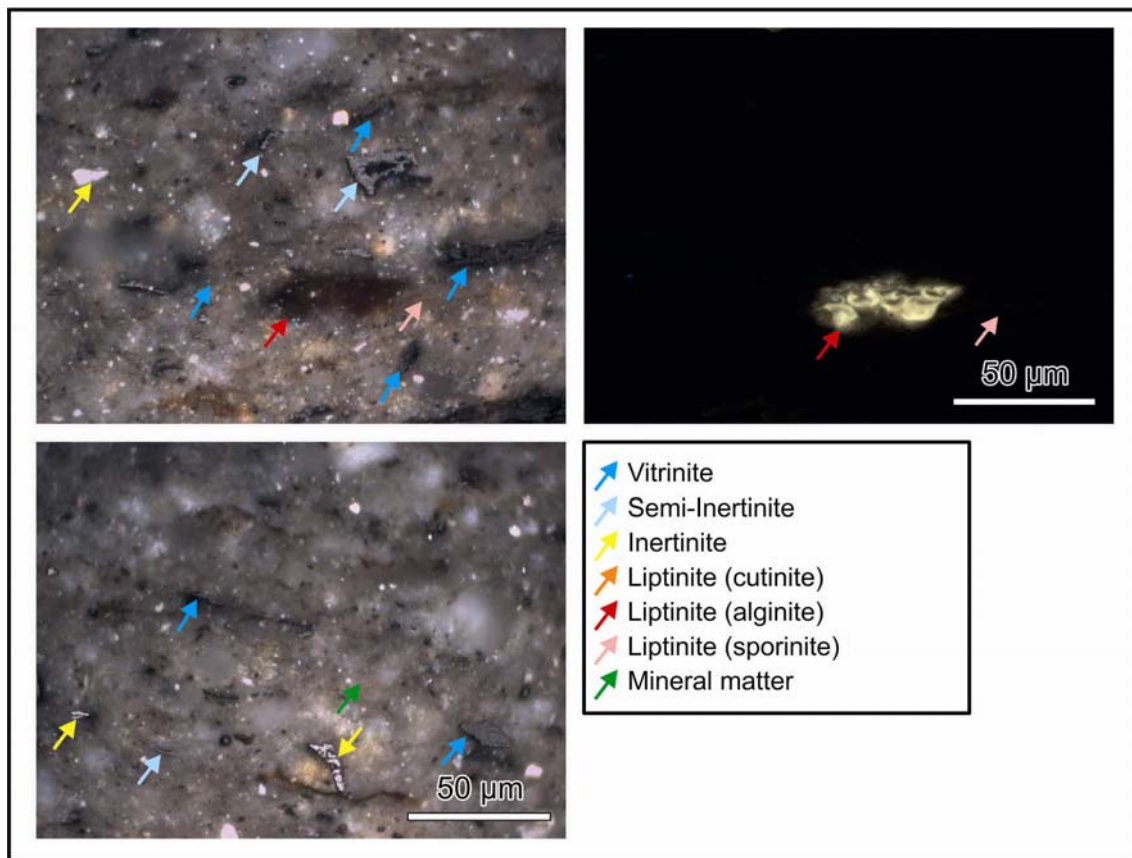
Photomicrographs (oil immersion) of sample G016504. Photographs are taken using incident white light (left side) and fluorescing light (right side).



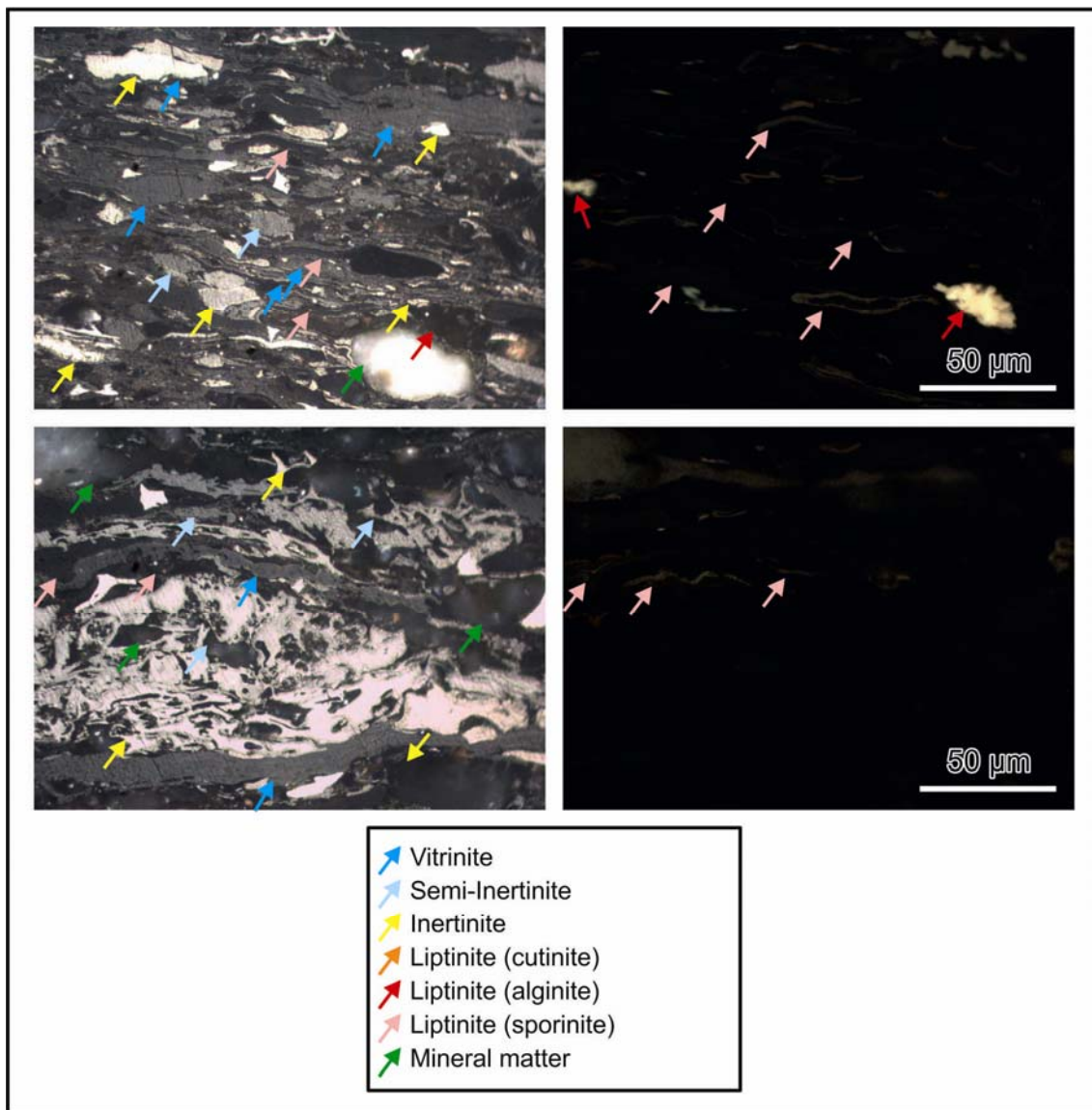
Photomicrographs (oil immersion) of sample G016505. Photographs are taken using incident white light (left side) and fluorescing light (right side).



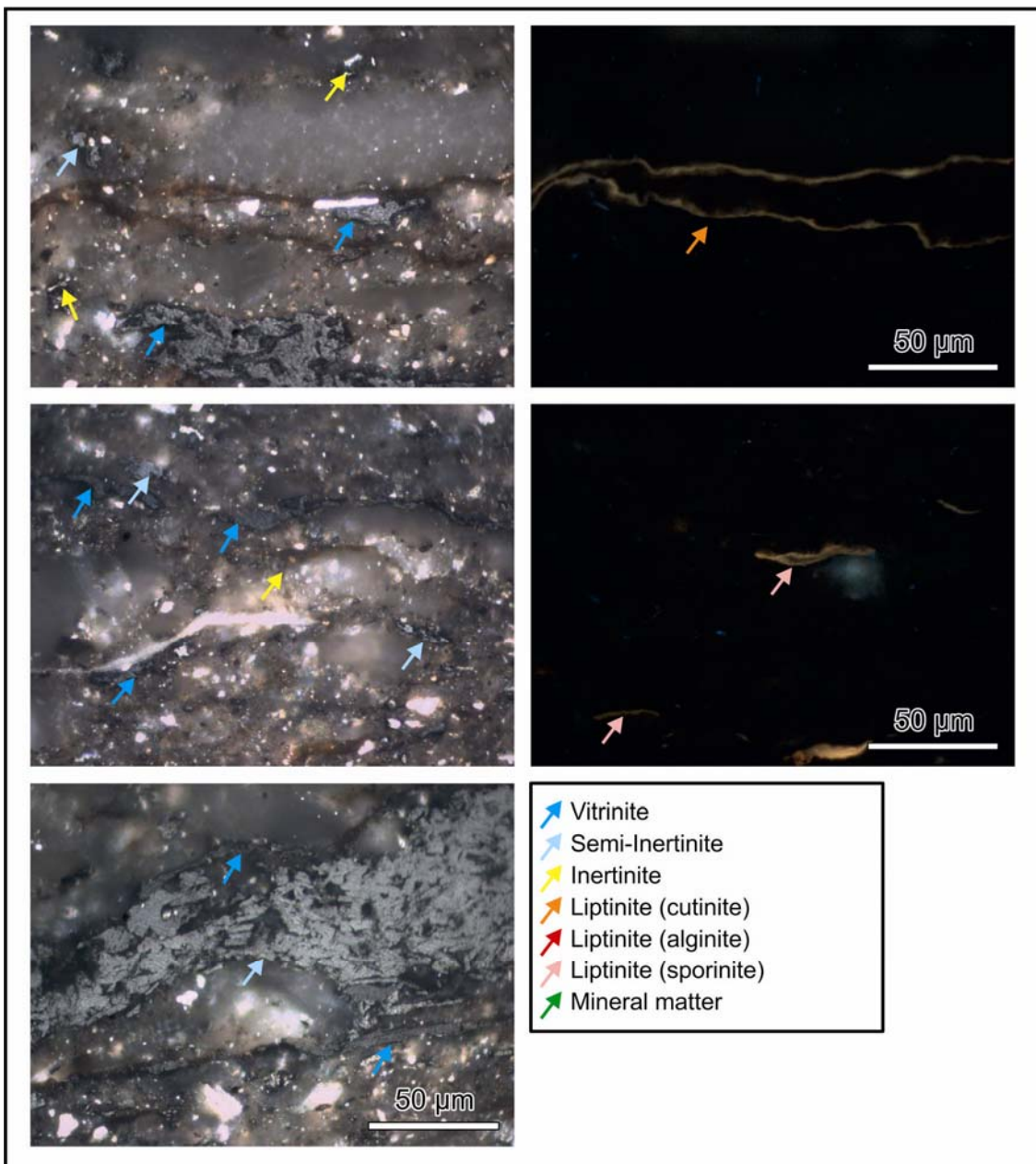
Photomicrographs (oil immersion) of sample G016511. Photographs are taken using incident white light (left side) and fluorescing light (right side).



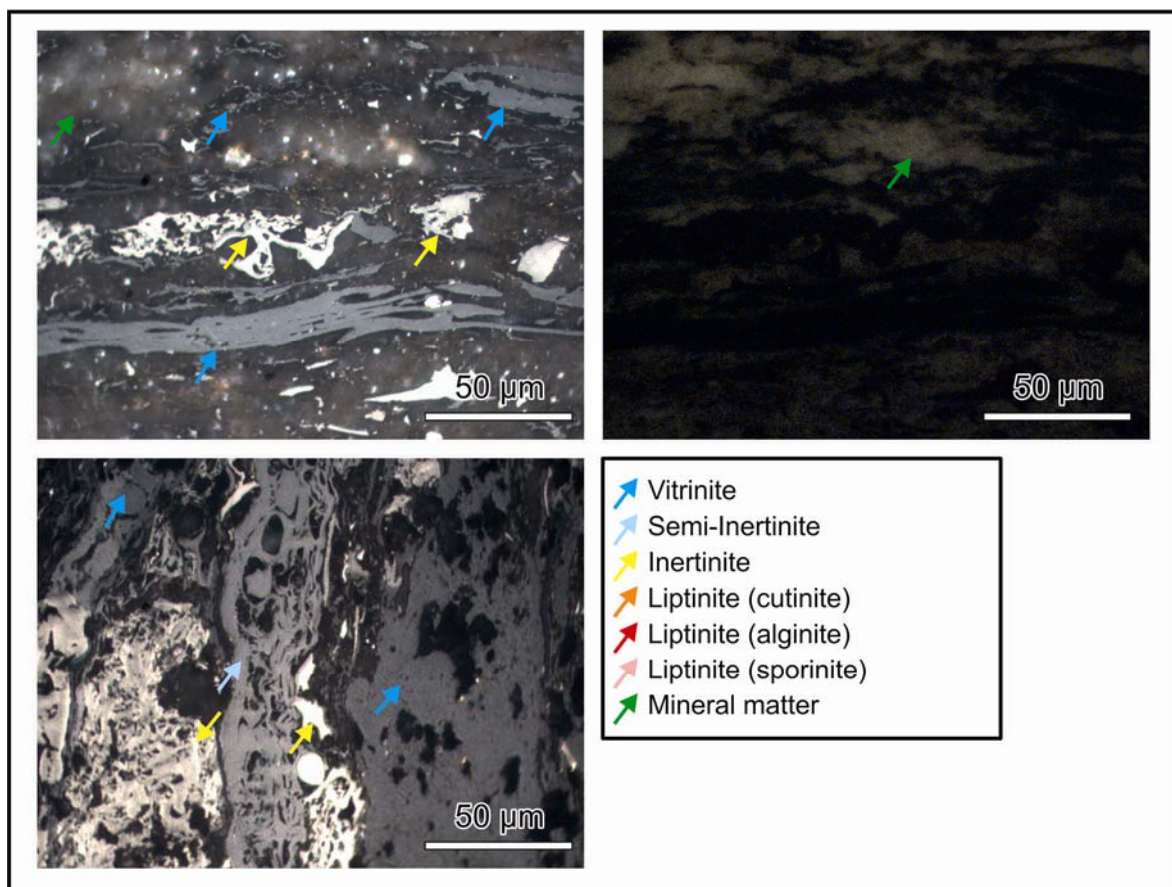
Photomicrographs (oil immersion) of sample G016513. Photographs are taken using incident white light (left side) and fluorescing light (right side).



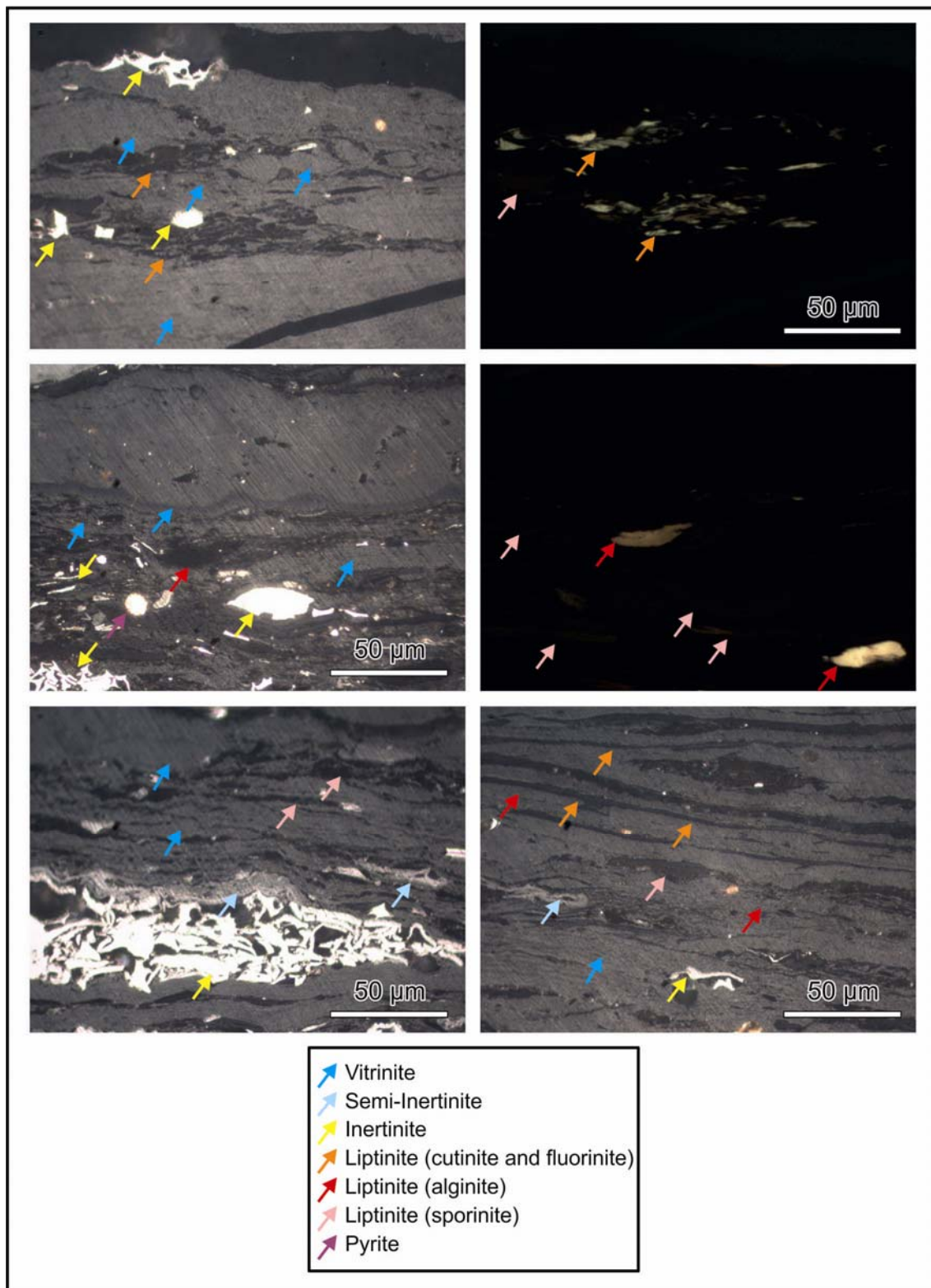
Photomicrographs (oil immersion) of sample G016522. Photographs are taken using incident white light (left side) and fluorescing light (right side).



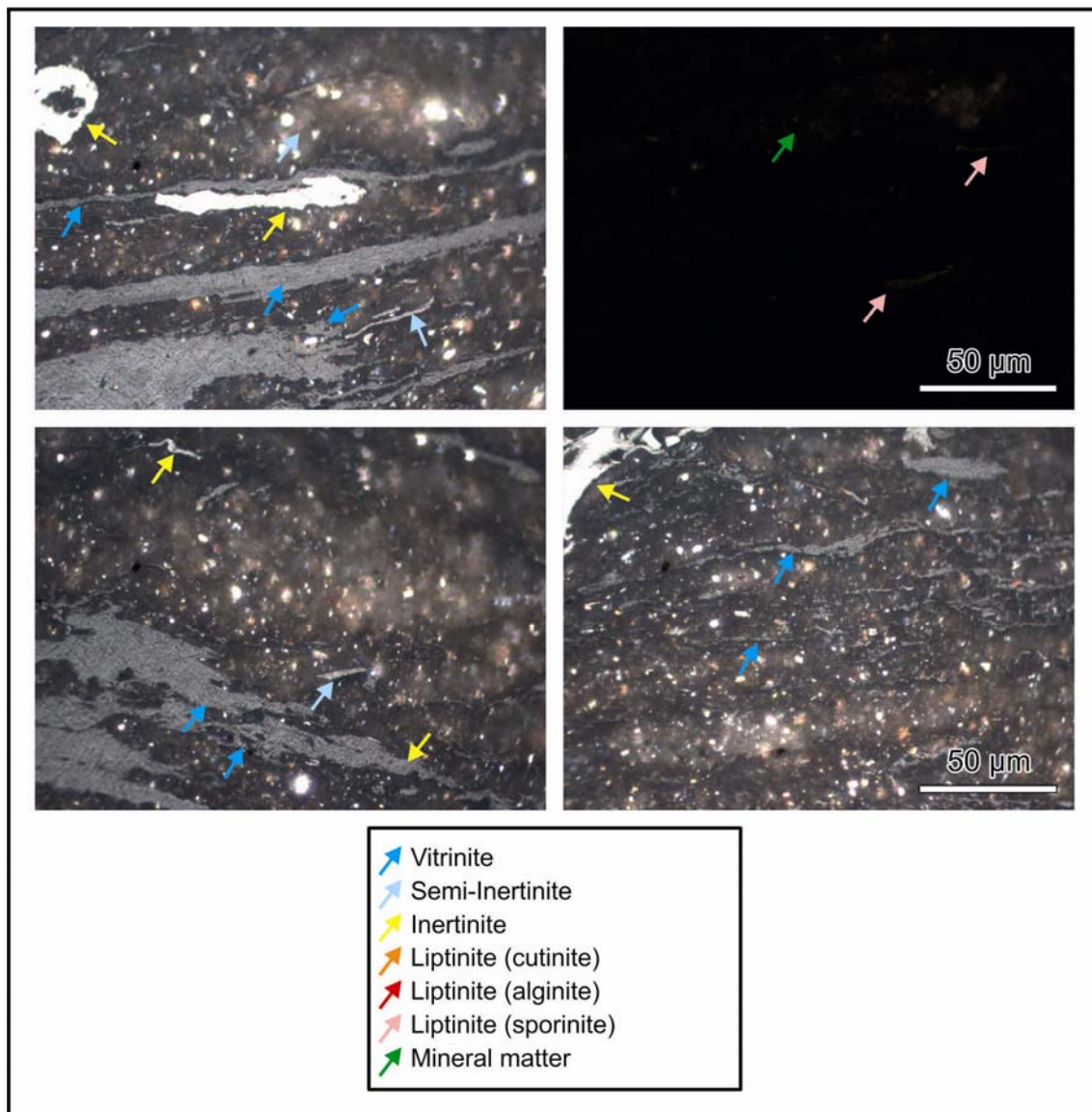
Microphotographs (oil immersion) of sample G016524. Photographs are taken using incident white light (left side) and fluorescing light (right side).



Photomicrographs (oil immersion) of sample G016531. Photographs are taken using incident white light (left side) and fluorescing light (right side).



Photomicrographs (oil immersion) of sample G016535. Photographs are taken using incident white light (left side and lower right side) and fluorescing light (right side).



Photomicrographs (oil immersion) of sample G016539. Photographs are taken using incident white light (left side and lower right side) and fluorescing light (right side).

4 Biomarkers & isotopes (maltenes)

Biomarkers and isotopes were evaluated in close collaboration with Steve Killops, APT, Norway.

GEOS4-ID	Basin	QLD i.d.	Rock Type	Rock Unit Name	Extracts
G016494	Cooper	GSV01	Carb'ceous mst	Patchawarra Formation	1
G016504	Eromanga	GSV11	Carb'ceous mst	Birkhead Formation	1
G016505	Eromanga	GSV12	Coal	Birkhead Formation	1
G016508	Adavale	GSV15	Carbonate	Bury Limestone	1
G016511	Bowen	GSV18	Shale	Bandanna Formation	1
G016522	Bowen	GSV29	Coal	Aldebaran Sandstone	1
G016529	Bowen	GSV39	Shale	Tinowon Formation	1
G016531	Bowen	GSV40	Coal	Tinowon Sandstone	1
G016535	Bowen	GSV45	Coal	Riverstone Sst Mr?-Cattle Creek Formation	1
RUNNING TOTALS					9

4.1 Bulk Compositional Characteristics

Bulk compositional information is effectively contained in extract yield and saturates/aromatics (Sat/Aro) ratio from the quantitative Medium Pressure Liquid Chromatography fractionation. These data are represented in Figure 4-1 and are typical of bitumen from mainly low maturity source rocks, other than the carbonaceous mudstone from the Birkhead Formation (G016504), which has a higher Sat/Aro ratio than the NSO-1 oil standard.

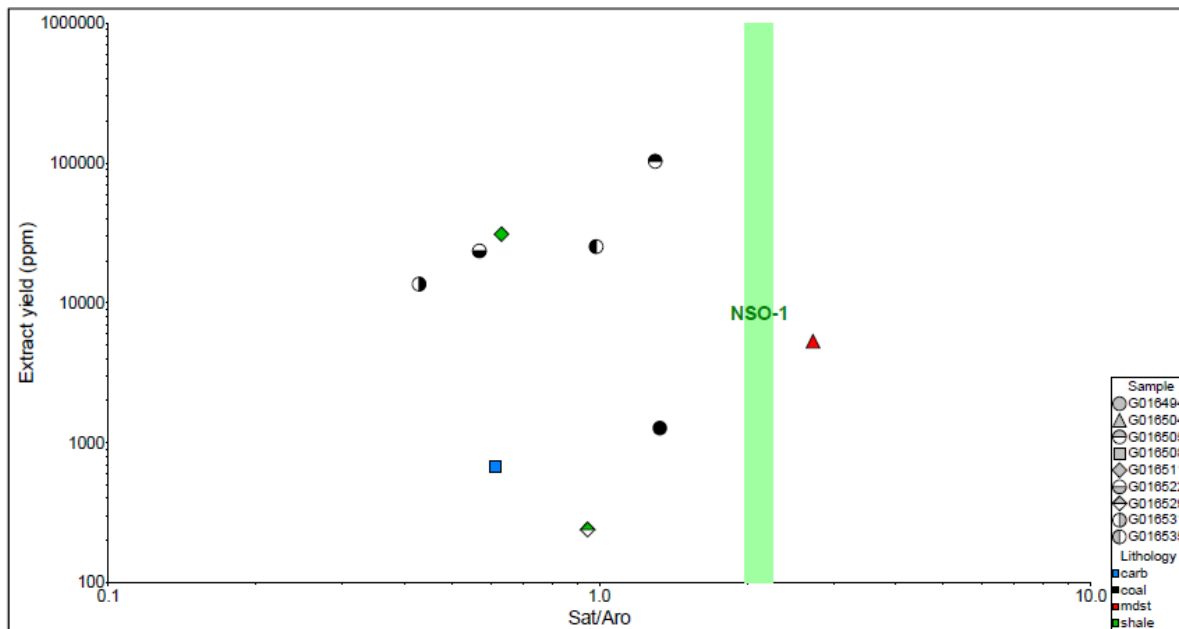


Figure 4-1: Sat/Aro ratio versus extract yield.

An idea of *n*-alkane distributions can be obtained from the mass/charge (*m/z*) 183 mass chromatograms shown in Figure 4-2. The carbonaceous mudstone G016504, shale G016511 and coals G016505, G016522 and G016535 all exhibit a significant odd-over-even preference in the higher plant wax range *nC*₂₃–*nC*₃₁ (NSO-1 is shown for comparison). The other samples exhibit a smaller carbon preference, consistent with higher maturity. The coal G016494 and carbonate G016508 have bimodal distributions, suggesting contributions from more than one major source of organic matter (OM), possibly a mixture of microbial and higher plant contributions (at least for the coal).

There are signs of extended acyclic isoprenoids in coals G016494 and G016531, carbonate G016505 and shale G016529, in the form of small but distinct peaks between *n*-alkanes from around *nC*₃₀ to >*nC*₃₅. It is likely that head-to-head linked components are present in the samples dominated by humic organic matter.

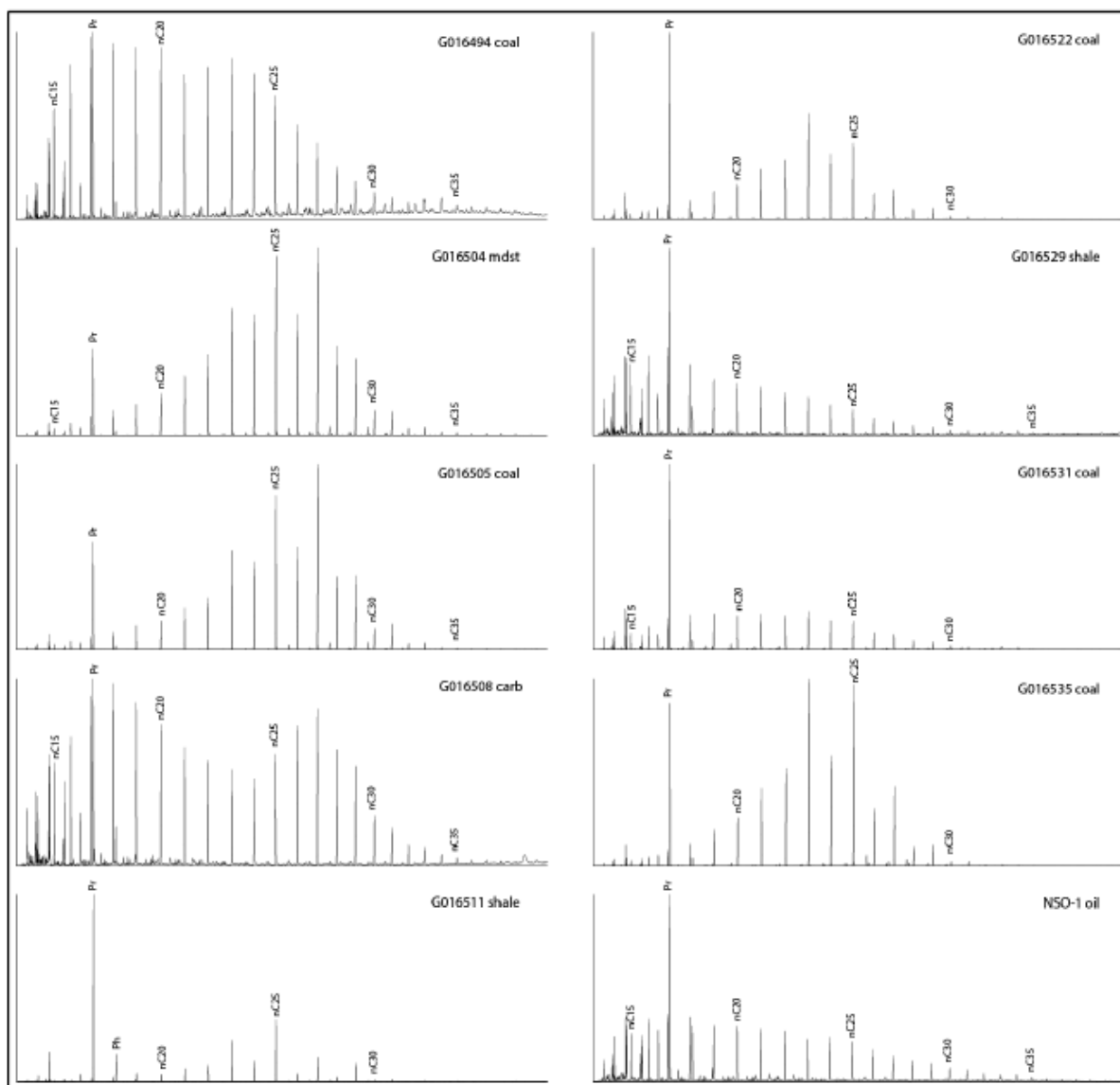


Figure 4-2: Broad indicators of bitumen sources based on *m/z* 183

4.2 Maturity

Maturity assessment has been largely achieved using Tmax, vitrinite reflectance and liptinite fluorescence colours, as laid out in earlier chapters of this report. Assessments based on biomarkers and aromatic compound ratios are here reported for completeness.

Biomarkers

Hopane seems to have reached, or is closely approaching, equilibrium in only the Tinowon Formation shale (G016529) and Tinowon Sandstone Member coal (G016531), which also have low carbon preferences among *n*-alkane distributions, and are suggested to have maturities of $\geq 0.7\% R_o$ based on generalised global occurrences (Figure 4-3). The Bandanna Formation shale (G016511) appears the least mature sample ($< 0.6\% R_o$), whereas the other samples are inferred to have maturities within the range 0.6–0.7% R_o despite maturity estimates sometimes being lower or greater (Table 1-3). Sterane isomerism does not seem to have reached equilibrium in any of the samples, although it is approaching equilibrium for the Tinowon Formation shale (G016529) and Patchawarra Formation coal (G016494) samples in Figure 4-4. That coal sample has a low carbon preference among *n*-alkanes, consistent with the suggested maturity level. Once again, the Bandanna Formation shale (G016511) appears the least mature sample, and the Bury Limestone carbonate (G016508) and Tinowon Sandstone Member coal (G016531) seem more mature than the three remaining coals and carbonaceous mudstone. It appears that the most mature samples correspond to no greater than 0.7% R_o .

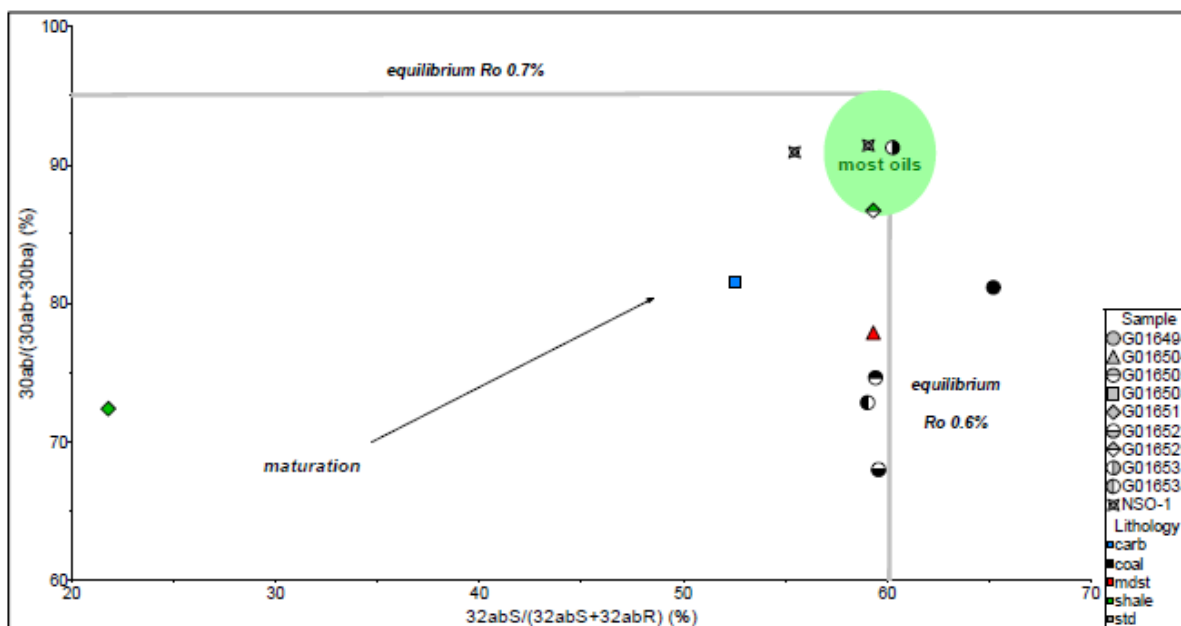


Figure 4-3: Maturity indications from hopane isomerism parameters using m/z 191.

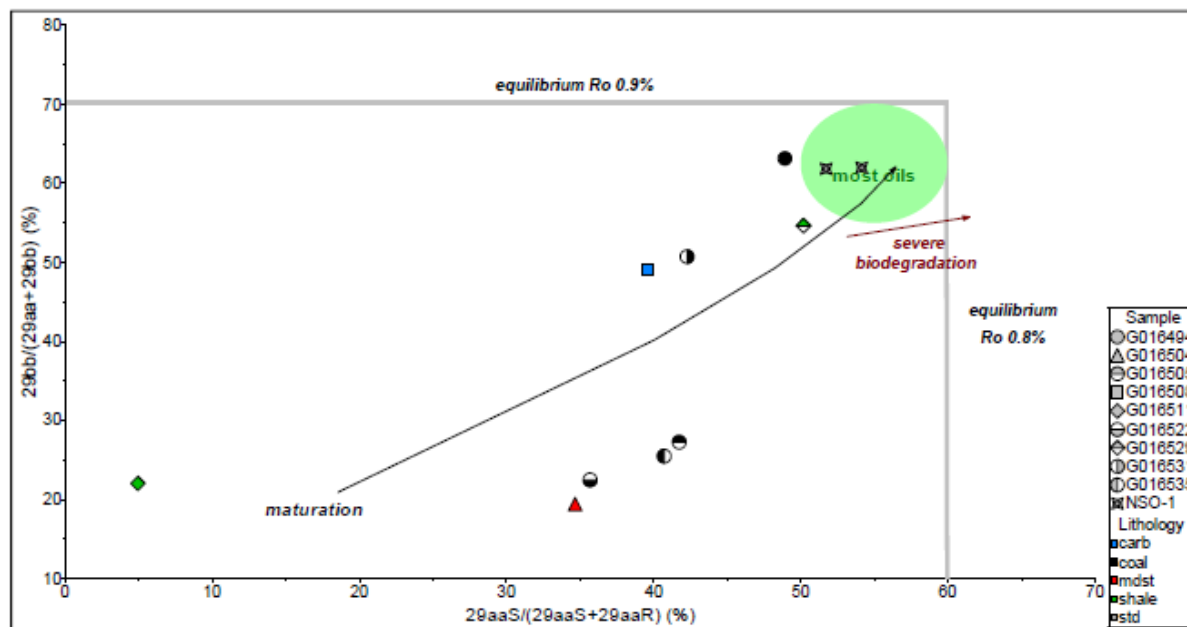


Figure 4-4: Maturity indications from sterane isomerism parameters using m/z 217.

The extent of steroid aromatization is variable in Figure 4-5, but surprisingly low for the Patchawarra Formation coal (G016494) considering its high proportion of short-chain triaromatic steroids. The Bury Limestone carbonate (G016508), Tinowon Formation shale (G016529) and Tinowon Sandstone Member coal (G016531) all appear more mature than suggested by hopane and sterane isomerism. Once again, the Bandanna Formation shale (G016511) is suggested to correspond to low maturity.

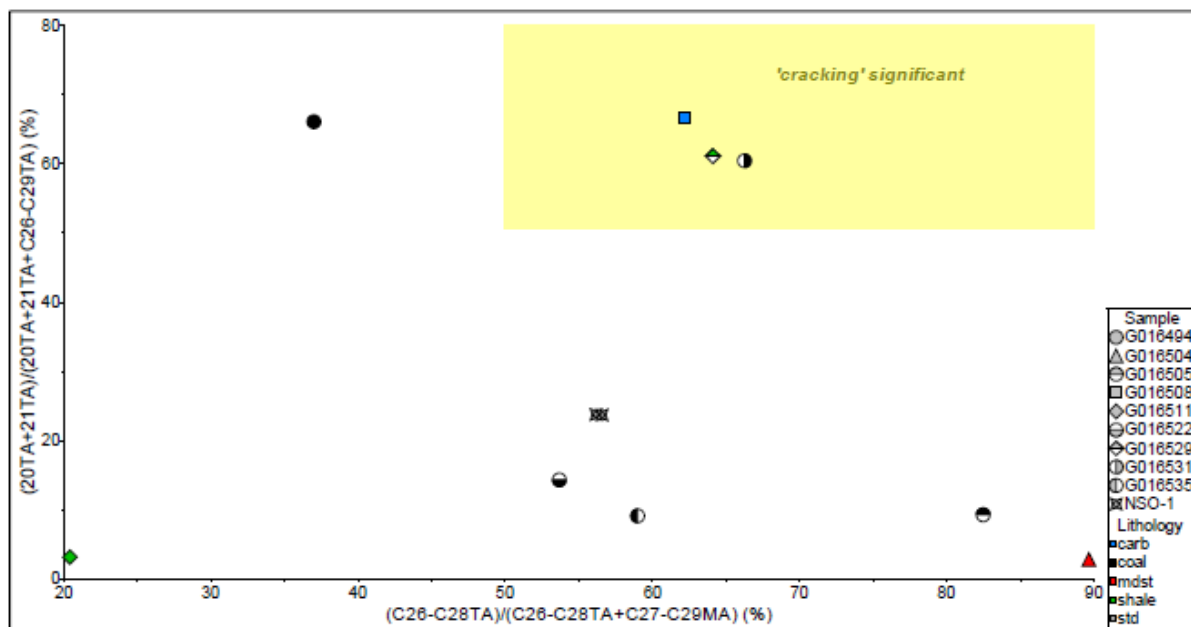


Figure 4-5: Steroid aromatization parameters using m/z 253 for monoaromatic steroids and m/z 231 for triaromatic steroids

Aromatic hydrocarbons

Non-biomarker aromatic maturity parameters based on methylphenanthrenes (MP), Dimethylphenanthrenes (DMP), dimethylnaphthalenes (DMN) and trimethylnaphthalenes (TMN) can

be more reliable indicators of maturity above ~0.9% R_o (due to a wider generation range), but they can be adversely affected by the presence of specific isomers attributable to higher plant contributions, especially in coals prior to the onset of expulsion. In this study, the Birkhead Formation mudstone (G016504) and coal (G016505) samples particularly contain abundant 1-MP, 1,7-DMP (pimanthrene), 1,5-DMN, 1,6-DMN and 1,2,5-TMN (agathalene). Elevated levels of pimanthrene and agathalane in bitumen from humic dominated organic matter are usually associated with gymnosperm-derived diterpenoid origins, although agathalene is less specific, having a potential contribution from hopanoids, which are also abundant in coaly organic matter. 1-MP is likely derived from additional methyl loss from the precursor(s) to pimanthrene, and the two DMNs similarly from precursors of agathalene. Until expulsion occurs, flushing the bulk of the original bitumen from the source rocks, maturity parameters based on methylated naphthalenes and phenanthrenes can be variable and unreliable. In a number of the following graphs, the maturity of the Birkhead Formation mudstone (G016504) and coal (G016505) samples appear exceptionally low because of the retention of initial bitumen and specific gymnosperm/bacterial contributions. In addition, the Cattle Creek Formation (?Riverstone Sandstone Member) coal (G016535) has elevated pimanthrene and agathalene, but not their further demethylated counterparts, which suggests different diagenetic conditions to the Birkhead Formation (G016504 and G016505) samples, although similar gymnosperm contributions.

Methylphenanthrene parameters suggest similar maturity trends to aromatic steroids, apart from the Birkhead Formation mudstone (G016504) and coal (G016505), which have particularly low values of MPI1 and MPR resulting from abundant 1-MP (Figure 4-6). Maturities are suggested to be <0.9% R_o for all samples.

Methylated naphthalene distributions yield maturity ratios that plot close to the empirical calibration line in Figure 4-7. However, the dimethylnaphthalene ratio DNR is adversely affected by abundant 1,5-DMN, which appears in the denominator of the ratio, and hence the Birkhead Formation samples (G016504 and G016505) plot at very low DNR, and slightly below the calibration line. It also appears that the Bandanna Formation sample (G016511) and the Aldebaran Sandstone sample (G016522) may be affected to an extent by specific contributions of pimanthrene, because they too plot below the calibration line. In contrast, the trimethylnaphthalene ratio-2 TNR2 is not expected to be so obviously affected by specific gymnosperm contributions. It suggests a maturity approaching 0.7% R_o for the Birkhead Formation (G016504 and G016505), ~0.85% for the Bandanna Formation (G016511) and Aldebaran Sandstone (G016522), 0.90–0.95% for Tinowon Sandstone member (G016531) and the Cattle Creek Formation (?Riverstone Sandstone Member) (G016535), ~1.0% for the Tinowon Formation (G016529) and approaching 1.1% for the Bury Limestone (G016508) and Patchawarra Formation (G016494). The trends are similar to those suggested by steroid aromatization and sterane isomerism, but maturity levels are slightly higher than the latter indicate.

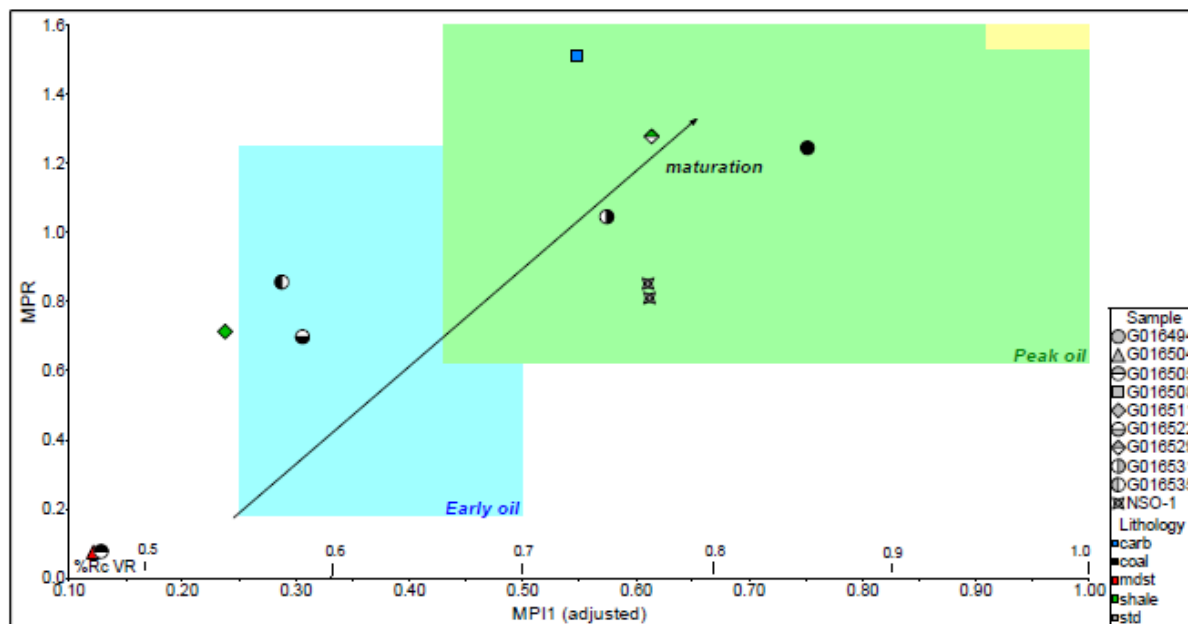


Figure 4-6: Maturity implications of methylphenanthrene distributions (after Radke 1988).

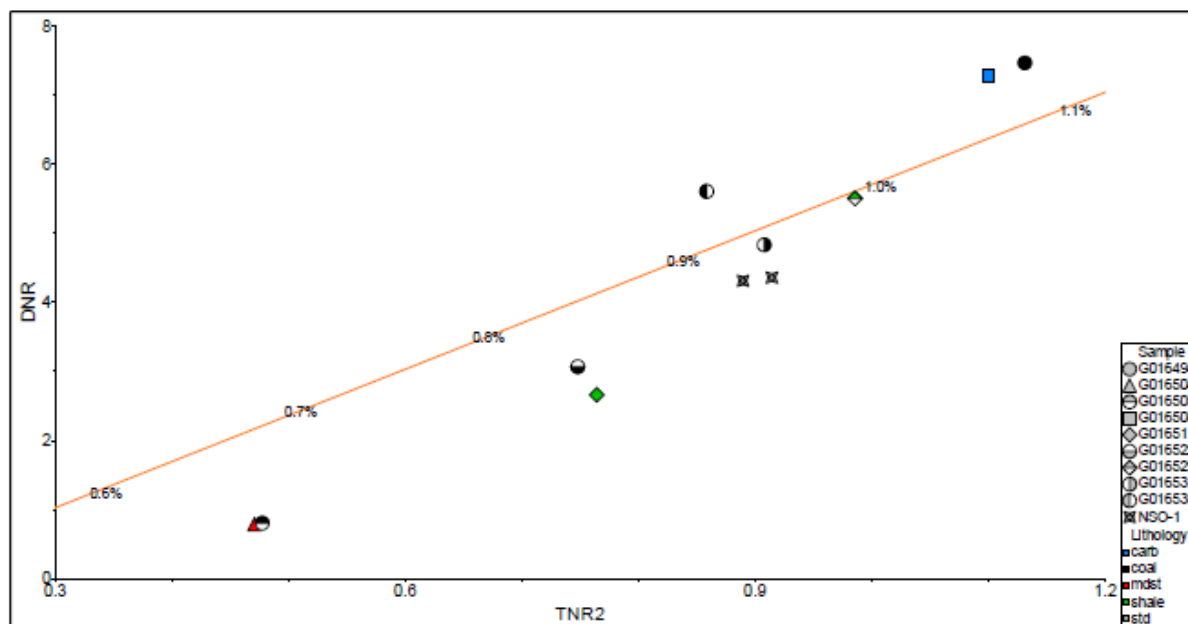


Figure 4-7: Maturity implications from methylnaphthalenes (equivalent VR scales after Radke et al. 1994).

The Methyldibenzothiophene Ratio (MDR) suggests similar maturity trends to those noted from TNR2, although estimated vitrinite reflectances differ for some of the samples, such as the carbonate G016508 (Figure 4-8). The ratio of 3-methylphenanthrene/retene 3MP/Ret can be useful, but is again affected by varying retene contributions to initial bitumen, which appear to be particularly high for the Birkhead Formation and the Cattle Creek Formation (?Riverstone Sandstone Member) coals (G016505 and G016535). The very high 3MP/Ret ratio for the Patchawarra Formation coal (G016494) suggests advanced maturity.

Two parameters that have proven useful in comparing maturities of oils in the North Sea are shown in Figure 4-9. They are affected by organofacies variation and severe biodegradation (which has a similar influence to increasing maturity), but are useful maturity indicators for oils from upper Jurassic, marine, sapropelic sources. Although their application to humic organic matter is limited, the high values for the Patchawarra Formation coal (G016494) again suggest advanced maturity.

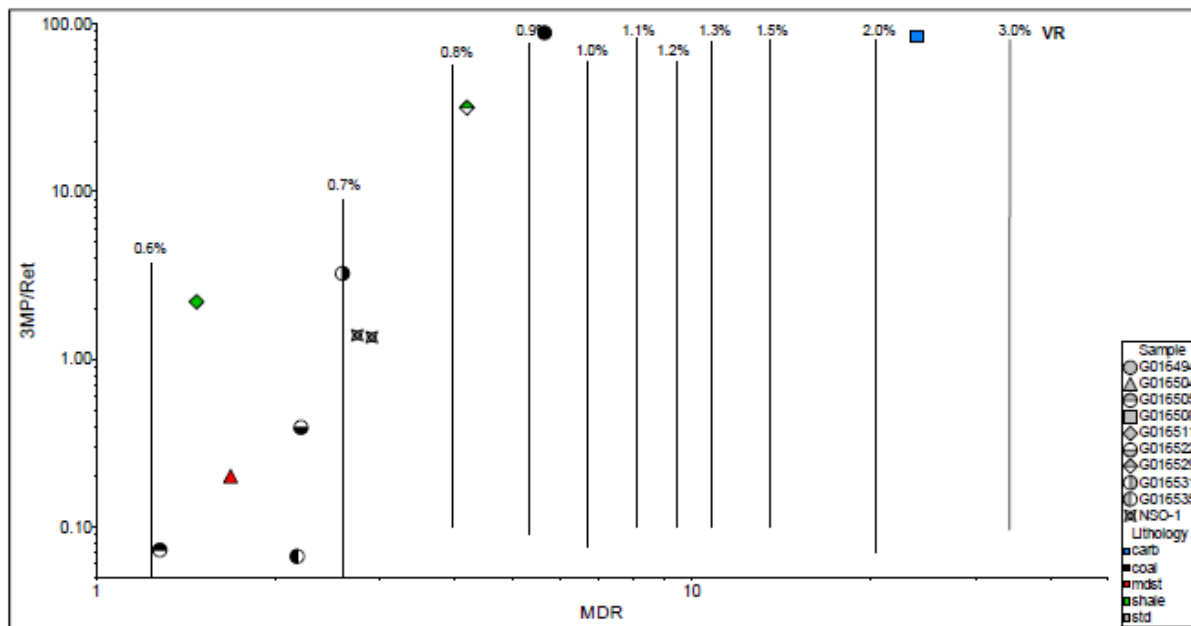


Figure 4-8: Maturity implications of methyldibenzothiophene distributions (MDR; equivalent VR scale after Radke 1988) and relative abundance of retene (3MP/Ret; Wilhelms et al. 1998).

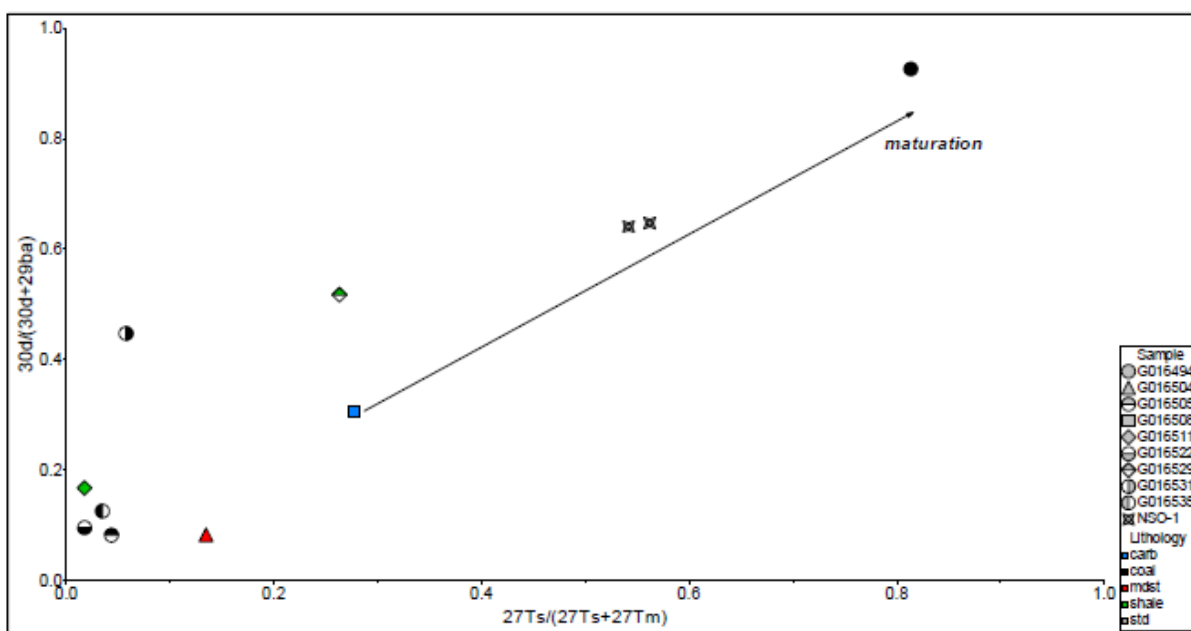


Figure 4-9: Maturity implications from rearranged hopanes.

Summary

The inferences for vitrinite reflectance ranges from the various molecular maturity parameters discussed above are summarized in Table 4-1. The discrepancy between aromatic and biomarker alkane is apparent, particularly for the (G016494) Patchawarra Formation coal and the Bury Limestone (G016508) carbonate, which appear to have likely maturities of ~1.0% R_o . Only very approximate equivalent VR values are suggested because of the discrepancies. The GEOS4 interim report 20161121 presents petrographic data on this topic.

Table 4-1: Summary of molecular maturity indications (equivalent VR values as % R_o).

GEOS4-ID	Lithology	Hopane isom	Sterane isom	Arom steroids	MPI 1	DNR	TNR2	MDR	Overall
G016494	Coal	0.6 -0.7	0.7-0.8	>1.0?	0.8-0.9	1.1.-12.	1.0-1.1	0.9-1.0	~1.0
G016504	Mdst	0.6 -0.7	<0.8	<1.0	<0.5	0.5-0.6	0.6-0.7	0.6-0.7	~0.6
G016505	Coal	0.6 -0.7	<0.8	<1.0	<0.5	0.5-0.6	0.6-0.7	0.6	~0.6
G016508	Carbonate	<0.6	<0.8	>1.0	0.7-0.8	1.1.-12.	1.0-1.1	2.0-2.5	~1.0
G016511	Shale	<<0.6	<<0.8	<<1.0	0.5-0.6	0.7-0.8	0.8-0.9	0.6-0.7	~0.6
G016522	Coal	0.6 -0.7	<0.8	<1.0	0.5-0.6	0.7-0.8	0.8-0.9	0.6-0.7	~0.7
G016529	Shale	~0.7	0.7-0.8	>1.0	0.7-0.8	1.0	1.0	0.8-0.9	~0.9
G016531	Coal	?0.7	<0.8	>1.0	0.7-0.8	0.9-1.0	0.9-1.0	0.7	~0.8
G016535	Coal	0.6 -0.7	<0.8	<1.0	0.5-0.6	1.0	0.9	0.6-0.7	~0.7

4.3 Alteration

Biodegradation

A significant degree of bacterial (and fungal) reworking of humic material is expected in coaly source rocks, so variation between samples may provide useful information. 25-Norhopanes can indicate biodegradation (Bennett et al. 2006 and refs therein). Although these compounds were present in very low abundance in most of the samples, they were more enriched in the carbonate and two shales, and particularly so in the Patchawara Formation coal (G016494) (Figure 4-10). This coal appears to have experienced more profound bacterial reworking than the other coals, which may, at least partially, account for its greater abundance of diahopane and neohopanes noted in Figure 4-9.

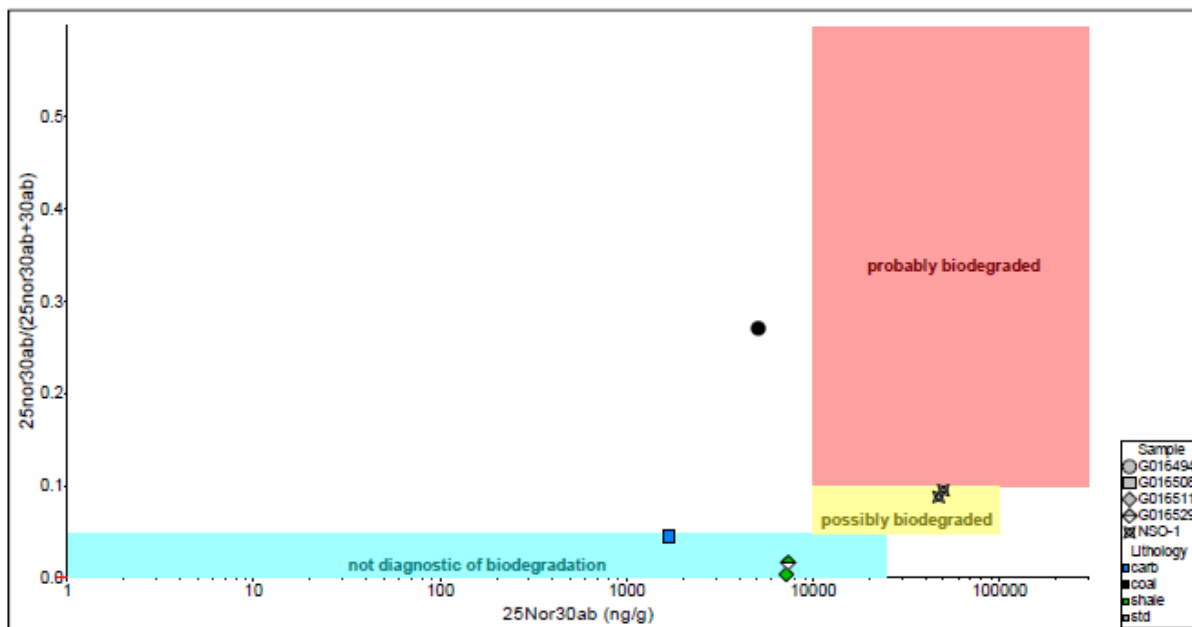


Figure 4-10: 25-Norhopane abundance.

Inspection of the m/z 191 mass chromatogram of the Patchawarra Formation coal (G016494) shows that the hopane range is dominated by a full set of diahopanes (Figure 4-11). The C₃₀ component is by far the most abundant, but even the other members of the series are more abundant than the regular hopanes. It is unusual to see such hopanoid distributions; the diahopanes are believed to be particularly thermally stable towards thermal and biodegradative alteration (Moldowan et al. 1991). The bacterial action responsible for the abundant 25-norhopanes is probably also the reason for the diahopane dominance.

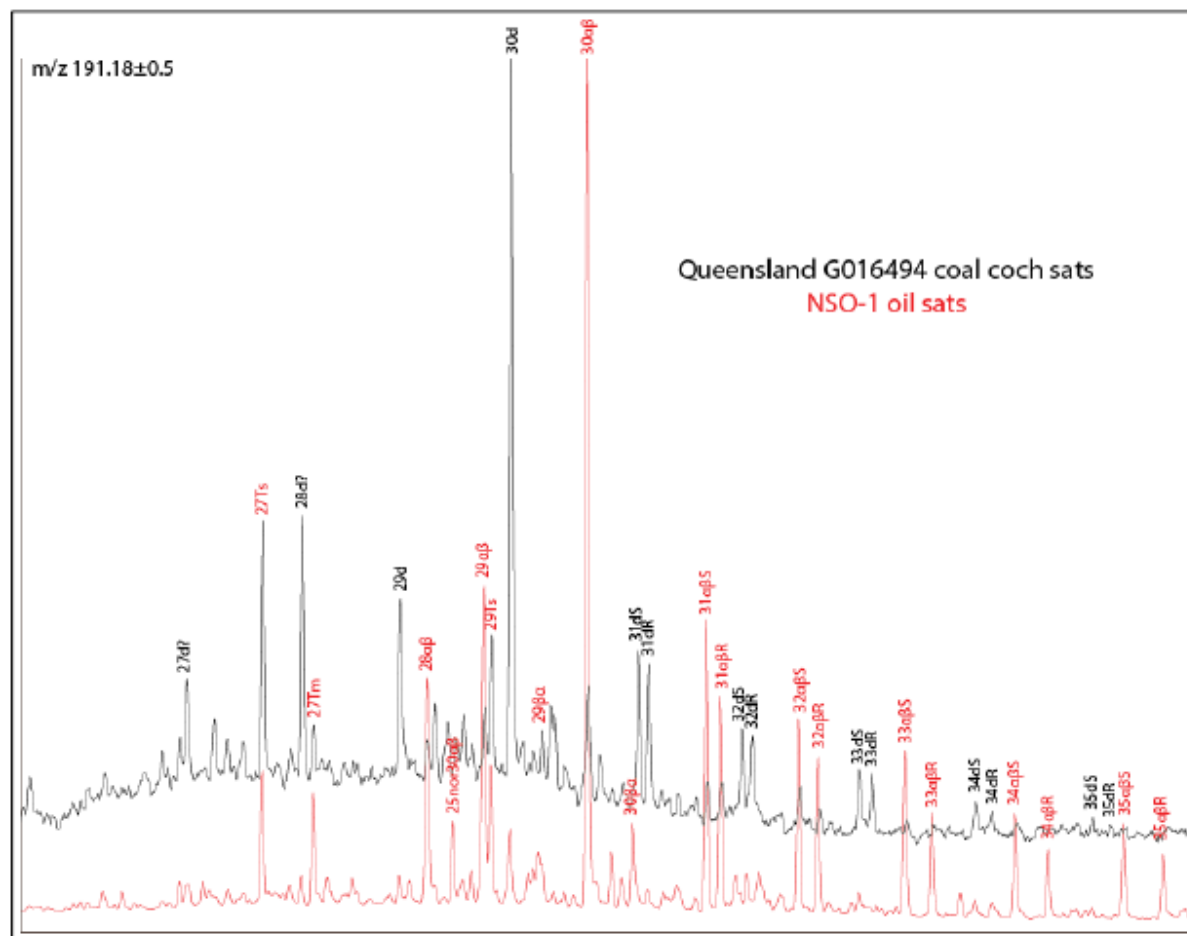


Figure 4-11: Diahopane distributions in m/z 191 mass chromatogram from G016494 coal (NSO-1 shown for comparison).

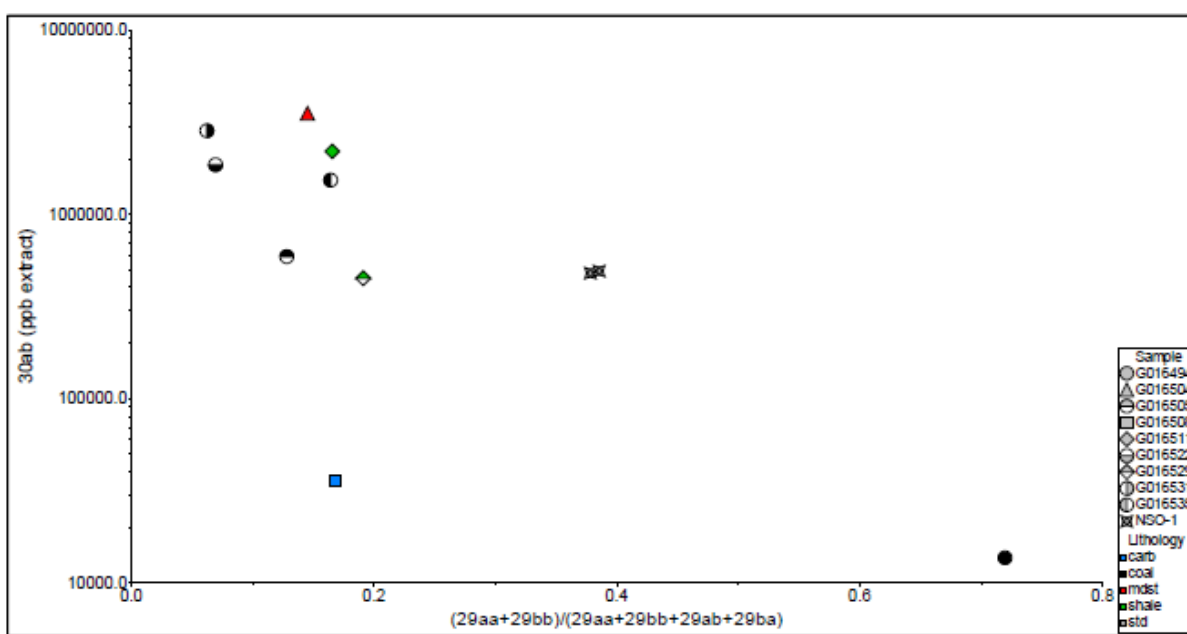


Figure 4-12: Hopane abundance.

Hopane abundance, both concentration within extracts and relative to steranes of similar volatility (both C_{29} and C_{30}), is high in all of the coals, mudstone and shales except for the Patchawarra

Formation sample G016494 (Figure 4-12), which is consistent with possible biodegradation of hopanes. The carbonate exhibits low concentrations, but relative abundance is quite high. Diasterane and cheilanthane content of Patchawarra Formation sample G016494 are also slightly elevated compared to the other coals (Figure 4-13), which could reflect generally greater influence from biodegradation in that sample, or slightly different environment (more clay catalysed rearrangement of regular steroids and higher salinity conducive to bacteria that synthesize cheilanthanes).

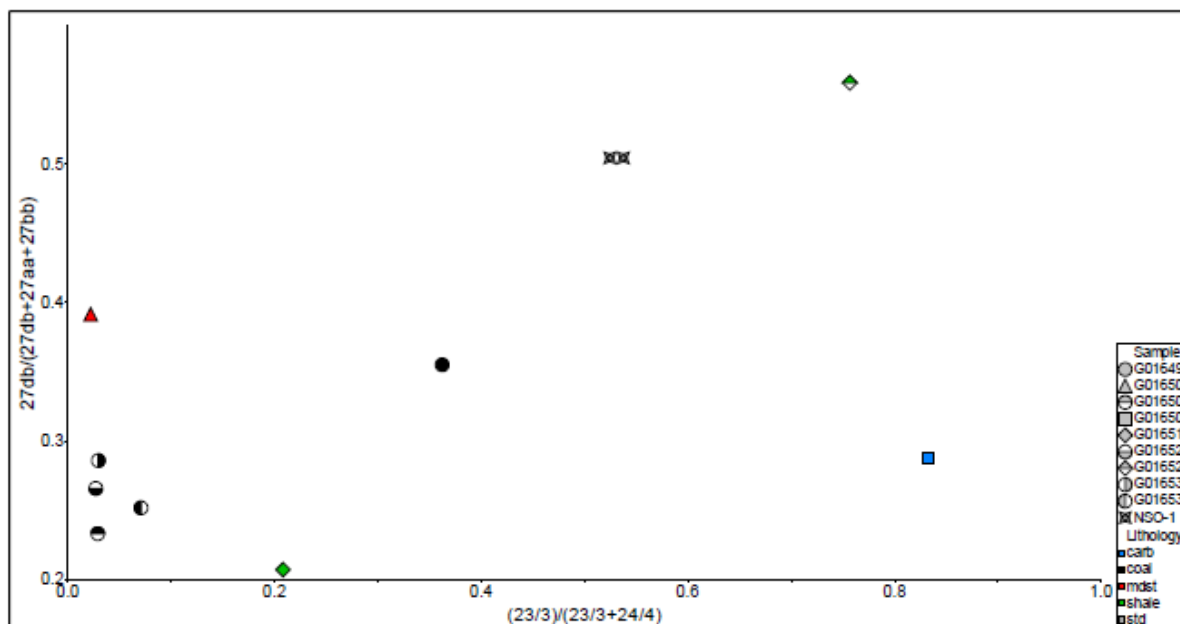


Figure 4-13: Relative abundance of diasteranes and cheilanthanes.

4.4 Sources and depositional environment

Environments

Dibenzothiophene/phenanthrene DBT/P and Pristane/Phytane (Pr/Ph) values (the latter estimated from m/z 183 mass chromatograms) are consistent with dominantly humic organic matter for all of the samples, except for the carbonate, although that sample exhibits an unexpectedly high Pr/Ph and very low DBT/P (Figure 4-14). Pristane/Phytane values are lower for the shale samples than the coals and mudstone, and the Patchawarra Formation coal (G016494) has an intermediate value between the shales and the other coals.

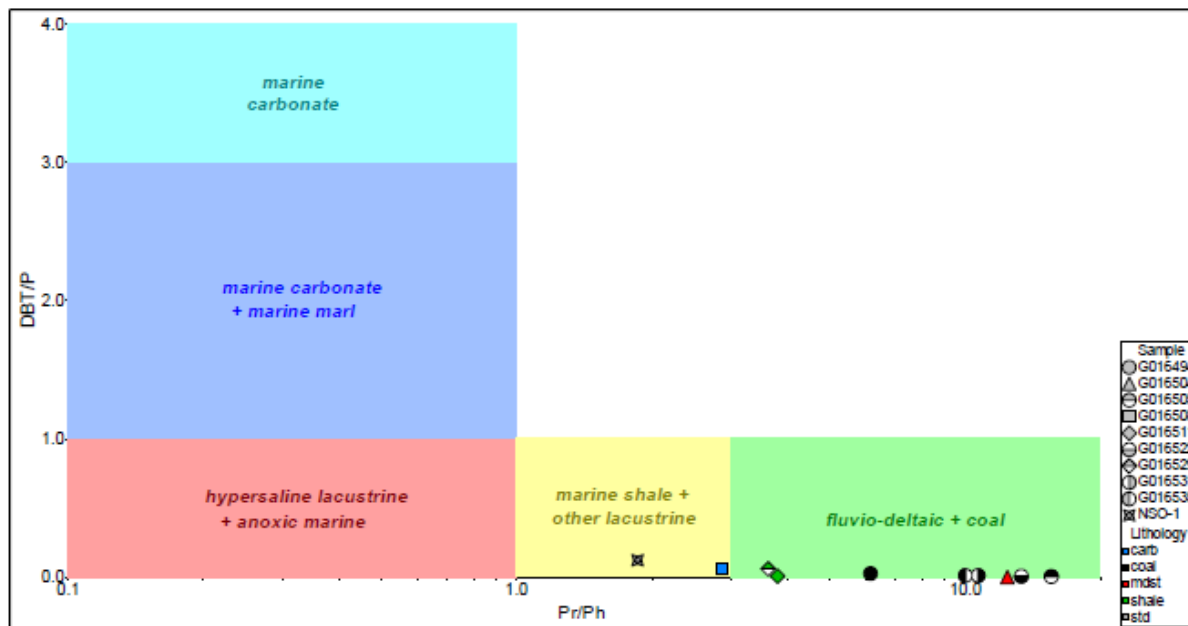


Figure 4-14: Inferred depositional environment (after Hughes et al. 1995). Pr/Ph estimated from m/z 183 signal [using Pr/(Ph*1.8)].

The abundance of 28,30-dinorhopane is generally low (Figure 4-15), consistent with the high Pr/Ph ratios that probably reflect relatively oxygenated conditions during diagenesis. Although the compound's abundance relative to $30\alpha\beta$ hopane is quite high in the Patchawarra Formation coal (G016494), this is due to biodegradative removal of regular hopanes, as demonstrated by a concentration towards the low end of the range for coals in Figure 4-15. The high relative abundance may reflect slightly poorer oxygenation during diagenesis, as also suggested by its Pr/Ph value conditions, and/or slightly greater biodegradative resistance than $30\alpha\beta$. Differing environmental conditions are suggested by the gammacerane and homohopane indices in Figure 4-16. However, extended hopane abundance is low in all coaly samples, so quantification may not be entirely reliable, and the high gammacerane index is a result of biodegradative removal of $30\alpha\beta$ (the gammacerane concentration in the G0156494 extract is nearly an order of magnitude lower than for the other coals).

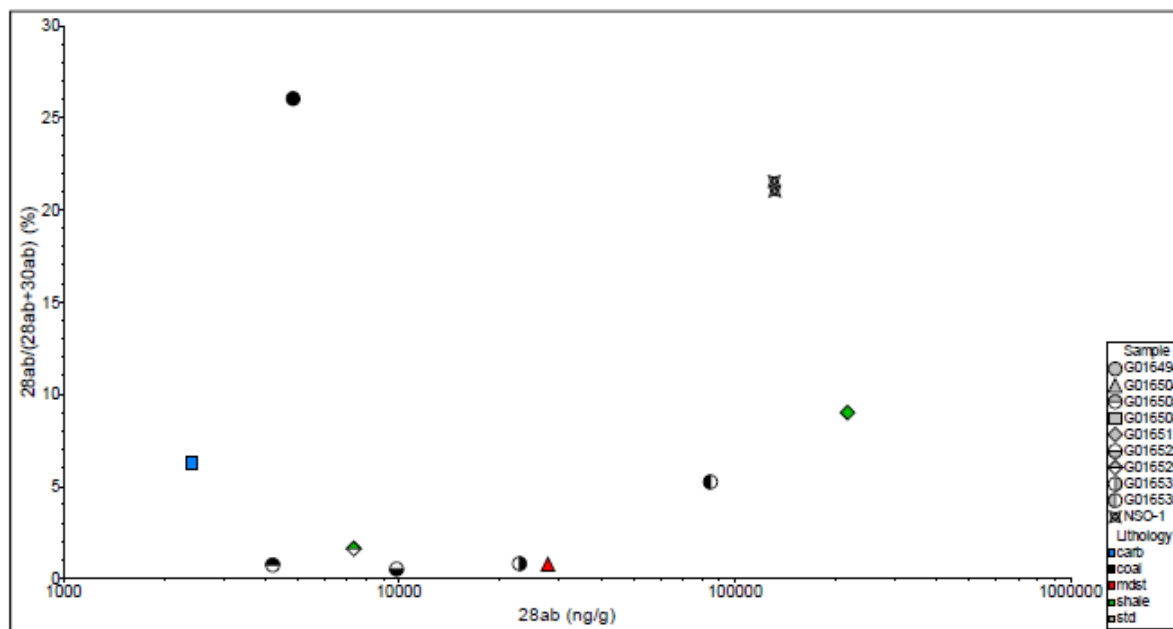


Figure 4-15: Abundance of 28,30-dinorhopane.

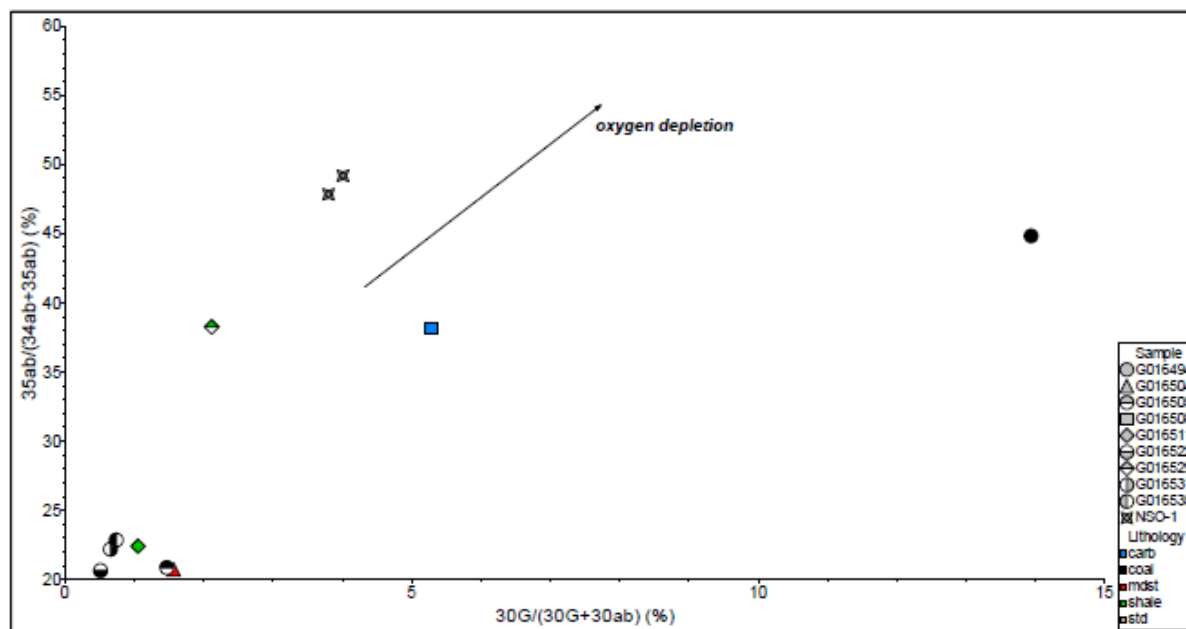


Figure 4-16: Gammacerane index and homohopane index.

A few parameters can be evaluated that help to identify carbonate settings, although it should be noted that they have been developed for oils, so may give erroneous indications for source rock bitumens, particularly at pre-oil window maturity. The tricyclic terpane (22/3)/(21/3) parameter for the Bury Limestone? carbonate sample is consistent with a carbonate setting in Figure 4-17, but the same is true for three of the coals, so the applicability to these extracts is questionable. In Figure 4-18, the carbonate sample is closest to the carbonate zone, but still not within the usual range for the parameters. Consequently, the few carbonate biomarker indicators are not appropriate for the bitumen extracted from the carbonate sample, possibly because it represents migrated hydrocarbons from a different facies, although the saturates/aromatics ratio is rather low for a migrated mature oil.

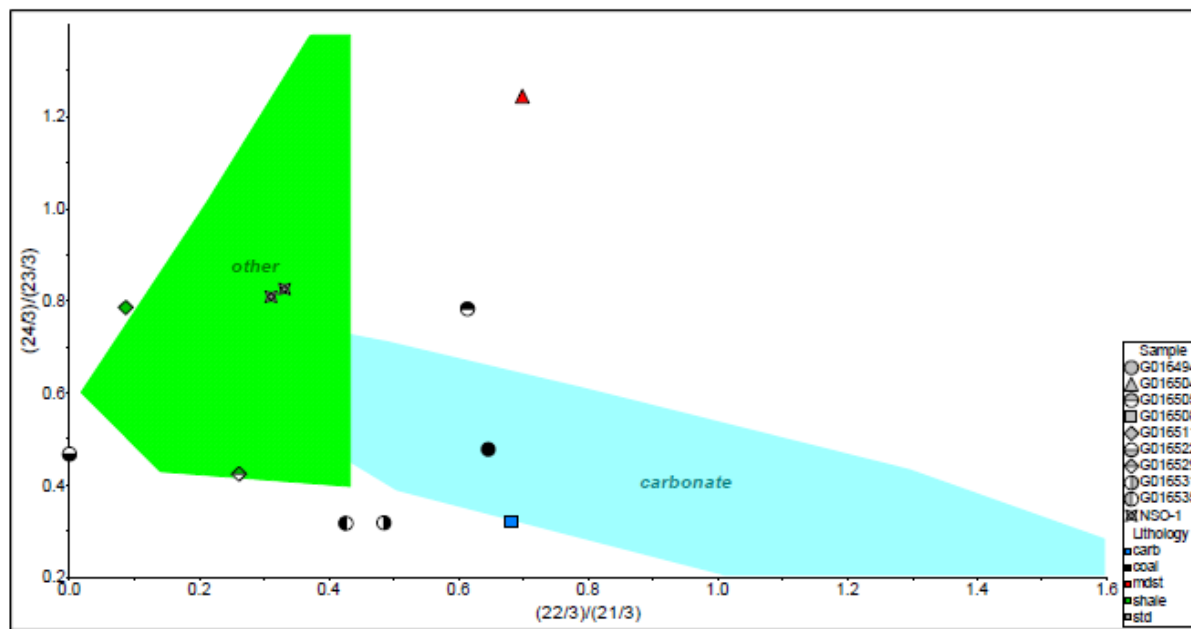


Figure 4-17: Identification of carbonate sourced oils from cheilanthane distributions (after Zumberge in Peters et al. 2005).

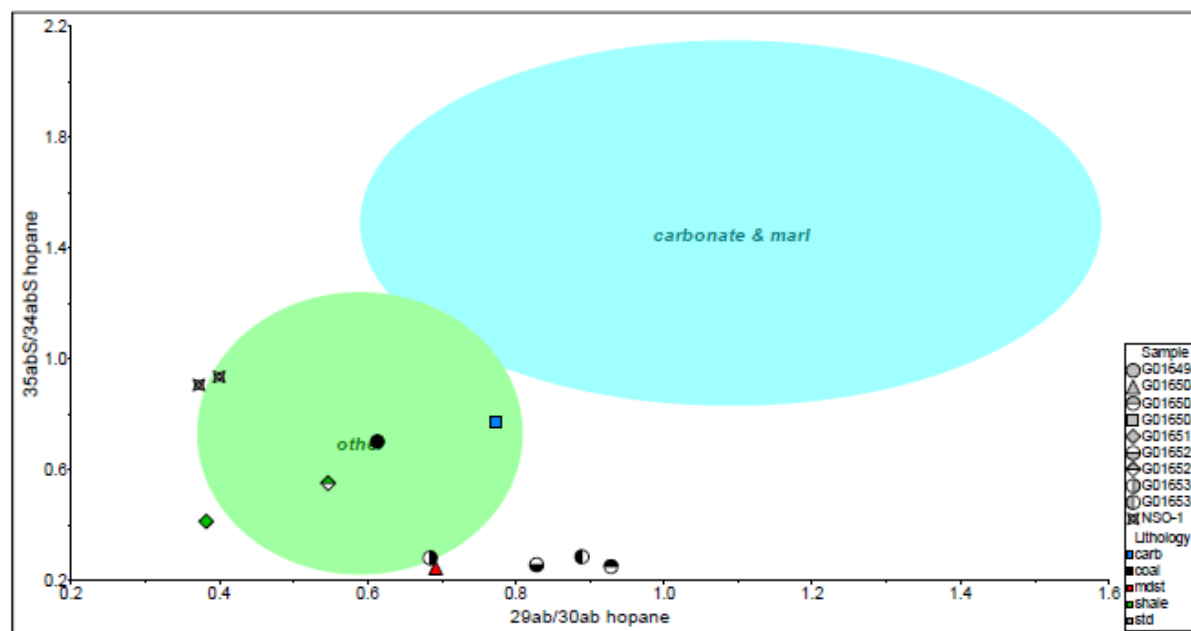


Figure 4-18: Identification of carbonate and marl sourced oils from hopane distributions (after Peters et al. 2005).

Sources

Sterane C-number distributions are shown in Figure 4-19. The coals, mudstone and Bandanna Formation shale (G016511) all plot in the deltaic-terrigenous zone, as expected for humic-dominated organic matter, although the Patchawarra Formation sample (G016494) plots closest to the proximal marine zone, towards the carbonate and the Tinowon Formation shale (G016529). 24-N-propylcholestanes, compounds which are believed to derive from marine phytoplankton (Moldowan et al. 1990), were detected in some of the extracts at very low levels ($\leq 2\%$ cf total C_{27} - C_{30} components), including the Patchawarra Formation coal (G016494) (Figure 4-20). All of the coals and the mudstone exhibit high $(19/3)/(19/3+23/3)$ cheilanthanes ratios, consistent with dominantly humic organic matter, although again the Patchawarra Formation coal (G016494) has the lowest value (Figure 4-20).

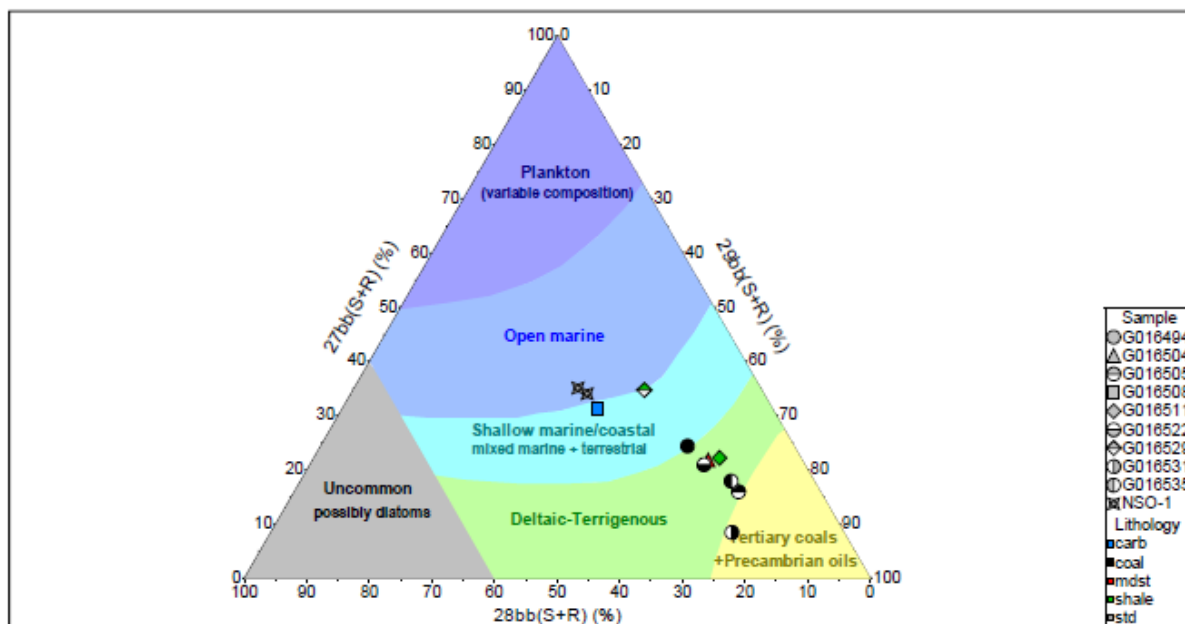


Figure 4-19: Distribution of C_{27} - C_{29} sterane fields for oil sources after Huang & Meinschein 1979, based on $(20S)+(20R)-5\alpha,14\beta,17\beta$ isomers.

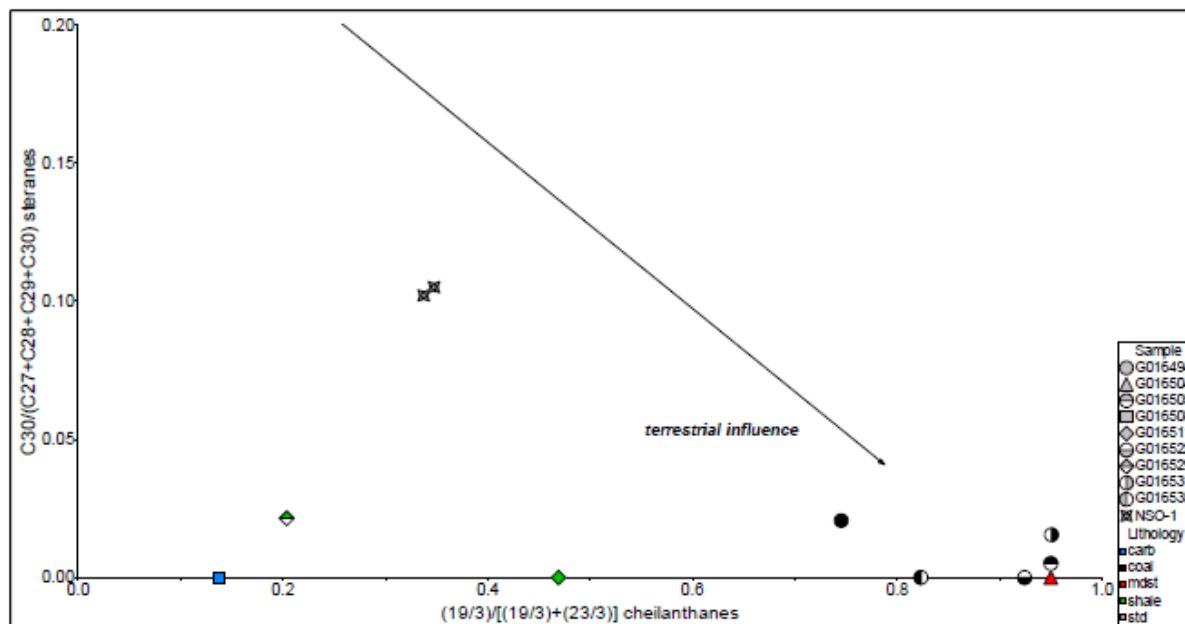


Figure 4-20: Sterane C-number distributions indicative of marine vs terrestrial contributions.

Oleanane, a woody angiosperm marker, was not detected in any of the samples and there are no obvious signs of des-A triterpanes derived from angiosperms. All of the coals and the mudstone exhibit a similar m/z 191 chromatogram to NSO-1 over the retention time range associated with des-A-oleanane (240), des-A-lupane (24L) and des-A-ursane (24U), dominated by cheilhanthes and des-E-hopane (24/4). However, the two shale samples (G016511 and G016529) contain some additional unknown compounds (A-G, Figure 4-21). The absence of detectable angiosperm derived terpanes suggests a pre-Cretaceous age for the coaly samples.

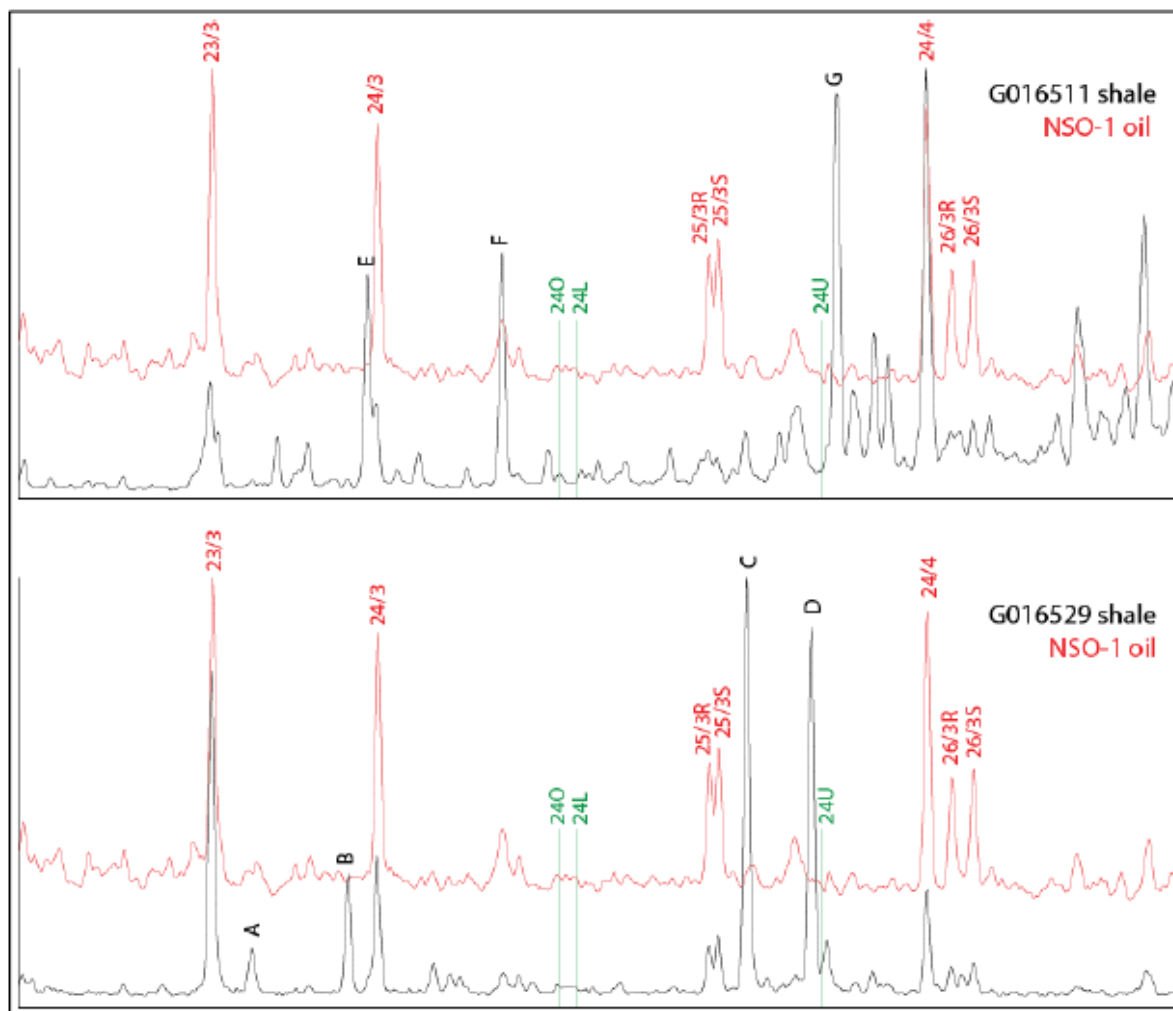


Figure 4-21: Des-A-triterpane region of m/z 191 mass chromatograms for shale samples. Green lines show elution positions of des-A-oleanane, -lupane and -ursane; A-G are major unidentified compounds.

There are significant amounts of diterpenoids in some of the samples, and lesser amounts in others, suggesting that gymnosperms are the main source of the humic organic matter (Figure 4-22). As previously noted, retene is particularly abundant in Birkhead Formation sample G016505 and Cattle Creek Formation (?Riverstone Sandstone Member) sample (G016535), and the tetracyclic diterpanes are major components in the Birkhead Formation mudstone and coals (G016504 and G016505), Cattle Creek Formation (?Riverstone Sandstone Member) sample G016535 and, in particular, the Aldebaran Sandstone sample (G016522). In addition, the first three of those four samples contain much enhanced abundances of diterpenoid derived aromatics (agathalene and pimanthrene), as noted above. On this basis, the coals are most likely to be of Carboniferous to Jurassic age. Of all the coals, the Patchawarra Formation sample G016494 has the least amount of gymnosperm derived diterpanes (although levels are almost as low in G016531 (Tinowon Sandstone Member)). Another distinctive feature of this Patchawarra Formation coal (G016494) is the low $(26/3)/(25/3)$ ratio, much lower than for the other coals but similar to those of the shale and carbonate samples. Beyerane dominates the tetracyclanes in the Birkhead Formation mudstone and coal (G016504 and G016505), but it is slightly subordinate to (α isane + 16β -kaurane) in the Bandanna Formation shale (G016511), whereas 16β -phyllocladane dominates in the Aldebaran Sandstone (G016522) and Cattle Creek Formation (?Riverstone Sandstone Member) (G016535) coals.

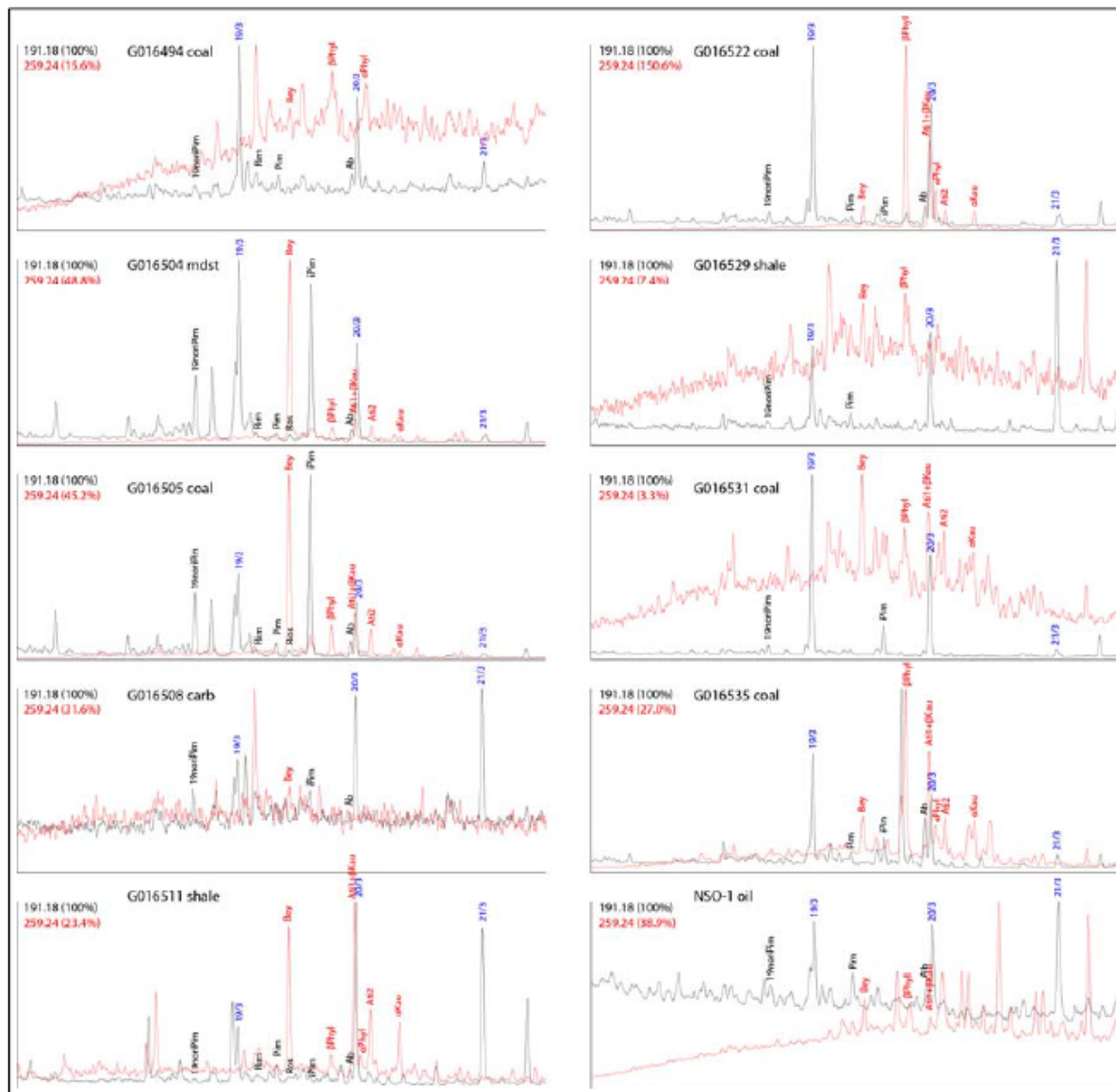


Figure 4-22: Diterpane distributions in m/z 191 and 259 mass chromatograms (NSO-1 shown for comparison).

Table 4-2: Key to diterpane abbreviations.

Tricyclics		Tetracyclics	
19noriPim	19-norisopimarane	Bey	beyerane
Rim	rimuane	β Phyl	16 β -phyllocladane
Pim	pimarane	Ati1	atisane isomer
Ros	rosane	β Kau	16 β -kaurane
iPim	isopimarane	α Phyl	16 α -phyllocladane
Ab	abietane	Ati2	atisane isomer
19/3, 20/3, 21/3	C ₁₉₋₂₁ cheilanthanes	α Kau	16 α -kaurane

Whereas the tetracyclines (m/z 259) are the best indicators of gymnosperm contributions among the diterpanes, the tricyclines (m/z 191) are mostly dominated by cheilanthanes of likely bacterial origin

(probably under saline conditions, possibly related to percolation of seawater into peat deposits during phases of marine transgressions). The exceptions are the samples with the greatest abundance of tetracyclics, which also exhibit abundant isopimarane and minor amounts of some other tricyclics of probably gymnosperm origin. The largest peak in the partial m/z 191 mass chromatogram for Cattle Creek Formation (?Riverstone Sandstone Member) coal (G016535) is of unknown identity. A key to diterpane abbreviations is provided in Table 4-2.

The $\delta^{13}\text{C}$ values for saturates and aromatics are relatively heavy for the coals and mudstone, consistent with humic OM, whereas the carbonate is isotopically lighter and the shales of intermediate isotopic composition (Figure 4-23). The coals tend to straddle the dividing line between terrigenous and marine sources according to Sofer (1984), but this linear discriminant function is known to be less than reliable. There is no clear difference between the coals, other than the slightly lighter Tinowon Sandstone Member sample (G016531), which may be related to greater marine influence in that coal.

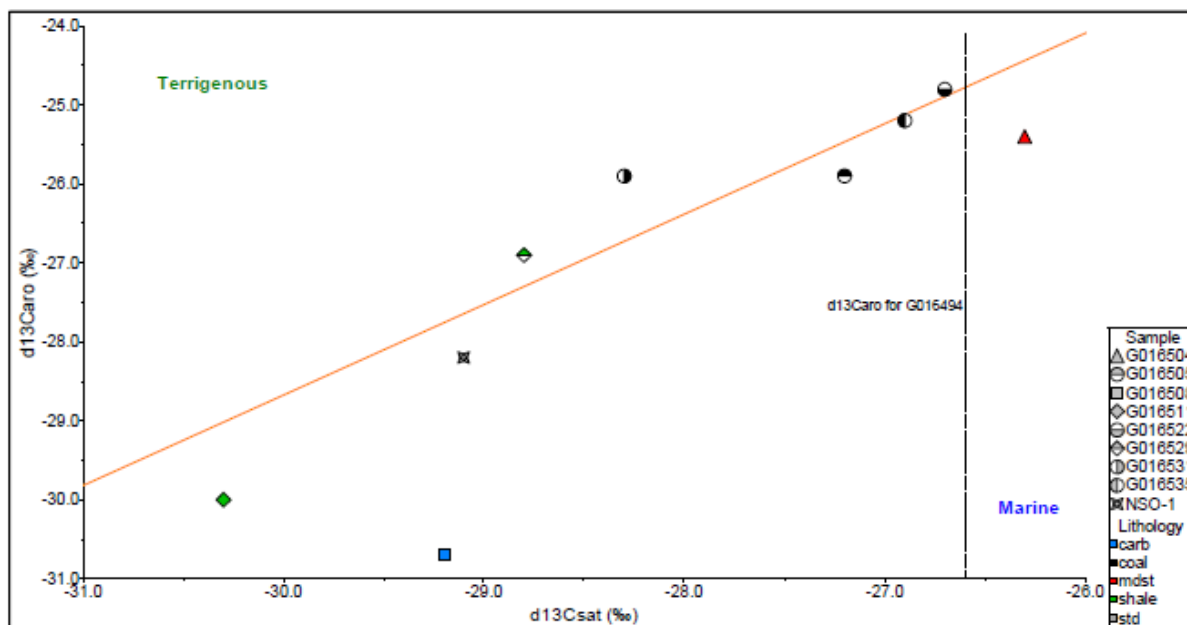


Figure 4-23: Stable C isotopic ratios for saturates and aromatics (terrigenous/marine division after Sofer 1983).

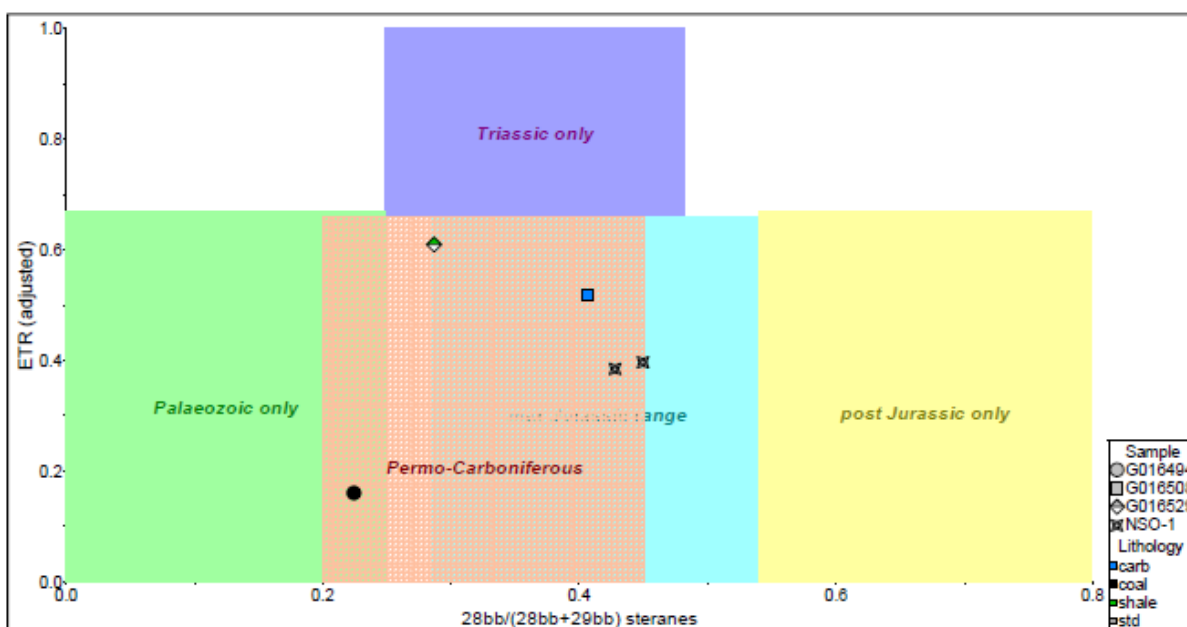


Figure 4-24: Age indications for oil sources based on sterane distributions and ETR.

The ages of the samples analysed in this study are known. However, we here add some age-related biomarker data for completeness.

The following age-related data are available: C₂₈/C₂₉ sterane distributions (after Grantham & Wakefield 1988) and the abundance of C₂₈ plus C₂₉ cheilanthanes (28/3 and 29/3) relative to C₂₇ neohopane (27Ts) (extended tricyclic terpane ratio, or ETR; Holba et al. 2001) are plotted in Figure 4-24. These ratios have been calibrated for marine sourced oils, so can give erroneous ages for oils from humic influenced kerogen and bitumen from immature source rocks. A high ETR was originally suggested to imply a Triassic source, but is now thought to indicate upwelling-associated blooms in general, not necessarily specifically Triassic (Holba et al. 2003). Where peak areas differ markedly between each of the resolved isomers of the cheilanthanes, it is to be suspected that co-elutants are inflating the areas of the most abundant components, and it is recommended that the lower value is doubled, to avoid erroneous ratios. It was only possible to evaluate ETR for a few samples, and age resolution from the sterane ratio is too low to differentiate periods.

Further age indications are possible using aromatic steroids from dinoflagellates and related compounds, as shown in Figure 4-25. The triaromatic dinosteroids (D1-D6) are usually abundant in marine sources of Mesozoic age and their oils, but undetectable in most Palaeozoic samples. However, they can occasionally be present at relatively high levels in Devonian and younger Palaeozoic sources, suggesting a likely origin from the acritarchs from which dinoflagellates evolved (Moldowan et al. 1996). Oils with a degree of contribution from terrestrial organic matter can have slightly lower values than fully marine oils of comparable age. On its own, this age parameter is not helpful, unless sources older than Carboniferous are unlikely, in which event parameter values >0.6 probably indicate post-Permian sources. 23,24-Dimethyl-triaromatic steroids (e.g. M2) are believed to derive from dinoflagellates, haptophytes and diatoms (Barbanti et al. 2011). A non-zero value for the parameter plotted on the y-axis usually suggests post-Palaeozoic origins, so a correlation with dinoflagellate sources appears likely. Again, the ratio appears to be slightly suppressed in the oils from sources containing a contribution from terrestrial organic matter. The data seem to suggest post-Palaeozoic origin for all of the samples, although this conflicts with the Permian age of the coals and on a molecular level by the presence of abundant gymnosperm markers.

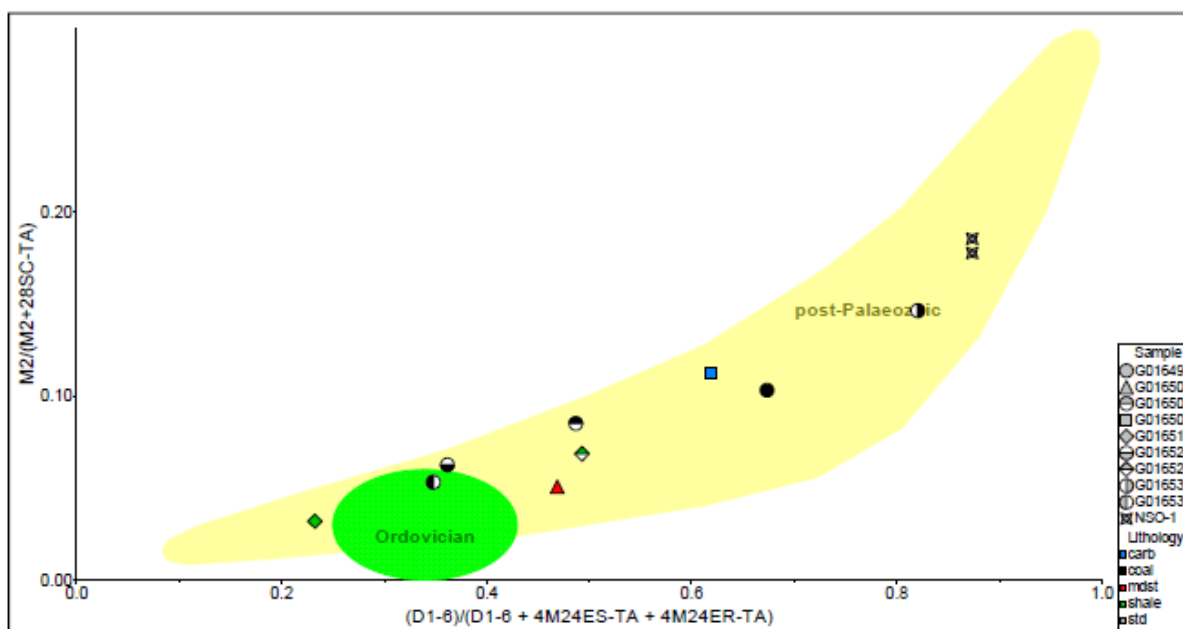


Figure 4-25: Age indications from relative abundance of triaromatic dinosteroids and related compounds (after Barbanti et al. 2011).

A number of attempts have been made to distinguish Permian from Jurassic oils in the Cooper-Eromanga system (see Arouri & McKirdy 2005 for summary review), with a source ratio (1MP/9MP)

plotted against a maturity ratio (2MP/1MP) being one of the most popular methods. These ratios are plotted in Figure 4-26 and are correct in identifying the Birkhead Formation mudstone and coal samples (G016504 and G016505) as Jurassic in age, whereas the other samples are Permian. However, it is questionable whether the parameters can be applied to differentiating individual coal samples (given the known variation in diterpane distributions over small vertical distances). In addition, if it is accepted that methyl group migration occurs during catagenesis, the influence of varying maturity on the 1MP/9MP ratio is an important factor.

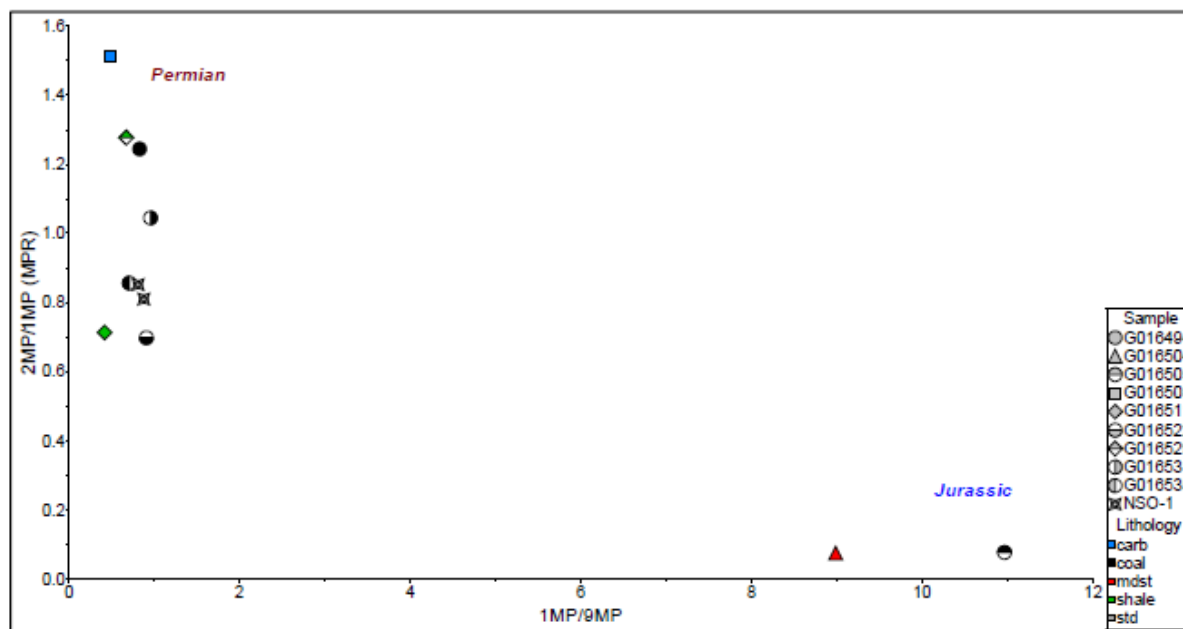


Figure 4-26: Source (1MP/9MP) vs maturity (2MP/1MP) ratios suggested to differentiate Permian from Jurassic sources in the Cooper-Eromanga petroleum system.

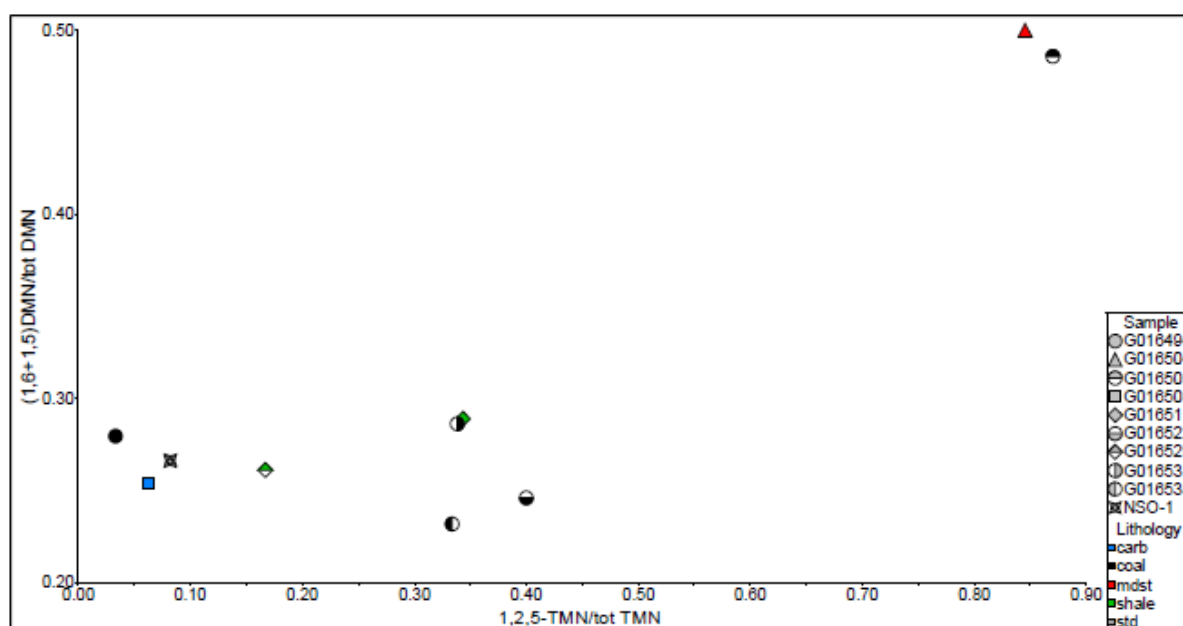


Figure 4-27: Relative abundance of methylated naphthalenes of potential gymnosperm diterpenoid origin.

The relative abundance of methylated naphthalenes and phenanthrenes of potential gymnosperm diterpenoid origin are shown in Figure 4-27 and Figure 4-28, respectively. Again, they demonstrate the difference between the Birkhead Formation mudstone and coal (G016504 and G016505) on the one hand and the other coals and shales on the other. Retene relative abundance does not exhibit such a clear difference (see Figure 4-8), but there is an approximate positive correlation between the concentrations of retene and 1,2,5TMN, but not between retene and 1,7DMP.

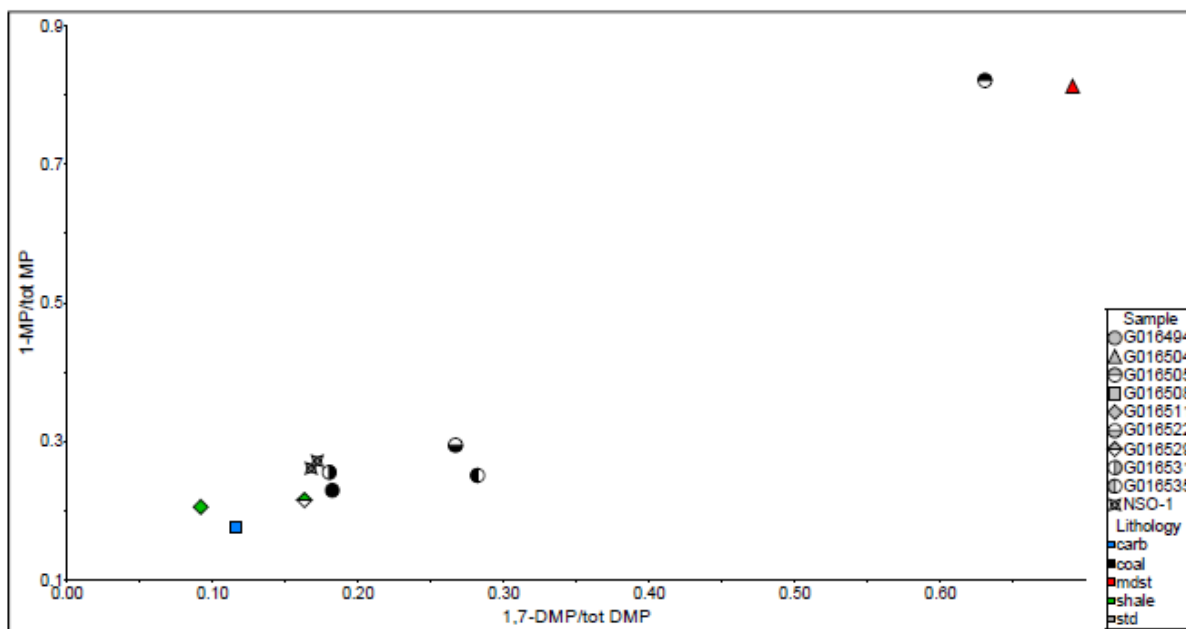


Figure 4-28: Relative abundance of methylated phenanthrenes of potential gymnosperm diterpenoid origin.

Conclusions

Aliphatic biomarker maturity parameters tend to suggest lower maturity than aromatic parameters, but overall the most mature samples appear to be the Patcawarra Formation coal (G016494) and Bury Limestone carbonate (G016508) ($\sim 1.0\% R_o$) and the least mature are the Birkhead Formation mudstone and coal (G016504 G016505) ($\sim 0.6\% R_o$). Variation in carbon preference among *n*-alkanes (monitored via *m/z* 183) generally agree with the inferred maturity differences. Dominant higher plant contributions are apparent for all of the coal, shale and mudstone samples. The carbonate sample exhibits a bimodal *n*-alkane distribution, with what appears to be a higher plant contribution, which appears to be reflected in an estimated Pr/Ph of ~ 3 and lack of obvious carbonate indications among available biomarker data.

The Patchawarra Formation coal sample (G016494) contains relatively abundant 25-norhopane, suggesting considerable bacterial reworking during diagenesis. This also appears to be reflected in the unusual dominance of a complete series of diahopanes over regular hopanes in its *m/z* 191 mass chromatogram. Regular hopane concentrations are low, and the compounds are depleted relative to steranes, so bacterial removal/alteration is confirmed. Cheilanthanes are relatively enriched, and so are diasteranes relative to regular steranes, which suggests that steranes have also been attacked to a degree.

Estimated Pr/Ph values of >3 were obtained for all the coal, shale and mudstone samples, although values for the shales were slightly lower than for the coals. This suggests different environmental conditions, which may be reflected in a range of unidentified compounds in the 23/3 to 26/3 region of their *m/z* 191 mass chromatograms. All samples except for the Bury Limestone carbonate (G016508)

and Tinowon Formation shale sample (G016529) exhibit C₂₉ dominance among steranes and high (19/3)/(23/3) ratios, typical of humicorganic matter.

No angiosperm derived triterpanes were detected in any of the samples, suggesting pre-Cretaceous ages. Gymnosperm derived tetracyclics dominate the diterpanes in the Birkhead Formation mudstone (G016504) and coals G016505 from the Birkhead Formation, G016535 from the Cattle Creek-?Riverstone Sandstone Member and, in particular, G016522 from the Aldebaran Sandstone. They are present but less abundant in the Bandanna Formation shale (G016511), and more sparse still in the other samples, including the Patchawarra Formation coal (G016494) and the Tinowon Sandstone Member coal (G016531). Beyerane is the major tetracycline in the Birkhead Formation samples G016504 and G016505, it is joined by the peak containing an atisane isomer and/or 16β-kaurane in coal G016511, but in the Aldebaran Sandstone sample G016522 and Cattle Creek-?Riverstone Sandstone Member sample G016535 16β-phyllocladane is the dominant diterpane. Whether these distributions have potential as age indicators is debatable, as there is evidence that beyerane/atisane dominance could be related to extent of clay-catalysed diagenetic rearrangement. Tricyclanes of likely gymnosperm origin are present in low abundance in the coaly samples, but subordinate to cheilanthanes in m/z 191 mass chromatograms, other than in the Birkhead Formation samples G016504 and G016505, in which isopimarane is particularly abundant.

The coals are mostly isotopically heavier than the shales and carbonate samples and there is no clear distinction between them, other than Tinowon Sandstone Member sample G016531. This coal is lighter than the others, tending towards the shale composition, but it is probably related to marine influence, given the low levels of gymnosperm diterpanes compared to cheilanthanes. The Birkhead Formation samples G016504 and G016505 appear related and differ markedly from the other coaly samples in terms of their considerable enrichment in aromatic compounds of probably gymnosperm diterpenoid origin: 1,2,5-TMN, 1,6- and 1,5-DMN, 1-MP and 1,7-DMP. These compounds are less obviously enriched in the other coaly samples. In contrast, retene shows a different enrichment pattern which does not clearly distinguish the Birkhead Formation samples G016504 and G016505. There appears to be a broad positive correlation between retene and 1,2,5-TMN concentrations in the extracts, but not between retene and 1,7-DMP.

References

- Arouri K.R., McKirdy D.M. (2005) The behaviour of aromatic hydrocarbons in artificial mixtures of Permian and Jurassic end-member oils: application to in-reservoir mixing in the Eromanga Basin, Australia. *Organic Geochemistry* 36, 105–115.
- Barbanti S.M., Moldowan L.M., Watt D.S., Kolaczkowska E. (2011) New triaromatic steroids distinguish Paleozoic from Mesozoic oil. *Organic Geochemistry* 42, 409–424.
- Bennett B., Fustic M., Farrimond P., Huang H., Larter S.R. (2006) 25-Norhopanes: Formation during biodegradation of petroleum in the subsurface. *Organic Geochemistry* 37, 787–797.
- Grantham P.J., Posthuma J., de Groot K. (1980) Variation and significance of the C₂₇ and C₂₈ triterpane content of a North Sea core and various North Sea crude oils. In (ed. Douglas A.G., Maxwell J.R.) *Advances in Organic Geochemistry 1979*, 29–38. Pergamon Press, Oxford.
- Holba A.G., Ellis L., Dzou I.L., Hallam A., Masterson W.D., Francu J., Fincannon A.L. (2001) Extended tricyclic terpanes as age discriminators between Triassic, Early Jurassic, and Middle-Late Jurassic oils. In: (abs.) 20th International Meeting on Organic Geochemistry, September 10–14, 2001, Nancy-France, vol. 1, p. 464.
- Holba A.G., Zumberge J., Huizinga B.J., Rosenstein H., Dzou L.I. (2003) Extended tricyclic terpanes as indicators of marine upwelling. Abstract OXX1, 21st International Meeting on Organic Geochemistry, September 8–12, 2003, Krakow, Book of Abstracts Part I, 131.
- Huang W.-Y., Meinschein W.G. (1979) Sterols as ecological indicators. *Geochimica et Cosmochimica Acta* 43, 739–745.
- Hughes W.B., Holba A.G., Dzou L.I.P. (1995) The ratios of dibenzothiophene to phenanthrene and pristane to phytane as indicators of depositional environment and lithology of petroleum source rocks. *Geochimica et Cosmochimica Acta* 59, 3581–3598.
- Moldowan J.M., Fago F.J., Lee C.Y., Jacobson S.R., Watt D.S., Slougui N.-E., Jeganathan A., Young D.C. (1990) Sedimentary 24-n-propylcholestanes, molecular fossils diagnostic of marine algae. *Science* 247, 309–312.
- Moldowan M., Fago F.J., Carlson R.M.K., Young D.C., Van Duyne G., Clardy J., Schoell M., Pillinger C.T., Watt D.S. (1991) Rearranged hopanes in sediments and petroleum, *Geochimica et Cosmochimica Acta* 55, 3333–3353.
- Moldowan J.M., Dahl J., Jacobson S.R., Huizinga B.J., Fago F.J., Shetty R., Watt D.S., Peters K.E. (1996) Chemostratigraphic reconstruction of biofacies: Molecular evidence linking cyst-forming dinoflagellates with pre-Triassic ancestors. *Geology* 24, 159–162.
- Peters K.E., Walters C.C., Moldowan J.M. (2005) *The Biomarker Guide* vol 2. Cambridge University Press, Cambridge.
- Radke M. (1988) Application of aromatic compounds as maturity indicators in source rocks and crude oils. *Marine & Petroleum Geology* 5, 224–236.
- Radke M., Welte D.H., Willsch H. (1986) Maturity parameters based on aromatic hydrocarbons: Influence of the organic matter type. *Organic Geochemistry* 10, 51–63.
- Radke M., Rullkötter J., Vriend S.P. (1994) Distribution of naphthalenes in crude oils from the Java Sea: Source and maturation effects. *Geochimica et Cosmochimica Acta* 17, 3675–3689.
- Sofer Z. (1984) Stable carbon isotope compositions of crude oils: application to source depositional environments and petroleum alteration. *AAPG Bulletin* 68, 31–49.
- Wilhelms A., Telnæs N., Steen A., Augustson J. (1998) A quantitative study of aromatic hydrocarbons in a natural maturity shale sequence – the 3-methylphenanthrene/retene ratio, a pragmatic maturity parameter. *Organic Geochemistry* 29, 97–105.
- Zumberge J. E. (1987) Prediction of source rock characteristics based on terpane biomarkers in crude oils: A multivariate statistical approach. *Geochimica et Cosmochimica Acta* 51, 1625–1637.

Appendix - Tables

Table 4-A1: Extraction, asphaltene precipitation and MPLC data.

GEOS4-ID	Basin	Rock weight	EOM	EOM	SAT	ARO	POL	ASP	HC
			g	mg	mg/kg rock	wt% of EOM/Oil			
G016494	Cooper	17.75	22.60	1273	57.00	43.00			100
G016504	Eromanga	16.82	89.30	5308	73.10	26.90			100
G016505	Eromanga	2.96	304.10	102876	56.50	43.50			100
G016508	Adavale	16.56	11.20	677	38.10	61.90			100
G016511	Bowen	8.98	278.60	31026	38.70	61.30			100
G016522	Bowen	7.21	169.20	23473	36.30	63.70			100
G016529	Bowen	20.88	5.00	240	48.60	51.40			100
G016531	Bowen	7.81	106.00	13573	30.00	70.00			100
G016535	Bowen	8.87	223.90	25242	49.60	50.40			100

Table 4-A2: GCMS SIR of saturated compounds (amounts in µg/g).

m/e		177				191			
		25nor28αβ	25nor29αβ	25nor30αβ	25nor31αβ	19/3	20/3	21/3	22/3
G016494	Cooper	2.43E+03	1.67E+03	1.95E+03	2.04E+03	2.27E+04	1.48E+04	4.58E+03	2.96E+03
G016504	Eromanga	0.00E+00	0.00E+00	0.00E+00	2.14E+05	1.02E+05	5.61E+04	4.44E+03	3.10E+03
G016505	Eromanga	5.18E+02	1.29E+03	0.00E+00	3.49E+04	2.20E+04	1.45E+04	1.08E+03	6.62E+02
G016508	Adavale	0.00E+00	1.88E+03	1.06E+03	2.26E+03	3.54E+03	6.90E+03	7.39E+03	5.03E+03
G016511	Bowen	0.00E+00	0.00E+00	2.95E+03	1.25E+05	2.95E+03	9.63E+03	8.29E+03	7.19E+02
G016522	Bowen	5.17E+03	5.64E+03	0.00E+00	1.08E+05	2.55E+04	1.74E+04	1.75E+03	0.00E+00
G016529	Bowen	8.62E+03	1.48E+04	4.21E+03	2.61E+04	4.17E+04	4.90E+04	8.55E+04	2.24E+04
G016531	Bowen	0.00E+00	1.61E+03	0.00E+00	1.67E+05	9.54E+04	5.20E+04	3.69E+03	1.79E+03
G016535	Bowen	0.00E+00	0.00E+00	0.00E+00	8.97E+04	1.51E+04	9.68E+03	1.82E+03	7.77E+02

m/e		191							
		23/3	24/3	25/3R	25/3S	24/4	26/3R	26/3S	28/3R
G016494	Cooper	7.75E+03	3.70E+03	1.29E+03	1.84E+03	1.36E+04	1.04E+03	1.78E+03	2.89E+03
G016504	Eromanga	5.43E+03	6.75E+03	0.00E+00	1.19E+03	2.40E+05	3.60E+03	4.20E+03	0.00E+00
G016505	Eromanga	1.17E+03	9.12E+02	0.00E+00	2.31E+02	3.91E+04	4.76E+02	7.38E+02	0.00E+00
G016508	Adavale	2.21E+04	7.10E+03	1.72E+03	2.30E+03	4.43E+03	1.88E+03	1.65E+03	1.97E+03
G016511	Bowen	3.34E+03	2.62E+03	9.68E+02	7.45E+02	1.27E+04	1.12E+03	1.42E+03	0.00E+00
G016522	Bowen	2.09E+03	9.79E+02	0.00E+00	6.45E+02	7.51E+04	2.15E+03	1.55E+03	0.00E+00
G016529	Bowen	1.63E+05	6.91E+04	2.38E+04	2.93E+04	5.24E+04	1.40E+04	1.61E+04	1.81E+04
G016531	Bowen	4.97E+03	1.58E+03	0.00E+00	7.47E+02	1.65E+05	1.74E+03	2.44E+03	0.00E+00
G016535	Bowen	3.25E+03	1.03E+03	0.00E+00	6.64E+02	4.26E+04	1.20E+03	1.38E+03	0.00E+00

m/e		191							
		28/3S	29/3R	29/3S	27Ts	27Tm	30/3R	30/3S	28αβ
G016494	Cooper	1.27E+03	5.69E+03	1.61E+03	3.00E+04	6.87E+03	2.76E+03	2.57E+03	4.82E+03
G016504	Eromanga	4.88E+03	1.53E+03	0.00E+00	2.34E+05	1.51E+06	1.98E+04	3.72E+04	2.77E+04
G016505	Eromanga	8.16E+02	2.58E+02	0.00E+00	1.78E+04	3.92E+05	3.08E+03	5.45E+03	4.20E+03
G016508	Adavale	1.51E+03	1.32E+03	1.07E+03	5.46E+03	1.43E+04	1.39E+03	1.65E+03	2.41E+03
G016511	Bowen	2.18E+03	0.00E+00	7.85E+03	1.64E+04	9.11E+05	3.30E+03	1.21E+04	2.17E+05
G016522	Bowen	2.58E+03	0.00E+00	0.00E+00	1.91E+04	1.07E+06	8.31E+03	1.27E+04	9.82E+03
G016529	Bowen	1.43E+04	1.06E+04	1.01E+04	3.40E+04	9.51E+04	8.98E+03	9.79E+03	7.33E+03
G016531	Bowen	1.90E+03	1.20E+03	0.00E+00	5.34E+04	8.79E+05	7.21E+03	1.33E+04	2.28E+04
G016535	Bowen	2.70E+03	0.00E+00	0.00E+00	2.27E+04	6.25E+05	0.00E+00	0.00E+00	8.45E+04

m/e		191							
GEOS4-ID	Basin	25nor30αβ	29αβ	29Ts	30d	29βα	300	30αβ	30βα
G016494	Cooper	5.07E+03	8.39E+03	1.66E+04	8.22E+04	6.52E+03	0.00E+00	1.37E+04	3.18E+03
G016504	Eromanga	0.00E+00	2.44E+06	5.05E+05	6.99E+04	7.62E+05	0.00E+00	3.52E+06	1.00E+06
G016505	Eromanga	0.00E+00	5.46E+05	5.08E+04	1.55E+04	1.72E+05	0.00E+00	5.88E+05	2.00E+05
G016508	Adavale	1.68E+03	2.78E+04	6.85E+03	3.12E+03	7.06E+03	0.00E+00	3.60E+04	8.14E+03
G016511	Bowen	7.14E+03	8.38E+05	3.21E+04	7.92E+04	3.93E+05	0.00E+00	2.19E+06	8.35E+05
G016522	Bowen	0.00E+00	1.53E+06	8.75E+04	6.92E+04	6.48E+05	0.00E+00	1.85E+06	8.73E+05
G016529	Bowen	7.34E+03	2.46E+05	5.14E+04	3.48E+04	3.25E+04	0.00E+00	4.49E+05	6.88E+04
G016531	Bowen	0.00E+00	1.94E+06	1.20E+05	1.13E+05	1.39E+05	0.00E+00	2.84E+06	2.72E+05
G016535	Bowen	0.00E+00	1.36E+06	8.61E+04	5.59E+04	3.89E+05	0.00E+00	1.53E+06	5.70E+05

m/e		191							
GEOS4-ID	Basin	31αβS	31αβR	30G	31βα	32αβS	32αβR	33αβS	33αβR
G016494	Cooper	4.74E+03	4.67E+03	2.22E+03	1.59E+03	5.37E+03	2.87E+03	2.49E+03	2.05E+03
G016504	Eromanga	1.20E+06	8.32E+05	5.61E+04	3.70E+05	4.75E+05	3.26E+05	1.89E+05	1.29E+05
G016505	Eromanga	2.54E+05	1.77E+05	8.80E+03	1.06E+05	9.71E+04	6.64E+04	3.78E+04	2.48E+04
G016508	Adavale	1.34E+04	1.09E+04	2.01E+03	4.79E+03	6.15E+03	5.56E+03	3.38E+03	2.34E+03
G016511	Bowen	1.48E+06	2.17E+06	2.34E+04	9.28E+05	1.05E+05	3.78E+05	2.51E+04	9.97E+04
G016522	Bowen	1.16E+06	8.19E+05	9.54E+03	4.34E+05	3.40E+05	2.30E+05	1.31E+05	9.27E+04
G016529	Bowen	1.89E+05	1.38E+05	9.71E+03	3.89E+04	1.04E+05	7.11E+04	5.36E+04	3.63E+04
G016531	Bowen	1.19E+06	7.86E+05	1.88E+04	1.30E+05	4.81E+05	3.17E+05	2.14E+05	1.35E+05
G016535	Bowen	8.45E+05	5.73E+05	1.15E+04	2.72E+05	3.00E+05	2.08E+05	1.79E+05	1.14E+05

m/e		191			
GEOS4-ID	Basin	34αβS	34αβR	35αβS	35αβR
G016494	Cooper	1.89E+03	1.28E+03	1.33E+03	1.25E+03
G016504	Eromanga	9.13E+04	5.83E+04	2.23E+04	1.68E+04
G016505	Eromanga	1.80E+04	1.08E+04	4.52E+03	3.10E+03
G016508	Adavale	2.89E+03	2.22E+03	2.23E+03	9.25E+02
G016511	Bowen	1.40E+04	5.32E+04	5.80E+03	1.36E+04
G016522	Bowen	6.08E+04	4.01E+04	1.56E+04	1.07E+04
G016529	Bowen	3.46E+04	2.25E+04	1.91E+04	1.63E+04
G016531	Bowen	9.86E+04	6.18E+04	2.77E+04	1.80E+04
G016535	Bowen	7.34E+04	4.57E+04	2.09E+04	1.43E+04

m/e		217							
GEOS4-ID	Basin	21 $\alpha\alpha$	21 $\beta\beta$	22 $\alpha\alpha$	22 $\beta\beta$	27d $\beta\$$	27d βR	27d αR	27d αS
G016494	Cooper	2.95E+03	4.20E+03	2.82E+03	2.40E+03	4.16E+03	2.75E+03	1.55E+03	1.69E+03
G016504	Eromanga	3.83E+03	3.32E+03	2.12E+03	1.80E+03	6.66E+03	5.02E+03	2.24E+03	2.87E+03
G016505	Eromanga	1.05E+03	1.05E+03	7.13E+02	3.77E+02	9.90E+02	6.58E+02	5.60E+02	4.84E+02
G016508	Adavale	1.42E+03	3.07E+03	1.07E+03	1.71E+03	1.38E+03	9.13E+02	5.76E+02	6.95E+02
G016511	Bowen	6.42E+02	2.44E+03	4.87E+02	9.84E+02	9.11E+03	6.99E+03	4.34E+03	3.81E+03
G016522	Bowen	2.32E+03	3.87E+03	1.55E+03	1.70E+03	2.78E+03	2.07E+03	1.23E+03	1.67E+03
G016529	Bowen	2.15E+04	1.93E+04	1.70E+04	8.97E+03	3.54E+04	2.13E+04	1.02E+04	1.21E+04
G016531	Bowen	3.32E+03	5.87E+03	3.01E+03	3.15E+03	2.39E+03	1.47E+03	9.93E+02	1.16E+03
G016535	Bowen	3.04E+03	4.90E+03	1.67E+03	1.79E+03	3.91E+03	2.43E+03	1.66E+03	1.84E+03

m/e		217								
GEOS4-ID	Basin	28d $\beta\$#1$	28d $\beta\$#2$	28d $\beta R#1$	28d $\beta R#2$	28d αR	27 $\alpha\alpha S$	27 $\beta\beta R+2$ 9d $\beta\$$	27 $\beta\beta S$	28d αS
G016494	Cooper	5.49E+03	8.67E+03	3.34E+03	4.88E+03	4.16E+03	1.73E+03	3.35E+04	4.18E+03	2.60E+03
G016504	Eromanga	1.86E+04	1.95E+04	9.92E+03	1.48E+04	1.12E+04	7.43E+03	1.42E+05	0.00E+00	8.08E+03
G016505	Eromanga	2.88E+03	3.01E+03	1.29E+03	2.18E+03	2.45E+03	1.55E+03	2.52E+04	1.10E+03	1.44E+03
G016508	Adavale	7.10E+02	6.58E+02	5.30E+02	6.06E+02	7.84E+02	1.48E+03	2.64E+03	1.08E+03	6.57E+02
G016511	Bowen	2.80E+03	2.97E+03	2.96E+03	3.93E+03	3.04E+03	1.25E+04	3.15E+04	3.73E+03	1.30E+03
G016522	Bowen	5.94E+03	6.01E+03	2.85E+03	5.12E+03	4.04E+03	3.35E+03	4.32E+04	2.21E+03	2.90E+03
G016529	Bowen	1.44E+04	1.37E+04	7.11E+03	8.91E+03	6.69E+03	1.05E+04	4.46E+04	1.13E+04	4.85E+03
G016531	Bowen	3.92E+03	3.87E+03	1.74E+03	3.43E+03	2.75E+03	1.67E+03	2.34E+04	2.51E+03	1.87E+03
G016535	Bowen	9.92E+03	1.06E+04	5.06E+03	7.28E+03	7.10E+03	3.80E+03	8.29E+04	4.09E+03	4.43E+03

m/e		217							
GEOS4-ID	Basin	27 $\alpha\alpha R$	29d βR	29d αR	28 $\alpha\alpha S$	29d αS	28 $\beta\beta R$	28 $\beta\beta S$	28 $\alpha\alpha R$
G016494	Cooper	1.75E+03	1.94E+04	9.91E+03	3.36E+03	1.25E+04	3.72E+03	5.38E+03	1.78E+03
G016504	Eromanga	1.07E+04	9.15E+04	3.89E+04	1.87E+04	7.71E+04	1.69E+04	1.36E+04	6.16E+04
G016505	Eromanga	1.28E+03	1.74E+04	6.40E+03	3.68E+03	1.60E+04	2.93E+03	2.78E+03	1.08E+04
G016508	Adavale	2.01E+03	1.58E+03	8.79E+02	0.00E+00	1.01E+03	8.76E+02	1.03E+03	8.71E+02
G016511	Bowen	3.88E+04	2.05E+04	9.67E+03	1.60E+03	2.98E+04	1.06E+04	5.53E+03	1.66E+04
G016522	Bowen	4.63E+03	2.70E+04	1.27E+04	5.40E+03	3.66E+04	6.29E+03	4.58E+03	1.37E+04
G016529	Bowen	9.49E+03	2.52E+04	1.17E+04	4.52E+03	1.71E+04	7.45E+03	1.02E+04	5.32E+03
G016531	Bowen	1.86E+03	1.54E+04	7.70E+03	3.88E+03	2.63E+04	7.71E+03	1.01E+04	1.19E+04
G016535	Bowen	4.70E+03	5.23E+04	2.18E+04	1.11E+04	4.42E+04	9.74E+03	1.03E+04	2.36E+04

m/e		217							
GEOS4-ID	Basin	29ααS	29ββR	29ββS	29ααR	30ααS	30ββR	30ββS	30ααR
G016494	Cooper	6.90E+03	1.30E+04	1.11E+04	7.21E+03	2.24E+03	1.70E+03	9.99E+02	6.76E+02
G016504	Eromanga	1.52E+05	5.99E+04	4.58E+04	2.86E+05	0.00E+00	0.00E+00	0.00E+00	1.70E+03
G016505	Eromanga	3.20E+04	1.65E+04	1.22E+04	4.47E+04	0.00E+00	0.00E+00	0.00E+00	3.16E+02
G016508	Adavale	1.41E+03	1.75E+03	1.68E+03	2.16E+03	5.40E+02	0.00E+00	0.00E+00	0.00E+00
G016511	Bowen	9.38E+03	3.46E+04	1.92E+04	1.81E+05	0.00E+00	0.00E+00	0.00E+00	2.68E+03
G016522	Bowen	4.51E+04	2.17E+04	1.50E+04	8.13E+04	0.00E+00	0.00E+00	0.00E+00	5.26E+02
G016529	Bowen	1.50E+04	1.94E+04	1.64E+04	1.49E+04	3.64E+03	0.00E+00	0.00E+00	1.20E+03
G016531	Bowen	2.87E+04	4.12E+04	2.88E+04	3.92E+04	4.22E+04	0.00E+00	0.00E+00	4.49E+03
G016535	Bowen	1.04E+05	5.30E+04	3.46E+04	1.52E+05	0.00E+00	0.00E+00	0.00E+00	6.31E+02

m/e		218							
GEOS4-ID	Basin	27ββR	27ββS	28ββR	28ββS	29ββR	29ββS	30ββR	30ββS
G016494	Cooper	1.51E+04	2.94E+03	4.88E+03	7.65E+03	2.34E+04	1.99E+04	9.23E+02	6.28E+02
G016504	Eromanga	6.17E+04	4.90E+03	2.14E+04	2.41E+04	1.03E+05	8.90E+04	0.00E+00	0.00E+00
G016505	Eromanga	1.15E+04	8.27E+02	4.45E+03	5.57E+03	3.05E+04	2.40E+04	0.00E+00	3.86E+02
G016508	Adavale	2.48E+03	1.67E+03	1.50E+03	2.18E+03	2.78E+03	2.60E+03	0.00E+00	0.00E+00
G016511	Bowen	1.86E+04	6.81E+03	8.36E+03	6.35E+03	4.27E+04	3.12E+04	0.00E+00	0.00E+00
G016522	Bowen	1.95E+04	1.97E+03	7.74E+03	8.60E+03	3.57E+04	2.83E+04	0.00E+00	0.00E+00
G016529	Bowen	3.27E+04	2.09E+04	1.35E+04	1.52E+04	3.63E+04	3.50E+04	1.43E+03	1.93E+03
G016531	Bowen	1.09E+04	3.58E+03	1.35E+04	1.70E+04	6.91E+04	5.61E+04	0.00E+00	2.68E+03
G016535	Bowen	3.68E+04	3.38E+03	1.22E+04	1.73E+04	8.61E+04	6.75E+04	0.00E+00	0.00E+00

Table 4-A3: GCMS SIR of saturated compounds (parameters).

Sample	Basin	%23:3	%28ab	%30D	%27Ts	%22S	%29Ts	%20S	%bb	%27dbs	%C27	%C29	28/29	24:4/23:3
G016494	Cooper	36.16	26.05	85.74	81.36	65.19	54.83	48.90	63.13	54.46	24.45	58.61	0.37	1.76
G016504	Eromanga	0.15	0.78	1.94	13.45	59.31	12.54	34.65	19.44	26.84	21.89	63.15	0.20	44.31
G016505	Eromanga	0.20	0.71	2.57	4.34	59.41	7.96	41.73	27.21	25.96	16.06	70.89	0.19	33.53
G016508	Adavale	38.10	6.27	7.98	27.64	52.52	16.01	39.59	49.00	28.38	31.41	40.74	0.40	0.20
G016511	Bowen	0.15	9.01	3.49	1.77	21.79	1.45	4.93	22.03	15.09	22.30	64.80	0.14	3.80
G016522	Bowen	0.11	0.53	3.60	1.75	59.57	4.51	35.68	22.50	25.87	21.06	62.88	0.18	35.88

G016529	Bowen	26.63	1.61	7.20	26.33	59.32	10.28	50.19	54.61	63.88	34.85	46.48	0.42	0.32
G016531	Bowen	0.17	0.80	3.81	5.72	60.25	4.06	42.26	50.73	40.36	8.50	73.60	0.24	33.11
G016535	Bowen	0.21	5.24	3.53	3.51	59.05	5.33	40.72	25.48	31.50	18.01	68.77	0.16	13.12

Table 4-A4: GCMS SIR of aromatic compounds (amounts in µg/g).

m/e		142		156					
		2-MN	1-MN	2-EN	1-EN	2,6-DMN	2,7-DMN	1,3- + 1,7-DMN	1,6-DMN
G016494	Cooper	2.56E+06	1.36E+06	1.29E+05	2.68E+04	8.62E+05	7.87E+05	1.36E+06	1.20E+06
G016504	Eromanga	1.61E+05	1.24E+05	1.90E+03	2.83E+03	2.17E+04	2.48E+04	7.80E+04	1.25E+05
G016505	Eromanga	4.75E+05	3.31E+05	1.55E+04	1.12E+04	5.51E+04	5.95E+04	1.70E+05	2.95E+05
G016508	Adavale	2.97E+06	1.71E+06	1.35E+05	4.63E+04	6.21E+05	6.80E+05	1.17E+06	8.85E+05
G016511	Bowen	4.07E+04	4.77E+04	2.93E+03	2.79E+03	1.03E+04	7.59E+03	2.85E+04	2.32E+04
G016522	Bowen	1.18E+06	6.26E+05	7.08E+04	4.36E+04	1.41E+05	1.49E+05	4.39E+05	3.04E+05
G016529	Bowen	3.71E+06	1.96E+06	2.03E+05	1.14E+05	6.19E+05	7.09E+05	1.38E+06	1.11E+06
G016531	Bowen	5.83E+06	2.60E+06	1.13E+05	6.99E+04	5.52E+05	5.76E+05	1.36E+06	1.17E+06
G016535	Bowen	4.83E+06	1.36E+06	1.37E+05	7.70E+04	3.06E+05	3.46E+05	8.32E+05	5.72E+05

m/e		156				170			
		2,3- + 1,4-DMN	1,5-DMN	1,2-DMN	1,8-DMN	1,3,7- TMN	1,3,6- TMN	1,3,5- + 1,4,6- TMN	2,3,6- TMN
G016494	Cooper	4.26E+05	2.21E+05	8.39E+04	4.02E+02	3.12E+05	4.06E+05	2.29E+05	3.93E+05
G016504	Eromanga	3.59E+04	5.91E+04	1.91E+04	2.66E+02	8.88E+03	1.91E+04	4.04E+04	1.10E+04
G016505	Eromanga	8.88E+04	1.43E+05	6.25E+04	1.19E+03	2.15E+04	4.03E+04	8.92E+04	2.59E+04
G016508	Adavale	3.74E+05	1.79E+05	1.00E+05	2.71E+02	1.62E+05	2.36E+05	1.26E+05	2.12E+05
G016511	Bowen	1.50E+04	6.74E+03	5.80E+03	7.63E+02	3.51E+03	6.45E+03	6.59E+03	3.71E+03
G016522	Bowen	2.76E+05	9.47E+04	9.89E+04	4.78E+03	6.16E+04	9.63E+04	1.15E+05	7.04E+04
G016529	Bowen	5.24E+05	2.41E+05	2.80E+05	6.50E+02	2.41E+05	3.85E+05	2.50E+05	3.37E+05
G016531	Bowen	5.70E+05	2.33E+05	2.53E+05	7.42E+02	1.76E+05	2.35E+05	2.18E+05	2.31E+05
G016535	Bowen	4.27E+05	1.16E+05	1.50E+05	6.22E+03	8.95E+04	1.27E+05	1.25E+05	1.04E+05

m/e		170			178	192				
		1,2,7- TMN	1,6,7 + 1,2,6- TMN	1,2,4- TMN	1,2,5- TMN	P	3-MP	2-MP	9-MP	1-MP
G016494	Cooper	2.83E+04	2.00E+05	1.08E+04	5.43E+04	2.07E+06	9.58E+05	1.31E+06	1.27E+06	1.05E+06
G016504	Eromanga	6.15E+03	2.81E+04	2.23E+03	6.33E+05	3.10E+05	3.99E+04	7.17E+04	1.05E+05	9.43E+05
G016505	Eromanga	1.68E+04	6.66E+04	7.49E+03	1.79E+06	3.59E+05	4.88E+04	7.71E+04	9.10E+04	9.98E+05
G016508	Adavale	2.57E+04	1.24E+05	1.19E+04	6.05E+04	6.36E+06	1.81E+06	2.47E+06	3.34E+06	1.64E+06
G016511	Bowen	1.26E+03	6.89E+03	1.12E+03	1.54E+04	6.82E+04	9.32E+03	8.70E+03	2.91E+04	1.22E+04
G016522	Bowen	2.29E+04	1.07E+05	1.62E+04	3.26E+05	1.51E+06	2.24E+05	2.66E+05	4.22E+05	3.81E+05
G016529	Bowen	8.32E+04	2.96E+05	3.87E+04	3.27E+05	4.68E+06	1.58E+06	2.27E+06	2.65E+06	1.78E+06
G016531	Bowen	6.36E+04	2.77E+05	3.14E+04	6.31E+05	2.25E+06	6.95E+05	8.88E+05	8.92E+05	8.50E+05
G016535	Bowen	3.40E+04	1.34E+05	2.11E+04	3.18E+05	2.06E+06	2.70E+05	3.27E+05	5.41E+05	3.81E+05

m/e		206									
		2-EP+9-EP+3,6-DMP	1-EP	2,6- + 2,7- + 3,5-DMP	1,3- + 2,10- + 3,9- + 3,10-DMP	1,6- + 2,5- + 2,9-DMP	1,7-DMP	2,3-DMP	1,9- + 4,9- + 4,10-DMP	1,8-DMP	1,2-DMP
G016494	Cooper	8.89E+04	2.38E+05	2.07E+05	8.49E+05	4.59E+05	5.23E+05	1.75E+05	2.02E+05	9.30E+04	3.63E+04
G016504	Eromanga	4.62E+03	7.93E+03	6.25E+03	2.86E+04	9.53E+04	6.87E+05	9.90E+03	3.38E+04	4.04E+04	8.07E+04
G016505	Eromanga	6.22E+03	1.04E+04	7.17E+03	3.51E+04	8.39E+04	5.71E+05	1.25E+04	3.60E+04	4.07E+04	1.03E+05
G016508	Adavale	1.32E+05	3.46E+05	2.50E+05	1.27E+06	6.24E+05	4.32E+05	2.41E+05	2.70E+05	9.05E+04	5.89E+04
G016511	Bowen	3.50E+03	2.94E+03	4.46E+03	9.77E+03	3.04E+03	3.01E+03	1.63E+03	2.21E+03	8.86E+02	1.32E+03
G016522	Bowen	2.26E+04	3.47E+04	1.73E+04	1.01E+05	5.93E+04	1.41E+05	3.19E+04	5.34E+04	3.04E+04	3.64E+04
G016529	Bowen	1.56E+05	3.50E+05	2.37E+05	1.13E+06	5.57E+05	6.42E+05	2.64E+05	3.28E+05	1.36E+05	1.34E+05
G016531	Bowen	7.49E+04	1.54E+05	9.58E+04	4.37E+05	2.62E+05	3.27E+05	1.38E+05	1.68E+05	7.17E+04	9.00E+04
G016535	Bowen	2.53E+04	3.68E+04	1.90E+04	1.13E+05	6.26E+04	1.66E+05	3.50E+04	5.77E+04	3.03E+04	4.24E+04

m/e		219	184	198			253		
		Retene	DBT	4-MDBT	(3+2)-MDBT	1-MDBT	C21MA	C22MA	βSC27MA
G016494	Cooper	1.08E+04	6.86E+04	1.01E+05	5.70E+04	1.78E+04	2.89E+02	4.70E+02	8.80E+01
G016504	Eromanga	1.99E+05	2.78E+02	3.65E+02	1.92E+02	2.17E+02	3.13E+02	4.89E+02	1.28E+02
G016505	Eromanga	6.71E+05	1.20E+03	1.38E+03	8.41E+02	1.08E+03	4.69E+02	3.95E+02	8.10E+01
G016508	Adavale	2.17E+04	4.69E+05	1.45E+06	2.49E+05	6.09E+04	2.10E+02	1.95E+02	5.70E+01
G016511	Bowen	4.22E+03	5.97E+02	6.56E+02	2.74E+02	4.45E+02	1.94E+03	1.41E+03	2.94E+03
G016522	Bowen	5.71E+05	1.57E+04	1.30E+04	8.21E+03	5.88E+03	2.81E+03	2.22E+03	2.55E+02
G016529	Bowen	4.99E+04	3.32E+05	3.22E+05	2.62E+05	7.67E+04	1.92E+03	1.78E+03	3.17E+02
G016531	Bowen	2.14E+05	3.32E+04	3.35E+04	3.18E+04	1.29E+04	4.92E+02	3.74E+02	5.30E+01
G016535	Bowen	4.03E+06	2.49E+04	1.78E+04	1.49E+04	8.19E+03	3.04E+03	2.19E+03	2.40E+02

m/e		253									
		Sample	Basin	βSC27DMA	βRC27MA+ βRC27DMA	αSC27MA	βSC28MA+ βSC28DMA+ αRC27DMA	αSC27DMA	αRC27MA	αSC28MA	βRC28MA+ βRC28DMA
G016494	Cooper			1.05E+02	1.51E+02	6.30E+01	2.82E+02	9.00E+01	7.40E+01	2.05E+02	1.20E+03
G016504	Eromanga			5.07E+02	3.79E+02	3.24E+02	2.48E+03	5.04E+02	0.00E+00	4.89E+02	1.81E+03
G016505	Eromanga			2.64E+02	1.72E+02	7.60E+01	1.22E+03	4.00E+02	2.10E+01	1.90E+02	9.32E+02
G016508	Adavale			7.50E+01	4.70E+01	3.70E+01	1.61E+02	4.10E+01	5.10E+01	1.38E+02	1.20E+02
G016511	Bowen			1.04E+04	1.25E+04	1.41E+04	1.46E+04	1.96E+03	8.69E+03	8.54E+03	1.39E+04
G016522	Bowen			1.75E+03	1.45E+03	4.98E+02	5.55E+03	1.75E+03	3.70E+02	1.25E+03	4.11E+03
G016529	Bowen			1.59E+03	1.31E+03	3.78E+02	2.19E+03	4.76E+02	2.45E+02	6.51E+02	1.15E+03
G016531	Bowen			1.53E+02	1.84E+02	8.50E+01	4.65E+02	3.44E+02	7.60E+01	6.08E+02	8.18E+02
G016535	Bowen			1.94E+03	1.54E+03	3.12E+02	7.52E+03	2.51E+03	2.23E+02	1.00E+03	5.58E+03

m/e		253				231			
		$\beta\text{SC29MA} + \beta\text{SC29DMA}$	αSC29MA	$\alpha\text{RC28MA} + \beta\text{RC29MA} + \beta\text{RC29DMA}$	αRC29MA	C20TA	C21TA	SC26TA	RC26TA + SC27TA
G016494	Cooper	1.20E+03	1.31E+02	2.84E+02	1.14E+02	2.12E+03	2.46E+03	2.50E+02	4.86E+02
G016504	Eromanga	9.05E+03	1.21E+03	6.01E+03	9.40E+02	2.67E+03	3.36E+03	5.10E+03	2.74E+04
G016505	Eromanga	4.79E+03	4.49E+02	3.13E+03	2.53E+02	3.32E+03	2.47E+03	1.69E+03	8.47E+03
G016508	Adavale	3.09E+02	7.50E+01	2.06E+02	5.60E+01	2.79E+03	1.72E+03	1.43E+02	3.53E+02
G016511	Bowen	4.83E+04	2.95E+04	4.00E+04	2.30E+04	1.10E+03	8.34E+02	6.24E+03	1.27E+04
G016522	Bowen	2.23E+04	2.74E+03	1.67E+04	1.53E+03	6.53E+03	5.17E+03	3.54E+03	1.18E+04
G016529	Bowen	2.43E+03	7.07E+02	1.86E+03	3.11E+02	2.18E+04	1.65E+04	4.04E+03	8.07E+03
G016531	Bowen	2.24E+03	3.35E+02	1.07E+03	2.99E+02	1.14E+04	8.77E+03	1.10E+03	2.16E+03
G016535	Bowen	3.33E+04	3.69E+03	2.32E+04	2.07E+03	6.97E+03	5.05E+03	4.42E+03	1.74E+04

m/e		231						245	
		M1	M2	SC28TA	RC27TA	M3	M4	RC28TA	3MS-TA
G016494	Cooper	9.50E+01	7.40E+01	6.43E+02	3.41E+02	1.07E+02	1.55E+02	6.27E+02	1.44E+02
G016504	Eromanga	9.94E+02	4.06E+03	7.62E+04	1.51E+04	9.60E+02	8.62E+02	8.27E+04	3.06E+03
G016505	Eromanga	2.80E+02	1.89E+03	2.03E+04	4.56E+03	3.44E+02	3.21E+02	2.14E+04	6.65E+02
G016508	Adavale	1.18E+02	1.07E+02	8.47E+02	2.24E+02	6.10E+01	9.50E+01	6.86E+02	7.30E+01
G016511	Bowen	3.43E+02	5.88E+02	1.78E+04	4.04E+03	8.59E+03	2.95E+02	1.78E+04	7.32E+02
G016522	Bowen	3.79E+02	1.55E+03	2.31E+04	5.61E+03	6.52E+02	2.71E+03	2.57E+04	8.64E+02
G016529	Bowen	3.13E+02	3.42E+02	4.64E+03	2.71E+03	2.55E+02	2.88E+02	4.86E+03	6.19E+02
G016531	Bowen	2.62E+02	7.33E+02	4.27E+03	1.22E+03	5.23E+02	5.12E+02	4.46E+03	3.97E+02
G016535	Bowen	2.90E+02	2.36E+03	4.21E+04	8.92E+03	7.17E+02	4.25E+02	4.69E+04	8.52E+02

m/e		245							
		4MS-TA	2,24DMS-TA	3,24DMS+3MR-TA	4,24DMS+4MR-TA	D1-TA	3M24ES-TA	D2-TA	4M24ES-TA
G016494	Cooper	1.39E+02	9.20E+01	2.56E+02	2.31E+02	1.47E+02	2.29E+02	2.30E+02	5.22E+02
G016504	Eromanga	1.14E+04	2.84E+03	8.54E+03	6.25E+04	1.05E+03	2.11E+04	1.73E+03	1.27E+04
G016505	Eromanga	4.01E+03	6.78E+02	2.16E+03	8.61E+03	3.53E+02	4.82E+03	5.67E+02	3.78E+03
G016508	Adavale	1.83E+02	0.00E+00	1.34E+02	4.04E+02	5.90E+01	2.71E+02	7.00E+01	1.94E+02
G016511	Bowen	5.63E+03	5.59E+02	2.62E+03	3.57E+03	7.79E+02	7.41E+03	5.87E+02	5.69E+03
G016522	Bowen	4.24E+03	6.65E+02	2.45E+03	3.13E+03	3.43E+02	6.92E+03	1.20E+03	5.59E+03
G016529	Bowen	7.48E+02	3.73E+02	1.01E+03	7.26E+02	7.40E+01	9.22E+02	2.10E+02	7.85E+02
G016531	Bowen	8.93E+02	4.99E+02	6.44E+02	5.89E+02	2.28E+02	1.36E+03	6.95E+02	1.29E+03
G016535	Bowen	4.62E+03	9.14E+02	4.01E+03	4.16E+03	3.58E+02	1.19E+04	1.22E+03	5.70E+03

m/e		245									
		3,24DMR-TA	4,24DMR-TA	D3-TA	D4-TA	2M24ER-TA	3M24ER-TA	D5-TA	4M24ER-TA	D6-TA	
G016494	Cooper	1.65E+02	1.98E+02	3.66E+02	2.42E+02	7.80E+01	2.79E+02	2.48E+02	2.46E+02	3.48E+02	
G016504	Eromanga	5.86E+03	3.15E+04	1.25E+04	3.66E+03	1.13E+04	2.29E+04	1.67E+03	1.29E+04	1.98E+03	
G016505	Eromanga	1.28E+03	4.99E+03	2.92E+03	1.40E+03	3.30E+03	4.74E+03	1.11E+03	4.08E+03	1.12E+03	
G016508	Adavale	1.37E+02	2.72E+02	2.16E+02	1.20E+02	1.63E+02	3.05E+02	8.50E+01	2.08E+02	1.01E+02	
G016511	Bowen	3.08E+03	1.50E+03	3.86E+02	5.82E+02	8.25E+02	3.97E+03	2.17E+02	4.56E+03	5.51E+02	
G016522	Bowen	1.89E+03	1.78E+03	2.28E+03	1.05E+03	3.00E+03	4.91E+03	3.68E+02	5.99E+03	1.31E+03	
G016529	Bowen	5.49E+02	3.70E+02	6.29E+02	1.34E+02	4.04E+02	9.83E+02	2.47E+02	7.20E+02	1.69E+02	
G016531	Bowen	7.99E+02	3.27E+02	6.60E+03	1.21E+03	1.59E+03	2.19E+03	4.34E+02	8.22E+02	4.73E+02	
G016535	Bowen	2.30E+03	2.37E+03	2.04E+03	5.58E+02	3.50E+03	9.82E+03	5.31E+02	6.19E+03	1.64E+03	

Table 4-A5: GCMS SIR of aromatic compounds (parameters).

GEO54-ID	Basin	AROM2	Crack1	Crack2	MSAro1	MSAro2	MSAro3	MSAro4	MSAro5	MSAro6	MSAro7	MSAro8	MSAro9
G016494	Cooper	0.78	0.77	0.66	0.39	5.66	0.49	1.88	7.47	1.47	0.03	88.68	0.69
G016504	Eromanga	0.97	0.03	0.03	0.11	1.68	0.10	1.30	0.79	1.31	0.00	0.20	0.93
G016505	Eromanga	0.94	0.13	0.09	0.23	1.28	0.10	1.43	0.80	1.15	0.00	0.07	0.87
G016508	Adavale	0.86	0.80	0.67	0.38	23.85	0.46	1.73	7.28	3.10	0.07	83.81	0.77
G016511	Bowen	0.34	0.06	0.03	0.03	1.47	0.30	0.85	2.66	1.10	0.01	2.21	0.31
G016522	Bowen	0.80	0.20	0.14	0.25	2.21	0.38	1.89	3.07	0.83	0.01	0.39	0.61
G016529	Bowen	0.86	0.82	0.61	0.36	4.19	0.47	1.89	5.50	0.97	0.07	31.57	0.72
G016531	Bowen	0.91	0.72	0.60	0.26	2.59	0.48	2.24	4.83	1.01	0.01	3.24	0.81
G016535	Bowen	0.84	0.13	0.09	0.21	2.18	0.39	3.54	5.60	0.72	0.01	0.07	0.67

AROM2: $(C_{20}TA + C_{21}TA + SC_{26}TA + RC_{26}TA + SC_{27}TA + SC_{28}TA + RC_{27}TA + RC_{28}TA) / (C_{20}TA + C_{21}TA + SC_{26}TA + RC_{26}TA + SC_{27}TA + SC_{28}TA + RC_{27}TA + RC_{28}TA + C21MA + C22MA + bSC27MA + bRC27MA + bRC27DMA + aSC27MA + bSC28MA + bSC28DMA + aRC27DMA + aSC27DMA + aRC27MA + aSC28MA + aSC29MA + aRC29MA)$

Crack1: $(C_{20}TA) / (C_{20}TA + RC_{28}TA)$

Crack2: $(C_{20}TA + C_{21}TA) / (C_{20}TA + C_{21}TA + SC_{26}TA + RC_{26}TA + SC_{27}TA + SC_{28}TA + RC_{27}TA + RC_{28}TA)$

MSAro1: $(C_{21}MA + C_{22}MA) / (C_{21}MA + C_{22}MA + bSC_{27}MA + bRC_{27}MA + bRC_{27DMA} + aSC_{27MA} + bSC28MA + bSC28DMA + aRC27DMA + aSC27DMA + aRC27MA + aSC28MA + aSC29MA + aRC29MA)$

MSAro2: 4-MDBT/1-MDBT

MSAro3: $(2\text{-MP} + 3\text{-MP}) / (1\text{-MP} + 2\text{-MP} + 3\text{-MP} + 9\text{-MP})$

MSAro4: 2-MN/1-MN

MSAro5: $(2,6\text{-DMN} + 2,7\text{-DMN}) / 1,5\text{-DMN}$

MSAro6: 4-MDBT/DBT

MSAro7: DBT/P

MSAro8: 3-MP/Retene

Table 4-A6: Isotopes of fractions, $\delta^{13}\text{C}$ (‰ VPDB).

GEOS4-ID	Basin	$\delta^{13}\text{C-Sat}$	$\delta^{13}\text{C-Aro}$
		(‰ VPDB)	
G016494	Cooper	-29.0	-26.6
G016504	Eromanga	-26.3	-25.4
G016505	Eromanga	-27.2	-25.9
G016508	Adavale	-29.2	-30.7
G016511	Bowen	-30.3	-30.0
G016522	Bowen	-26.7	-24.8
G016529	Bowen	-28.8	-26.9
G016531	Bowen	-28.3	-25.9
G016535	Bowen	-26.9	-25.2

5 Late Gas Potential

Table 5-1: Sample overview.

GEOS4-ID	Basin	QLD i.d.	Rock Type	Rock Unit Name	Late Gas
COOPER BASIN	G016494	GSV01	Carb'ceous mst	Patchawarra Formation	1
COOPER BASIN	G016496	GSV03	Coal	Patchawarra Formation	1
COOPER BASIN	G016499	GSV06	Coal	Toolachee Formation	1
COOPER BASIN	G016500	GSV07	Coal	Toolachee Formation	1
COOPER BASIN	G016501	GSV08	Coal	Toolachee Formation	1
ADAVALE BASIN	G016508	GSV15	Carbonate	Bury limestone	1
RUNNING TOTALS					6

MSSV-Pyrolysis: Late Gas Potentials

Six mature samples from the Cooper and Adavale Basins, Queensland were subjected to closed-system high temperature pyrolysis to evaluate their late gas potential following the approach of Mahlstedt and Horsfield (2012b).

MSSV-pyrolysis gas chromatograms are shown in Figure 5-A1 and individual compound and boiling range yields are listed in Table 5-A1 and Table 5-2. Two MSSV pyrolysis experiments were performed for each sample using a heating rate of 2.0°C/min. One tube was heated from 200°C to 560°C and another one from 200°C to 700°C. The temperature range between 560°C and 700°C represents the main stage of late methane generation and occurs subsequently to primary C₁₊ generation as well as subsequently to secondary cracking of the major portion of C₆₊ compounds.

Total C₁₋₅ and C₆₊ product yields at MSSV temperatures 560°C and 700°C, calculated total late gas yields, late secondary gas (A) yields from oil cracking, and late secondary gas (B) yields from cracking of a refractory kerogen moiety, as well as late gas ratios LGP and LGT for all samples are given in Table 5-2.

Table 5-2: High temperature MSSV-Pyrolysis GC-FID

G-Number	R_r	C₁₋₅	C₁₋₅	C₆₊	C₆₊	Late Gas	sec. Gas (A)	sec. Gas (B)	LGP	LGT					
		560°C	700°C	560°C	700°C										
		mg/g TOC								kg/kg					
G016494	1.25	108.1	147.4	22.4	17.5	39.2	1.5	37.8	0.58	1.34					
G016496	0.96	101.7	147.8	22.6	4.3	46.1	5.5	40.6	0.59	1.38					
G016499	0.95	75.9	120.4	18.3	2.9	44.5	4.6	39.9	0.61	1.50					
G016500	0.78	97.9	141.2	29.3	5.4	43.3	7.2	36.1	0.59	1.34					
G016501	1.44	64.8	113.0	11.2	3.0	48.2	2.5	45.8	0.64	1.68					
G016508	1.20	41.4	58.0	16.0	4.9	16.6	3.3	13.2	0.58	1.30					

R_r: assessed vitrinite reflectance taking into account T_{max} values as well as organic petrology
Late Gas: Yield C₁₋₅(700°C) – Yield C₁₋₅(560°C)
sec. Gas (A): Late Gas from late oil cracking: (Yield C₆₊(560°C) – Yield C₆₊(700°C))*0.3
sec. Gas (B): Late Gas from refractory OM: Late Gas – sec. Gas (A)
LGP: Late Gas Potential ratio: Yield C₁₋₅(700°C)/(Yield C₁₋₅(560°C) + Yield C₁₋₅(700°C))
LGT: Late Gas Type ratio: Yield C₁₋₅(700°C)/(Yield C₁₋₅(560°C) + sec. Gas (A))

For all investigated samples gas yields at 700°C are higher than gas yields at 560°C. Those samples generate late gas and exhibit high late gas potentials (LGP >0.55). This means that generated late gas has to be largely explained by the cracking of a refractory kerogen moiety (formed during catagenesis) as input of secondary gas from oil cracking (sec. Gas (A)) is neglectable (LGT >>1). Late gas yields (sec. Gas (B)) range around 40 mg/g TOC for Cooper Basin samples and around 13 mg/g TOC Bury Limestone (G016508) from the Adavale Basin.

The two late gas potential ratios are shown in Figure 5-1 for investigated Queensland samples in comparison to earlier published results (Mahlstedt and Horsfield, 2012a) of Type II and Type III source rocks. All source rocks fall on the previously established trend, their ratios even exceeding borders previously defined by an immature sample set (Mahlstedt and Horsfield, 2012b). This maturity trend is systematic and can be described by a logarithmic function implying that late gas potentials increase up to infinity, which is of course only true for ratios but not for absolute yields, which will be shown in the following paragraphs. It should be stated here that the higher late gas potentials are all associated with mature, rather than immature, samples.

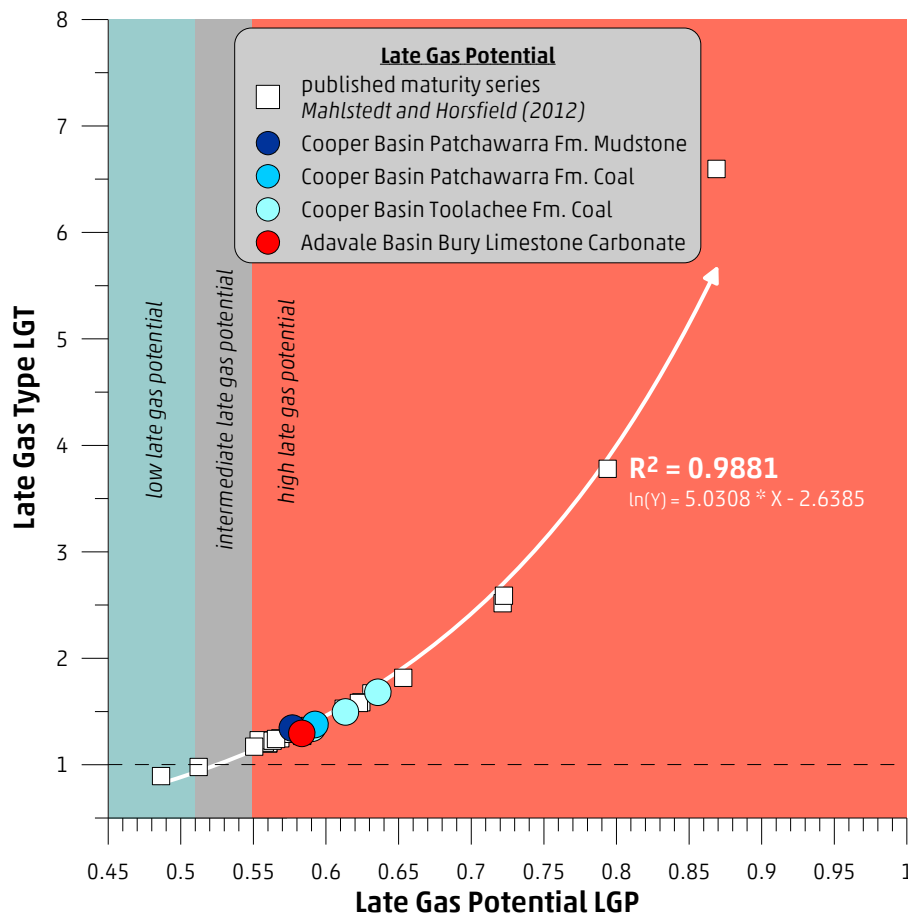


Figure 5-1: Late Gas Potential ratios evolution with maturity for Queensland samples (colored circles) as well as for published (Mahlstedt and Horsfield, 2012a) maturity series samples (white squares). (Data in Table 5-2)

The evolution of late gas potentials as a function of maturity is shown in Figure 5-2 in comparison to earlier published results (Mahlstedt and Horsfield, 2012a) of Type II and Type III source rocks. For the latter it could be shown that late gas potentials are underestimates for immature samples and that late gas potentials increase during catagenesis up to values of ~40 mg/g TOC at 2.0% vitrinite reflectance for possibly any given kerogen type. Relevant late gas precursor structures, i.e. methyl-aromatics, are formed during catagenesis within the residual organic matter by chain shortening reactions via β -scission as well as by concentration of refractory kerogen. The late methane forming reaction itself can be described by a final demethylation of residual aromatic nuclei within spent organic matter via α -cleavage mechanisms involving condensation reactions of aromatic clusters. Based on kinetic parameters published in Mahlstedt (2012) late gas generation takes place between 2.5 and 3.5% R_o for a simplified geological heating history ($3^\circ\text{C}/\text{ma}$ heating rate), a prediction directly confirmed by decreasing late gas potentials of naturally matured samples of Type II and Type III origin exhibiting vitrinite reflectance $>2.0\% R_o$ (Figure 5-2).

Late gas potentials of investigated samples from Queensland follow generally very well the previously described evolution trend for shales and coals with maturity, i.e. increasing late gas potentials going from low maturities ($<1\% R_r$) to $R_r \sim 2.0\%$. The vitrinite-rich coals of the Toolachee and Patchawarra formations of the Cooper Basin exhibit high late gas potentials already at lower maturity stages than the Patchawarra Formation mudstone sample. The late gas potential of ~13 mg/g TOC at $\sim 1.2\% VR_{\text{calc}}$.

for the Bury Limestone sample (G016508) from the Adavale Basin fits very well to the trend of source rocks that have low LGP values at low maturity and only develop their late gas potential during catagenesis.

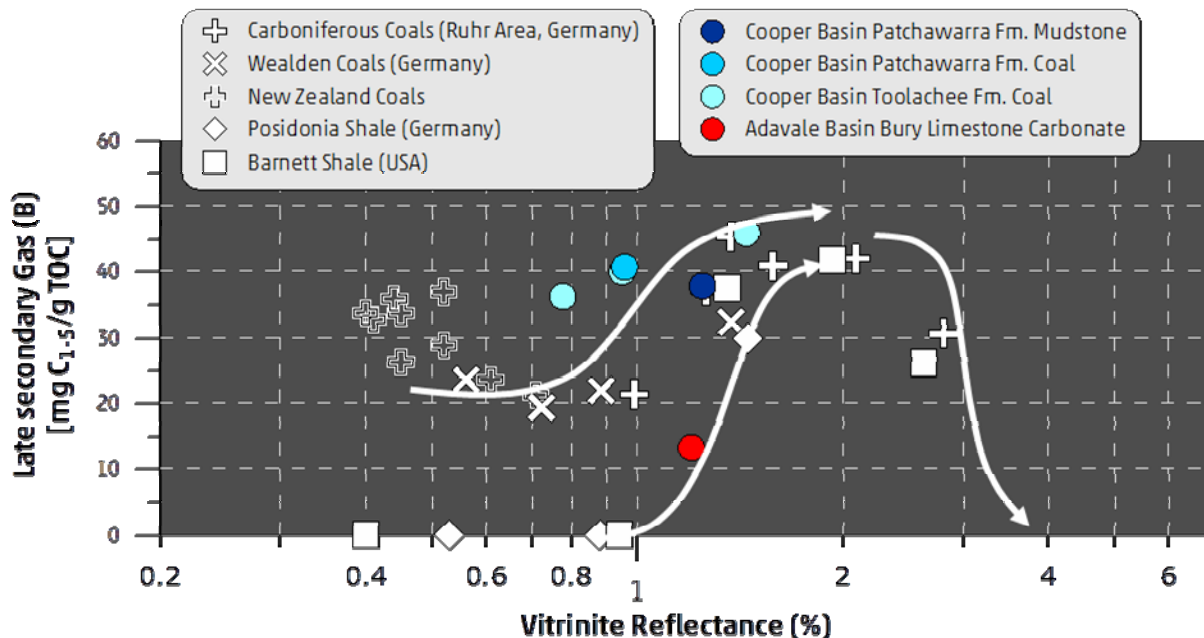


Figure 5-2: Late Gas potential evolution with maturity (vitrinite reflectance) for Queensland samples (colored circles) as well as for published (Mahlstedt and Horsfield, 2012a) maturity series samples (white symbols). White arrows indicate the evolution of late gas potentials with maturity. (Data in Table 5-2)

References

- Mahlstedt, N., 2012. Evaluating the late gas potential of source rocks stemming from different sedimentary environments. Dissertation. Technische Universität Berlin, Berlin, p. 342.
- Mahlstedt, N., Horsfield, B., 2012a. Gas Generation at High Maturities ($> Ro = 2.0\%$) in Gas Shales. Search and Discovery Article #40873.
- Mahlstedt, N., Horsfield, B., 2012b. Metagenetic methane generation in gas shales I. Screening protocols using immature samples. Marine and Petroleum Geology - Insights into Shale Gas Exploration and Exploitation 31, 27-42.

Appendix 5-1 – MSSV Chromatograms

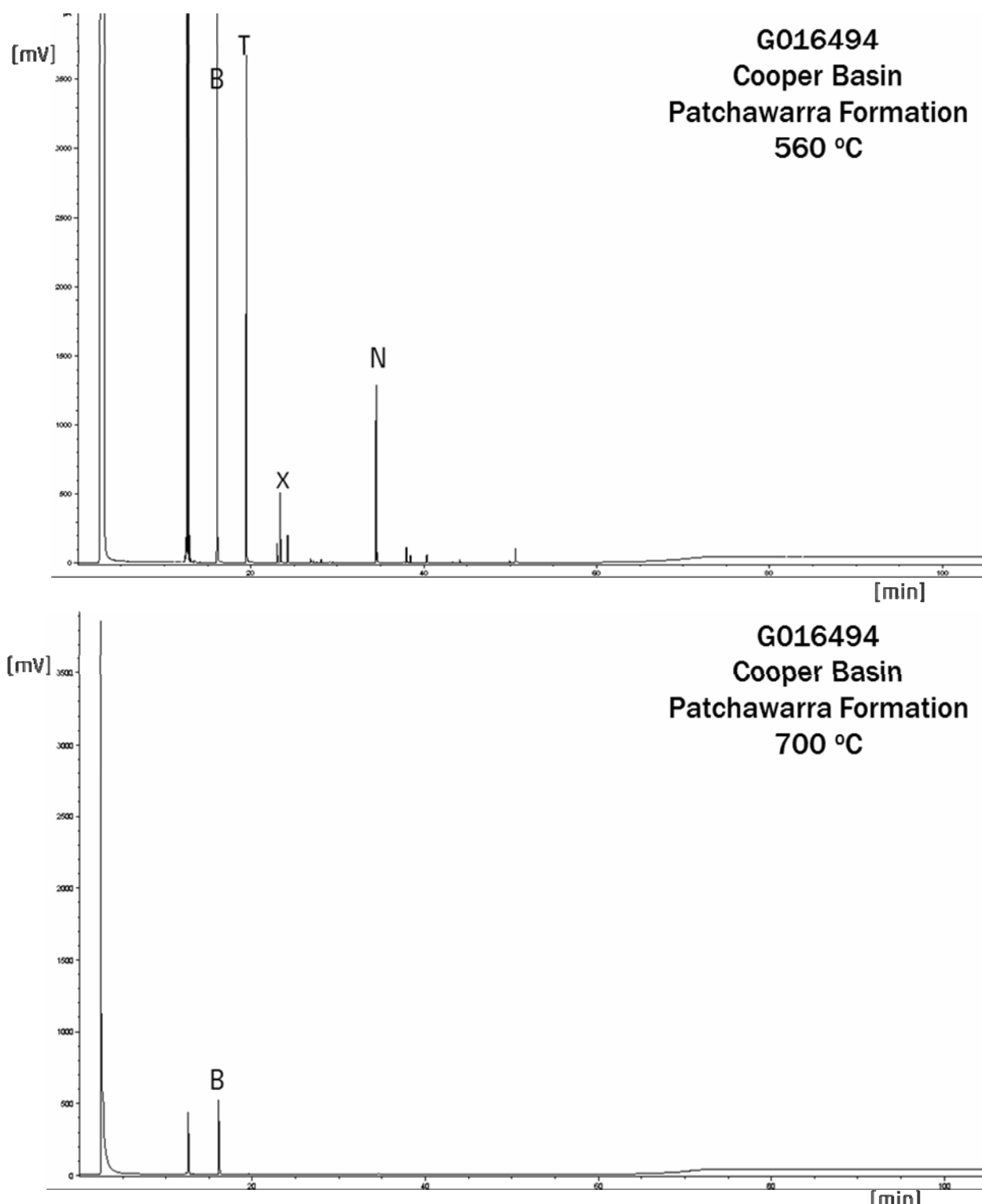


Table 5-A1: MSSV-Pyrolysis GC-FID. Chromatograms Patchawarra Formation mudstone.
For reference, selected peaks are marked: B= benzene; T= toluene; X= meta/para-xylene; N= naphthalene.

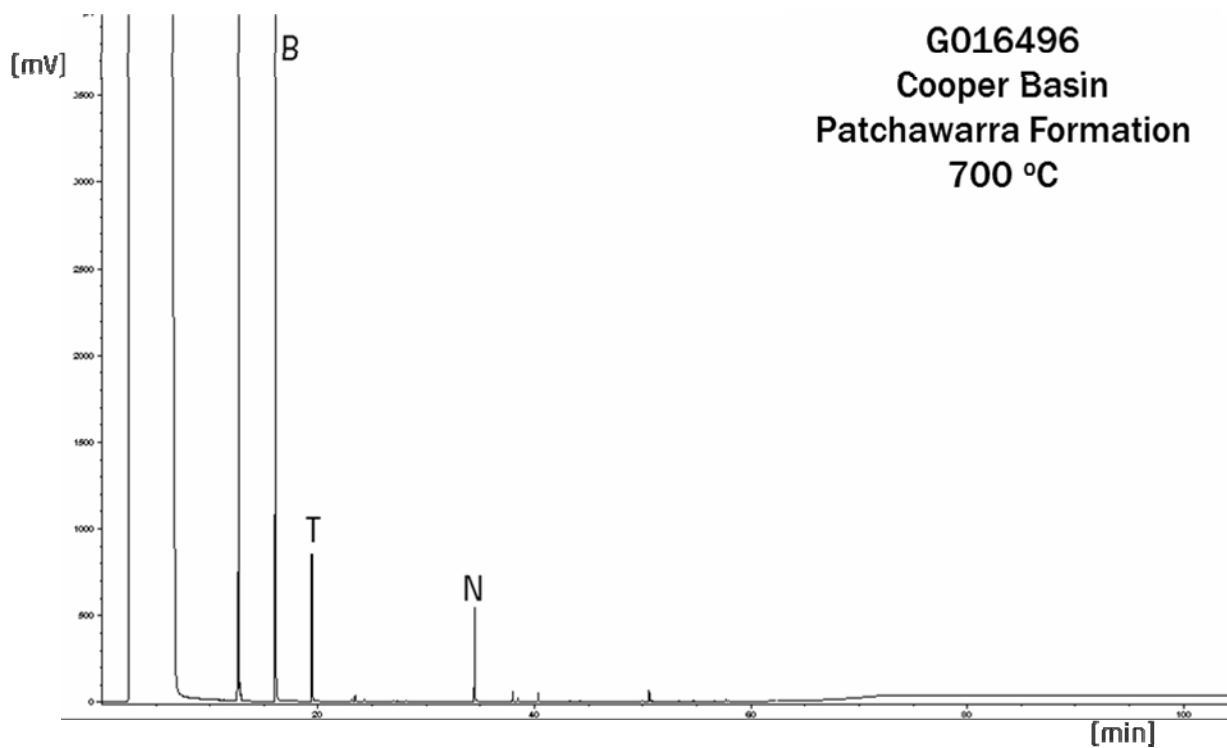
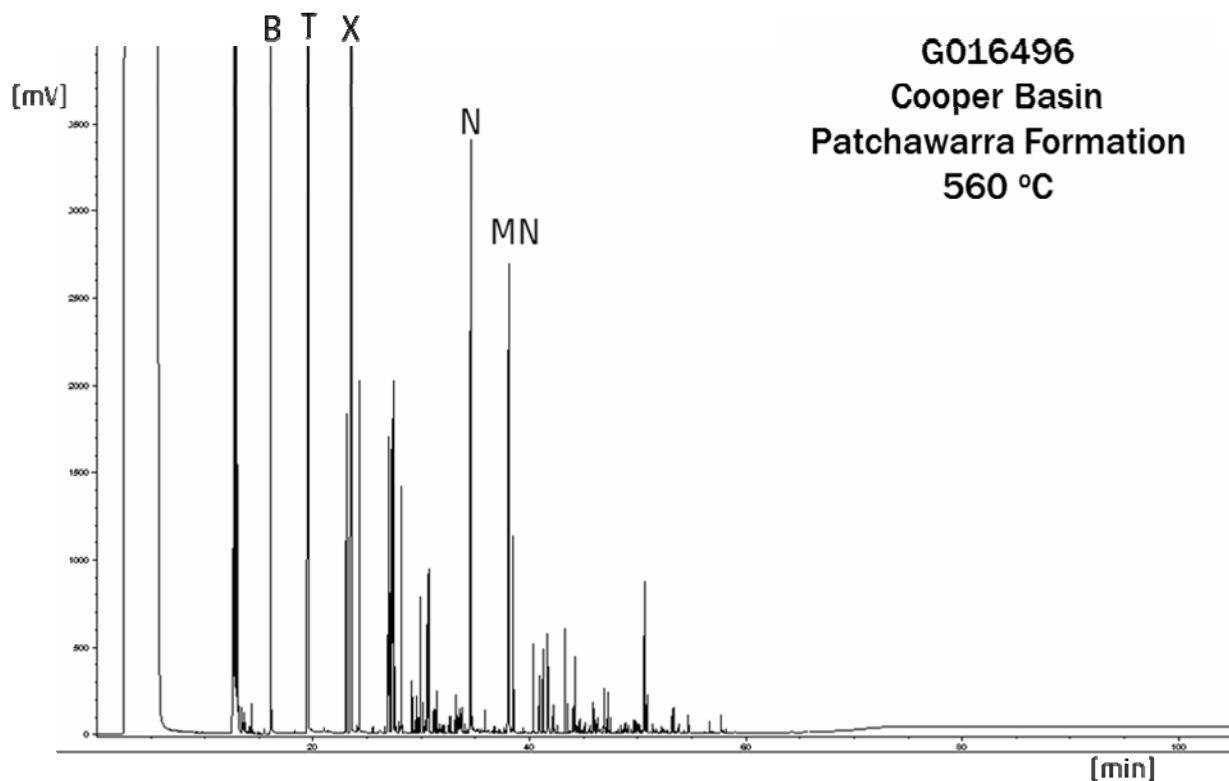


Table 5-A1 (contd.): MSSV-Pyrolysis GC-FID. Chromatograms Patchawarra Formation coal. For reference, selected peaks are marked: B= benzene; T= toluene; X= meta/para-xylene; N= naphthalene; MN= methylnaphthalene.

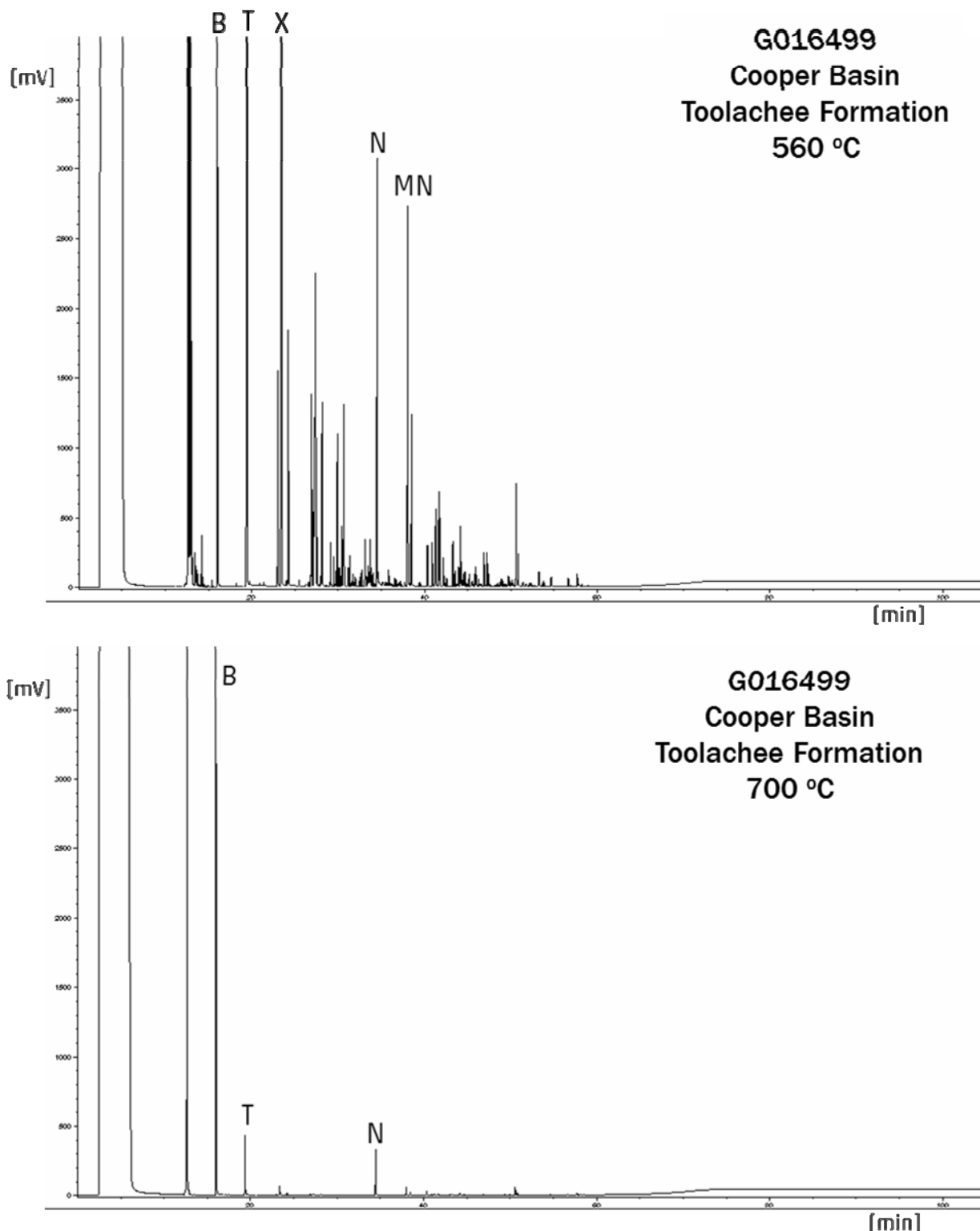


Table 5-A1 (contd.): MSSV-Pyrolysis GC-FID. Chromatograms Toolachee Formation coal.
For reference, selected peaks are marked: B= benzene; T= toluene; X= meta/para-xylene; N= naphthalene; MN= methylnaphthalene.

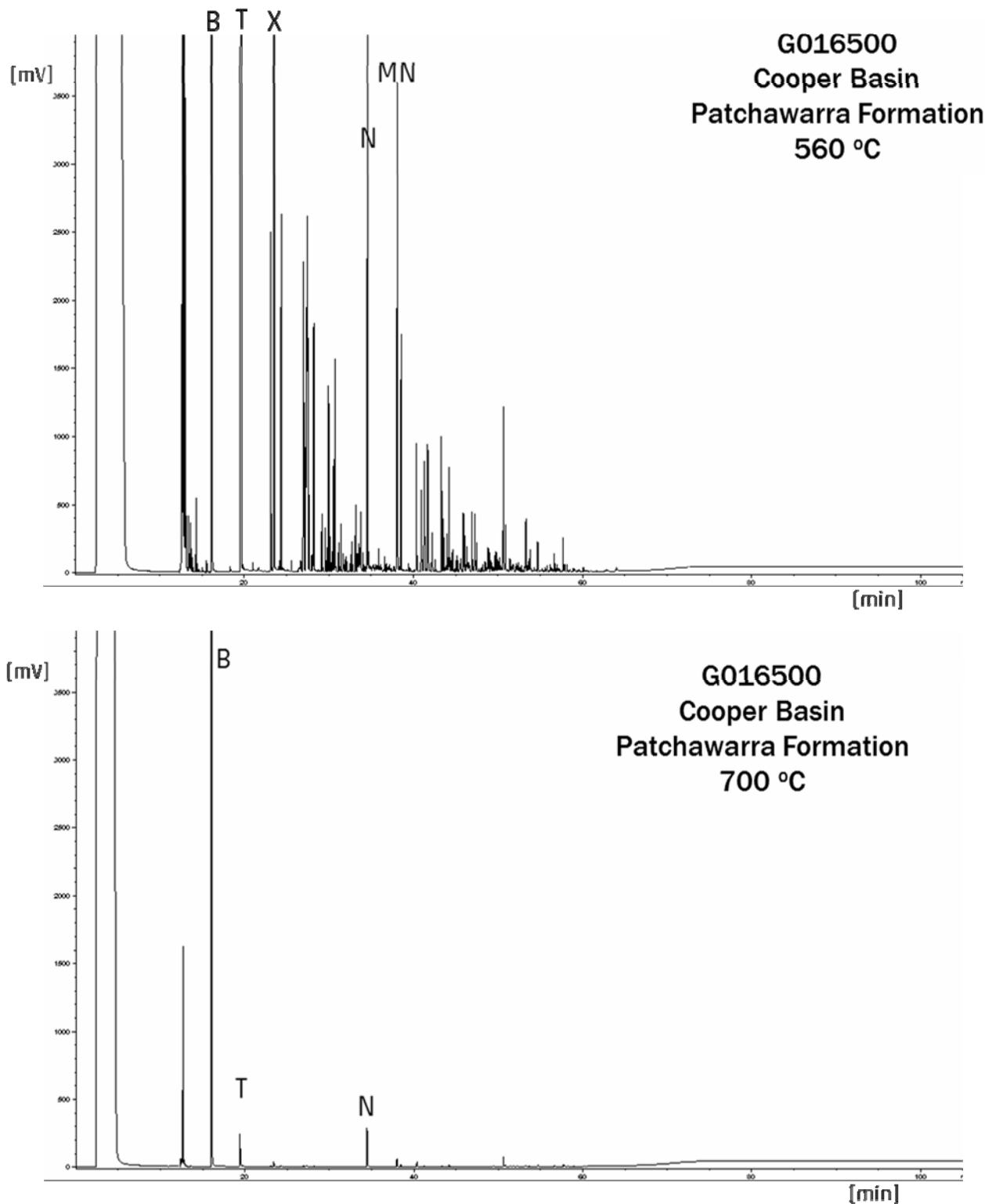


Table 5-A1 (contd.): MSSV-Pyrolysis GC-FID. Chromatograms Toolachee Formation coal.
For reference, selected peaks are marked: B= benzene; T= toluene; X= meta/para-xylene; N= naphthalene; MN= methylnaphthalene.

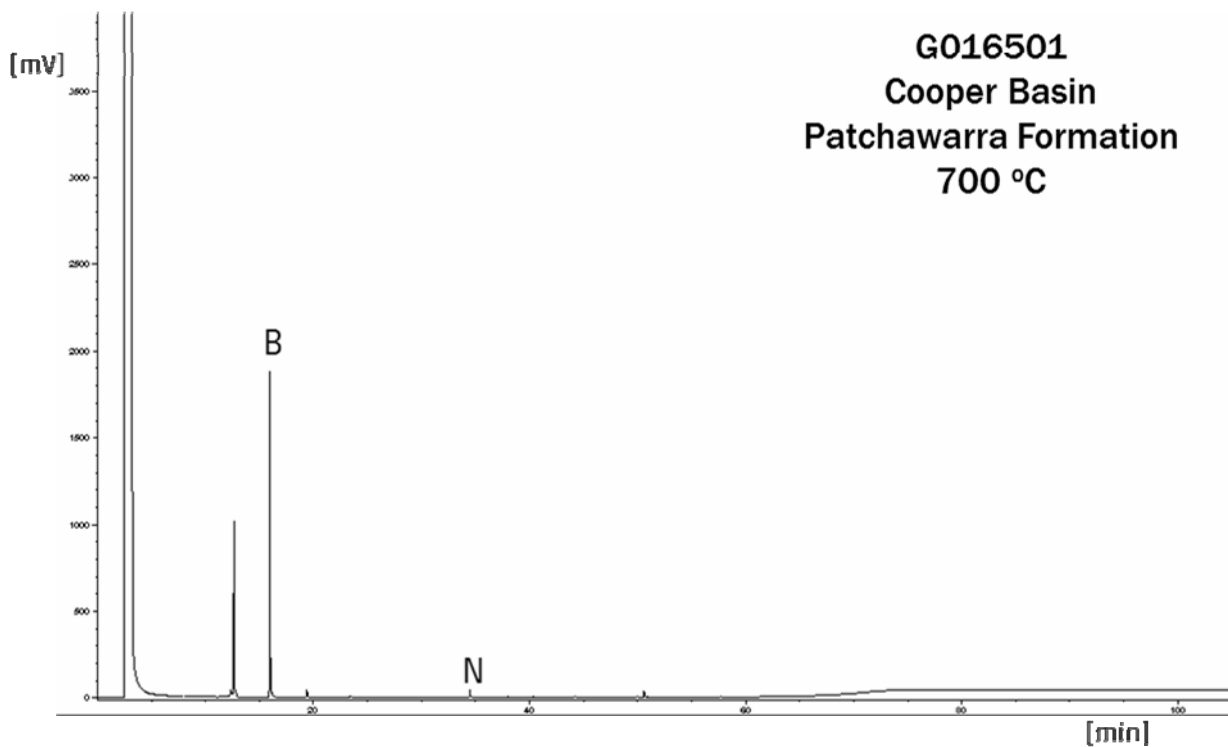
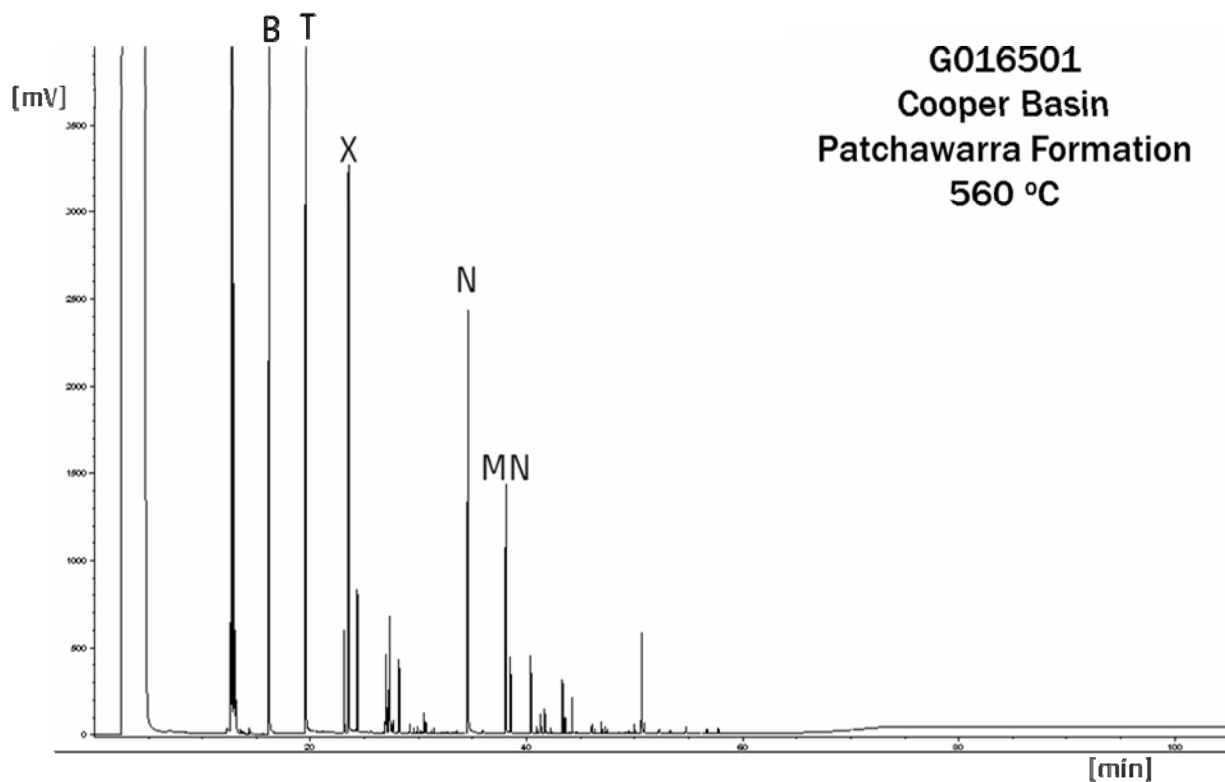


Table 5-A1 (contd.): MSSV-Pyrolysis GC-FID. Chromatograms Toolachee Formation coaly shale. For reference, selected peaks are marked: B= benzene; T= toluene; X= meta/para-xylene; N= naphthalene; MN= methylnaphthalene.

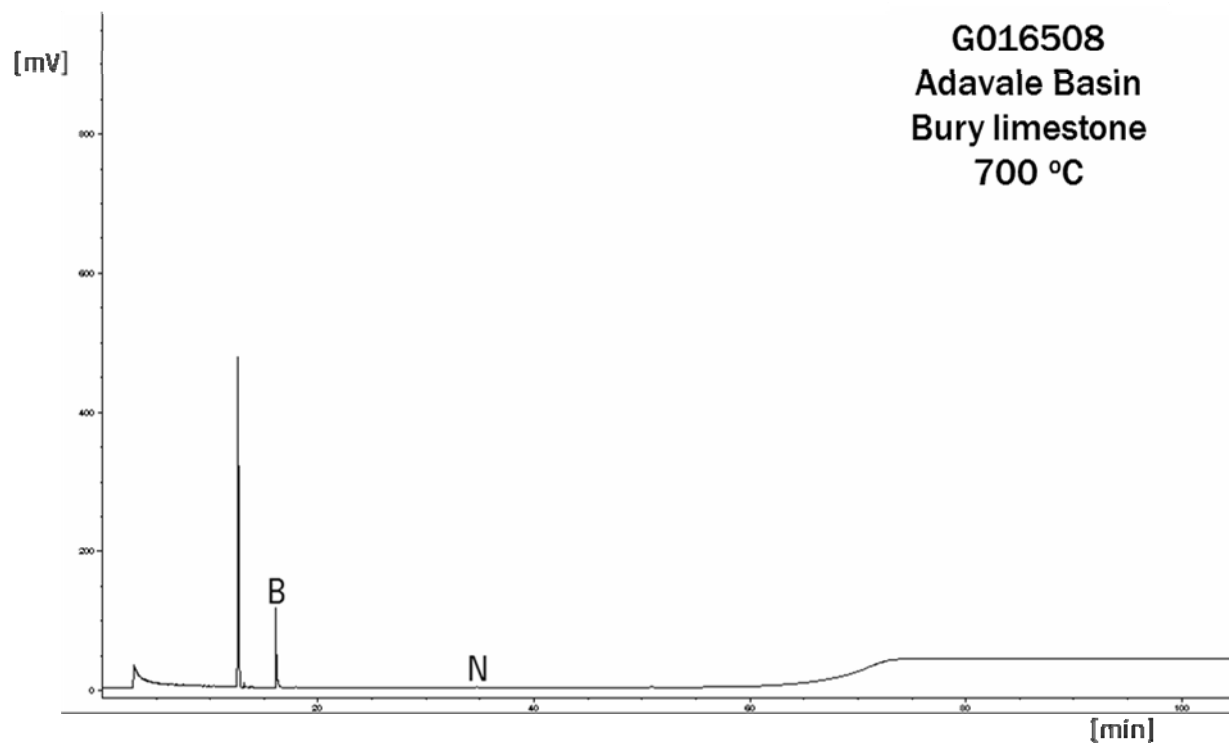
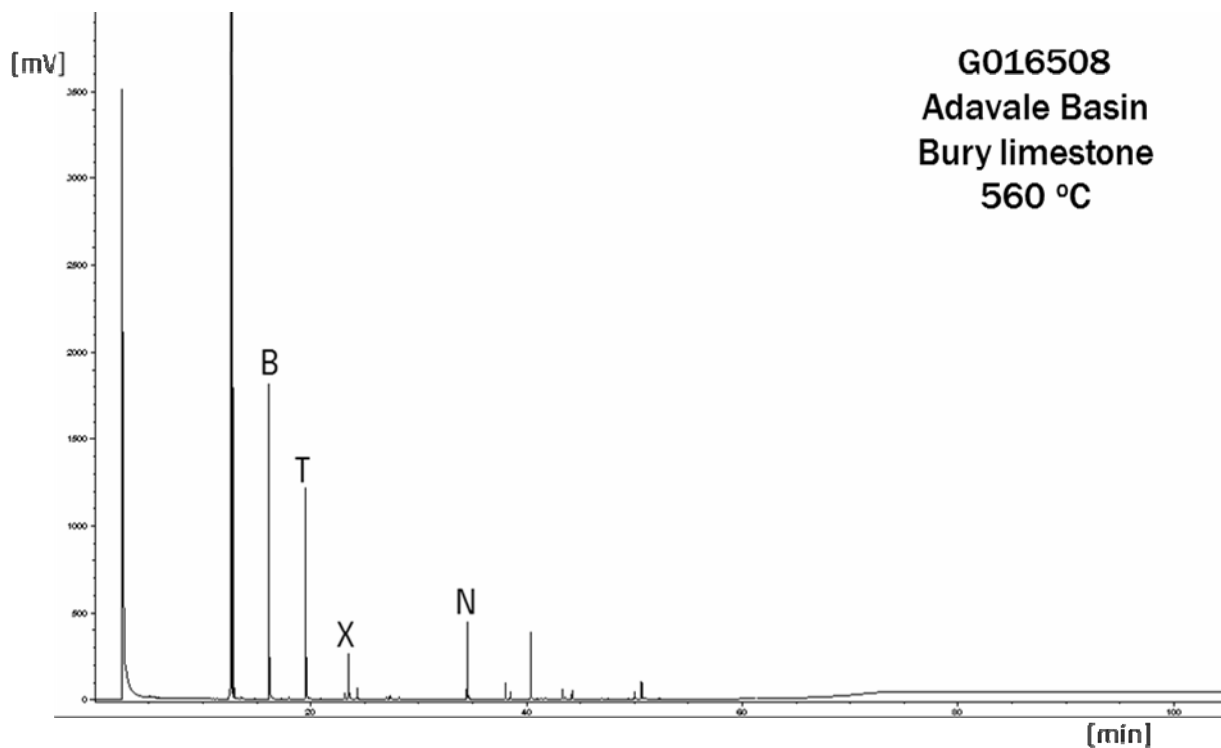


Table 5-A1 (contd.): MSSV-Pyrolysis GC-FID. Chromatograms Bury limestone.

For reference, selected peaks are marked: B= benzene; T= toluene; X= meta/para-xylene; N= naphthalene.

Appendix 5-2 – Tables

Table 5-A1: MSSV-Pyrolysis GC-FID. (Late Gas Potential)

Sample	G016494		G016496		G016499		G016500		G016501		G016508	
Heated to, °C	560	700	560	700	560	700	560	700	595	700	560	700
Weight, mg	38.90	6.18	6.18	4.10	6.48	4.11	6.60	2.20	17.84	3.10	36.04	3.93
(µg/g sample)												
C1	1690	2979	58807	114725	44556	95732	52889	111687	13771	29073	355	550
C2-5	549	71	20889	1111	16288	794	25151	866	3195	533	117	111
C6+	463	362	17757	3387	14661	2347	23323	4290	2946	787	183	56

6 PhaseKinetics

Table 6-1: Sample overview.

GEOS4-ID	Basin	QLD i.d.	Rock Type	Rock Unit Name	BulkKin	PhaseKin
COOPER BASIN	G016500	GSV07	Coal	Toolachee Formation	1	
EROMANGA BASIN	G016504	GSV11	Carb'ceous mst	Birkhead Formation	1	1
EROMANGA BASIN	G016505	GSV12	Coal	Birkhead Formation	1	1
ADAVALE BASIN	G016508	GSV15	carbonate	Bury Limestone	1	
BOWEN BASIN	G016511	GSV18	shale	Bandanna Formation	1	1
BOWEN BASIN	G016522	GSV29	Coal	Aldebaran Sandstone	1	1
BOWEN BASIN	G016524	GSV34	shale	Snake Creek Mudstone Mbr	1	
BOWEN BASIN	G016531	GSV40	Coal	Tinowon Sandstone	1	1
BOWEN BASIN	G016535	GSV45	Coal	Riverstone Sst Mr?-Cattle Creek Formation	1	1
BOWEN BASIN	G016539	GSV49	Coal	Reids Dome beds	1	1
RUNNING TOTALS					10	7

6.1 Open System Pyrolysis Bulk Kinetics

Table 6-A1 lists the activation energy distributions and frequency factors determined for the ten samples analysed using a Source Rock Analyzer and 4 heating rates (0.7, 2.0, 5.0 and 15.0°C/min). Kinetics parameters are determined using the three slow heating rates and shown in Figure 6-1a & b.

Cooper Basin

The activation energy distribution of the Toolachee Formation sample G016500 with five dominant energies between 55 and 59 kcal/mol accounting for ~85% of the total kerogen to petroleum conversion reaction and the single frequency factor are indicative of stable, i.e., in this case, relatively mature organic matter ($T_{max} = 441^\circ\text{C}$).

Adavale Basin

The broad activation energy distribution of the Bury Limestone sample G016508 with four dominant energies between 55 and 58 kcal/mol accounting for ~65% of the total kerogen to petroleum conversion reaction and the single frequency factor are indicative of stable, i.e., in this case, mature organic matter ($T_{max} = 458^\circ\text{C}$).

Eromanga Basin

The single frequency factor and the narrow activation energy distribution of the Type I Birkhead Formation sample G016504 with one dominant energy at 51 kcal/mol and four main energies between 50 and 53 kcal/mol accounting for >90% of the total kerogen to petroleum conversion reaction are indicative of relatively homogeneous organic matter, likely derived from algae deposited in an aquatic environment. Nevertheless, we know from maceral analysis (Interim report 3) that, besides alginite, sporinite and vitrinite are abundant (27% and 35% of OM, respectively).

The single frequency factor and broader activation energy distribution of the Type II/III Birkhead Fm. coal sample G016505 with five main energies between 51 and 55 kcal/mol accounting for >80% of the total kerogen to petroleum conversion reaction are indicative of more heterogeneous organic matter, which is in line with deposition of algal material in a mixed terrestrial-aquatic (lacustrine) environment.

Bowen Basin

Pyrolysis GC-FID indicated that investigated Bowen Basin samples were most likely "formed" by input of algal or bacterial organic matter into a lacustrine/brackish environment. Thus, a broad activation energy distribution can be observed for all samples accounting for the heterogeneous, mixed terrestrial-lacustrine organic matter mix. Single main energies only occur for the Bandanna Formation shale (coal) G016511, Aldebaran Sandstone coal G016522, and the Snake Creek Mudstone Member G016524 indicating that certain H-rich structures, such as plant or algal/bacterial lipids might prevail.

Application of the kinetic models to a geologic heating rate of 3 K/Ma was performed based on the activation energy distributions calculated for each sample (Figure 6-1a and 1b). Figure 6-2 shows the comparison of predicted transformation ratio rate and generation rate curves for each sample indicating kinetic variability related to differences in maturity and the organic matter structure. In line with relatively broad activation energy distributions (in line with presence of higher land plant material) petroleum generation occurs over moderately broad to broad temperature intervals of >30°C. Onset temperatures (10% TR) of all samples exceed 110°C indicative of relatively stable organic matter, which is in line with low organic sulphur contents.

Cooper Basin and Adavale Basin

Onset temperatures >140°C for Cooper Basin sample G016500 (Toolachee Formation) and Adavale Basin sample G016508 (Bury Limestone) are in line with presence of mature organic matter.

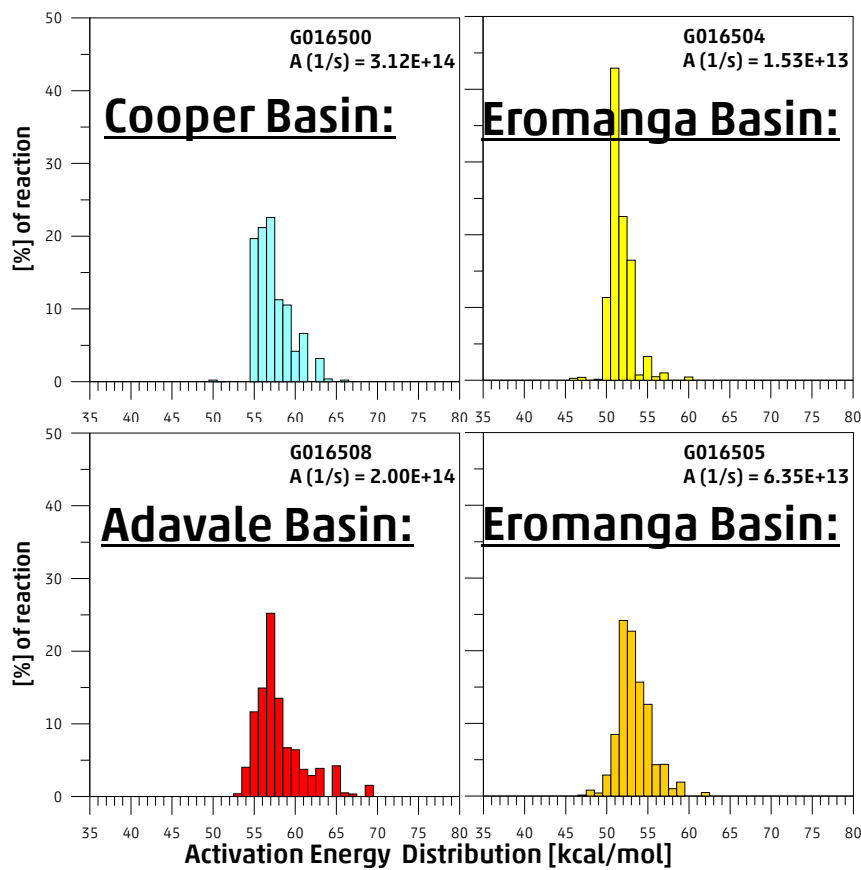


Figure 6-1a: Bulk kinetic parameters of four samples from the Cooper, Eromanga, and Adavale Basins based on slow heating rates (0.7; 2.0; 5.0K/min). (Data in Table 6-A1)

Bowen Basin:

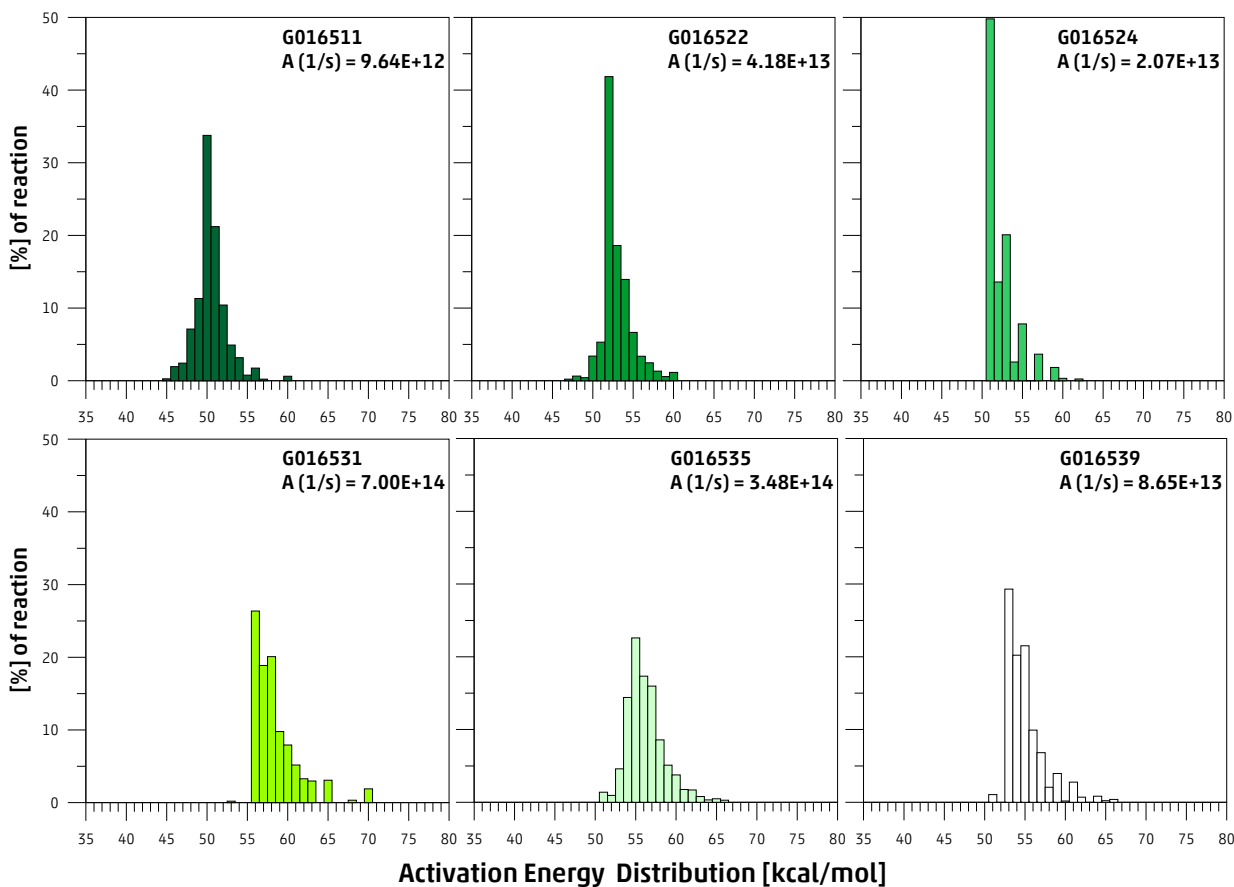


Figure 6-1b: Bulk kinetic parameters of six samples from the Bowen Basin based on slow heating rates (0.7; 2.0; 5.0K/min). (Data in Table 6-A1)

Eromanga Basin

Petroleum generation occurs between 126°C (10%TR) and 157°C (90% TR) for the Type I Birkhead Formation sample G016504 and between 125°C and 167°C for the Type II/III Birkhead Fm. coal sample (G016505).

Bowen Basin

Onset temperatures between 130 and 140°C for most Bowen Basin shales and coals are line in with presence of early oil window mature, mixed lacustrine-terrestrial organic matter. Bandanna Formation shale (coal) sample G016511, being the least mature Bowen Basin sample (Tmax 426°C; 0.40% R_r), exhibits the lowest onset temperature of 114°C, whereas the Tinowon Sandstone Member coal sample G016531, being the most mature Bowen Basin sample (Tmax 439°C; 0.63% R_r), exhibits the highest onset temperature of 147°C.

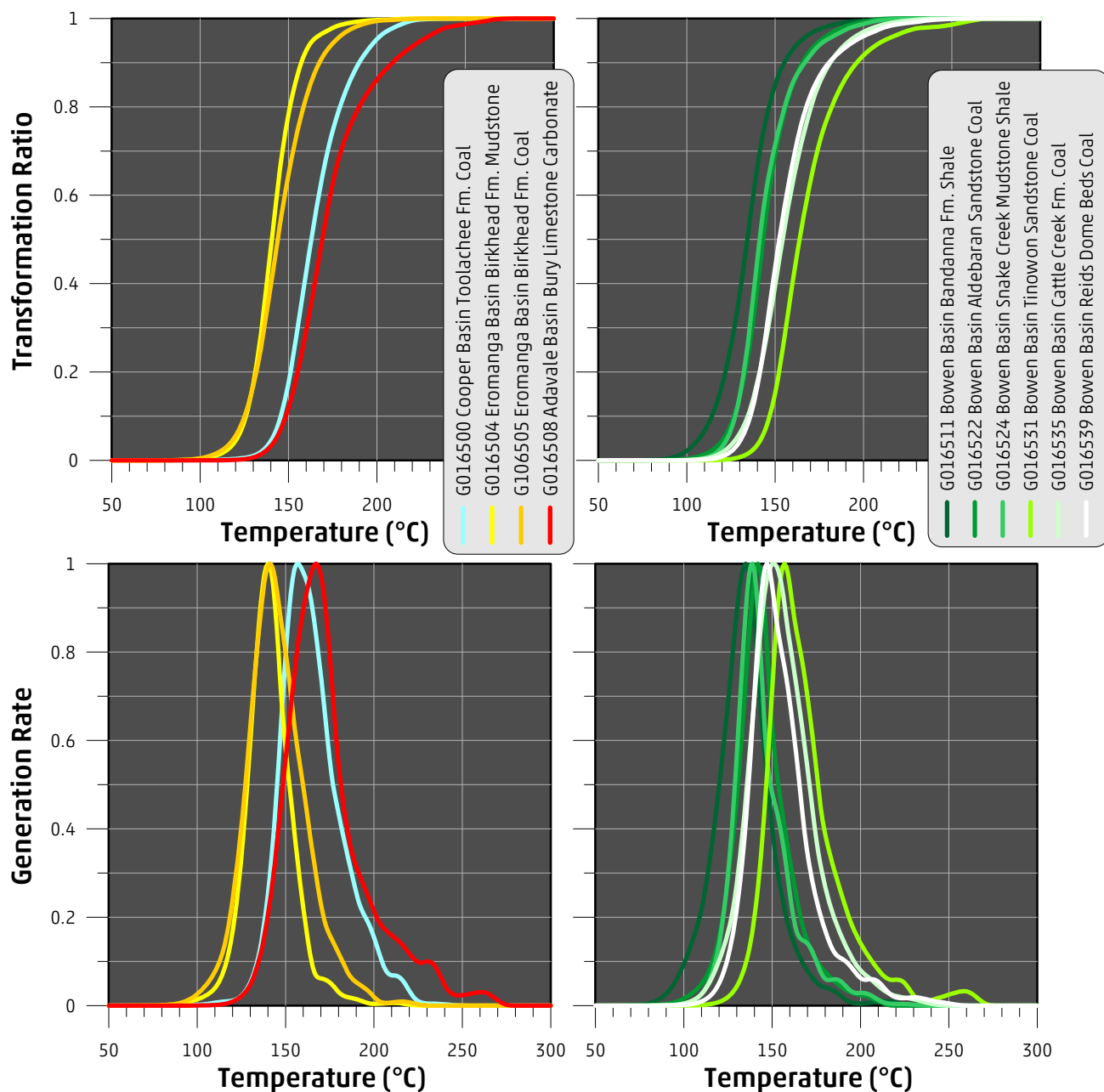


Figure 6-2: Transformation ratio rate curves (top) and generation rate curves (bottom) calculated using the bulk kinetic models shown in Figure 6-1 applied to a geologic heating rate of 3K/Ma.

6.2 MSSV-Pyrolysis: PhaseKinetics

Primary cracking products

Following the two-level screening (Rock-Eval and pyrolysis gas chromatography) and bulk kinetics analyses seven samples from the Eromanga and Bowen Basin were subjected to close-system pyrolysis and data synthesis following the PhaseKinetic approach (di Primio and Horsfield, 2006).

Five MSSV pyrolysis experiments were performed using a heating rate of 0.7 K/min up to temperatures representing 10, 30, 50, 70 and 90% kerogen transformation (TR). The end temperatures for each heating experiment (Table 6-A2) were determined based on bulk pyrolysis at 0.7 K/min. Thermovaporation for identification of previously generated hydrocarbons was not performed. Solvent extracted samples were used to minimize the influence of earlier formed products on the evolution of physical properties of artificially generated fluids.

MSSV-pyrolysis gas chromatograms for the five temperatures are shown in Figure 6-A1. With increasing simulated maturation, a mixture of aromatic/phenolic and mainly paraffinic products was generated for all samples. Paraffinicity increased as did the content of low molecular weight hydrocarbons as the level of maturity increased. Individual compound and boiling range yields are listed in Table 6-A2. We report cumulative yields (Table 6-A2a) and instantaneous yields (Table 6-A2b). Instantaneously generated fluids are products generated between two TR ratio stages (e.g. 10% and 30% TR) and can simply be calculated by subtraction of yields of the lower TR experiment from yields of the higher TR experiment.

Compositional information at each transformation ratio, after correction of the gas composition as discussed in Appendix 1 was used to determine molar proportions of selected compounds for the characterisation of the generated fluids physical properties (PVT-properties). Through integration of the individual, instantaneous PVT-datasets with the bulk kinetics of the sample, following the PhaseKinetic approach (di Primio and Horsfield, 2006), a phase predictive compositional kinetic model was developed using the methodology described in Appendix 1.

Table 6-A3 shows the molar composition of the final corrected, cumulative (a) and instantaneous (b) fluid descriptions. Table 6-A4 gives the physical properties of the pseudo compounds used for the 14 compound models. Standard "wet gas" and "black oil" definitions from Petromod® are recommended for the 2-compound kinetic models. The final compositional subdivision of the models for the individual transformation ratio stages are based on instantaneous data and shown in Figure 6-3. The complete compositional kinetic models, including two and four compound compositional kinetics, are listed in Table 6-A5.

It is very important to note that the final compositional kinetic model discussed to this point predicts the generation of petroleum (cumulative) as a function of primary cracking exclusively. Generally we assume that the compositions predicted are representative of the expelled fluid phase which then migrates to the reservoir (and accumulates there). This assumption is most likely valid for good quality oil-prone source rocks, which are efficient expellers. In the case of poor samples, however, expulsion efficiency and the secondary cracking of retained compounds should be taken into account.

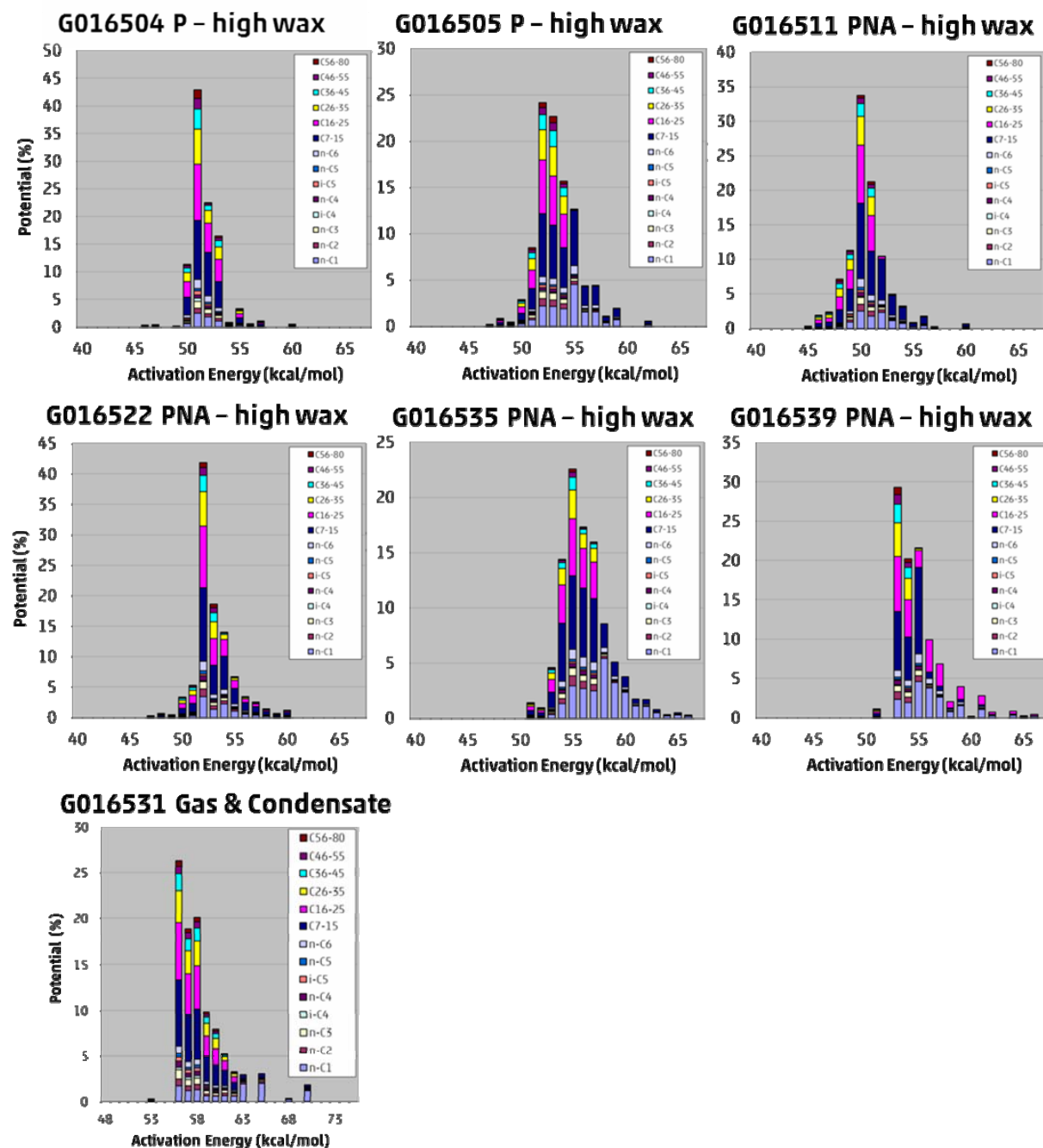


Figure 6-3: PhaseKinetic 14-compound models for seven samples. (Data in Table A5)

Concerning physical properties (GOR, saturation pressure Psat, formation volume factor Bo) predictions of the compositional kinetic models (using instantaneous compositions) closely follow the physical properties of fluids cumulatively generated during MSSV-pyrolysis (Figure 6-4 and Table 6-A6a) as a function of primary cracking.

Eromanga Basin

A Paraffinic-high wax petroleum type was inferred for the two Birkhead Formation samples (G016504 and G016505). Nevertheless, only fluids generated from the predominantly algal Type I mudstone sample G016504 fall within the black oil class over the entire primary kerogen conversion range. They exhibit more or less uniform and low saturation pressures between 120 and 150 bar, and the GOR values increase only slightly from 80 to 120 Sm³/Sm³ with maturity. Fluids generated from the heterogeneous Type II/III coal sample G016505 exhibit saturation pressures of >200 bars (approximate beginning of volatile oil) already at lowest maturity levels (10% TR) and increase to >300 bar at highest maturity levels (90% TR) where secondary cracking is likely to have set in in the closed system. GOR values also strongly increase from 160 Sm³/Sm³ to 200 Sm³/Sm³ at 70% TR and to 425 Sm³/Sm³ at 90% TR.

The physical properties of fluids generated from the Type I sample G016504 can therefore be described as typically lacustrine (uniform Psat and GOR values), whereas the physical properties of fluids generated from the heterogeneous Type II/III coal sample G016505 can be described as mixed lacustrine-terrestrial (gradually increasing Psat and GOR values).

Bowen Basin

A gas and condensate petroleum type was predicted for the Tinowon Sandstone coal sample G016531 and a P-N-A high wax petroleum type was predicted for the remaining four Bowen Basin coals and shales. Thus, fluids generated from sample G016531 (Tinowon Sandstone Member), exhibiting saturation pressures of >200 bars already at low maturity levels (>10% TR) which increase to ~450 bar at highest maturity levels (90% TR), fall within the volatile oil class. Cattle Creek Formation - ?Riverstone Sandstone Member sample G016535 and Reids Dome Beds sample G016539 generate volatile oil (Psat >200 bar) from 50% TR onward, whereas Bandanna Formation sample G0165311 and Aldebaran Sandstone sample G0165322 generate fluids with Psat values exceeding 200 bar only at highest maturity levels (90% TR). At lower transformation ratios Psat values range between 150 and 200 bar indicating generation of black oil.

The evolution of GOR values are similar for all samples. They gradually increase between 10 and 70% TR and then rapidly increase reaching 90% TR (secondary cracking is likely to have set in in the closed system) to values above 400 Sm³/Sm³ (G016531 (Tinowon Sandstone Member), G016535 (Cattle Creek Formation - ?Riverstone Sandstone Member), G016539 (Reids Dome beds)) or above 200 Sm³/Sm³ (G016511 (Bandanna Formation), G016522 (Aldebaran Sandstone)). The initial gradual increase is steepest for the gas and condensate sample G016531 (160 - 350 Sm³/Sm³ between 10 and 70% TR), less steep for samples G016535 and G016539 (100 - 240 Sm³/Sm³ between 10 and 70% TR), and least steep for samples G016511 and G016522 (<100 - 150 Sm³/Sm³ between 10 and 70% TR).

Due to overall increasing Psat and GOR values, the physical properties of fluids generated from all samples can be described as typical for heterogeneous mixed aquatic/lacustrine – terrestrial organic matter deposited in a fluviodeltaic environment.

The increase in saturation pressure with increasing transformation ratio is positively correlated to Bo for all samples from the two basins (Figure 6-4a and b bottom). Hence, closed-system artificial maturation experiments at maturation stages below 90% TR reflect the behaviour of naturally occurring petroleum, i.e. black (waxy) to volatile oil, very well.

Compositional kinetic models were developed for each of these source rocks. The calculation of petroleum phase behaviour under the subsurface conditions of hydrocarbon migration and entrapment is therefore possible.

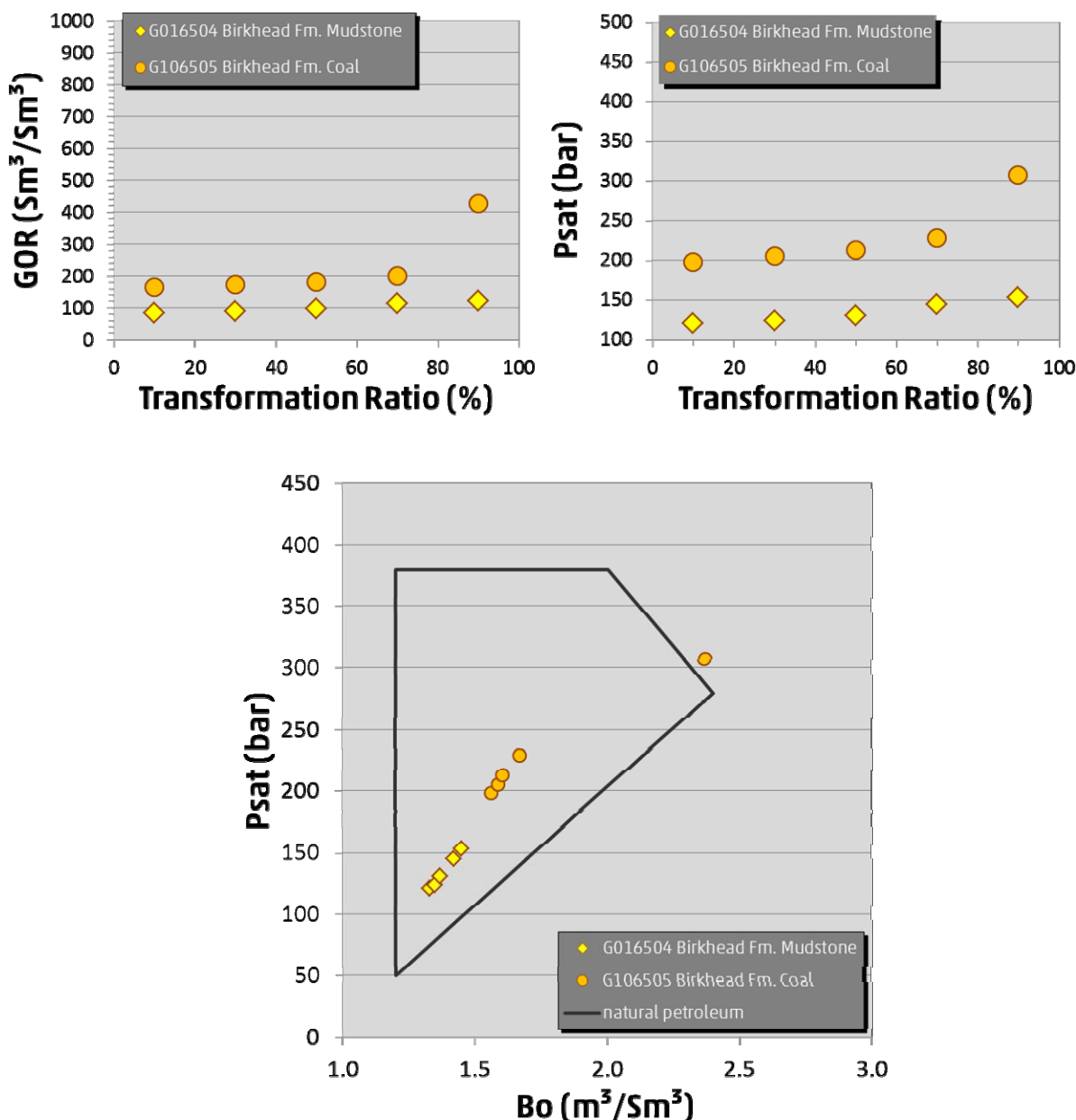


Figure 6-4a: GOR and saturation pressure (P_{sat}) as a function of kerogen transformation, as well as P_{sat} and formation volume factor (B_o) for Eromanga Basin samples (bottom). The outlined area marks physical properties of naturally occurring petroleum. (Data in Table 6-A6a)

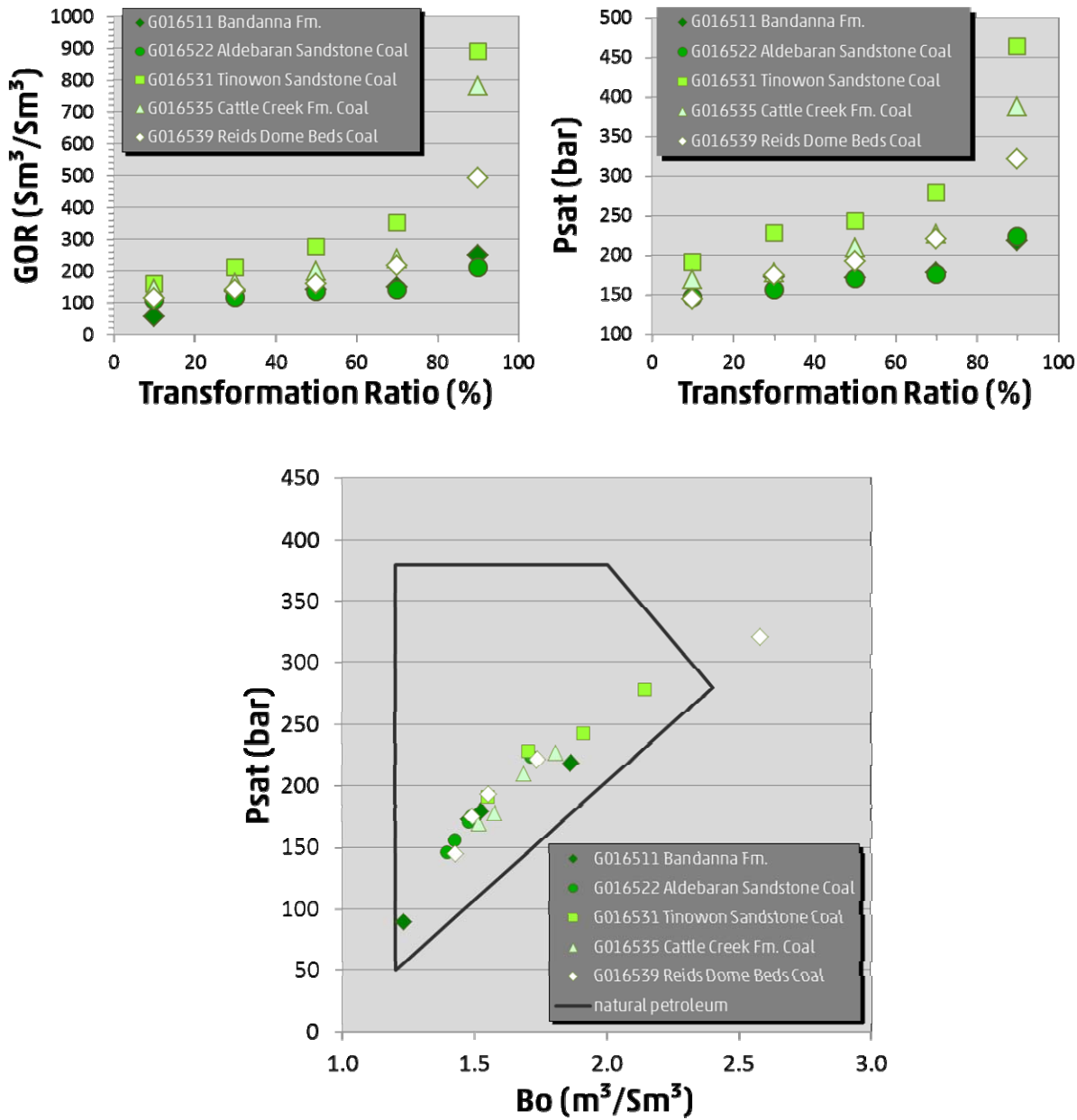


Figure 6-4b: GOR and saturation pressure (Psat) as a function of kerogen transformation, as well as Psat and formation volume factor (Bo) for Bowen Basin samples (bottom). The outlined area marks physical properties of naturally occurring petroleum. (Data in Table 6-A6a)

Secondary cracking products

The characterisation of secondary cracking effects is not as well constrained, and has been implemented into the PhaseKinetic approach based on the following assumptions:

- PhaseKinetics describe the hydrocarbon composition generated and expelled from the source rock.
- A proportion of the entire generated phase is retained in the kerogen by adsorption.
- The proportion retained depends on the dead carbon content of the kerogen and a specific sorption coefficient, which applies to the entire petroleum phase.
- Dead carbon proportion and sorption coefficients are based on the Pepper and Corvi (1995a) approach, these numbers are defined for the secondary cracking versions of each 14-compound phase-predictive model.
- Expulsion occurs once the sorption capacity of the kerogen is exceeded.
- Retained fluids will mix with newly generated fluids, cracking kinetics of exclusively the liquid pseudo-compounds are also defined based on Pepper and Corvi (1995b).
- The only compound generated by cracking is methane.

In order to implement the secondary cracking kinetics the specific kinetic model must be assigned to a source rock facies. In the Petromod® V2012 kinetic editor under the Adsorption tab the Component Adsorption Model "Expelled Composition" should be selected. The simulator will then calculate expulsion of the generated phase from the source rock.

References

- Andresen, B., Throndsen, T., Barth, T., Bolstad, J., 1994. Thermal generation of carbon dioxide and organic acids from different source rocks. *Organic Geochemistry* 21, 1229-1242.
- Behar, F., Ungerer, P., Kressmann, S., Rudkiewicz, J.L., 1991. Thermal evolution of crude oils in sedimentary basins; experimental simulation in a confined system and kinetic modeling. *Revue de l'Institut Francais du Petrole* 46, 151-181.
- Berner, U., Faber, E., Scheeder, G., Panten, D., 1995. Primary cracking of algal and landplant kerogens; kinetic models of isotope variations in methane, ethane and propane, *Processes of natural gas formation*. Elsevier, Amsterdam, Netherlands, pp. 233-245.
- di Primio, R., Dieckmann, V., Mills, N., 1998. PVT and phase behaviour analysis in petroleum exploration. *Organic Geochemistry* 29, 207-222.
- di Primio, R., Horsfield, B., 2006. From petroleum-type organofacies to hydrocarbon phase prediction. *Aapg Bulletin* 90, 1031-1058.
- Dieckmann, V., Schenk, H.J., Horsfield, B., Welte, D.H., 1998. Kinetics of petroleum generation and cracking by programmed-temperature closed-system pyrolysis of Toarcian Shales. *Fuel* 77, 23-31.
- Erdmann, M., 1999a. Gas Generation from Overmature Upper Jurassic Source Rocks, Northern Viking Graben. RWTH Aachen, Aachen, p. 128.
- Erdmann, M., 1999b. Gas generation from overmature Upper Jurassic source rocks, Northern Viking Graben. Berichte des Forschungszentrum Jülich, p. 128.
- Horsfield, B., Disko, U., Leistner, F., 1989. The micro-scale simulation of maturation: outline of a new technique and its potential applications. *Geologische Rundschau* 78, 361-374.
- Horsfield, B., Dueppenbecker, S.J., 1991. The decomposition of posidonia shale and green river shale kerogens using microscale sealed vessel (MSSV) pyrolysis. *Journal of Analytical and Applied Pyrolysis* 20, 107-123.
- Mahlstedt, N., Horsfield, B., di Primio, R., 2013. GORFit – From Liquids to Late Gas: Deconvoluting Primary from Secondary Gas Generation Kinetics, 26th International Meeting on Organic Geochemistry (IMOG), Tenerife, Canary Islands (Spain). Book of Abstracts, p. 193.
- Mango, F.D., 1996. Transition metal catalysis in the generation of natural gas. *Organic Geochemistry* 24, 977-984.
- Mango, F.D., 1997. The light hydrocarbons in petroleum: a critical review. *Organic Geochemistry* 26, 417-440.
- Michels, R., Enjelvin-Raoult, N., Elie, M., Mansuy, L., Faure, P., Oudin, J.-L., 2002. Understanding of reservoir gas compositions in a natural case using stepwise semi-open artificial maturation. *Marine and Petroleum Geology* 19, 589-599.
- Pedersen, K.S., Fredenslund, A., Thomassen, P., 1989. Properties of oils and natural gases. Gulf Publishing Company, Houston.

Pepper, A.S., Corvi, P.J., 1995a. Simple kinetic models of petroleum formation. Part I: oil and gas generation from kerogen. *Marine and Petroleum Geology* 12, 291-319.

Pepper, A.S., Corvi, P.J., 1995b. Simple kinetic models of petroleum formation. Part III: Modelling an open system. *Marine and Petroleum Geology* 12, 417-452.

Schenk, H.J., Horsfield, B., Krooss, B., Schaefer, R.G., Schwochau, K., 1997. Kinetics of petroleum formation and cracking, in: Welte, D.H., Horsfield, B., Backer, D.R. (Eds.), *Petroleum and Basin Evolution*. Springer, Berlin, pp. 231-270.

Appendix-PhaseKinetics approach

Methodology and background information on the PhaseKinetics approach.

The phase behaviour of migrating petroleum fluids is controlled by the fluids composition. The geological conditions upon which a migrating oil separates into oil and gas are strongly controlled by the gas (C1-C5) composition of the fluid (di Primio et al., 1998). For petroleum phase behaviour gas composition plays the dominant role with respect to the fluids saturation pressure and shrinkage behaviour, however, influence of the liquid fraction composition should not be neglected.

The gross description of oil and gas generation from closed system pyrolysis results, and the surface GORs derived therefrom, are very similar to the GOR distributions observed in nature. Hence, it appears that the relative gas and oil proportions generated as a function of maturity can be estimated based on laboratory experiments.

Compositional predictions are, however, not as straight forward. High methane contents generally result in phase separation at relatively high pressures, i.e. at great depth. A very wet gas composition results in a much lower saturation pressure (P_{sat}) for a given fluid. The sensitivity of gas composition on phase behaviour of migrating hydrocarbons has severe implications for the prediction of petroleum phase behaviour during petroleum generation and migration. Mango (1996, 1997) documented the discrepancy between gas compositions generated by pyrolysis of source rocks or oils and natural fluids. As discussed by Mango (1996; 1997) natural fluids display a much stronger predominance of methane in their gas fractions than observed in source rock pyrolysates. Interestingly, the lack of predictive ability of laboratory experiments is common to all experimental approaches: published gas compositions from closed system hydrous pyrolysis (Andresen et al., 1994), closed system anhydrous pyrolysis (Behar et al., 1991; Dieckmann et al., 1998; Erdmann, 1999; Michels et al., 2002) and open system pyrolysis (Berner et al., 1995) of Type I, II and III source rocks all show the same systematics.

It is commonly known that for genetically related fluids saturation pressure correlates linearly to GOR and formation volume factor (Bo). As discussed above the methane content of a fluid is the most important factor controlling its saturation pressure. Hence, a correction of the gas compositions generated by pyrolysis is possible assuming a linear relationship between the methane proportion of the gas phase (C1-C5) and the fluids GOR. The equation used for methane correction in this study is based on linear regression using a natural dataset from the North Sea representative of the black oil to gas-condensate range (correlation coefficient for the relationship between GOR and C1/C2-5 $r^2=0.98$). The original GOR used as a starting point for the methane correction was that determined on the MSSV pyrolysates and converted to volumetric data by a single stage flash using PVT simulation software.

The characterisation of the generated fluids oil composition (C6+) for phase behaviour assessment is based on the compositional information from MSSV analysis. The resolved compounds from C6 onwards were quantified, their proportions converted to molar amounts and these were summed to a total description of the liquid phase which consisted of a pseudo compound C6 (containing all

resolved compounds in the range eluting after Pentane until and including Hexane) and a C7+ fraction (containing the rest of the resolved compounds). The C7+ fraction was further characterised by a molecular weight and density. The molecular weight of the C7+ fraction was determined by subdividing the GC hump (MSSV total minus resolved compounds) into boiling ranges according to the resolved n-alkanes, and using the average molecular weights of the resolved compounds as representative of the respective hump range. Quantification of the subdivisions led thus to an averaged molecular weight of the entire hump. The density of the C7+ fraction was determined using a C7+ molecular weight – density correlation for natural petroleums from the North Sea.

The compositional description obtained by these methods is ideal for initial phase behaviour calculations. For the determination of a compositional kinetic model, however, a C7+ fraction consisting of molar amount, molecular weight and density was inappropriate. In PVT simulators the C7+ fraction definition is used to calculate a distribution of components representing the total liquid phase. This so called C7+ characterisation consists in representing the hydrocarbons with seven and more carbon atoms as a reasonable number (generally 12) of pseudo-components (with specific equation of state parameters) whereby a logarithmic relationship between the molar concentration z_N of a given fraction and the corresponding carbon number, CN, for $CN > 7$ is assumed (Pedersen et al., 1989). This characterisation leads to the automatic definition of a set of additional compounds of increasing molecular weight (usually up to the molecular weight range corresponding to alkane chainlengths of C80-C100). For this study a series of 6 pseudo compounds were defined: P10, P20, P30, P40, P50 and P60+. The physical properties of the individual pseudo compounds remain constant for all sample types, only their molar proportion varies depending on the samples original composition. This subdivision of the C7+ fraction into 6 additional fractions was tested to be the minimum number of pseudo compounds required for satisfactory calculation of phase behaviour.

The determined PVT descriptions of the fluids at different transformation ratios are used for the definition of the compositional kinetic models. The individual potentials per activation energy derived from the bulk kinetic analysis of the samples are subdivided into 14 sub-potentials, one for each compound described in the PVT dataset. The PVT data is assigned to individual bulk potentials based on its transformation ratio. For example bulk potentials below a TR of 10% were assigned the compositional description of the 10% TR MSSV experiment, from 10 to under 30% TR the 30% TR compositional description is used, etc. The final compositional kinetic models, hence, consist of an activation energy distribution for each compound (potentials normalised to 100%) as well as a total potential for each compound (again normalised to 100%). In combination with the sample HI and TOC absolute potentials can be calculated.

Appendix 6-1 - Tables

Table 6-A1: Activation energy distribution and frequency factors based on slow heating rates (0.7; 2.0; 5.0K/min).

slow rates	G016500	G016504	G016505	G016508	G016511	G016522	G016524	G016531	G016535	G016539
10% TR (°C)	145.6	125.8	125.1	148.4	114.2	126.8	127.4	146.9	134.5	135.9
50% TR (°C)	162.9	140.5	143.8	169.1	134.3	143.1	141.2	163.8	154.2	152.3
90% TR (°C)	189.9	157.2	167.4	208.9	155.2	165.4	166.7	196.1	181.2	180.4
T_{max} (°C)	156.9	140.2	141.2	167.2	135.1	142.0	138.6	157.0	150.8	147.1
A (1/sec)	3.12E+14	1.53E+13	6.35E+13	2.00E+14	9.64E+12	4.18E+13	2.07E+13	7.00E+14	3.48E+14	8.65E+13
Ea (kcal/mol)	(%)									
45					0.28					
46		0.26			1.95					
47		0.40	0.14		2.42	0.24				
48			0.82		7.13	0.65				
49		0.14	0.42		11.34	0.42				
50	0.23	11.37	2.89		33.77	3.39				
51	0.01	42.90	8.48		21.22	5.32	49.81		1.39	1.06
52		22.50	24.15		10.42	41.86	13.60		0.94	
53		16.50	22.67	0.38	4.91	18.61	20.09	0.20	4.59	29.31
54		0.73	15.68	4.03	3.18	13.95	2.59		14.41	20.21
55	19.66	3.28	12.63	11.66	0.78	6.65	7.82		22.59	21.52
56	21.17	0.48	4.33	14.92	1.75	3.38	0.02	26.36	17.32	9.93
57	22.58	1.00	4.36	25.21	0.22	2.47	3.66	18.86	15.96	6.83
58	11.26		1.03	13.52		1.33		20.09	8.57	2.06
59	10.54		1.91	6.71		0.57	1.82	9.78	5.10	3.96
60	4.18	0.44		6.43	0.62	1.15	0.34	7.94	3.75	0.18
61	6.61			3.74				5.19	1.76	2.78
62			0.49	2.89			0.25	3.29	1.70	0.70
63	3.19			3.88				2.98	0.79	
64	0.36								0.33	0.84
65				4.22				3.09	0.49	0.22
66	0.22			0.50					0.29	0.39
67				0.35						
68							0.32			
69				1.55						
70							1.90			

Table 6-A2a: cumulative MSSV-yields: individual, resolved, total compounds.

Sample	G016504X				
Heated to, °C	373.2	390.2	401.8	413.5	432.3
Weight, mg	18.13	16.50	14.80	13.35	10.55
Resolved	(µg/g)				
C1	62.2	112.4	189.3	302.0	553.7
C2	33.1	79.1	124.6	217.9	452.0
C3	78.4	155.4	220.7	343.6	600.6
i-C4	37.7	78.0	110.8	136.2	172.3
n-C4	40.3	73.6	104.1	165.3	311.1
i-C5	71.8	140.9	176.1	225.7	521.4
n-C5	25.6	49.7	72.8	116.9	219.4
R06	82.0	159.1	219.9	322.5	534.3
R07	93.9	183.1	251.9	361.7	602.4
R08	100.8	191.4	258.0	362.6	585.4
R09	96.8	177.8	240.7	338.2	535.2
R10	92.0	167.1	229.5	319.1	488.4
R11	78.6	141.3	203.9	294.7	480.9
R12	81.0	141.6	207.2	289.4	488.0
R13	65.6	120.4	169.5	241.7	427.0
R14	46.7	87.3	127.9	190.9	312.5
R15	54.2	102.1	152.2	230.0	355.4
R16	62.2	115.5	164.5	233.0	361.2
R17	40.4	73.6	106.0	161.7	294.0
R18	32.6	60.1	95.6	154.1	280.3
R19	26.6	51.5	91.9	150.4	279.8
R20	23.5	49.3	93.1	149.0	266.3
R21	27.7	61.4	111.2	169.3	298.6
R22	29.0	69.9	122.9	162.3	295.2
R23	25.4	64.1	112.2	128.2	287.5
R24	25.0	62.3	105.0	103.6	270.4
R25	20.3	50.6	91.1	75.9	247.9
R26	16.8	42.3	77.7	63.4	211.3
R27	13.5	36.5	68.4	55.1	178.0
R28	7.5	21.4	45.3	37.8	115.0
R29	3.9	12.1	24.7	24.1	68.6
R30-32	10.4	29.2	50.0	42.9	115.2
Totals	(µg/g)				
T06 -Blank	90.8	177.4	239.4	343.7	576.9
T07 -Blank	104.4	205.8	271.1	384.7	640.4
T08 -Blank	112.9	212.9	279.4	391.4	625.7
T09 -Blank	119.0	222.8	293.6	408.8	633.8
T10 -Blank	119.1	223.5	300.3	416.0	605.3
T11 -Blank	109.9	200.3	278.8	401.2	614.6
T12 -Blank	116.6	212.1	293.1	420.1	651.8
T13 -Blank	109.4	201.6	279.3	400.0	626.2
T14 -Blank	98.9	185.3	257.9	371.0	571.9
T15 -Blank	106.9	199.4	285.4	421.2	618.6
T16 -Blank	108.3	207.3	290.3	407.7	606.5
T17 -Blank	88.3	169.1	238.0	347.3	543.8
T18 -Blank	86.8	167.0	239.3	354.3	564.1
T19 -Blank	78.0	151.1	229.8	348.2	552.6
T20 -Blank	73.3	149.2	230.8	346.1	547.2
T21 -Blank	73.4	155.3	243.4	355.6	566.0
T22 -Blank	72.5	159.6	251.5	342.6	562.7
T23 -Blank	69.2	154.7	241.4	295.2	533.9
T24 -Blank	69.9	152.1	234.9	259.9	504.3
T25 -Blank	68.5	138.8	215.0	216.7	460.3
T26 -Blank	68.9	136.1	203.5	200.8	424.6
T27 -Blank	73.4	133.4	195.0	190.7	369.1
T28 -Blank	73.9	120.1	173.3	175.8	294.0
T29 -Blank	74.6	116.3	157.5	163.9	237.9
T30-32 -Blank	270.8	377.2	475.1	510.8	535.2

Sample	G016505X				
Heated to,	370.0	390.4	404.8	421.5	458.3
Weight, mg	5.29	4.86	3.79	3.12	2.66
Resolved	(µg/g)				
C1	925.3	2196.2	3860.1	6458.3	17566.7
C2	337.6	1052.0	2121.1	4211.4	11650.6
C3	406.9	1103.0	2113.0	3980.5	10985.4
i-C4	53.3	171.1	341.1	620.9	1532.1
n-C4	229.3	536.6	1086.3	2065.0	6546.8
i-C5	215.8	454.5	757.1	1207.7	2470.0
n-C5	130.6	339.1	642.8	1286.6	4144.1
R06	334.6	784.0	1435.1	2483.3	6233.9
R07	389.8	909.2	1617.6	2767.1	6691.6
R08	431.6	990.5	1723.2	2850.6	6734.6
R09	414.5	985.0	1701.7	2765.1	6266.3
R10	424.9	1014.1	1800.2	2973.7	5729.4
R11	557.7	1476.1	2580.8	4302.4	7363.4
R12	457.3	1297.5	2357.8	4084.1	6255.6
R13	358.4	971.9	1769.8	3008.4	4337.5
R14	255.4	630.3	1104.0	1770.7	2132.8
R15	371.5	937.5	1650.7	2479.1	2792.4
R16	590.5	1344.5	2095.7	2757.2	2436.8
R17	242.8	598.0	1055.8	1624.1	1512.6
R18	285.8	711.0	1228.4	1674.7	1217.8
R19	222.7	533.1	922.8	1431.9	1032.0
R20	228.2	495.9	847.0	1301.2	714.5
R21	256.7	613.1	1033.3	1575.3	776.2
R22	246.3	563.3	940.3	1391.4	543.7
R23	239.9	485.9	843.2	1351.4	373.3
R24	210.8	428.9	790.2	1270.5	239.0
R25	165.3	357.3	695.1	1159.3	133.4
R26	111.2	279.6	566.0	924.5	74.5
R27	96.5	252.7	518.9	822.1	64.5
R28	67.6	172.6	359.4	548.2	32.2
R29	44.1	114.3	257.9	361.1	17.2
R30-32	83.5	203.2	397.5	473.7	25.9
Totals	(µg/g)				
T06 -Blank	385.0	864.7	1536.9	2617.1	6456.8
T07 -Blank	447.2	997.7	1732.7	2903.5	6961.5
T08 -Blank	499.4	1071.9	1823.9	3006.7	6981.6
T09 -Blank	530.7	1185.0	2005.7	3241.5	6743.3
T10 -Blank	590.0	1365.4	2279.4	3623.5	6639.1
T11 -Blank	757.6	1846.2	3118.8	5079.3	8376.7
T12 -Blank	697.0	1769.5	3112.3	5124.3	7694.1
T13 -Blank	671.6	1634.5	2854.7	4565.9	6046.7
T14 -Blank	656.2	1518.0	2542.6	3786.3	4104.8
T15 -Blank	818.1	1886.3	3109.6	4477.3	4499.0
T16 -Blank	1026.5	2269.9	3551.7	4651.2	3920.7
T17 -Blank	666.3	1561.6	2604.3	3635.6	2816.9
T18 -Blank	766.3	1715.8	2794.2	3747.8	2502.6
T19 -Blank	645.3	1486.4	2478.0	3428.1	2156.1
T20 -Blank	643.6	1450.0	2390.8	3263.6	1773.5
T21 -Blank	658.7	1495.9	2487.0	3465.9	1691.9
T22 -Blank	612.1	1387.3	2311.3	3206.9	1298.2
T23 -Blank	575.6	1214.2	2092.1	3027.4	979.2
T24 -Blank	518.3	1076.7	1917.5	2802.2	734.1
T25 -Blank	450.5	924.2	1734.6	2572.1	535.8
T26 -Blank	395.7	834.8	1551.5	2281.3	412.1
T27 -Blank	376.0	781.1	1450.0	2049.1	336.1
T28 -Blank	338.7	657.7	1213.8	1655.3	267.6
T29 -Blank	322.3	610.9	1066.9	1360.6	261.9
T30-32 -Blank	1019.9	1639.1	2661.5	3079.9	877.1

Table 6-A2a (contd.): cumulative MSSV-yields: individual, resolved, total compounds.

Sample	G016511X					Sample	G016522X				
Heated to,	361.2	382.7	396.4	409.4	429.7	Heated to,	371.4	389.8	402.0	415.0	440.0
Weight, mg	5.13	5.27	3.56	3.13	3.12	Weight, mg	4.93	4.07	3.32	2.93	3.22
Resolved	(µg/g)					Resolved	(µg/g)				
C1	109.5	1137.3	1610.5	2433.8	5108.5	C1	355.0	813.5	1474.0	2193.5	6324.1
C2	62.4	518.2	882.7	1578.7	3589.6	C2	187.9	528.8	1062.8	1787.0	5214.2
C3	70.9	475.4	849.4	1450.8	3235.8	C3	222.1	565.0	1049.2	1718.1	4736.8
i-C4	8.8	78.6	120.5	202.9	452.9	i-C4	23.6	62.8	115.6	201.8	592.6
n-C4	44.6	274.0	502.7	852.6	1831.6	n-C4	149.5	334.3	651.3	1040.0	3010.2
i-C5	48.5	328.9	453.4	665.1	1085.6	i-C5	124.4	216.7	349.2	484.9	1089.6
n-C5	36.5	188.8	341.1	582.3	1240.7	n-C5	93.5	238.4	440.0	752.4	2177.8
R06	68.1	468.9	762.5	1245.3	2356.6	R06	184.5	452.5	835.6	1309.3	3449.3
R07	79.7	516.4	860.6	1379.3	2571.1	R07	253.4	585.9	1059.7	1619.9	3975.4
R08	142.9	709.5	1134.3	1770.2	3089.3	R08	319.9	713.7	1195.9	1798.7	4175.4
R09	139.4	711.3	1142.8	1747.9	2976.4	R09	276.3	639.1	1093.7	1668.7	3801.9
R10	169.6	830.7	1286.3	1878.7	2899.4	R10	291.7	676.3	1158.5	1775.5	3705.0
R11	210.1	894.8	1411.6	2151.2	3460.9	R11	337.4	774.7	1370.8	2063.4	4541.9
R12	164.3	715.7	1136.2	1825.5	2919.6	R12	306.3	734.7	1275.3	1956.9	4146.2
R13	144.7	564.7	916.3	1436.7	2433.8	R13	266.0	625.2	1046.7	1628.9	3188.6
R14	113.9	449.9	709.9	1089.0	1720.9	R14	179.8	416.4	671.4	1071.2	2011.0
R15	164.3	591.1	875.8	1295.5	1963.6	R15	209.7	483.7	782.4	1198.3	2281.8
R16	290.5	962.5	1299.3	1708.5	2314.1	R16	247.4	513.5	857.5	1162.3	1951.5
R17	92.0	341.1	488.7	706.1	1005.5	R17	160.1	339.0	582.2	857.3	1504.3
R18	125.0	408.5	533.8	745.9	1003.5	R18	208.3	391.3	640.4	880.0	1468.3
R19	79.4	277.1	406.6	595.6	801.8	R19	150.7	323.1	530.3	737.6	1287.1
R20	69.6	245.5	358.7	511.0	624.6	R20	152.8	314.4	514.0	705.1	1044.1
R21	74.6	248.6	315.2	471.1	542.8	R21	156.6	312.0	523.8	704.6	967.8
R22	58.0	205.6	286.2	443.9	387.3	R22	154.2	321.7	487.0	687.7	852.6
R23	58.6	211.5	277.5	425.3	277.5	R23	160.0	323.1	426.7	658.4	789.9
R24	45.8	159.0	195.2	302.6	142.2	R24	120.2	247.6	319.0	518.3	622.5
R25	41.9	131.3	148.2	252.8	96.3	R25	88.4	183.6	219.6	354.9	421.3
R26	33.5	96.2	96.3	188.4	49.9	R26	52.4	116.7	142.2	253.5	318.9
R27	31.6	87.6	79.1	149.6	29.2	R27	44.6	94.0	107.3	196.6	238.4
R28	24.6	75.4	65.3	117.1	15.0	R28	33.3	76.9	88.8	145.8	167.3
R29	26.9	73.4	52.7	93.5	11.2	R29	25.2	45.3	68.9	109.6	115.8
R30-32	242.2	436.1	399.2	490.4	41.4	R30-32	153.1	262.9	244.7	335.5	178.4
Totals	(µg/g)					Totals	(µg/g)				
T06 -Blank	93.1	513.2	838.6	1346.7	2587.7	T06 -Blank	222.2	510.0	903.0	1433.4	3575.2
T07 -Blank	109.3	578.0	958.2	1519.5	2851.7	T07 -Blank	298.4	658.3	1133.0	1738.9	4129.6
T08 -Blank	185.7	786.0	1248.6	1905.5	3373.5	T08 -Blank	373.2	790.3	1297.5	1947.4	4342.1
T09 -Blank	201.6	840.5	1319.4	2006.6	3526.0	T09 -Blank	369.3	784.1	1314.8	1941.4	4227.2
T10 -Blank	252.9	1061.5	1608.7	2343.0	3737.8	T10 -Blank	405.7	863.6	1453.6	2159.0	4363.9
T11 -Blank	308.8	1167.0	1802.0	2663.3	4296.8	T11 -Blank	462.2	1002.1	1724.2	2508.9	5247.9
T12 -Blank	283.7	1028.5	1641.2	2467.5	3940.4	T12 -Blank	459.8	1011.8	1738.0	2572.2	5239.0
T13 -Blank	278.7	960.2	1538.8	2333.7	3700.9	T13 -Blank	456.9	989.8	1684.1	2525.3	4665.5
T14 -Blank	280.5	980.2	1526.4	2256.1	3360.7	T14 -Blank	426.2	915.5	1534.6	2222.6	3840.4
T15 -Blank	368.4	1214.2	1826.4	2630.5	3670.1	T15 -Blank	493.2	1048.2	1747.0	2473.9	4037.4
T16 -Blank	489.3	1558.4	2138.9	2900.1	3769.7	T16 -Blank	521.8	1088.7	1779.3	2418.9	3638.3
T17 -Blank	289.9	913.2	1311.3	1839.3	2282.1	T17 -Blank	446.5	931.4	1518.9	2088.3	3089.9
T18 -Blank	322.6	965.1	1331.9	1880.0	2158.9	T18 -Blank	497.9	982.8	1591.6	2147.9	3038.2
T19 -Blank	270.9	823.7	1182.7	1691.3	1781.5	T19 -Blank	437.9	900.1	1479.7	2005.8	2807.3
T20 -Blank	272.8	798.6	1146.2	1665.5	1558.6	T20 -Blank	443.7	907.0	1491.0	1989.6	2598.0
T21 -Blank	270.2	771.7	1073.9	1539.2	1352.4	T21 -Blank	445.4	909.1	1490.4	1949.1	2468.1
T22 -Blank	236.8	684.9	942.2	1374.8	1076.7	T22 -Blank	428.7	876.2	1383.6	1881.4	2209.2
T23 -Blank	219.6	655.3	867.2	1274.2	840.7	T23 -Blank	411.9	835.5	1298.9	1752.0	2014.6
T24 -Blank	194.8	552.2	720.9	1062.1	594.2	T24 -Blank	354.5	740.4	1080.1	1504.7	1737.1
T25 -Blank	189.1	489.8	617.5	930.7	432.6	T25 -Blank	309.7	622.0	892.5	1260.8	1457.8
T26 -Blank	185.8	443.9	530.0	805.6	311.6	T26 -Blank	268.7	547.3	754.8	1096.2	1229.6
T27 -Blank	196.0	436.5	500.2	730.9	216.0	T27 -Blank	257.7	504.9	679.9	1000.0	1047.5
T28 -Blank	207.7	432.4	493.8	689.0	145.6	T28 -Blank	240.1	468.3	621.0	936.6	877.9
T29 -Blank	233.5	484.2	527.9	685.5	109.7	T29 -Blank	247.2	448.3	600.2	860.0	765.7
T30-32 -Blank	951.1	1585.1	1887.1	2108.9	263.8	T30-32 -Blank	870.9	1432.4	1691.4	2470.8	1706.1

Table 6-A2a (contd.): cumulative MSSV-yields: individual, resolved, total compounds.

Sample	G016531X					Sample	G016535X				
Heated to,	389.5	407.8	421.7	439.4	480.1	Heated to,	375.5	396.5	411.2	428.5	472.0
Weight, mg	5.01	3.99	3.60	3.04	2.45	Weight, mg	4.98	2.50	3.49	1.69	1.35
Resolved	(\mu g/g)					Resolved	(\mu g/g)				
C1	385.0	763.2	1860.7	4070.5	11617.4	C1	509.5	1036.6	2038.6	3555.2	12390.3
C2	242.9	546.3	1371.0	2956.3	6911.7	C2	284.0	698.5	1557.3	2623.9	7921.2
C3	315.3	561.5	1207.9	2503.3	5546.1	C3	286.1	693.3	1359.7	2300.1	6463.7
i-C4	101.0	96.7	197.8	349.9	750.2	i-C4	39.4	84.0	179.9	249.4	747.8
n-C4	214.8	303.2	646.7	1355.0	2783.9	n-C4	173.5	412.7	743.4	1297.9	3545.2
i-C5	153.3	192.7	343.1	566.4	884.9	i-C5	226.2	322.5	460.9	726.0	1404.5
n-C5	123.9	196.1	253.3	816.1	1364.0	n-C5	108.1	249.1	448.3	790.4	1867.6
R06	209.8	332.6	735.2	1359.5	1797.0	R06	239.0	502.3	917.8	1582.6	2732.9
R07	340.7	477.7	940.2	1695.9	2099.3	R07	309.9	692.0	1138.1	1829.9	2806.2
R08	504.8	631.6	1141.5	1910.6	2325.0	R08	422.5	865.9	1327.7	2092.5	3262.4
R09	359.1	497.1	941.9	1608.7	1967.3	R09	354.4	758.9	1187.0	1928.9	2830.6
R10	249.4	375.5	782.9	1391.4	1693.6	R10	386.2	752.3	1261.0	1949.1	2690.8
R11	239.3	424.1	933.2	1686.5	1984.3	R11	439.1	874.1	1610.7	2466.9	3140.7
R12	239.9	430.2	897.2	1626.0	1648.3	R12	395.6	809.6	1448.5	2282.1	2323.0
R13	246.1	391.8	752.0	1258.0	1135.6	R13	306.0	648.2	1096.7	1646.9	1432.8
R14	136.4	231.9	406.3	691.4	476.9	R14	189.1	393.1	659.3	932.6	562.0
R15	190.2	277.5	473.8	755.6	680.2	R15	221.6	440.7	706.5	993.3	715.5
R16	156.7	236.3	431.1	662.1	471.0	R16	219.6	430.7	689.3	976.9	513.7
R17	112.7	164.9	302.3	469.3	312.1	R17	163.0	331.2	524.9	740.8	300.8
R18	130.6	197.2	323.4	471.0	274.9	R18	201.5	373.9	568.9	737.5	249.9
R19	92.8	140.4	260.6	387.5	272.4	R19	162.8	327.5	521.2	665.0	220.3
R20	71.9	112.1	207.5	293.1	168.8	R20	171.8	331.2	481.9	590.0	121.9
R21	72.0	117.1	210.1	297.7	161.8	R21	171.2	321.8	478.9	557.8	124.0
R22	62.1	92.4	154.0	196.0	114.4	R22	146.6	295.3	402.6	473.9	44.2
R23	55.6	88.1	148.7	185.8	99.6	R23	176.9	296.0	363.4	427.2	47.1
R24	49.8	70.8	119.0	152.6	72.8	R24	102.0	188.4	220.2	282.2	24.1
R25	36.9	55.6	84.7	101.1	34.3	R25	80.9	135.4	144.3	189.1	13.9
R26	29.8	39.6	65.5	86.1	40.6	R26	49.6	73.1	68.9	120.3	17.0
R27	23.0	34.8	51.4	67.8	30.1	R27	39.5	54.2	45.6	85.1	8.4
R28	18.5	27.7	42.0	44.5	14.1	R28	16.8	26.0	31.9	46.1	7.0
R29	19.7	26.9	34.3	44.8	27.2	R29	18.5	20.7	19.9	46.0	4.0
R30-32	47.6	58.9	48.3	75.2	19.5	R30-32	49.5	54.9	39.5	66.6	9.0
Totals	(\mu g/g)					Totals	(\mu g/g)				
T06 -Blank	245.1	382.8	767.7	1467.5	1953.1	T06 -Blank	282.1	578.3	989.9	1714.1	2936.2
T07 -Blank	380.2	539.8	1024.4	1822.0	2242.4	T07 -Blank	366.8	781.6	1222.9	1998.2	2980.2
T08 -Blank	564.2	714.4	1240.8	2056.5	2492.4	T08 -Blank	498.0	988.0	1414.0	2308.0	3467.9
T09 -Blank	457.2	628.7	1127.1	1902.6	2188.8	T09 -Blank	463.7	949.0	1393.3	2262.5	3116.5
T10 -Blank	360.6	533.8	1022.6	1756.2	1957.6	T10 -Blank	524.7	984.9	1579.5	2419.5	3053.7
T11 -Blank	366.1	599.9	1210.9	2133.8	2282.9	T11 -Blank	603.0	1135.9	1957.0	3026.0	3573.9
T12 -Blank	387.4	648.8	1260.9	2205.6	2060.1	T12 -Blank	582.9	1122.3	1898.0	2951.0	2878.3
T13 -Blank	409.7	636.3	1177.8	1918.4	1571.1	T13 -Blank	521.1	1042.9	1680.4	2512.1	1983.2
T14 -Blank	321.1	535.1	955.4	1525.2	942.5	T14 -Blank	429.2	857.6	1338.8	1968.8	1124.9
T15 -Blank	398.5	625.4	1066.7	1652.1	1115.9	T15 -Blank	487.1	942.4	1422.3	2019.0	1202.9
T16 -Blank	351.1	556.3	946.0	1400.1	849.7	T16 -Blank	469.9	876.4	1333.8	1854.0	934.6
T17 -Blank	300.0	474.5	803.3	1186.9	662.3	T17 -Blank	406.2	760.5	1151.3	1605.8	687.1
T18 -Blank	316.5	493.3	811.4	1179.2	660.1	T18 -Blank	447.6	821.6	1181.0	1609.4	629.9
T19 -Blank	280.0	444.7	744.9	1059.9	605.9	T19 -Blank	384.2	729.8	1063.5	1448.0	558.3
T20 -Blank	265.5	417.1	677.8	957.7	513.1	T20 -Blank	396.1	722.8	1031.9	1371.0	453.6
T21 -Blank	259.6	408.3	661.1	916.5	483.0	T21 -Blank	384.1	705.8	997.7	1284.4	430.0
T22 -Blank	235.4	363.0	573.4	783.4	404.7	T22 -Blank	352.7	642.3	876.0	1111.4	281.3
T23 -Blank	229.7	344.3	533.9	703.9	342.9	T23 -Blank	366.3	626.5	782.7	992.5	253.4
T24 -Blank	207.4	305.2	456.8	585.5	312.9	T24 -Blank	269.0	465.8	568.1	756.2	205.1
T25 -Blank	190.5	270.6	392.4	488.3	251.5	T25 -Blank	230.1	376.1	436.4	582.2	150.4
T26 -Blank	180.2	255.2	340.1	442.8	269.1	T26 -Blank	186.0	278.4	309.8	451.7	128.9
T27 -Blank	158.3	226.7	274.4	372.0	204.2	T27 -Blank	157.7	222.7	252.6	349.4	86.7
T28 -Blank	139.1	195.5	220.1	310.9	171.1	T28 -Blank	126.0	157.1	206.1	244.1	40.3
T29 -Blank	141.0	202.8	183.8	290.7	188.1	T29 -Blank	136.1	139.1	189.0	210.8	40.3
T30-32 -Blank	428.9	566.9	312.1	659.6	515.0	T30-32 -Blank	407.6	328.1	594.5	429.2	103.8

Table 6-A2a (contd.): cumulative MSSV-yields: individual, resolved, total compounds.

Sample	G016539X				
Heated to,	383.7	402.5	415.6	431.0	463.0
Weight, mg	20.04	18.09	16.10	14.02	10.16
Resolved	(µg/g)				
C1	113.3	320.6	604.2	1027.3	2608.8
C2	83.3	234.3	471.9	819.2	1873.4
C3	109.9	231.9	447.0	740.7	1684.7
i-C4	16.9	32.6	58.9	98.0	202.9
n-C4	47.9	132.1	243.0	434.3	982.5
i-C5	60.1	82.0	142.6	181.6	346.3
n-C5	34.4	79.9	156.5	278.4	639.7
R06	79.3	169.5	312.3	481.8	945.0
R07	103.7	221.2	384.4	580.7	995.5
R08	126.3	255.9	424.3	634.5	1013.0
R09	106.2	218.7	372.4	564.0	884.0
R10	109.0	234.9	412.4	592.4	826.9
R11	120.0	291.0	513.2	767.4	991.4
R12	113.0	274.1	486.6	705.2	832.7
R13	99.6	220.2	377.7	535.3	543.2
R14	65.2	137.4	234.9	316.8	249.7
R15	79.3	164.7	276.2	356.6	285.1
R16	79.4	162.2	268.1	331.6	227.3
R17	61.1	128.3	221.8	275.5	146.6
R18	72.5	147.0	242.0	283.6	133.2
R19	61.4	137.2	217.9	248.7	110.9
R20	61.0	130.9	201.6	217.7	70.8
R21	65.7	135.3	206.0	206.7	61.5
R22	58.6	118.9	174.0	164.7	35.0
R23	65.4	110.8	153.2	128.3	26.5
R24	37.7	68.4	103.9	71.4	13.8
R25	31.3	49.5	76.2	49.3	7.5
R26	17.5	30.4	45.2	26.4	5.3
R27	14.6	22.7	31.7	17.7	3.4
R28	7.0	14.3	20.5	13.7	2.0
R29	6.1	10.5	16.6	9.0	2.4
R30-32	18.1	25.6	29.8	12.8	3.7
Totals	(µg/g)				
T06 -Blank	92.5	182.3	329.4	519.7	984.5
T07 -Blank	122.0	235.8	403.1	610.7	1035.5
T08 -Blank	149.0	274.9	446.3	664.2	1056.1
T09 -Blank	139.1	258.5	430.9	642.0	957.9
T10 -Blank	153.7	295.1	493.0	709.2	962.1
T11 -Blank	163.9	357.0	612.1	896.5	1145.0
T12 -Blank	164.2	360.5	618.8	892.3	1020.4
T13 -Blank	159.7	321.4	543.7	756.6	742.6
T14 -Blank	137.5	275.4	456.9	599.0	476.4
T15 -Blank	159.2	306.8	500.0	631.1	480.3
T16 -Blank	156.2	297.5	476.6	577.5	384.2
T17 -Blank	139.1	265.7	434.0	507.3	291.3
T18 -Blank	154.3	293.7	456.3	511.7	267.4
T19 -Blank	139.1	280.5	442.1	476.4	228.8
T20 -Blank	142.2	282.5	436.1	444.7	187.1
T21 -Blank	148.0	288.9	436.3	422.9	165.1
T22 -Blank	136.3	262.5	395.9	359.7	120.3
T23 -Blank	139.5	246.0	361.4	301.8	92.2
T24 -Blank	104.4	186.6	279.0	215.3	68.4
T25 -Blank	93.7	163.2	232.3	163.5	50.2
T26 -Blank	74.7	132.4	191.8	123.1	41.7
T27 -Blank	63.9	115.7	172.9	96.7	33.0
T28 -Blank	49.9	98.9	149.9	81.3	26.3
T29 -Blank	47.1	91.6	134.7	71.8	27.4
T30-32 -Blank	113.9	237.7	330.4	187.2	100.0

Table 6-A2b: instantaneous MSSV-yields: individual, resolved, total compounds.

Sample	G016504X					Sample	G016505X				
Heated to,	373.2	390.2	401.8	413.5	432.3	Heated to,	370.0	390.4	404.8	421.5	458.3
Weight, mg	18.13	16.50	14.80	13.35	10.55	Weight, mg	5.29	4.86	3.79	3.12	2.66
Resolved	(µg/g)					Resolved	(µg/g)				
C1	62.2	50.2	76.8	112.7	251.7	C1	925.3	1270.9	1663.8	2598.3	11108.3
C2	33.1	46.0	45.5	93.3	234.1	C2	337.6	714.4	1069.1	2090.3	7439.3
C3	78.4	77.0	65.3	122.8	257.0	C3	406.9	696.1	1010.0	1867.5	7004.9
i-C4	37.7	40.3	32.8	25.4	36.1	i-C4	53.3	117.8	170.0	279.8	911.2
n-C4	40.3	33.3	30.5	61.3	145.8	n-C4	229.3	307.3	549.7	978.6	4481.8
i-C5	71.8	69.2	35.1	49.6	95.7	i-C5	215.8	238.7	302.6	450.5	1262.4
n-C5	25.6	24.1	23.1	44.1	102.5	n-C5	130.6	208.5	303.7	643.9	2857.5
R06	82.0	77.1	60.8	102.6	211.8	R06	334.6	449.5	651.0	1048.2	3750.7
R07	93.9	89.2	68.8	109.9	240.7	R07	389.8	519.4	708.4	1149.5	3924.5
R08	100.8	90.6	66.6	104.5	222.8	R08	431.6	558.9	732.7	1127.5	3884.0
R09	96.8	81.0	62.9	97.5	197.0	R09	414.5	570.5	716.7	1063.5	3501.2
R10	92.0	75.1	62.4	89.6	169.3	R10	424.9	589.3	786.1	1173.5	2755.7
R11	78.6	62.7	62.6	90.8	186.3	R11	557.7	918.3	1104.7	1721.6	3061.0
R12	81.0	60.6	65.6	82.2	198.6	R12	457.3	840.3	1060.3	1726.3	2171.6
R13	65.6	54.8	49.2	72.2	185.3	R13	358.4	613.5	797.9	1238.5	1329.1
R14	46.7	40.6	40.6	63.0	121.6	R14	255.4	375.0	473.6	666.7	362.1
R15	54.2	47.9	50.0	77.8	125.4	R15	371.5	566.0	713.1	828.5	313.3
R16	62.2	53.3	49.0	68.4	128.2	R16	590.5	753.9	751.2	661.5	0.0
R17	40.4	33.2	32.4	55.7	132.3	R17	242.8	355.2	457.8	568.3	0.0
R18	32.6	27.4	35.5	58.5	126.2	R18	285.8	425.2	517.4	446.3	0.0
R19	26.6	25.0	40.4	58.4	129.4	R19	222.7	310.4	389.8	509.0	0.0
R20	23.5	25.8	43.8	55.9	117.2	R20	228.2	267.7	351.0	454.3	0.0
R21	27.7	33.7	49.8	58.1	129.3	R21	256.7	356.4	420.2	542.0	0.0
R22	29.0	40.9	53.0	39.4	132.9	R22	246.3	317.0	377.0	451.1	0.0
R23	25.4	38.7	48.1	16.0	159.3	R23	239.9	246.0	357.3	508.1	0.0
R24	25.0	37.3	42.8	0.0	166.8	R24	210.8	218.1	361.3	480.3	0.0
R25	20.3	30.2	40.6	0.0	172.0	R25	165.3	192.0	337.8	464.2	0.0
R26	16.8	25.5	35.4	0.0	147.9	R26	111.2	168.3	286.4	358.5	0.0
R27	13.5	23.0	31.9	0.0	122.9	R27	96.5	156.2	266.2	303.2	0.0
R28	7.5	13.9	24.0	0.0	77.2	R28	67.6	104.9	186.8	188.8	0.0
R29	3.9	8.1	12.6	0.0	44.5	R29	44.1	70.2	143.6	103.2	0.0
R30-32	10.4	18.8	20.8	0.0	72.3	R30-32	83.5	119.6	194.3	76.2	0.0
Totals	(µg/g)					Totals	(µg/g)				
T06 -Blank	90.8	86.6	62.0	104.2	233.2	T06 -Blank	385.0	479.7	672.2	1080.2	3839.7
T07 -Blank	104.4	101.4	65.2	113.6	255.8	T07 -Blank	447.2	550.5	735.0	1170.7	4058.0
T08 -Blank	112.9	100.0	66.4	112.0	234.3	T08 -Blank	499.4	572.5	752.0	1182.9	3974.9
T09 -Blank	119.0	103.8	70.9	115.2	224.9	T09 -Blank	530.7	654.3	820.7	1235.8	3501.7
T10 -Blank	119.1	104.4	76.8	115.7	189.4	T10 -Blank	590.0	775.4	914.0	1344.0	3015.6
T11 -Blank	109.9	90.4	78.5	122.4	213.4	T11 -Blank	757.6	1088.5	1272.7	1960.4	3297.5
T12 -Blank	116.6	95.5	81.0	127.0	231.7	T12 -Blank	697.0	1072.4	1342.9	2012.0	2569.8
T13 -Blank	109.4	92.2	77.7	120.7	226.2	T13 -Blank	671.6	962.9	1220.1	1711.3	1480.7
T14 -Blank	98.9	86.4	72.6	113.1	200.9	T14 -Blank	656.2	861.9	1024.5	1243.7	318.5
T15 -Blank	106.9	92.5	86.0	135.9	197.3	T15 -Blank	818.1	1068.3	1223.3	1367.7	21.6
T16 -Blank	108.3	99.0	83.0	117.3	198.8	T16 -Blank	1026.5	1243.4	1281.7	1099.5	0.0
T17 -Blank	88.3	80.8	68.9	109.3	196.5	T17 -Blank	666.3	895.3	1042.7	1031.3	0.0
T18 -Blank	86.8	80.2	72.3	114.9	209.8	T18 -Blank	766.3	949.5	1078.4	953.5	0.0
T19 -Blank	78.0	73.2	78.6	118.5	204.4	T19 -Blank	645.3	841.1	991.6	950.0	0.0
T20 -Blank	73.3	76.0	81.6	115.3	201.1	T20 -Blank	643.6	806.4	940.8	872.8	0.0
T21 -Blank	73.4	81.9	88.1	112.1	210.4	T21 -Blank	658.7	837.2	991.2	978.9	0.0
T22 -Blank	72.5	87.1	91.9	91.2	220.1	T22 -Blank	612.1	775.2	924.0	895.6	0.0
T23 -Blank	69.2	85.6	86.7	53.9	238.7	T23 -Blank	575.6	638.6	877.9	935.3	0.0
T24 -Blank	69.9	82.2	82.8	24.9	244.4	T24 -Blank	518.3	558.4	840.8	884.7	0.0
T25 -Blank	68.5	70.3	76.2	1.7	243.6	T25 -Blank	450.5	473.6	810.5	837.4	0.0
T26 -Blank	68.9	67.2	67.4	0.0	223.8	T26 -Blank	395.7	439.1	716.7	729.8	0.0
T27 -Blank	73.4	60.0	61.6	0.0	178.4	T27 -Blank	376.0	405.0	668.9	599.1	0.0
T28 -Blank	73.9	46.2	53.2	2.4	118.2	T28 -Blank	338.7	319.0	556.1	441.5	0.0
T29 -Blank	74.6	41.6	41.2	6.4	74.0	T29 -Blank	322.3	288.6	456.0	293.7	0.0
T30-32 -Blank	270.8	106.4	97.9	35.8	24.3	T30-32 -Blank	1019.9	619.2	1022.4	418.4	0.0

Table 6-A2b (contd.): instantaneous MSSV-yields: individual, resolved, total compounds.

Sample	G016511X					Sample	G016522X				
Heated to,	361.2	382.7	396.4	409.4	429.7	Heated to,	371.4	389.8	402.0	415.0	440.0
Weight, mg	5.13	5.27	3.56	3.13	3.12	Weight, mg	4.93	4.07	3.32	2.93	3.22
Resolved	(µg/g)					Resolved	(µg/g)				
C1	109.5	1027.8	473.3	823.3	2674.7	C1	355.0	458.5	660.5	719.6	4130.5
C2	62.4	455.9	364.4	696.0	2011.0	C2	187.9	340.8	534.0	724.2	3427.2
C3	70.9	404.5	374.0	601.5	1784.9	C3	222.1	342.9	484.2	668.9	3018.7
i-C4	8.8	69.8	41.9	82.5	250.0	i-C4	23.6	39.2	52.8	86.2	390.8
n-C4	44.6	229.4	228.7	349.9	979.1	n-C4	149.5	184.8	317.0	388.7	1970.2
i-C5	48.5	280.5	124.5	211.7	420.5	i-C5	124.4	92.2	132.6	135.6	604.7
n-C5	36.5	152.3	152.3	241.2	658.4	n-C5	93.5	144.9	201.6	312.4	1425.4
R06	68.1	400.7	293.7	482.8	1111.3	R06	184.5	268.0	383.1	473.7	2140.1
R07	79.7	436.8	344.2	518.7	1191.8	R07	253.4	332.5	473.8	560.1	2355.5
R08	142.9	566.6	424.8	635.8	1319.1	R08	319.9	393.9	482.1	602.8	2376.7
R09	139.4	571.9	431.6	605.0	1228.5	R09	276.3	362.8	454.6	575.0	2133.2
R10	169.6	661.1	455.7	592.4	1020.7	R10	291.7	384.7	482.2	617.0	1929.4
R11	210.1	684.7	516.8	739.7	1309.7	R11	337.4	437.3	596.1	692.6	2478.6
R12	164.3	551.4	420.5	689.3	1094.1	R12	306.3	428.3	540.6	681.6	2189.3
R13	144.7	419.9	351.6	520.4	997.1	R13	266.0	359.2	421.5	582.2	1559.7
R14	113.9	336.1	260.0	379.1	631.8	R14	179.8	236.7	255.0	399.8	939.7
R15	164.3	426.8	284.7	419.7	668.1	R15	209.7	274.0	298.7	415.9	1083.5
R16	290.5	672.0	336.7	409.2	605.6	R16	247.4	266.1	344.0	304.8	789.2
R17	92.0	249.2	147.5	217.5	299.4	R17	160.1	178.9	243.3	275.0	647.1
R18	125.0	283.5	125.3	212.1	257.6	R18	208.3	183.0	249.0	239.7	588.2
R19	79.4	197.7	129.6	188.9	206.2	R19	150.7	172.5	207.2	207.3	549.4
R20	69.6	175.9	113.2	152.3	113.6	R20	152.8	161.6	199.6	191.1	339.1
R21	74.6	174.0	66.6	155.9	71.7	R21	156.6	155.5	211.8	180.7	263.3
R22	58.0	147.5	80.7	157.7	0.0	R22	154.2	167.5	165.3	200.6	165.0
R23	58.6	153.0	65.9	147.8	0.0	R23	160.0	163.1	103.6	231.8	131.5
R24	45.8	113.2	36.2	107.3	0.0	R24	120.2	127.4	71.4	199.3	104.2
R25	41.9	89.4	16.9	104.6	0.0	R25	88.4	95.2	36.0	135.4	66.4
R26	33.5	62.7	0.1	92.1	0.0	R26	52.4	64.3	25.4	111.3	65.5
R27	31.6	56.1	0.0	70.5	0.0	R27	44.6	49.4	13.3	89.3	41.7
R28	24.6	50.7	0.0	51.9	0.0	R28	33.3	43.6	11.9	57.0	21.5
R29	26.9	46.5	0.0	40.8	0.0	R29	25.2	20.1	23.6	40.7	6.2
R30-32	242.2	193.9	0.0	91.1	0.0	R30-32	153.1	109.8	0.0	90.8	0.0
Totals	(µg/g)					Totals	(µg/g)				
T06 -Blank	93.1	420.2	325.3	508.2	1241.0	T06 -Blank	222.2	287.7	393.0	530.4	31.0
T07 -Blank	109.3	468.6	380.3	561.3	1332.2	T07 -Blank	298.4	359.9	474.7	605.9	2390.7
T08 -Blank	185.7	600.4	462.5	656.9	1468.1	T08 -Blank	373.2	417.0	507.2	649.9	2394.7
T09 -Blank	201.6	638.9	478.9	687.2	1519.4	T09 -Blank	369.3	414.8	530.7	626.6	2285.8
T10 -Blank	252.9	808.7	547.2	734.3	1394.8	T10 -Blank	405.7	457.8	590.0	705.5	2204.9
T11 -Blank	308.8	858.2	635.0	861.3	1633.5	T11 -Blank	462.2	539.9	722.1	784.6	2739.1
T12 -Blank	283.7	744.8	612.7	826.3	1472.9	T12 -Blank	459.8	552.0	726.3	834.1	2666.8
T13 -Blank	278.7	681.5	578.6	794.9	1367.2	T13 -Blank	456.9	532.8	694.3	841.2	2140.2
T14 -Blank	280.5	699.6	546.2	729.7	1104.6	T14 -Blank	426.2	489.4	619.0	688.1	1617.8
T15 -Blank	368.4	845.8	612.2	804.0	1039.6	T15 -Blank	493.2	555.0	698.8	727.0	1563.5
T16 -Blank	489.3	1069.1	580.5	761.2	869.6	T16 -Blank	521.8	566.9	690.5	639.6	1219.4
T17 -Blank	289.9	623.4	398.1	528.0	442.8	T17 -Blank	446.5	484.9	587.5	569.4	1001.6
T18 -Blank	322.6	642.5	366.8	548.1	278.9	T18 -Blank	497.9	484.9	608.8	556.3	890.3
T19 -Blank	270.9	552.8	359.0	508.6	90.2	T19 -Blank	437.9	462.2	579.6	526.1	801.5
T20 -Blank	272.8	525.8	347.6	519.3	0.0	T20 -Blank	443.7	463.3	584.0	498.6	608.4
T21 -Blank	270.2	501.5	302.2	465.3	0.0	T21 -Blank	445.4	463.7	581.3	458.7	519.0
T22 -Blank	236.8	448.1	257.3	432.6	0.0	T22 -Blank	428.7	447.6	507.4	497.8	327.8
T23 -Blank	219.6	435.8	211.9	407.0	0.0	T23 -Blank	411.9	423.6	463.4	453.1	262.6
T24 -Blank	194.8	357.4	168.7	341.2	0.0	T24 -Blank	354.5	385.9	339.7	424.6	232.4
T25 -Blank	189.1	300.7	127.7	313.2	0.0	T25 -Blank	309.7	312.2	270.6	368.3	197.0
T26 -Blank	185.8	258.1	86.1	275.6	0.0	T26 -Blank	268.7	278.6	207.5	341.4	133.3
T27 -Blank	196.0	240.5	63.7	230.8	0.0	T27 -Blank	257.7	247.2	175.0	320.1	47.5
T28 -Blank	207.7	224.7	61.5	195.2	0.0	T28 -Blank	240.1	228.2	152.6	315.6	0.0
T29 -Blank	233.5	250.6	43.8	157.5	0.0	T29 -Blank	247.2	201.1	151.9	259.8	0.0
T30-32 -Blank	951.1	634.0	301.9	221.8	0.0	T30-32 -Blank	870.9	561.5	259.0	779.4	0.0

Table 6-A2b (contd.): instantaneous MSSV-yields: individual, resolved, total compounds.

Sample	G016531X					Sample	G016535X				
Heated to,	389.5	407.8	421.7	439.4	480.1	Heated to,	375.5	396.5	411.2	428.5	472.0
Weight, mg	5.01	3.99	3.60	3.04	2.45	Weight, mg	4.98	2.50	3.49	1.69	1.35
Resolved	(µg/g)					Resolved	(µg/g)				
C1	385.0	378.2	1097.5	2209.7	7547.0	C1	509.5	527.1	1002.0	1516.6	8835.1
C2	242.9	303.4	824.7	1585.3	3955.4	C2	284.0	414.4	858.9	1066.5	5297.3
C3	315.3	246.3	646.4	1295.3	3042.9	C3	286.1	407.1	666.4	940.4	4163.6
i-C4	101.0	-4.3	101.0	152.1	400.3	i-C4	39.4	44.6	95.9	69.4	498.4
n-C4	214.8	88.4	343.5	708.2	1428.9	n-C4	173.5	239.3	330.7	554.5	2247.3
i-C5	153.3	39.4	150.4	223.3	318.5	i-C5	226.2	96.4	138.4	265.1	678.5
n-C5	123.9	72.2	57.2	562.8	547.9	n-C5	108.1	141.0	199.2	342.2	1077.2
R06	209.8	122.8	402.6	624.4	437.5	R06	239.0	263.3	415.5	664.8	1150.3
R07	340.7	137.0	462.5	755.7	403.4	R07	309.9	382.0	446.2	691.7	976.3
R08	504.8	126.8	509.9	769.1	414.4	R08	422.5	443.4	461.7	764.8	1169.9
R09	359.1	138.1	444.8	666.8	358.7	R09	354.4	404.5	428.2	741.9	901.7
R10	249.4	126.1	407.4	608.6	302.2	R10	386.2	366.2	508.7	688.1	741.7
R11	239.3	184.9	509.0	753.3	297.8	R11	439.1	434.9	736.6	856.3	673.7
R12	239.9	190.4	466.9	728.8	22.3	R12	395.6	414.1	638.9	833.6	40.9
R13	246.1	145.6	360.3	506.0	0.0	R13	306.0	342.2	448.5	550.2	0.0
R14	136.4	95.4	174.5	285.1	0.0	R14	189.1	203.9	266.2	273.3	0.0
R15	190.2	87.3	196.4	281.8	0.0	R15	221.6	219.1	265.8	286.8	0.0
R16	156.7	79.5	194.8	231.1	0.0	R16	219.6	211.1	258.6	287.7	0.0
R17	112.7	52.2	137.5	167.0	0.0	R17	163.0	168.2	193.7	215.8	0.0
R18	130.6	66.6	126.2	147.5	0.0	R18	201.5	172.5	195.0	168.5	0.0
R19	92.8	47.5	120.2	126.9	0.0	R19	162.8	164.7	193.6	143.8	0.0
R20	71.9	40.2	95.5	85.5	0.0	R20	171.8	159.4	150.7	108.0	0.0
R21	72.0	45.1	93.0	87.6	0.0	R21	171.2	150.5	157.2	78.9	0.0
R22	62.1	30.3	61.7	42.0	0.0	R22	146.6	148.7	107.3	71.3	0.0
R23	55.6	32.4	60.6	37.1	0.0	R23	176.9	119.1	67.4	63.8	0.0
R24	49.8	21.1	48.2	33.6	0.0	R24	102.0	86.4	31.8	62.0	0.0
R25	36.9	18.7	29.1	16.4	0.0	R25	80.9	54.5	8.9	44.8	0.0
R26	29.8	9.9	25.9	20.5	0.0	R26	49.6	23.5	0.0	51.4	0.0
R27	23.0	11.8	16.6	16.4	0.0	R27	39.5	14.7	0.0	39.5	0.0
R28	18.5	9.2	14.3	2.6	0.0	R28	16.8	9.1	5.9	14.1	0.0
R29	19.7	7.2	7.4	10.5	0.0	R29	18.5	2.2	0.0	26.2	0.0
R30-32	47.6	11.3	0.0	26.9	0.0	R30-32	49.5	5.4	0.0	27.1	0.0
Totals		(µg/g)					(µg/g)				
T06 -Blank	245.1	137.7	384.9	699.9	485.5	T06 -Blank	282.1	296.2	411.6	724.2	1222.1
T07 -Blank	380.2	159.7	484.6	797.5	420.5	T07 -Blank	366.8	414.8	441.2	775.3	982.0
T08 -Blank	564.2	150.2	526.4	815.7	435.9	T08 -Blank	498.0	490.0	426.0	894.0	1159.9
T09 -Blank	457.2	171.5	498.4	775.5	286.2	T09 -Blank	463.7	485.4	444.2	869.2	854.1
T10 -Blank	360.6	173.2	488.7	733.6	201.4	T10 -Blank	524.7	460.2	594.6	840.0	634.2
T11 -Blank	366.1	233.8	611.0	922.9	149.1	T11 -Blank	603.0	532.8	821.2	1069.0	547.8
T12 -Blank	387.4	261.4	612.0	944.8	0.0	T12 -Blank	582.9	539.5	775.7	1053.0	0.0
T13 -Blank	409.7	226.6	541.5	740.6	0.0	T13 -Blank	521.1	521.8	637.4	831.7	0.0
T14 -Blank	321.1	214.0	420.3	569.8	0.0	T14 -Blank	429.2	428.4	481.2	630.0	0.0
T15 -Blank	398.5	226.9	441.4	585.3	0.0	T15 -Blank	487.1	455.3	479.9	596.8	0.0
T16 -Blank	351.1	205.2	389.7	454.1	0.0	T16 -Blank	469.9	406.5	457.5	520.1	0.0
T17 -Blank	300.0	174.5	328.9	383.5	0.0	T17 -Blank	406.2	354.3	390.8	454.5	0.0
T18 -Blank	316.5	176.9	318.0	367.9	0.0	T18 -Blank	447.6	374.0	359.3	428.4	0.0
T19 -Blank	280.0	164.7	300.2	315.0	0.0	T19 -Blank	384.2	345.6	333.7	384.6	0.0
T20 -Blank	265.5	151.6	260.7	279.9	0.0	T20 -Blank	396.1	326.7	309.2	339.0	0.0
T21 -Blank	259.6	148.8	252.8	255.3	0.0	T21 -Blank	384.1	321.7	291.9	286.7	0.0
T22 -Blank	235.4	127.6	210.4	210.1	0.0	T22 -Blank	352.7	289.6	233.7	235.4	0.0
T23 -Blank	229.7	114.7	189.6	170.0	0.0	T23 -Blank	366.3	260.2	156.2	209.8	0.0
T24 -Blank	207.4	97.7	151.6	128.7	0.0	T24 -Blank	269.0	196.8	102.3	188.1	0.0
T25 -Blank	190.5	80.1	121.9	95.8	0.0	T25 -Blank	230.1	146.0	60.2	145.8	0.0
T26 -Blank	180.2	75.0	84.9	102.8	0.0	T26 -Blank	186.0	92.4	31.4	141.8	0.0
T27 -Blank	158.3	68.5	47.7	97.5	0.0	T27 -Blank	157.7	65.0	29.9	96.8	0.0
T28 -Blank	139.1	56.4	24.6	90.8	0.0	T28 -Blank	126.0	31.2	49.0	38.0	0.0
T29 -Blank	141.0	61.8	0.0	107.0	0.0	T29 -Blank	136.1	3.1	49.9	21.8	0.0
T30-32 -Blank	428.9	138.0	0.0	347.5	0.0	T30-32 -Blank	407.6	0.0	266.4	0.0	0.0

Table 6-A2b (contd.): instantaneous MSSV-yields: individual, resolved, total compounds.

Sample	G016539X				
Heated to,	383.7	402.5	415.6	431.0	463.0
Weight, mg	20.04	18.09	16.10	14.02	10.16
Resolved	(µg/g)				
C1	113.3	207.3	283.6	423.1	1581.6
C2	83.3	151.0	237.6	347.3	1054.2
C3	109.9	122.1	215.0	293.7	944.1
i-C4	16.9	15.6	26.3	39.1	104.9
n-C4	47.9	84.2	110.9	191.3	548.3
i-C5	60.1	21.9	60.6	39.0	164.7
n-C5	34.4	45.5	76.6	121.9	361.2
R06	79.3	90.2	142.9	169.5	463.1
R07	103.7	117.5	163.3	196.3	414.8
R08	126.3	129.6	168.4	210.2	378.5
R09	106.2	112.5	153.7	191.6	319.9
R10	109.0	125.8	177.5	180.0	234.5
R11	120.0	171.0	222.2	254.2	223.9
R12	113.0	161.2	212.5	218.6	127.5
R13	99.6	120.6	157.5	157.6	7.8
R14	65.2	72.2	97.4	81.9	0.0
R15	79.3	85.4	111.5	80.4	0.0
R16	79.4	82.9	105.8	63.5	0.0
R17	61.1	67.3	93.5	53.7	0.0
R18	72.5	74.5	95.0	41.6	0.0
R19	61.4	75.8	80.7	30.8	0.0
R20	61.0	69.9	70.7	16.0	0.0
R21	65.7	69.6	70.7	0.7	0.0
R22	58.6	60.3	55.1	0.0	0.0
R23	65.4	45.4	42.5	0.0	0.0
R24	37.7	30.7	35.5	0.0	0.0
R25	31.3	18.2	26.7	0.0	0.0
R26	17.5	12.9	14.8	0.0	0.0
R27	14.6	8.0	9.0	0.0	0.0
R28	7.0	7.3	6.2	0.0	0.0
R29	6.1	4.4	6.1	0.0	0.0
R30-32	18.1	7.5	4.2	0.0	0.0
Totals	(µg/g)				
T06 -Blank	92.5	89.8	147.1	190.3	464.9
T07 -Blank	122.0	113.8	167.3	207.6	424.7
T08 -Blank	149.0	125.9	171.4	217.9	391.9
T09 -Blank	139.1	119.4	172.3	211.2	315.9
T10 -Blank	153.7	141.4	197.8	216.2	252.9
T11 -Blank	163.9	193.1	255.1	284.4	248.5
T12 -Blank	164.2	196.4	258.2	273.5	128.0
T13 -Blank	159.7	161.7	222.3	212.9	0.0
T14 -Blank	137.5	137.9	181.5	142.1	0.0
T15 -Blank	159.2	147.7	193.2	131.1	0.0
T16 -Blank	156.2	141.2	179.1	100.8	0.0
T17 -Blank	139.1	126.6	168.3	73.2	0.0
T18 -Blank	154.3	139.4	162.6	55.4	0.0
T19 -Blank	139.1	141.4	161.6	34.3	0.0
T20 -Blank	142.2	140.3	153.7	8.6	0.0
T21 -Blank	148.0	140.9	147.5	0.0	0.0
T22 -Blank	136.3	126.1	133.5	0.0	0.0
T23 -Blank	139.5	106.5	115.4	0.0	0.0
T24 -Blank	104.4	82.2	92.4	0.0	0.0
T25 -Blank	93.7	69.4	69.1	0.0	0.0
T26 -Blank	74.7	57.7	59.4	0.0	0.0
T27 -Blank	63.9	51.9	57.1	0.0	0.0
T28 -Blank	49.9	49.0	51.1	0.0	0.0
T29 -Blank	47.1	44.5	43.1	0.0	0.0
T30-32 -Blank	113.9	123.8	92.7	0.0	0.0

Table 6-A3: Molar compositions of final corrected a) cumulative and b) instantaneous fluids.

a)	G016504X					b)	G016504X				
Mol%	10	30	50	70	90		10	30	50	70	90
n-C1	31.80	32.64	33.99	36.97	38.60		31.80	33.60	36.85	42.18	40.19
n-C2	4.53	5.20	5.73	6.41	7.36		4.53	5.80	6.93	7.72	8.76
n-C3	7.32	6.97	6.92	6.89	6.67		7.32	6.61	6.78	6.94	6.56
i-C4	2.67	2.65	2.63	2.07	1.45		2.67	2.62	2.58	1.09	0.70
n-C4	2.85	2.50	2.47	2.51	2.62		2.85	2.17	2.40	2.62	2.82
i-C5	4.09	3.86	3.37	2.77	2.18		4.09	3.63	2.23	1.71	1.49
n-C5	1.46	1.36	1.40	1.43	1.49		1.46	1.27	1.47	1.52	1.60
n-C6	5.86	5.89	5.46	5.37	5.05		5.86	5.92	4.60	5.15	4.62
C7-15	20.45	21.16	20.67	20.03	19.81		20.45	22.09	18.08	20.84	19.67
C16-25	10.58	10.35	10.11	9.37	9.04		10.58	10.02	8.85	7.26	8.57
C26-35	4.71	4.34	4.24	3.74	3.52		4.71	3.87	3.71	2.11	3.18
C36-45	2.10	1.82	1.78	1.49	1.37		2.10	1.50	1.55	0.62	1.18
C46-55	0.93	0.76	0.74	0.60	0.53		0.93	0.58	0.65	0.18	0.44
C56-80	0.65	0.49	0.48	0.36	0.31		0.65	0.33	0.42	0.07	0.24
a)	G016505X					b)	G016505X				
Mol%	10	30	50	70	90		10	30	50	70	90
n-C1	46.10	47.19	48.12	50.70	66.24		46.10	47.93	49.29	54.60	77.95
n-C2	7.86	8.68	8.91	8.91	6.16		7.86	9.11	9.12	8.64	3.13
n-C3	6.46	6.21	6.05	5.74	3.96		6.46	6.05	5.88	5.26	2.01
i-C4	0.64	0.73	0.74	0.68	0.42		0.64	0.78	0.75	0.60	0.20
n-C4	2.76	2.29	2.36	2.26	1.79		2.76	2.03	2.43	2.09	0.98
i-C5	2.09	1.56	1.33	1.07	0.54		2.09	1.27	1.08	0.78	0.22
n-C5	1.27	1.17	1.13	1.13	0.91		1.27	1.11	1.08	1.11	0.50
n-C6	3.16	2.99	3.02	3.03	3.14		3.16	2.87	3.06	3.05	3.15
C7-15	16.77	16.87	16.17	15.30	11.68		16.77	16.98	15.31	14.37	11.72
C16-25	7.79	7.60	7.43	6.90	3.77		7.79	7.46	7.20	6.09	0.14
C26-35	3.09	2.92	2.91	2.65	1.01		3.09	2.78	2.89	2.19	0.00
C36-45	1.23	1.12	1.14	1.02	0.27		1.23	1.04	1.16	0.79	0.00
C46-55	0.49	0.43	0.45	0.39	0.07		0.49	0.39	0.47	0.28	0.00
C56-80	0.29	0.24	0.26	0.22	0.03		0.29	0.21	0.28	0.15	0.00
a)	G016511X					b)	G016511X				
Mol%	10	30	50	70	90		10	30	50	70	90
n-C1	23.85	41.46	41.71	43.09	53.21		23.85	45.77	42.23	45.69	65.62
n-C2	7.75	9.10	8.96	9.18	7.92		7.75	8.88	8.63	9.31	5.28
n-C3	6.01	5.69	5.88	5.75	4.87		6.01	5.37	6.04	5.49	3.19
i-C4	0.57	0.71	0.63	0.61	0.52		0.57	0.70	0.51	0.57	0.34
n-C4	2.87	2.49	2.64	2.56	2.09		2.87	2.31	2.80	2.42	1.33
i-C5	2.51	2.41	1.92	1.61	1.00		2.51	2.28	1.23	1.18	0.46
n-C5	1.89	1.38	1.44	1.41	1.14		1.89	1.24	1.50	1.35	0.72
n-C6	3.04	3.27	3.49	3.62	3.53		3.04	3.31	3.90	3.87	3.40
C7-15	27.65	19.02	19.44	19.02	18.48		27.65	17.82	20.90	18.47	19.08
C16-25	13.75	8.79	8.65	8.29	5.47		13.75	7.77	8.20	7.60	0.58
C26-35	5.86	3.46	3.27	3.07	1.34		5.86	2.88	2.72	2.65	0.01
C36-45	2.50	1.37	1.24	1.14	0.33		2.50	1.07	0.90	0.92	0.00
C46-55	1.07	0.54	0.47	0.42	0.08		1.07	0.40	0.30	0.32	0.00
C56-80	0.70	0.32	0.26	0.23	0.03		0.70	0.21	0.14	0.16	0.00
a)	G016522X					b)	G016522X				
Mol%	10	30	50	70	90		10	30	50	70	90
n-C1	36.46	38.17	40.99	41.83	51.05		36.46	39.48	44.89	43.33	59.14
n-C2	8.12	8.96	9.20	9.36	8.58		8.12	9.47	9.24	9.63	7.00
n-C3	6.55	6.53	6.19	6.14	5.32		6.55	6.49	5.71	6.06	4.20
i-C4	0.53	0.55	0.52	0.55	0.50		0.53	0.56	0.47	0.59	0.41
n-C4	3.34	2.93	2.92	2.82	2.56		3.34	2.66	2.84	2.67	2.08
i-C5	2.24	1.53	1.26	1.06	0.75		2.24	1.07	0.96	0.75	0.51
n-C5	1.68	1.68	1.59	1.64	1.49		1.68	1.68	1.45	1.73	1.21
n-C6	3.41	3.58	3.69	3.75	3.83		3.41	3.71	3.83	3.85	3.88
C7-15	20.84	20.05	19.11	18.58	15.74		20.84	19.47	18.26	17.36	16.30
C16-25	9.97	9.54	8.83	8.63	6.58		9.97	9.21	7.85	8.31	4.17
C26-35	4.08	3.88	3.48	3.43	2.33		4.08	3.72	2.87	3.40	0.87
C36-45	1.67	1.58	1.37	1.36	0.82		1.67	1.51	1.05	1.39	0.18
C46-55	0.68	0.64	0.54	0.54	0.29		0.68	0.61	0.38	0.57	0.04
C56-80	0.42	0.39	0.32	0.32	0.15		0.42	0.37	0.20	0.35	0.01

Table 6-A3 (contd.): Molar compositions of final corrected a) cumulative and b) instantaneous fluids.

a)	G016531X					b)	G016531X				
Mol%	10	30	50	70	90		10	30	50	70	90
n-C1	39.58	44.17	48.23	52.90	70.09		39.58	51.52	52.09	58.16	88.60
n-C2	8.45	10.98	12.24	12.18	9.83		8.45	13.78	12.96	11.72	4.61
n-C3	7.48	7.70	7.35	7.03	5.38		7.48	7.63	6.93	6.53	2.42
i-C4	1.82	1.01	0.91	0.75	0.55		1.82	0.00	0.82	0.58	0.24
n-C4	3.87	3.15	2.99	2.89	2.05		3.87	2.08	2.79	2.71	0.86
i-C5	2.22	1.61	1.28	0.97	0.52		2.22	0.75	0.98	0.69	0.15
n-C5	1.80	1.64	0.94	1.40	0.81		1.80	1.37	0.37	1.73	0.27
n-C6	3.49	3.18	3.17	2.87	1.69		3.49	2.76	3.16	2.58	0.73
C7-15	18.25	15.70	14.50	12.04	5.83		18.25	12.17	13.60	9.78	2.11
C16-25	8.12	6.85	5.64	4.69	2.21		8.12	5.12	4.54	3.74	0.00
C26-35	3.07	2.54	1.85	1.54	0.71		3.07	1.83	1.26	1.21	0.00
C36-45	1.16	0.94	0.61	0.50	0.23		1.16	0.65	0.35	0.39	0.00
C46-55	0.44	0.35	0.20	0.17	0.07		0.44	0.23	0.10	0.13	0.00
C56-80	0.25	0.19	0.09	0.08	0.03		0.25	0.12	0.04	0.06	0.00
a)	G016535X					b)	G016535X				
Mol%	10	30	50	70	90		10	30	50	70	90
n-C1	42.11	44.19	49.45	53.03	77.52		42.11	46.20	55.94	58.90	91.04
n-C2	8.28	8.55	9.02	8.47	4.62		8.28	8.62	9.09	7.42	1.72
n-C3	5.69	5.79	5.37	5.06	2.57		5.69	5.78	4.81	4.46	0.92
i-C4	0.59	0.53	0.54	0.42	0.23		0.59	0.48	0.53	0.25	0.08
n-C4	2.61	2.61	2.23	2.17	1.07		2.61	2.58	1.81	2.00	0.38
i-C5	2.75	1.65	1.11	0.98	0.34		2.75	0.84	0.61	0.77	0.09
n-C5	1.31	1.27	1.08	1.06	0.45		1.31	1.22	0.88	0.99	0.15
n-C6	3.34	3.34	3.28	3.41	2.25		3.34	3.34	3.20	3.60	1.50
C7-15	20.34	20.60	17.77	16.88	8.10		20.34	21.05	14.51	15.52	4.12
C16-25	8.43	7.81	6.86	6.00	2.21		8.43	7.11	5.74	4.60	0.00
C26-35	2.96	2.49	2.23	1.78	0.49		2.96	2.00	1.92	1.12	0.00
C36-45	1.04	0.80	0.73	0.53	0.11		1.04	0.56	0.64	0.28	0.00
C46-55	0.37	0.25	0.24	0.16	0.03		0.37	0.16	0.21	0.07	0.00
C56-80	0.18	0.11	0.11	0.06	0.01		0.18	0.06	0.10	0.02	0.00
a)	G016539X					b)	G016539X				
Mol%	10	30	50	70	90		10	30	50	70	90
n-C1	36.94	41.84	45.02	51.40	68.91		36.94	45.41	49.08	64.61	85.44
n-C2	7.85	9.23	9.33	8.64	5.84		7.85	10.18	9.28	5.91	1.90
n-C3	7.07	6.23	6.03	5.32	3.58		7.07	5.61	5.72	3.41	1.16
i-C4	0.83	0.66	0.60	0.53	0.33		0.83	0.55	0.53	0.34	0.10
n-C4	2.34	2.69	2.49	2.37	1.58		2.34	2.94	2.24	1.68	0.51
i-C5	2.36	1.35	1.18	0.80	0.45		2.36	0.61	0.99	0.28	0.12
n-C5	1.35	1.31	1.29	1.22	0.83		1.35	1.28	1.25	0.86	0.27
n-C6	3.90	3.48	3.49	3.38	3.20		3.90	3.17	3.51	3.18	2.95
C7-15	22.19	19.12	17.67	16.76	10.92		22.19	16.74	15.98	17.79	2.06
C16-25	9.61	8.67	7.96	6.47	3.28		9.61	8.01	7.11	1.79	5.48
C26-35	3.53	3.35	3.06	2.10	0.81		3.53	3.28	2.69	0.14	0.00
C36-45	1.30	1.30	1.17	0.68	0.20		1.30	1.34	1.02	0.01	0.00
C46-55	0.48	0.50	0.45	0.22	0.05		0.48	0.55	0.39	0.00	0.00
C56-80	0.26	0.29	0.26	0.10	0.02		0.26	0.34	0.21	0.00	0.00

Table 6-A4: Physical properties of the pseudo compounds used for the 14 compounds model.

PNA-Oil (low wax/low sulphur)							
	Mol Wt (g/mol)	T _b (K)	T _c (K)	P _c (MPa)	V _c (m ³ /mol)	Acentric Factor	Rackett Factor
							(Zra)
P10	137	182	335	2.39	0.63	0.612	0.256
P20	268	337	465	1.58	1.18	0.934	0.226
P30	406	444	570	1.40	1.83	1.189	0.194
P40	545	520	661	1.35	2.54	1.338	0.180
P50	683	583	746	1.33	3.29	1.361	0.168
P60+	866	657	857	1.34	4.36	1.160	0.157

PNA-Oil (low wax/high sulphur)							
	Mol Wt (g/mol)	T _b (K)	T _c (K)	P _c (MPa)	V _c (m ³ /mol)	Acentric Factor	Rackett Factor
							(Zra)
P10	140	183	336	2.40	0.63	0.614	0.256
P20	273	338	466	1.58	1.18	0.935	0.226
P30	414	446	577	1.51	1.85	1.194	0.194
P40	554	521	668	1.44	2.58	1.340	0.180
P50	694	585	752	1.56	3.34	1.360	0.168
P60+	895	664	869	1.42	4.51	1.130	0.157

Paraffinic-oil (high wax)							
	Mol Wt (g/mol)	T _b (K)	T _c (K)	P _c (MPa)	V _c (m ³ /mol)	Acentric Factor	Rackett Factor
							(Zra)
P10	140	184	328	2.16	0.69	0.614	0.239
P20	273	338	456	1.40	1.21	0.936	0.189
P30	412	445	560	1.23	1.83	1.190	0.161
P40	552	520	651	1.17	2.50	1.338	0.243
P50	692	581	735	1.15	3.20	1.360	0.190
P60+	885	656	848	1.14	4.23	1.149	0.185

Gas/Condensate							
	Mol Wt (g/mol)	T _b (K)	T _c (K)	P _c (MPa)	V _c (m ³ /mol)	Acentric Factor	Rackett Factor
							(Zra)
P10	129	182	335	2.39	0.63	0.612	0.256
P20	250	337	465	1.58	1.18	0.934	0.226
P30	378	444	570	1.40	1.83	1.189	0.194
P40	506	520	661	1.35	2.54	1.338	0.180
P50	635	583	746	1.33	3.29	1.361	0.168
P60+	806	657	857	1.34	4.36	1.160	0.157

Table 6-A5: 2-, 4-, and 14-compound compositional kinetic model: instantaneous.

14 compound kinetics															
G016504X	n-C1	n-C2	n-C3	i-C4	n-C4	i-C5	n-C5	n-C6	C7-15	C16-25	C26-35	C36-45	C46-55	C56-80	
kcal/mol									(%)						
42	0.00	0.00	0.00	0.00	0.00	0.00	0.00	0.00	0.00	0.00	0.00	0.00	0.00	0.00	0.00
43	0.00	0.00	0.00	0.00	0.00	0.00	0.00	0.00	0.00	0.00	0.00	0.00	0.00	0.00	0.00
44	0.00	0.00	0.00	0.00	0.00	0.00	0.00	0.00	0.00	0.00	0.00	0.00	0.00	0.00	0.00
45	0.00	0.00	0.00	0.00	0.00	0.00	0.00	0.00	0.00	0.00	0.00	0.00	0.00	0.00	0.00
46	0.17	0.13	0.22	0.31	0.23	0.40	0.20	0.25	0.21	0.26	0.30	0.35	0.40	0.48	
47	0.26	0.19	0.34	0.48	0.36	0.62	0.31	0.38	0.33	0.39	0.47	0.54	0.62	0.74	
48	0.00	0.00	0.00	0.00	0.00	0.00	0.00	0.00	0.00	0.00	0.00	0.00	0.00	0.00	0.00
49	0.09	0.07	0.12	0.17	0.12	0.22	0.11	0.13	0.12	0.14	0.16	0.19	0.22	0.26	
50	8.65	7.77	9.73	14.74	8.50	17.36	8.45	12.05	11.22	11.72	12.04	12.17	12.12	11.80	
51	38.89	38.05	40.91	59.40	38.63	43.72	40.10	38.37	37.67	42.44	47.30	51.84	55.97	61.01	
52	28.35	27.02	26.66	15.94	26.89	21.38	26.52	27.36	27.65	22.17	17.17	13.06	9.80	6.54	
53	17.36	19.70	16.20	6.59	18.59	11.98	17.89	15.79	16.77	16.84	16.59	16.07	15.35	14.11	
54	0.77	0.87	0.72	0.29	0.82	0.53	0.79	0.70	0.74	0.74	0.73	0.71	0.68	0.62	
55	3.45	3.92	3.22	1.31	3.70	2.38	3.56	3.14	3.33	3.35	3.30	3.19	3.05	2.80	
56	0.50	0.57	0.47	0.19	0.54	0.35	0.52	0.46	0.49	0.49	0.48	0.47	0.45	0.41	
57	1.05	1.19	0.98	0.40	1.13	0.73	1.08	0.96	1.02	1.02	1.01	0.97	0.93	0.85	
58	0.00	0.00	0.00	0.00	0.00	0.00	0.00	0.00	0.00	0.00	0.00	0.00	0.00	0.00	
59	0.00	0.00	0.00	0.00	0.00	0.00	0.00	0.00	0.00	0.00	0.00	0.00	0.00	0.00	
60	0.46	0.53	0.43	0.18	0.50	0.32	0.48	0.42	0.45	0.45	0.44	0.43	0.41	0.38	
61	0.00	0.00	0.00	0.00	0.00	0.00	0.00	0.00	0.00	0.00	0.00	0.00	0.00	0.00	
62	0.00	0.00	0.00	0.00	0.00	0.00	0.00	0.00	0.00	0.00	0.00	0.00	0.00	0.00	
63	0.00	0.00	0.00	0.00	0.00	0.00	0.00	0.00	0.00	0.00	0.00	0.00	0.00	0.00	
64	0.00	0.00	0.00	0.00	0.00	0.00	0.00	0.00	0.00	0.00	0.00	0.00	0.00	0.00	
65	0.00	0.00	0.00	0.00	0.00	0.00	0.00	0.00	0.00	0.00	0.00	0.00	0.00	0.00	
Potential	6.39	2.30	3.07	1.06	1.52	1.55	1.11	4.34	28.26	23.95	13.58	6.96	3.38	2.54	
2 compound		4 compound kinetics													
kcal/mol	Gas	Oil	kcal/mol	C1	C2-5	C6-14	C15+								
42	0.00	0.00	42	0.00	0.00	0.00	0.00								
43	0.00	0.00	43	0.00	0.00	0.00	0.00								
44	0.00	0.00	44	0.00	0.00	0.00	0.00								
45	0.00	0.00	45	0.00	0.00	0.00	0.00								
46	0.21	0.27	46	0.17	0.24	0.22	0.30								
47	0.32	0.42	47	0.26	0.36	0.34	0.47								
48	0.00	0.00	48	0.00	0.00	0.00	0.00								
49	0.11	0.15	49	0.09	0.13	0.12	0.16								
50	9.87	11.68	50	8.65	10.61	11.33	11.90								
51	40.91	43.31	51	38.89	42.14	37.77	46.89								
52	26.20	21.74	52	28.35	24.91	27.61	17.95								
53	16.45	16.51	53	17.36	15.90	16.64	16.43								
54	0.73	0.73	54	0.77	0.70	0.74	0.73								
55	3.27	3.28	55	3.45	3.16	3.31	3.27								
56	0.48	0.48	56	0.50	0.46	0.48	0.48								
57	1.00	1.00	57	1.05	0.96	1.01	1.00								
58	0.00	0.00	58	0.00	0.00	0.00	0.00								
59	0.00	0.00	59	0.00	0.00	0.00	0.00								
60	0.44	0.44	60	0.46	0.42	0.44	0.44								
61	0.00	0.00	61	0.00	0.00	0.00	0.00								
62	0.00	0.00	62	0.00	0.00	0.00	0.00								
63	0.00	0.00	63	0.00	0.00	0.00	0.00								
64	0.00	0.00	64	0.00	0.00	0.00	0.00								
65	0.00	0.00	65	0.00	0.00	0.00	0.00								
Potential	17.00	83.00	Potential	6.39	10.61	32.60	50.41								

Table 6-A5 (contd.): 2-, 4-, and 14-compound compositional kinetic model: instantaneous.

14 compound kinetics														
G016505X	n-C1	n-C2	n-C3	i-C4	n-C4	i-C5	n-C5	n-C6	C7-15	C16-25	C26-35	C36-45	C46-55	C56-80
kcal/mol	()													
42	0.00	0.00	0.00	0.00	0.00	0.00	0.00	0.00	0.00	0.00	0.00	0.00	0.00	0.00
43	0.00	0.00	0.00	0.00	0.00	0.00	0.00	0.00	0.00	0.00	0.00	0.00	0.00	0.00
44	0.00	0.00	0.00	0.00	0.00	0.00	0.00	0.00	0.00	0.00	0.00	0.00	0.00	0.00
45	0.00	0.00	0.00	0.00	0.00	0.00	0.00	0.00	0.00	0.00	0.00	0.00	0.00	0.00
46	0.00	0.00	0.00	0.00	0.00	0.00	0.00	0.00	0.00	0.00	0.00	0.00	0.00	0.00
47	0.07	0.12	0.15	0.13	0.16	0.26	0.14	0.10	0.11	0.18	0.19	0.20	0.21	0.22
48	0.42	0.70	0.87	0.75	0.91	1.50	0.84	0.58	0.67	1.08	1.14	1.17	1.21	1.26
49	0.21	0.36	0.45	0.38	0.47	0.77	0.43	0.30	0.34	0.55	0.58	0.60	0.62	0.65
50	1.48	2.47	3.07	2.64	3.21	5.29	2.95	2.04	2.37	3.81	4.00	4.14	4.28	4.44
51	4.34	7.24	8.99	7.73	9.43	15.54	8.67	6.00	6.96	11.17	11.75	12.15	12.56	13.03
52	13.62	25.35	25.45	28.26	20.91	28.42	22.89	16.42	21.31	32.29	31.93	31.07	30.14	28.84
53	13.20	23.94	23.30	25.73	23.60	22.73	21.04	16.53	18.10	29.39	31.30	32.78	34.28	36.33
54	11.76	18.23	16.78	16.50	16.36	13.18	17.37	13.23	13.67	20.00	19.07	17.88	16.71	15.23
55	28.02	11.02	10.69	9.13	12.73	6.28	13.10	22.86	18.60	0.78	0.01	0.00	0.00	0.00
56	9.61	3.78	3.67	3.13	4.37	2.15	4.49	7.84	6.38	0.27	0.00	0.00	0.00	0.00
57	9.67	3.81	3.69	3.15	4.40	2.17	4.52	7.89	6.42	0.27	0.01	0.00	0.00	0.00
58	2.29	0.90	0.87	0.74	1.04	0.51	1.07	1.86	1.52	0.06	0.00	0.00	0.00	0.00
59	4.24	1.67	1.62	1.38	1.93	0.95	1.98	3.46	2.81	0.12	0.00	0.00	0.00	0.00
60	0.00	0.00	0.00	0.00	0.00	0.00	0.00	0.00	0.00	0.00	0.00	0.00	0.00	0.00
61	0.00	0.00	0.00	0.00	0.00	0.00	0.00	0.00	0.00	0.00	0.00	0.00	0.00	0.00
62	1.09	0.43	0.41	0.35	0.49	0.24	0.51	0.89	0.72	0.03	0.00	0.00	0.00	0.00
63	0.00	0.00	0.00	0.00	0.00	0.00	0.00	0.00	0.00	0.00	0.00	0.00	0.00	0.00
64	0.00	0.00	0.00	0.00	0.00	0.00	0.00	0.00	0.00	0.00	0.00	0.00	0.00	0.00
65	0.00	0.00	0.00	0.00	0.00	0.00	0.00	0.00	0.00	0.00	0.00	0.00	0.00	0.00
Potential	16.08	3.08	2.99	0.45	1.60	0.92	0.99	4.28	31.78	17.97	10.22	5.25	2.53	1.84
2 compound		4 compound kinetics												
kcal/mol	Gas	Oil	kcal/mol	C1	C2-5	C6-	C15+							
42	0.00	0.00	42	0.00	0.00	0.00	0.00							
43	0.00	0.00	43	0.00	0.00	0.00	0.00							
44	0.00	0.00	44	0.00	0.00	0.00	0.00							
45	0.00	0.00	45	0.00	0.00	0.00	0.00							
46	0.00	0.00	46	0.00	0.00	0.00	0.00							
47	0.10	0.15	47	0.07	0.15	0.11	0.19							
48	0.59	0.90	48	0.42	0.87	0.66	1.13							
49	0.30	0.46	49	0.21	0.45	0.34	0.58							
50	2.09	3.17	50	1.48	3.08	2.33	3.97							
51	6.14	9.31	51	4.34	9.03	6.85	11.65							
52	17.93	26.35	52	13.62	24.84	20.73	31.71							
53	17.11	24.64	53	13.20	23.38	17.92	31.04							
54	13.72	16.37	54	11.76	16.87	13.61	19.00							
55	21.44	9.52	55	28.02	10.88	19.11	0.37							
56	7.35	3.26	56	9.61	3.73	6.55	0.13							
57	7.40	3.29	57	9.67	3.76	6.60	0.13							
58	1.75	0.78	58	2.29	0.89	1.56	0.03							
59	3.24	1.44	59	4.24	1.65	2.89	0.06							
60	0.00	0.00	60	0.00	0.00	0.00	0.00							
61	0.00	0.00	61	0.00	0.00	0.00	0.00							
62	0.83	0.37	62	1.09	0.42	0.74	0.01							
63	0.00	0.00	63	0.00	0.00	0.00	0.00							
64	0.00	0.00	64	0.00	0.00	0.00	0.00							
65	0.00	0.00	65	0.00	0.00	0.00	0.00							
Potential	26.11	73.89	Potential	16.08	10.03	36.07	37.82							

Table 6-A5 (contd.): 2-, 4-, and 14-compound compositional kinetic model: instantaneous.

14 compound kinetics														
G016511X	n-C1	n-C2	n-C3	i-C4	n-C4	i-C5	n-C5	n-C6	C7-15	C16-25	C26-35	C36-45	C46-55	C56-80
kcal/mol	(%)													
42	0.00	0.00	0.00	0.00	0.00	0.00	0.00	0.00	0.00	0.00	0.00	0.00	0.00	0.00
43	0.00	0.00	0.00	0.00	0.00	0.00	0.00	0.00	0.00	0.00	0.00	0.00	0.00	0.00
44	0.00	0.00	0.00	0.00	0.00	0.00	0.00	0.00	0.00	0.00	0.00	0.00	0.00	0.00
45	0.07	0.15	0.19	0.17	0.20	0.33	0.24	0.13	0.21	0.36	0.45	0.54	0.63	0.77
46	0.49	1.07	1.29	1.22	1.38	2.31	1.65	0.88	1.44	2.53	3.14	3.73	4.38	5.37
47	0.61	1.33	1.60	1.51	1.72	2.87	2.05	1.09	1.79	3.14	3.89	4.62	5.43	6.66
48	1.79	3.91	4.71	4.45	5.06	8.46	6.04	3.20	5.28	9.25	11.46	13.62	16.01	19.62
49	8.96	11.69	10.99	14.40	10.62	20.01	10.30	9.09	8.86	13.63	14.68	15.16	15.48	15.63
50	24.01	32.97	35.85	30.48	37.37	31.34	36.34	31.08	30.16	41.76	40.19	37.09	33.89	29.39
51	17.21	23.56	21.57	22.46	21.39	19.94	21.53	20.42	17.66	25.64	25.97	25.23	24.18	22.57
52	22.32	12.05	11.34	12.06	10.60	7.01	10.41	16.25	16.47	1.75	0.11	0.01	0.00	0.00
53	10.52	5.68	5.34	5.68	4.99	3.30	4.90	7.65	7.76	0.83	0.05	0.00	0.00	0.00
54	6.81	3.68	3.46	3.68	3.23	2.14	3.18	4.96	5.03	0.54	0.03	0.00	0.00	0.00
55	1.67	0.90	0.85	0.90	0.79	0.53	0.78	1.22	1.23	0.13	0.01	0.00	0.00	0.00
56	3.75	2.02	1.90	2.02	1.78	1.18	1.75	2.73	2.77	0.29	0.02	0.00	0.00	0.00
57	0.47	0.25	0.24	0.25	0.22	0.15	0.22	0.34	0.35	0.04	0.00	0.00	0.00	0.00
58	0.00	0.00	0.00	0.00	0.00	0.00	0.00	0.00	0.00	0.00	0.00	0.00	0.00	0.00
59	0.00	0.00	0.00	0.00	0.00	0.00	0.00	0.00	0.00	0.00	0.00	0.00	0.00	0.00
60	1.33	0.72	0.67	0.72	0.63	0.42	0.62	0.97	0.98	0.10	0.01	0.00	0.00	0.00
61	0.00	0.00	0.00	0.00	0.00	0.00	0.00	0.00	0.00	0.00	0.00	0.00	0.00	0.00
62	0.00	0.00	0.00	0.00	0.00	0.00	0.00	0.00	0.00	0.00	0.00	0.00	0.00	0.00
63	0.00	0.00	0.00	0.00	0.00	0.00	0.00	0.00	0.00	0.00	0.00	0.00	0.00	0.00
64	0.00	0.00	0.00	0.00	0.00	0.00	0.00	0.00	0.00	0.00	0.00	0.00	0.00	0.00
65	0.00	0.00	0.00	0.00	0.00	0.00	0.00	0.00	0.00	0.00	0.00	0.00	0.00	0.00
Potential	10.54	2.94	2.78	0.37	1.63	1.06	1.12	4.04	36.25	20.06	10.40	5.00	2.27	1.55
2 compound kinetics		4 compound kinetics												
kcal/mol	Gas	Oil	kcal/mol	C1	C2-5	C6-14	C15+							
42	0.00	0.00	42	0.00	0.00	0.00	0.00							
43	0.00	0.00	43	0.00	0.00	0.00	0.00							
44	0.00	0.00	44	0.00	0.00	0.00	0.00							
45	0.13	0.32	45	0.07	0.20	0.20	0.44							
46	0.92	2.21	46	0.49	1.39	1.39	3.06							
47	1.15	2.75	47	0.61	1.72	1.72	3.80							
48	3.38	8.09	48	1.79	5.07	5.07	11.19							
49	10.51	11.55	49	8.96	12.15	8.89	14.29							
50	29.14	34.97	50	24.01	34.62	30.26	39.80							
51	19.52	21.66	51	17.21	21.99	17.94	25.47							
52	16.79	8.79	52	22.32	10.89	16.45	0.92							
53	7.91	4.14	53	10.52	5.13	7.75	0.44							
54	5.12	2.68	54	6.81	3.32	5.02	0.28							
55	1.26	0.66	55	1.67	0.82	1.23	0.07							
56	2.82	1.48	56	3.75	1.83	2.76	0.16							
57	0.35	0.19	57	0.47	0.23	0.35	0.02							
58	0.00	0.00	58	0.00	0.00	0.00	0.00							
59	0.00	0.00	59	0.00	0.00	0.00	0.00							
60	1.00	0.52	60	1.33	0.65	0.98	0.06							
61	0.00	0.00	61	0.00	0.00	0.00	0.00							
62	0.00	0.00	62	0.00	0.00	0.00	0.00							
63	0.00	0.00	63	0.00	0.00	0.00	0.00							
64	0.00	0.00	64	0.00	0.00	0.00	0.00							
65	0.00	0.00	65	0.00	0.00	0.00	0.00							
Potential	20.43	79.57	Potential	10.54	9.89	40.28	39.29							

Table 6-A5 (contd.): 2-, 4-, and 14-compound compositional kinetic model: instantaneous.

14 compound kinetics														
G016522X	n-C1	n-C2	n-C3	i-C4	n-C4	i-C5	n-C5	n-C6	C7-15	C16-25	C26-35	C36-45	C46-55	C56-80
kcal/mol	(%)													
42	0.00	0.00	0.00	0.00	0.00	0.00	0.00	0.00	0.00	0.00	0.00	0.00	0.00	0.00
43	0.00	0.00	0.00	0.00	0.00	0.00	0.00	0.00	0.00	0.00	0.00	0.00	0.00	0.00
44	0.00	0.00	0.00	0.00	0.00	0.00	0.00	0.00	0.00	0.00	0.00	0.00	0.00	0.00
45	0.00	0.00	0.00	0.00	0.00	0.00	0.00	0.00	0.00	0.00	0.00	0.00	0.00	0.00
46	0.00	0.00	0.00	0.00	0.00	0.00	0.00	0.00	0.00	0.00	0.00	0.00	0.00	0.00
47	0.13	0.17	0.22	0.19	0.23	0.46	0.21	0.15	0.21	0.26	0.31	0.36	0.40	0.44
48	0.34	0.46	0.59	0.52	0.61	1.25	0.56	0.42	0.56	0.71	0.85	0.98	1.08	1.20
49	0.22	0.29	0.38	0.34	0.40	0.80	0.36	0.27	0.36	0.46	0.55	0.63	0.70	0.78
50	1.79	2.38	3.05	2.73	3.20	6.50	2.90	2.17	2.90	3.68	4.44	5.09	5.64	6.27
51	2.81	3.73	4.79	4.29	5.02	10.20	4.54	3.41	4.55	5.77	6.97	7.98	8.85	9.83
52	33.83	41.57	40.96	37.54	41.73	42.58	38.43	37.59	39.04	44.53	47.93	49.01	48.40	45.98
53	13.48	17.89	17.95	19.46	16.24	13.82	18.89	15.57	15.33	19.45	23.47	26.90	29.81	33.08
54	22.42	15.85	15.16	16.51	15.40	11.53	16.13	19.11	17.53	11.89	7.32	4.29	2.42	1.15
55	10.69	7.55	7.23	7.87	7.34	5.50	7.69	9.11	8.35	5.67	3.49	2.04	1.15	0.55
56	5.43	3.84	3.67	4.00	3.73	2.79	3.91	4.63	4.25	2.88	1.77	1.04	0.59	0.28
57	3.97	2.81	2.68	2.92	2.73	2.04	2.86	3.38	3.10	2.10	1.30	0.76	0.43	0.20
58	2.14	1.51	1.45	1.57	1.47	1.10	1.54	1.82	1.67	1.13	0.70	0.41	0.23	0.11
59	0.92	0.65	0.62	0.67	0.63	0.47	0.66	0.78	0.72	0.49	0.30	0.18	0.10	0.05
60	1.85	1.31	1.25	1.36	1.27	0.95	1.33	1.58	1.44	0.98	0.60	0.35	0.20	0.09
61	0.00	0.00	0.00	0.00	0.00	0.00	0.00	0.00	0.00	0.00	0.00	0.00	0.00	0.00
62	0.00	0.00	0.00	0.00	0.00	0.00	0.00	0.00	0.00	0.00	0.00	0.00	0.00	0.00
63	0.00	0.00	0.00	0.00	0.00	0.00	0.00	0.00	0.00	0.00	0.00	0.00	0.00	0.00
64	0.00	0.00	0.00	0.00	0.00	0.00	0.00	0.00	0.00	0.00	0.00	0.00	0.00	0.00
65	0.00	0.00	0.00	0.00	0.00	0.00	0.00	0.00	0.00	0.00	0.00	0.00	0.00	0.00
Potential	10.07	3.16	2.91	0.35	1.87	0.77	1.29	4.16	30.98	22.80	11.66	5.58	2.58	1.84
2 compound kinetics		4 compound kinetics												
kcal/mol	Gas	Oil	kcal/mol	C1	C2-5	C6-14	C15+							
42	0.00	0.00	42	0.00	0.00	0.00	0.00							
43	0.00	0.00	43	0.00	0.00	0.00	0.00							
44	0.00	0.00	44	0.00	0.00	0.00	0.00							
45	0.00	0.00	45	0.00	0.00	0.00	0.00							
46	0.00	0.00	46	0.00	0.00	0.00	0.00							
47	0.17	0.26	47	0.13	0.22	0.20	0.30							
48	0.47	0.70	48	0.34	0.59	0.54	0.82							
49	0.30	0.45	49	0.22	0.38	0.35	0.53							
50	2.45	3.63	50	1.79	3.10	2.81	4.28							
51	3.85	5.70	51	2.81	4.86	4.42	6.71							
52	37.45	43.00	52	33.83	40.97	38.87	46.27							
53	15.51	19.40	53	13.48	17.48	15.35	22.61							
54	18.82	12.70	54	22.42	15.31	17.71	8.74							
55	8.97	6.05	55	10.69	7.30	8.44	4.17							
56	4.56	3.08	56	5.43	3.71	4.29	2.12							
57	3.33	2.25	57	3.97	2.71	3.14	1.55							
58	1.79	1.21	58	2.14	1.46	1.69	0.83							
59	0.77	0.52	59	0.92	0.63	0.72	0.36							
60	1.55	1.05	60	1.85	1.26	1.46	0.72							
61	0.00	0.00	61	0.00	0.00	0.00	0.00							
62	0.00	0.00	62	0.00	0.00	0.00	0.00							
63	0.00	0.00	63	0.00	0.00	0.00	0.00							
64	0.00	0.00	64	0.00	0.00	0.00	0.00							
65	0.00	0.00	65	0.00	0.00	0.00	0.00							
Potential	20.41	79.59	Potential	10.07	10.34	35.14	44.46							

Table 6-A5 (contd.): 2-, 4-, and 14-compound compositional kinetic model: instantaneous.

14 compound kinetics														
G016531X	n-C1	n-C2	n-C3	i-C4	n-C4	i-C5	n-C5	n-C6	C7-15	C16-25	C26-35	C36-45	C46-55	C56-80
kcal/mol	(%)													
50	0.00	0.00	0.00	0.00	0.00	0.00	0.00	0.00	0.00	0.00	0.00	0.00	0.00	0.00
51	0.00	0.00	0.00	0.00	0.00	0.00	0.00	0.00	0.00	0.00	0.00	0.00	0.00	0.00
52	0.00	0.00	0.00	0.00	0.00	0.00	0.00	0.00	0.00	0.00	0.00	0.00	0.00	0.00
53	0.11	0.16	0.19	0.21	0.20	0.22	0.21	0.20	0.21	0.22	0.23	0.23	0.23	0.23
54	0.00	0.00	0.00	0.00	0.00	0.00	0.00	0.00	0.00	0.00	0.00	0.00	0.00	0.00
55	0.00	0.00	0.00	0.00	0.00	0.00	0.00	0.00	0.00	0.00	0.00	0.00	0.00	0.00
56	14.41	21.43	24.58	28.21	26.10	28.96	27.54	25.77	27.35	29.19	29.71	30.11	30.43	30.76
57	10.31	15.33	17.59	20.18	18.67	20.72	19.70	18.44	19.57	20.88	21.25	21.55	21.77	22.01
58	10.98	16.33	18.73	21.50	19.89	22.07	20.99	19.64	20.84	22.25	22.64	22.95	23.19	23.44
59	5.35	7.95	9.12	10.47	9.68	10.74	10.22	9.56	10.15	10.83	11.02	11.17	11.29	11.41
60	4.34	6.45	7.40	8.50	7.86	8.72	8.30	7.76	8.24	8.79	8.95	9.07	9.17	9.27
61	5.74	9.94	6.88	3.85	5.70	3.88	1.74	7.07	6.17	4.94	3.70	2.76	2.05	1.37
62	4.56	6.39	4.62	1.94	3.93	1.93	5.72	4.11	3.16	2.90	2.51	2.16	1.86	1.51
63	15.89	5.76	3.91	1.84	2.86	0.99	2.01	2.68	1.56	0.00	0.00	0.00	0.00	0.00
64	0.00	0.00	0.00	0.00	0.00	0.00	0.00	0.00	0.00	0.00	0.00	0.00	0.00	0.00
65	16.48	5.97	4.06	1.91	2.97	1.03	2.08	2.78	1.62	0.00	0.00	0.00	0.00	0.00
66	0.00	0.00	0.00	0.00	0.00	0.00	0.00	0.00	0.00	0.00	0.00	0.00	0.00	0.00
67	0.00	0.00	0.00	0.00	0.00	0.00	0.00	0.00	0.00	0.00	0.00	0.00	0.00	0.00
68	1.71	0.62	0.42	0.20	0.31	0.11	0.22	0.29	0.17	0.00	0.00	0.00	0.00	0.00
69	0.00	0.00	0.00	0.00	0.00	0.00	0.00	0.00	0.00	0.00	0.00	0.00	0.00	0.00
70	10.13	3.67	2.50	1.18	1.83	0.63	1.28	1.71	0.99	0.00	0.00	0.00	0.00	0.00
71	0.00	0.00	0.00	0.00	0.00	0.00	0.00	0.00	0.00	0.00	0.00	0.00	0.00	0.00
72	0.00	0.00	0.00	0.00	0.00	0.00	0.00	0.00	0.00	0.00	0.00	0.00	0.00	0.00
73	0.00	0.00	0.00	0.00	0.00	0.00	0.00	0.00	0.00	0.00	0.00	0.00	0.00	0.00
Potential	12.61	3.40	3.84	1.07	2.47	1.59	1.35	3.34	26.17	21.33	12.02	6.02	2.83	1.97
2 compound kinetics		4 compound kinetics												
kcal/mol	Gas	Oil	kcal/mol	C1	C2-5	C6-	C15+							
50	0.00	0.00	50	0.00	0.00	0.00	0.00							
51	0.00	0.00	51	0.00	0.00	0.00	0.00							
52	0.00	0.00	52	0.00	0.00	0.00	0.00							
53	0.15	0.22	53	0.11	0.19	0.21	0.22							
54	0.00	0.00	54	0.00	0.00	0.00	0.00							
55	0.00	0.00	55	0.00	0.00	0.00	0.00							
56	20.01	28.63	56	14.41	25.15	27.17	29.61							
57	14.31	20.48	57	10.31	18.00	19.44	21.18							
58	15.25	21.82	58	10.98	19.17	20.71	22.56							
59	7.42	10.62	59	5.35	9.33	10.08	10.98							
60	6.03	8.62	60	4.34	7.58	8.18	8.92							
61	6.05	4.88	61	5.74	6.34	6.27	3.96							
62	4.54	2.84	62	4.56	4.52	3.26	2.56							
63	9.43	0.67	63	15.89	3.49	1.68	0.00							
64	0.00	0.00	64	0.00	0.00	0.00	0.00							
65	9.78	0.70	65	16.48	3.62	1.75	0.00							
66	0.00	0.00	66	0.00	0.00	0.00	0.00							
67	0.00	0.00	67	0.00	0.00	0.00	0.00							
68	1.01	0.07	68	1.71	0.38	0.18	0.00							
69	0.00	0.00	69	0.00	0.00	0.00	0.00							
70	6.01	0.43	70	10.13	2.23	1.07	0.00							
71	0.00	0.00	71	0.00	0.00	0.00	0.00							
72	0.00	0.00	72	0.00	0.00	0.00	0.00							
73	0.00	0.00	73	0.00	0.00	0.00	0.00							
Potential	26.32	73.68	Potential	12.61	13.71	29.50	44.18							

Table 6-A5 (contd.): 2-, 4-, and 14-compound compositional kinetic model: instantaneous.

14 compound kinetics														
G016535X	n-C1	n-C2	n-C3	i-C4	n-C4	i-C5	n-C5	n-C6	C7-15	C16-25	C26-35	C36-45	C46-55	C56-80
kcal/mol	(%)													
44	0.00	0.00	0.00	0.00	0.00	0.00	0.00	0.00	0.00	0.00	0.00	0.00	0.00	0.00
45	0.00	0.00	0.00	0.00	0.00	0.00	0.00	0.00	0.00	0.00	0.00	0.00	0.00	0.00
46	0.00	0.00	0.00	0.00	0.00	0.00	0.00	0.00	0.00	0.00	0.00	0.00	0.00	0.00
47	0.00	0.00	0.00	0.00	0.00	0.00	0.00	0.00	0.00	0.00	0.00	0.00	0.00	0.00
48	0.00	0.00	0.00	0.00	0.00	0.00	0.00	0.00	0.00	0.00	0.00	0.00	0.00	0.00
49	0.00	0.00	0.00	0.00	0.00	0.00	0.00	0.00	0.00	0.00	0.00	0.00	0.00	0.00
50	0.00	0.00	0.00	0.00	0.00	0.00	0.00	0.00	0.00	0.00	0.00	0.00	0.00	0.00
51	0.41	1.13	1.33	1.70	1.43	3.84	1.51	0.93	1.34	2.00	2.42	2.88	3.35	3.98
52	0.28	0.76	0.90	1.15	0.97	2.60	1.02	0.63	0.91	1.35	1.64	1.95	2.27	2.69
53	1.36	3.73	4.38	5.60	4.74	12.68	5.00	3.07	4.43	6.59	8.00	9.50	11.06	13.13
54	5.43	14.11	16.13	16.43	16.92	13.99	16.88	11.12	16.61	20.13	19.58	18.65	17.47	15.61
55	12.06	27.30	24.65	32.96	21.83	18.76	22.26	19.57	21.02	29.86	34.47	38.97	43.17	47.76
56	11.09	19.46	19.97	13.70	21.02	20.63	21.96	19.24	19.63	20.86	17.64	14.60	11.80	8.76
57	10.22	17.93	18.40	12.63	19.37	19.01	20.23	17.73	18.09	19.22	16.25	13.45	10.88	8.07
58	22.25	5.85	5.35	5.95	5.16	3.20	4.19	10.42	6.76	0.00	0.00	0.00	0.00	0.00
59	13.24	3.48	3.19	3.54	3.07	1.90	2.49	6.20	4.02	0.00	0.00	0.00	0.00	0.00
60	9.73	2.56	2.34	2.61	2.26	1.40	1.83	4.56	2.96	0.00	0.00	0.00	0.00	0.00
61	4.57	1.20	1.10	1.22	1.06	0.66	0.86	2.14	1.39	0.00	0.00	0.00	0.00	0.00
62	4.41	1.16	1.06	1.18	1.02	0.63	0.83	2.07	1.34	0.00	0.00	0.00	0.00	0.00
63	2.05	0.54	0.49	0.55	0.48	0.29	0.39	0.96	0.62	0.00	0.00	0.00	0.00	0.00
64	0.86	0.23	0.21	0.23	0.20	0.12	0.16	0.40	0.26	0.00	0.00	0.00	0.00	0.00
65	1.27	0.33	0.31	0.34	0.29	0.18	0.24	0.60	0.39	0.00	0.00	0.00	0.00	0.00
66	0.78	0.20	0.19	0.21	0.18	0.11	0.15	0.36	0.24	0.00	0.00	0.00	0.00	0.00
67	0.00	0.00	0.00	0.00	0.00	0.00	0.00	0.00	0.00	0.00	0.00	0.00	0.00	0.00
Potential	24.43	3.29	2.82	0.30	1.58	0.77	0.93	4.62	31.74	17.26	7.53	2.98	1.13	0.61
2 compound kinetics		4 compound kinetics												
kcal/mol	Gas	Oil	kcal/mol	C1	C2-5	C6-	C15+							
44	0.00	0.00	44	0.00	0.00	0.00	0.00							
45	0.00	0.00	45	0.00	0.00	0.00	0.00							
46	0.00	0.00	46	0.00	0.00	0.00	0.00							
47	0.00	0.00	47	0.00	0.00	0.00	0.00							
48	0.00	0.00	48	0.00	0.00	0.00	0.00							
49	0.00	0.00	49	0.00	0.00	0.00	0.00							
50	0.00	0.00	50	0.00	0.00	0.00	0.00							
51	0.72	1.74	51	0.41	1.51	1.29	2.29							
52	0.49	1.17	52	0.28	1.02	0.87	1.55							
53	2.39	5.73	53	1.36	4.98	4.25	7.55							
54	8.29	17.58	54	5.43	15.49	15.91	19.64							
55	15.64	26.21	55	12.06	24.65	20.83	32.83							
56	13.63	19.23	56	11.09	20.02	19.58	18.81							
57	12.56	17.72	57	10.22	18.44	18.04	17.33							
58	17.41	3.99	58	22.25	5.23	7.23	0.00							
59	10.36	2.37	59	13.24	3.11	4.30	0.00							
60	7.62	1.75	60	9.73	2.29	3.16	0.00							
61	3.57	0.82	61	4.57	1.07	1.48	0.00							
62	3.45	0.79	62	4.41	1.04	1.43	0.00							
63	1.60	0.37	63	2.05	0.48	0.67	0.00							
64	0.67	0.15	64	0.86	0.20	0.28	0.00							
65	1.00	0.23	65	1.27	0.30	0.41	0.00							
66	0.61	0.14	66	0.78	0.18	0.25	0.00							
67	0.00	0.00	67	0.00	0.00	0.00	0.00							
Potential	34.13	65.87	Potential	24.43	9.70	36.37	29.50							

Table 6-A5 (contd.): 2-, 4-, and 14-compound compositional kinetic model: instantaneous.

14 compound kinetics														
G016539X	n-C1	n-C2	n-C3	i-C4	n-C4	i-C5	n-C5	n-C6	C7-15	C16-25	C26-35	C36-45	C46-55	C56-80
kcal/mol	(%)													
44	0.00	0.00	0.00	0.00	0.00	0.00	0.00	0.00	0.00	0.00	0.00	0.00	0.00	0.00
45	0.00	0.00	0.00	0.00	0.00	0.00	0.00	0.00	0.00	0.00	0.00	0.00	0.00	0.00
46	0.00	0.00	0.00	0.00	0.00	0.00	0.00	0.00	0.00	0.00	0.00	0.00	0.00	0.00
47	0.00	0.00	0.00	0.00	0.00	0.00	0.00	0.00	0.00	0.00	0.00	0.00	0.00	0.00
48	0.00	0.00	0.00	0.00	0.00	0.00	0.00	0.00	0.00	0.00	0.00	0.00	0.00	0.00
49	0.00	0.00	0.00	0.00	0.00	0.00	0.00	0.00	0.00	0.00	0.00	0.00	0.00	0.00
50	0.00	0.00	0.00	0.00	0.00	0.00	0.00	0.00	0.00	0.00	0.00	0.00	0.00	0.00
51	0.31	0.83	1.27	1.56	0.90	3.54	1.05	0.71	1.20	1.04	2.00	1.91	1.78	1.59
52	0.00	0.00	0.00	0.00	0.00	0.00	0.00	0.00	0.00	0.00	0.00	0.00	0.00	0.00
53	11.87	33.51	31.54	32.16	35.33	28.80	30.90	18.03	28.19	27.01	58.04	61.53	63.69	66.32
54	9.86	23.47	24.74	24.09	20.71	35.55	23.14	15.33	20.69	18.43	36.63	35.93	34.41	32.08
55	23.37	26.92	26.51	28.10	28.03	17.94	28.91	24.98	41.47	8.35	3.33	0.63	0.13	0.00
56	19.43	5.44	5.67	5.02	5.35	5.04	5.70	14.57	3.01	16.08	0.00	0.00	0.00	0.00
57	13.36	3.74	3.90	3.45	3.68	3.47	3.92	10.02	2.07	11.06	0.00	0.00	0.00	0.00
58	4.03	1.13	1.18	1.04	1.11	1.05	1.18	3.02	0.62	3.34	0.00	0.00	0.00	0.00
59	7.75	2.17	2.26	2.00	2.13	2.01	2.27	5.81	1.20	6.41	0.00	0.00	0.00	0.00
60	0.35	0.10	0.10	0.09	0.10	0.09	0.10	0.26	0.05	0.29	0.00	0.00	0.00	0.00
61	5.44	1.52	1.59	1.40	1.50	1.41	1.60	4.08	0.84	4.50	0.00	0.00	0.00	0.00
62	1.37	0.38	0.40	0.35	0.38	0.36	0.40	1.03	0.21	1.13	0.00	0.00	0.00	0.00
63	0.00	0.00	0.00	0.00	0.00	0.00	0.00	0.00	0.00	0.00	0.00	0.00	0.00	0.00
64	1.64	0.46	0.48	0.42	0.45	0.43	0.48	1.23	0.25	1.36	0.00	0.00	0.00	0.00
65	0.43	0.12	0.13	0.11	0.12	0.11	0.13	0.32	0.07	0.36	0.00	0.00	0.00	0.00
66	0.78	0.22	0.23	0.20	0.22	0.20	0.23	0.59	0.12	0.65	0.00	0.00	0.00	0.00
67	0.00	0.00	0.00	0.00	0.00	0.00	0.00	0.00	0.00	0.00	0.00	0.00	0.00	0.00
Potential	19.55	2.91	2.50	0.31	1.54	0.49	0.95	4.83	26.49	25.83	7.41	3.84	1.90	1.45
2 compound kinetics		4 compound kinetics												
kcal/mol	Gas	Oil	kcal/mol	C1	C2-5	C6-	C15+							
44	0.00	0.00	44	0.00	0.00	0.00	0.00							
45	0.00	0.00	45	0.00	0.00	0.00	0.00							
46	0.00	0.00	46	0.00	0.00	0.00	0.00							
47	0.00	0.00	47	0.00	0.00	0.00	0.00							
48	0.00	0.00	48	0.00	0.00	0.00	0.00							
49	0.00	0.00	49	0.00	0.00	0.00	0.00							
50	0.00	0.00	50	0.00	0.00	0.00	0.00							
51	0.57	1.25	51	0.31	1.17	1.12	1.35							
52	0.00	0.00	52	0.00	0.00	0.00	0.00							
53	18.28	33.65	53	11.87	32.67	26.62	39.10							
54	14.22	22.57	54	9.86	24.01	19.86	24.67							
55	24.41	20.38	55	23.37	26.75	38.92	6.01							
56	15.13	7.88	56	19.43	5.48	4.80	10.27							
57	10.41	5.42	57	13.36	3.77	3.30	7.07							
58	3.14	1.64	58	4.03	1.14	0.99	2.13							
59	6.03	3.14	59	7.75	2.19	1.91	4.10							
60	0.27	0.14	60	0.35	0.10	0.09	0.19							
61	4.24	2.21	61	5.44	1.53	1.34	2.88							
62	1.07	0.56	62	1.37	0.39	0.34	0.72							
63	0.00	0.00	63	0.00	0.00	0.00	0.00							
64	1.28	0.67	64	1.64	0.46	0.41	0.87							
65	0.34	0.17	65	0.43	0.12	0.11	0.23							
66	0.61	0.32	66	0.78	0.22	0.19	0.41							
67	0.00	0.00	67	0.00	0.00	0.00	0.00							
Potential	28.25	71.75	Potential	19.55	8.70	31.33	40.42							

Table 6-A6: Physical properties of a) cumulatively and b) instantaneously generated fluids.

a)	G016504X					b)	G016504X				
TR (%)	10	30	50	70	90		10	30	50	70	90
GOR (Sm³/Sm³)	83.3	89.3	95.4	112.0	121.8		83.3	96.6	109.2	139.8	127.8
Bo (m³/Sm³)	1.328	1.350	1.368	1.421	1.450		1.328	1.379	1.406	1.496	1.456
Psat (bar)	120.7	123.4	130.7	144.4	153.3		120.7	125.8	147.1	177.2	168.1
G016505X						G016505X					
TR (%)	10	30	50	70	90		10	30	50	70	90
GOR (Sm³/Sm³)	163.2	173.1	179.1	200.6	425.0		163.2	180.2	186.9	240.0	1052.4
Bo (m³/Sm³)	1.563	1.591	1.606	1.668	2.369		1.563	1.613	1.624	1.788	5.019
Psat (bar)	198.0	205.2	212.6	228.7	307.3		198.0	209.3	222.8	249.8	276.7
G016511X						G016511X					
TR (%)	10	30	50	70	90		10	30	50	70	90
GOR (Sm³/Sm³)	54.9	134.8	138.7	148.5	248.1		54.9	164.7	148.3	169.4	524.4
Bo (m³/Sm³)	1.231	1.479	1.495	1.526	1.863		1.231	1.573	1.537	1.593	2.926
Psat (bar)	89.2	172.6	171.9	178.8	218.2		89.2	193.3	168.6	190.8	244.2
G016522X						G016522X					
TR (%)	10	30	50	70	90		10	30	50	70	90
GOR (Sm³/Sm³)	106.8	116.6	133.7	138.5	210.2		106.8	124.6	161.7	146.6	327.9
Bo (m³/Sm³)	1.395	1.423	1.476	1.489	1.710		1.395	1.446	1.566	1.509	2.125
Psat (bar)	146.2	156.2	170.5	175.7	223.7		146.2	164.2	188.5	186.9	245.8
G016531X						G016531X					
TR (%)	10	30	50	70	90		10	30	50	70	90
GOR (Sm³/Sm³)	159.7	211.4	274.3	350.7	889.8		159.7	321.6	350.1	464.6	>3200
Bo (m³/Sm³)	1.550	1.701	1.913	2.141			1.550	2.014	2.182	2.478	
Psat (bar)	191.1	228.2	243.2	278.7	464.2		191.1	292.1	251.5	321.1	
G016535X						G016535X					
TR (%)	10	30	50	70	90		10	30	50	70	90
GOR (Sm³/Sm³)	142.9	161.1	199.9	236.7	779.4		142.9	181.3	260.1	315.2	>2671
Bo (m³/Sm³)	1.516	1.578	1.687	1.806	3.406		1.516	1.647	1.852	2.063	
Psat (bar)	169.3	177.7	209.9	226.6	388.3		169.3	185.0	255.4	252.3	
G016539X						G016539X					
TR (%)	10	30	50	70	90		10	30	50	70	90
GOR (Sm³/Sm³)	114.0	139.4	159.8	216.7	491.1		114.0	159.1	189.9	461.9	2046.4
Bo (m³/Sm³)	1.427	1.493	1.553	1.737	2.576		1.427	1.541	1.641	2.633	
Psat (bar)	144.4	174.8	192.9	221.1	321.4		144.4	201.3	217.2	253.5	241.5

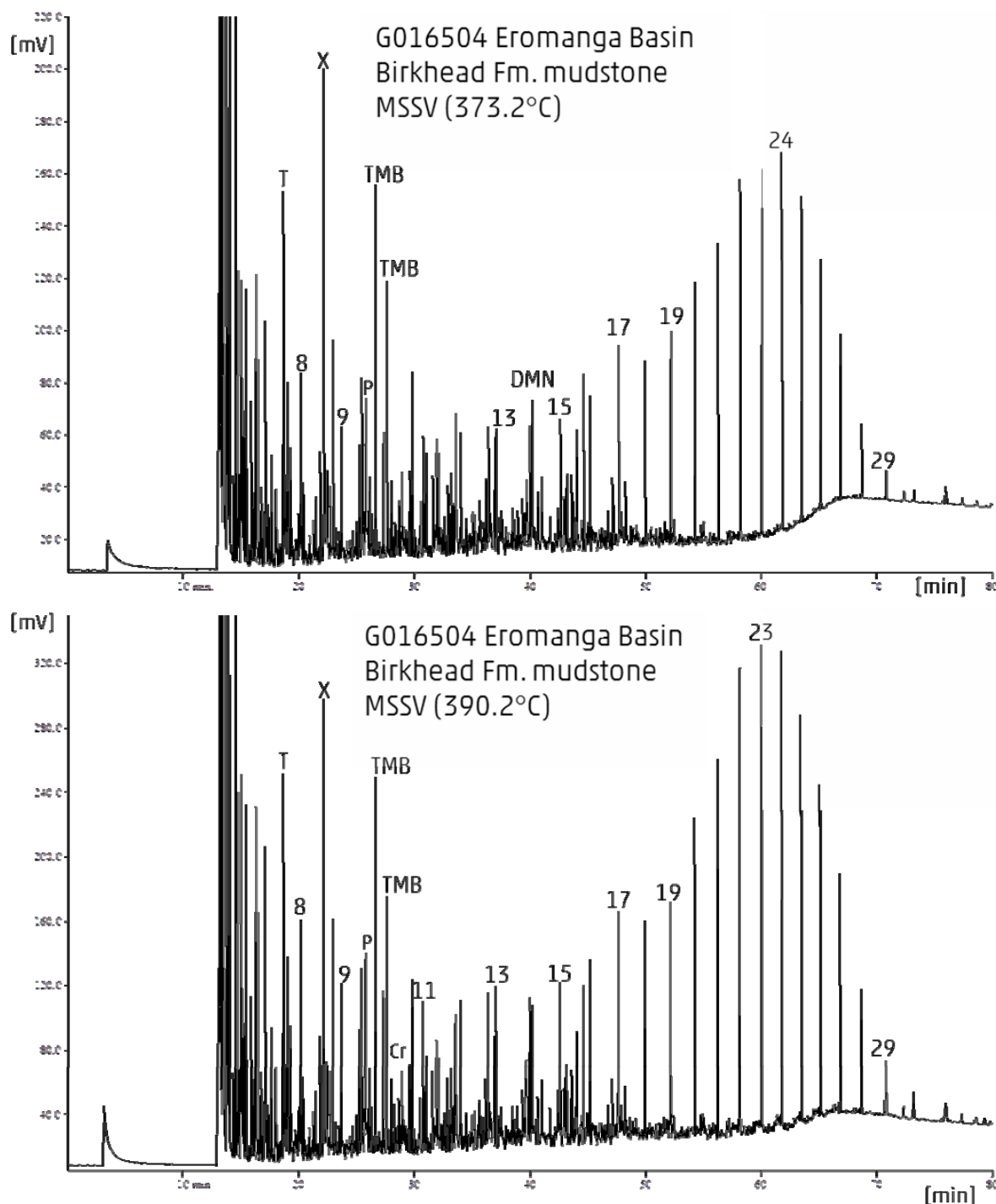
Appendix 6-2 - Figures

Figure 6-A1: MSSV chromatograms

a) sample G016504: Transformation ratio (TR) of 10 % (top) and 30% (bottom).

For reference, selected peaks are marked: numbers= n-alkanes, T = toluene, X = meta/para-xylene, P = phenol, Cr = cresol, TMB = trimethylbenzene, N = naphthalene, MN = methylnaphthalene, DMN = dimethylnaphthalene.

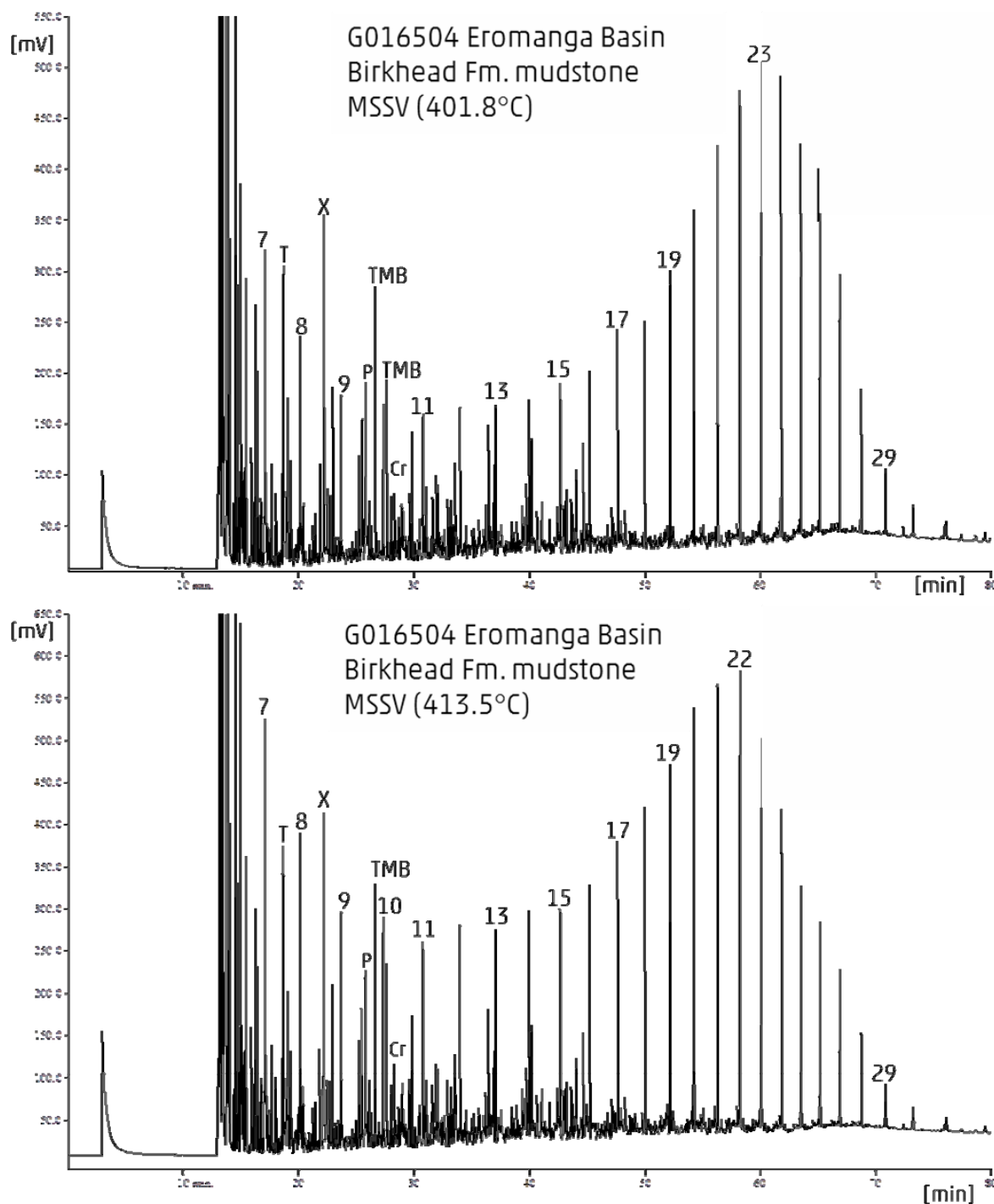


Figure 6-A1: MSSV chromatograms

a) sample G016504: Transformation ratio (TR) of 50 % (top) and 70% (bottom).

For reference, selected peaks are marked: numbers= n-alkanes, T = toluene, X = meta/para-xylene, P = phenol, Cr = cresol, TMB = trimethylbenzene, N = naphthalene, MN = methylnaphthalene, DMN = dimethylnaphthalene.

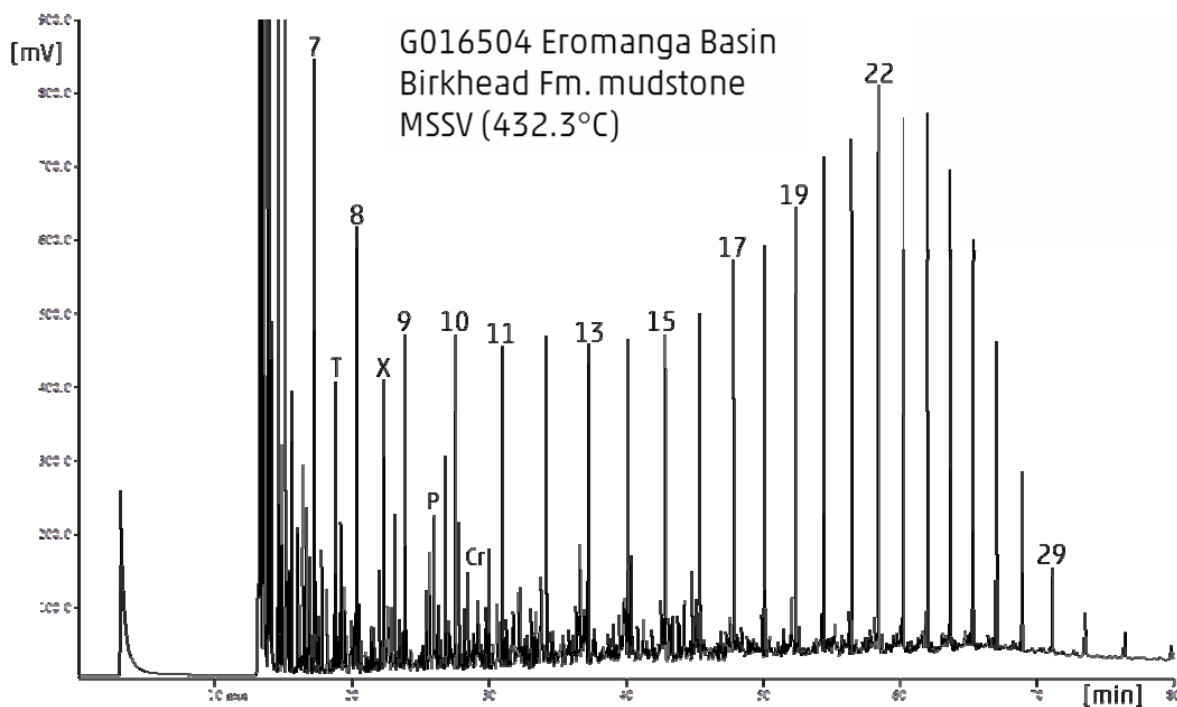


Figure 6-A1: MSSV chromatograms

a) sample G016504: Transformation ratio (TR) of 90 % (top).

For reference, selected peaks are marked: numbers= n-alkanes, T = toluene, X = meta/para-xylene, P = phenol, Cr = cresol, TMB = trimethylbenzene, N = naphthalene, MN = methylnaphthalene, DMN = dimethylnaphthalene.

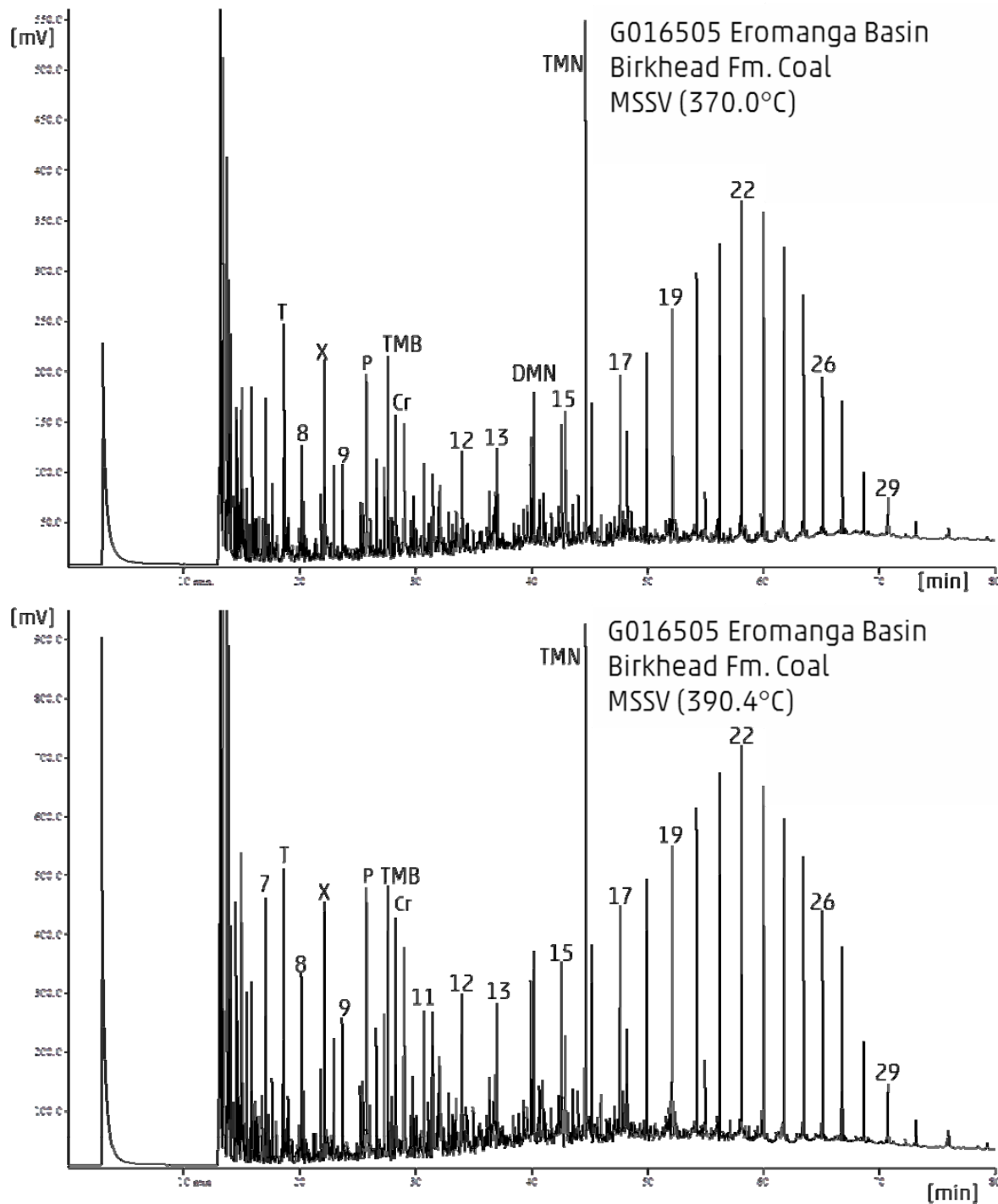


Figure 6-A1: MSSV chromatograms

b) sample G016505: Transformation ratio (TR) of 10 % (top) and 30% (bottom).

For reference, selected peaks are marked: numbers= n-alkanes, T = toluene, X = meta/para-xylene, P = phenol, Cr = cresol, TMB = trimethylbenzene, N = naphthalene, MN = methylnaphthalene, DMN = dimethylnaphthalene.

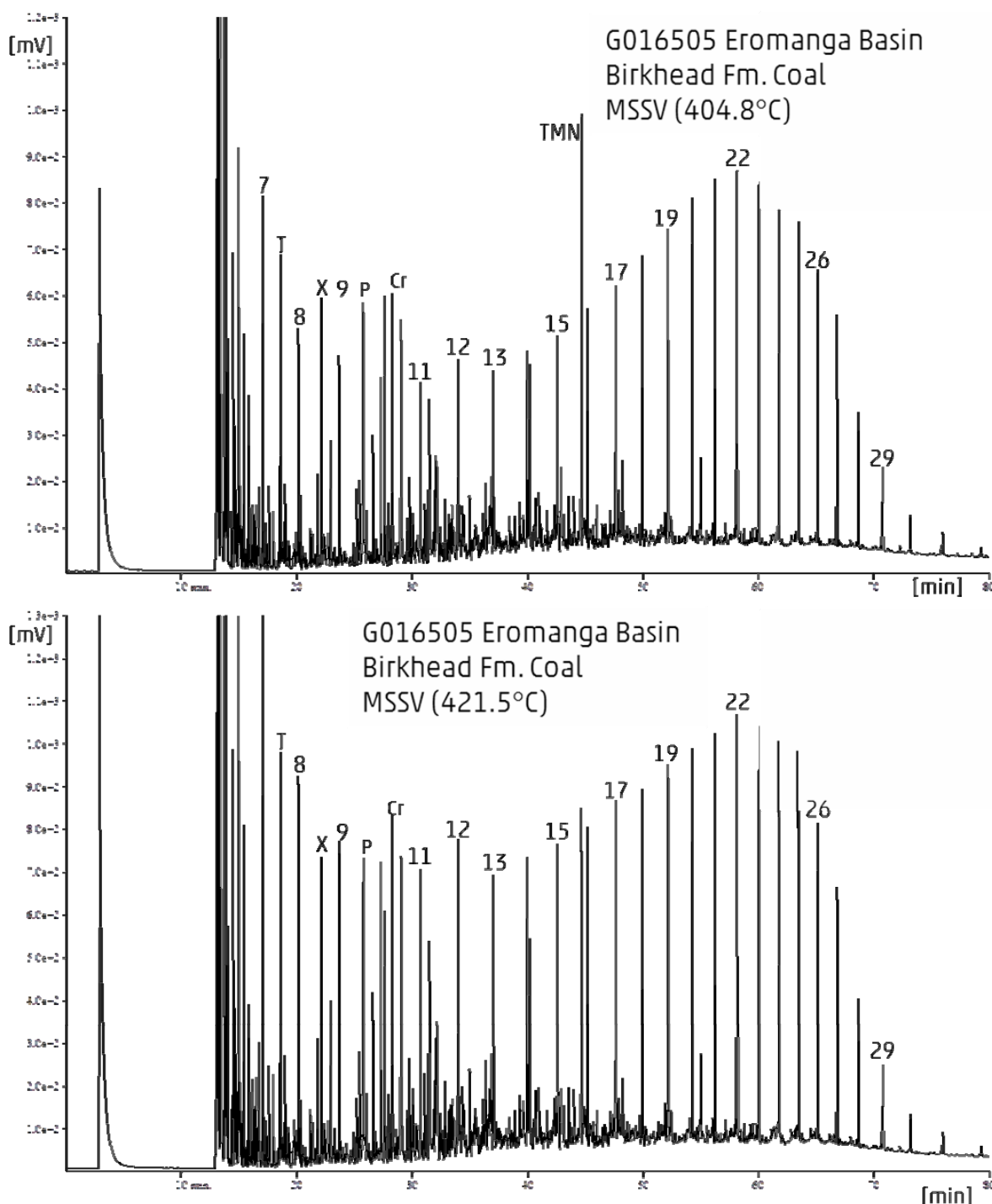


Figure 6-A1: MSSV chromatograms

b) sample G016505: Transformation ratio (TR) of 50 % (top) and 70% (bottom).

For reference, selected peaks are marked: numbers= n-alkanes, T = toluene, X = meta/para-xylene, P = phenol, Cr = cresol, TMB = trimethylbenzene, N = naphthalene, MN = methylnaphthalene, DMN = dimethylnaphthalene.

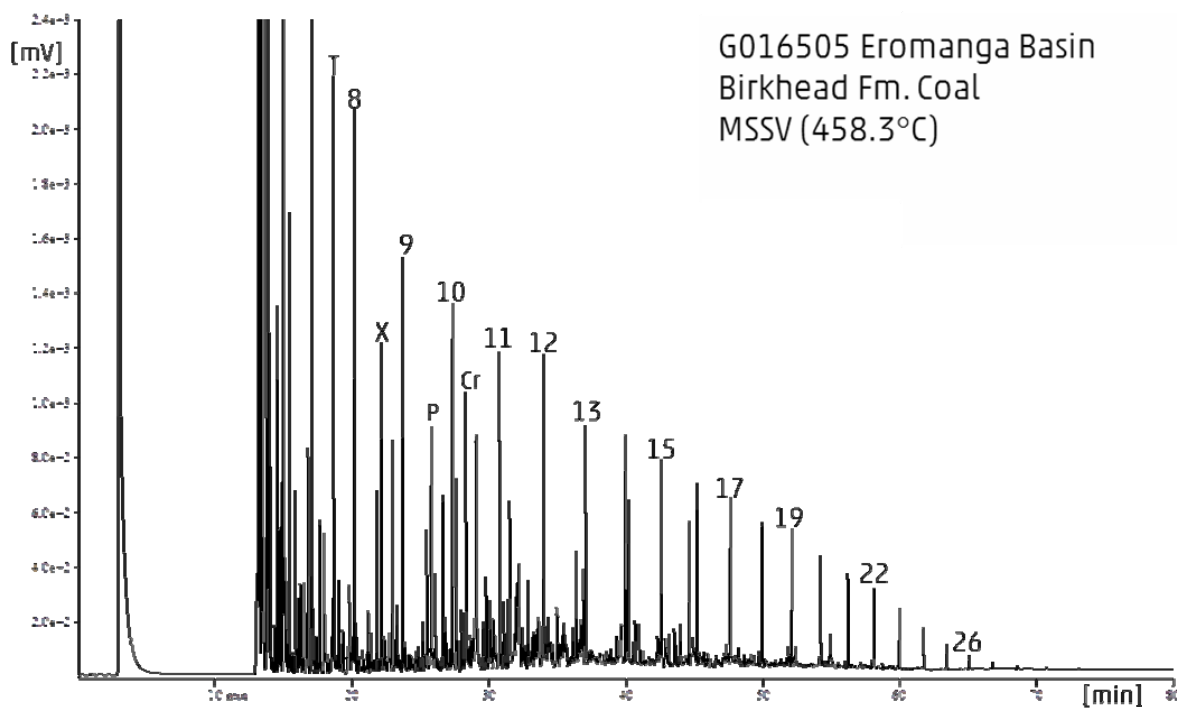


Figure 6-A1: MSSV chromatograms

b) sample G016505: Transformation ratio (TR) of 90 % (top).

For reference, selected peaks are marked: numbers= n-alkanes, T = toluene, X = meta/para-xylene, P = phenol, Cr = cresol, TMB = trimethylbenzene, N = naphthalene, MN = methylnaphthalene, DMN = dimethylnaphthalene.

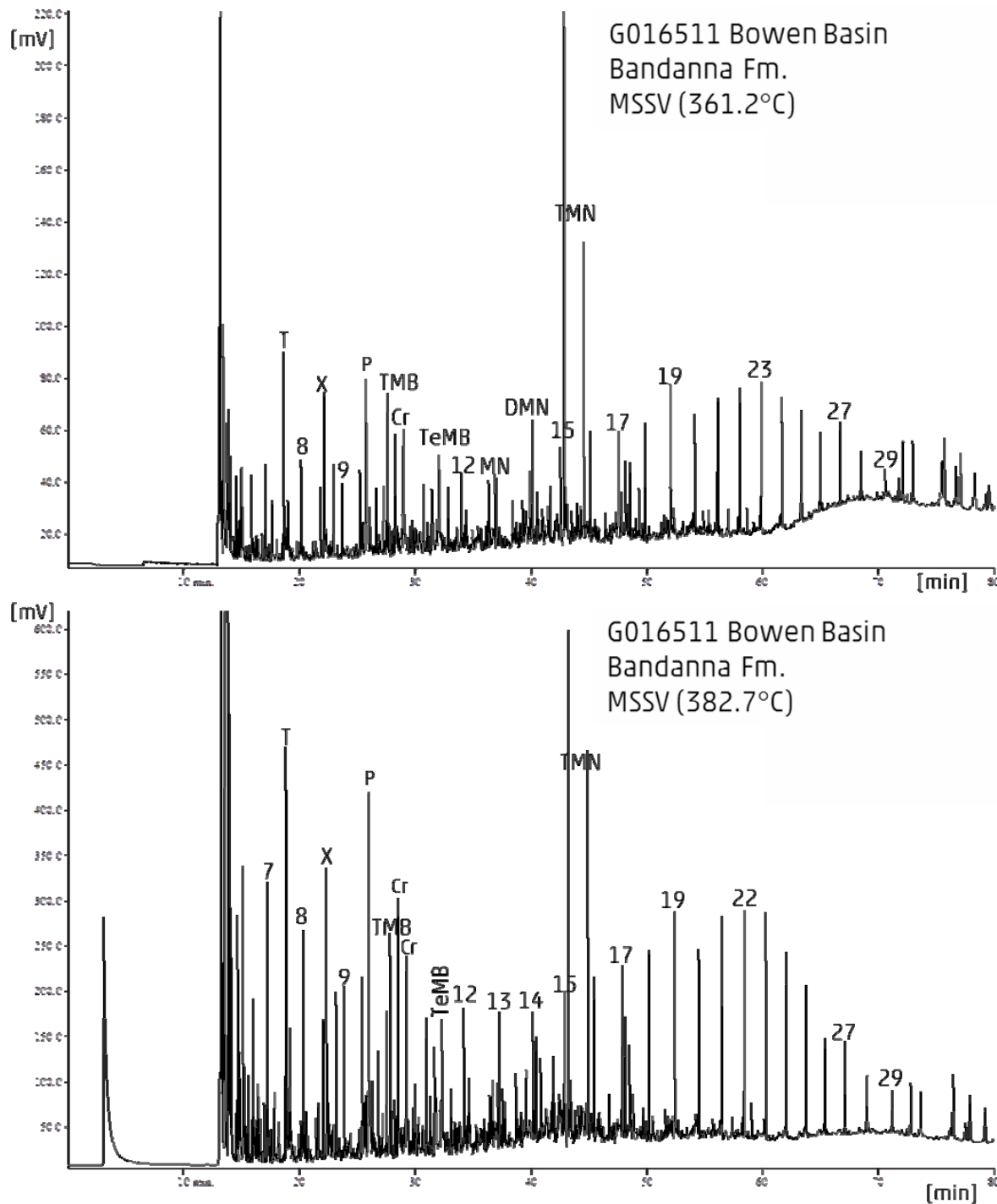


Figure 6-A1: MSSV chromatograms

c) sample G016511: Transformation ratio (TR) of 10 % (top) and 30% (bottom).

For reference, selected peaks are marked: numbers = n-alkanes, T = toluene, X = meta/para-xylene, P = phenol, Cr = cresol, TMB = trimethylbenzene, N = naphthalene, MN = methylnaphthalene, DMN = dimethylnaphthalene.

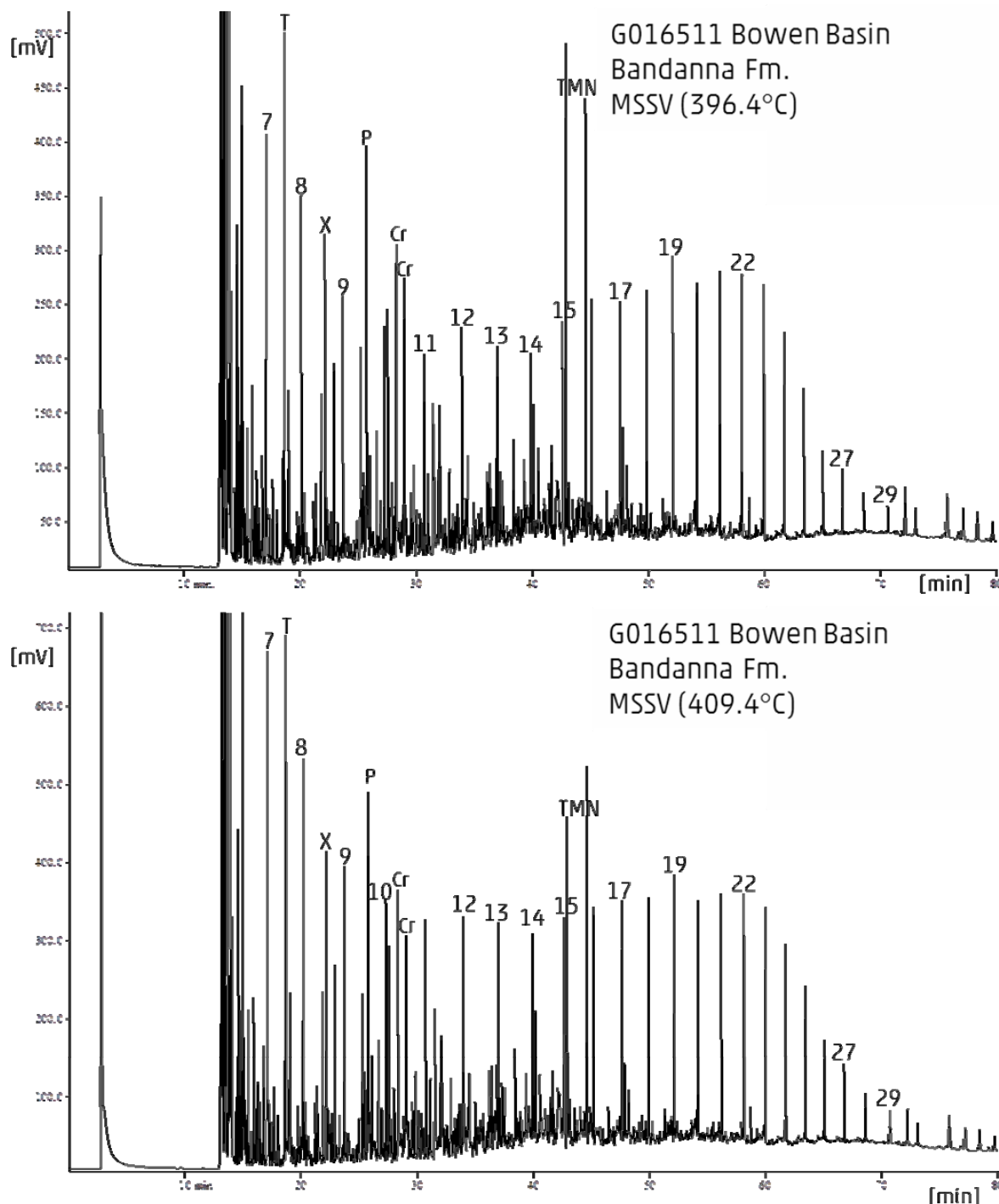


Figure 6-A1: MSSV chromatograms

c) sample G016511: Transformation ratio (TR) of 50 % (top) and 70% (bottom).

For reference, selected peaks are marked: numbers = n-alkanes, T = toluene, X = meta/para-xylene, P = phenol, Cr = cresol, TMB = trimethylbenzene, N = naphthalene, MN = methylnaphthalene, DMN = dimethylnaphthalene.

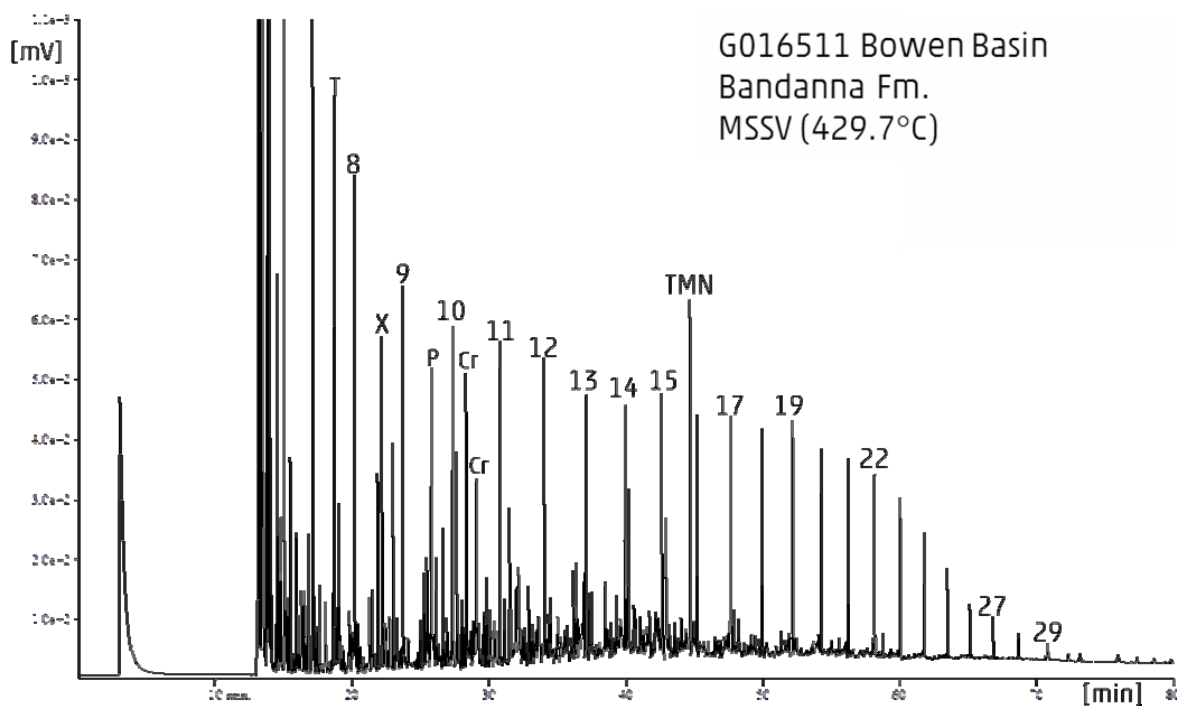


Figure 6-A1: MSSV chromatograms

c) sample G016511: Transformation ratio (TR) of 90 % (top).

For reference, selected peaks are marked: numbers = n-alkanes, T = toluene, X = meta/para-xylene, P = phenol, Cr = cresol, TMB = trimethylbenzene, N = naphthalene, MN = methylnaphthalene, DMN = dimethylnaphthalene.

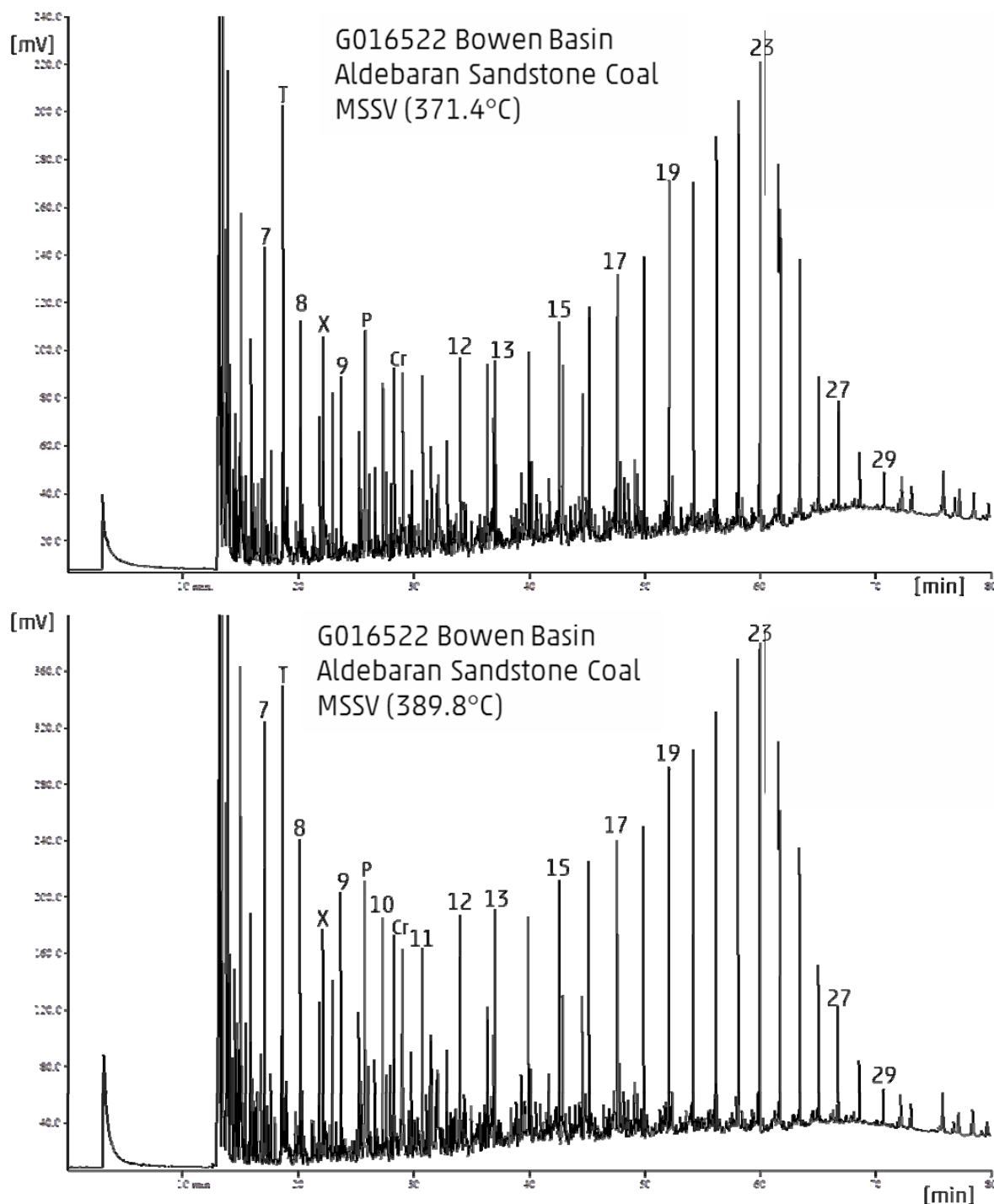
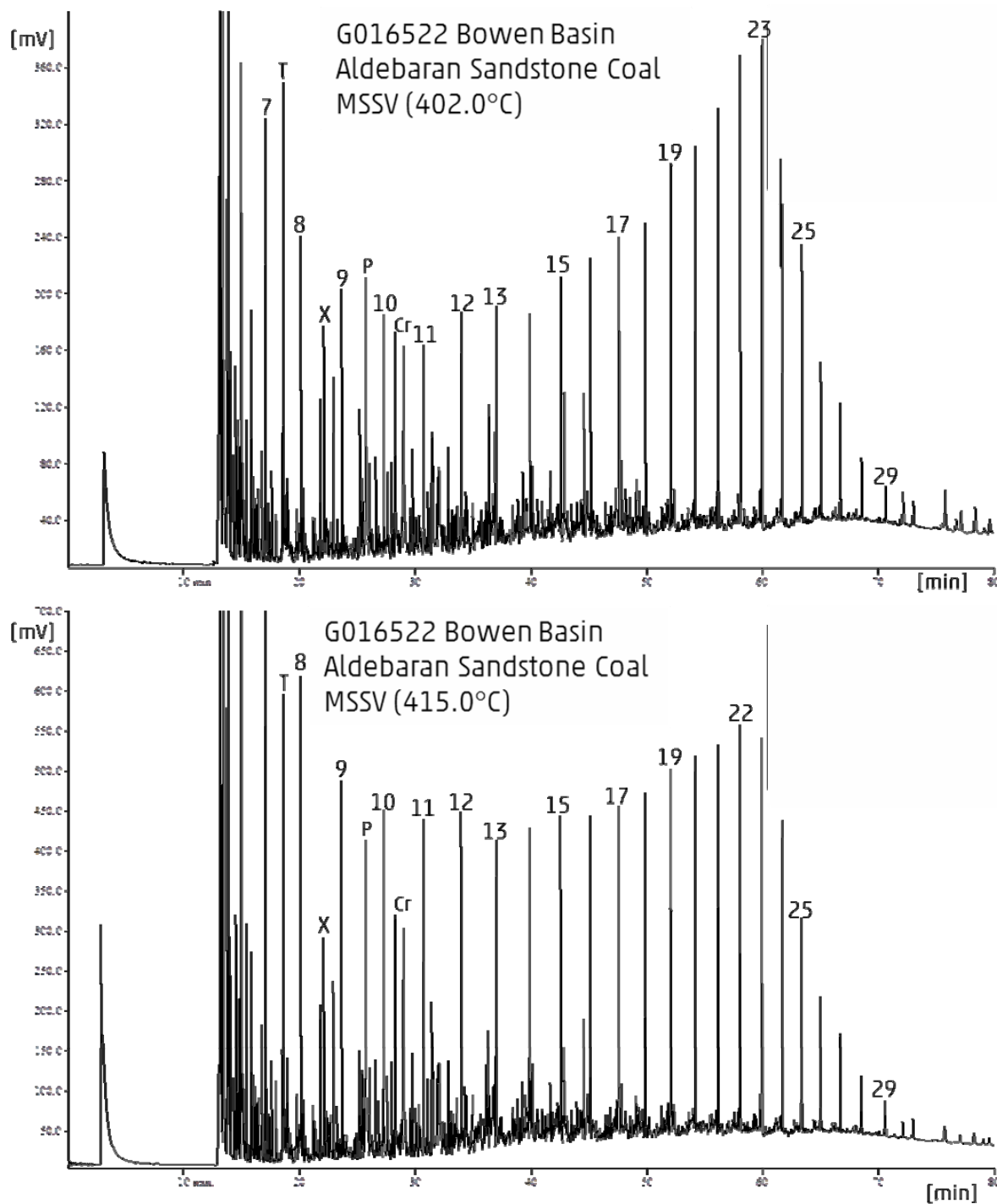


Figure 6-A1: MSSV chromatograms

d) sample G016522: Transformation ratio (TR) of 10 % (top) and 30% (bottom).

For reference, selected peaks are marked: numbers= n-alkanes, T = toluene, X = meta/para-xylene, P = phenol, Cr = cresol, TMB = trimethylbenzene, N = naphthalene, MN = methylnaphthalene, DMN = dimethylnaphthalene.



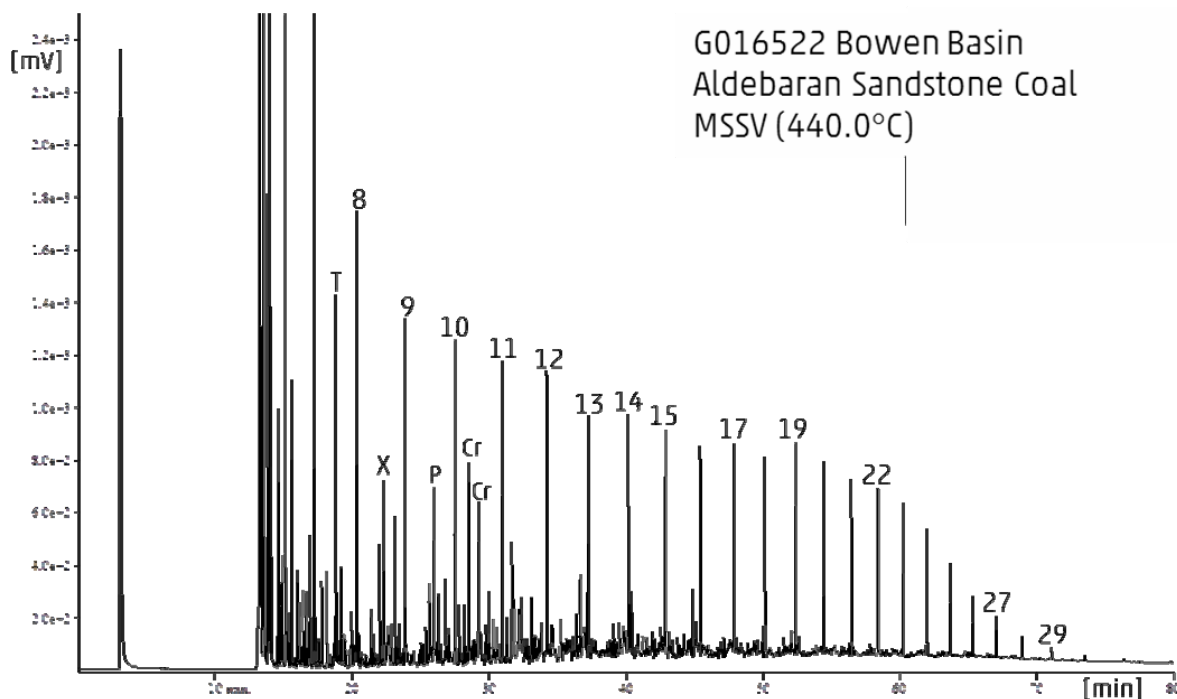


Figure 6-A1: MSSV chromatograms

d) sample G016522: Transformation ratio (TR) of 90 % (top).

For reference, selected peaks are marked: numbers= n-alkanes, T = toluene, X = meta/para-xylene, P = phenol, Cr = cresol, TMB = trimethylbenzene, N = naphthalene, MN = methylnaphthalene, DMN = dimethylnaphthalene.

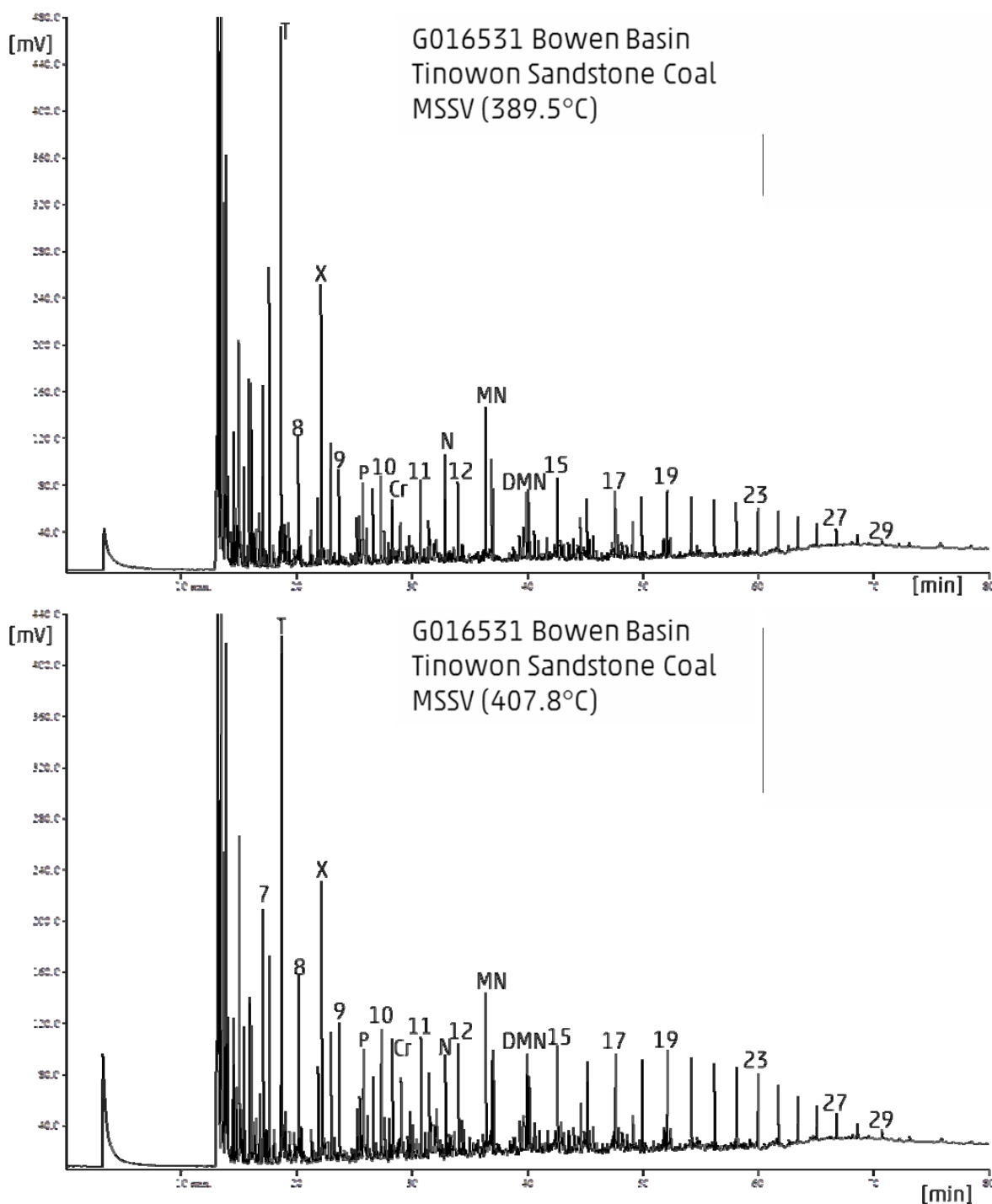


Figure 6-A1: MSSV chromatograms

e) sample G016531: Transformation ratio (TR) of 10 % (top) and 30% (bottom).

For reference, selected peaks are marked: numbers= n-alkanes, T = toluene, X = meta/para-xylene, P = phenol, Cr = cresol, TMB = trimethylbenzene, N = naphthalene, MN = methylnaphthalene, DMN = dimethylnaphthalene.

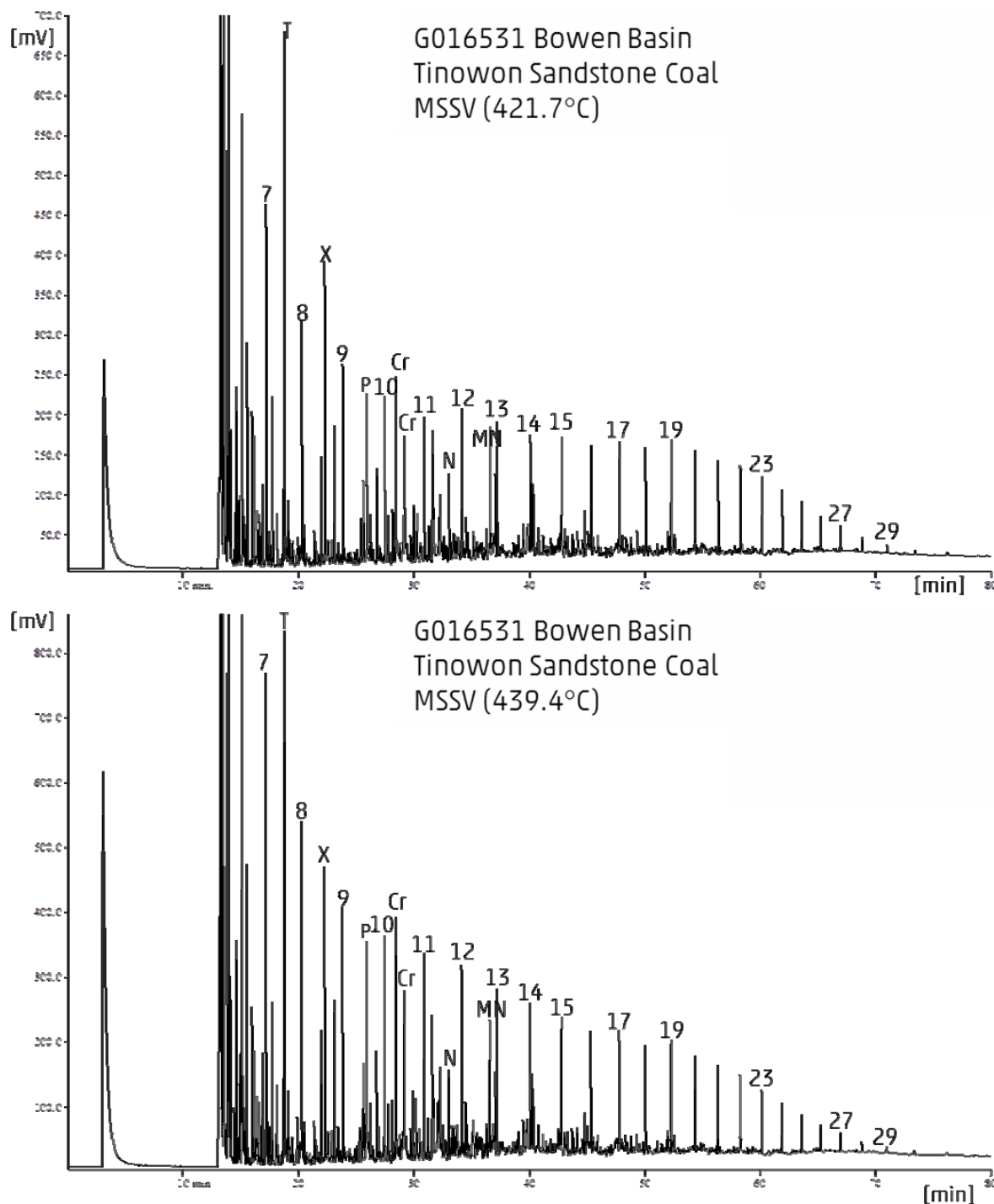


Figure 6-A1: MSSV chromatograms

e) sample G016531: Transformation ratio (TR) of 50 % (top) and 70% (bottom).

For reference, selected peaks are marked: numbers= n-alkanes, T = toluene, X = meta/para-xylene, P = phenol, Cr = cresol, TMB = trimethylbenzene, N = naphthalene, MN = methylnaphthalene, DMN = dimethylnaphthalene.

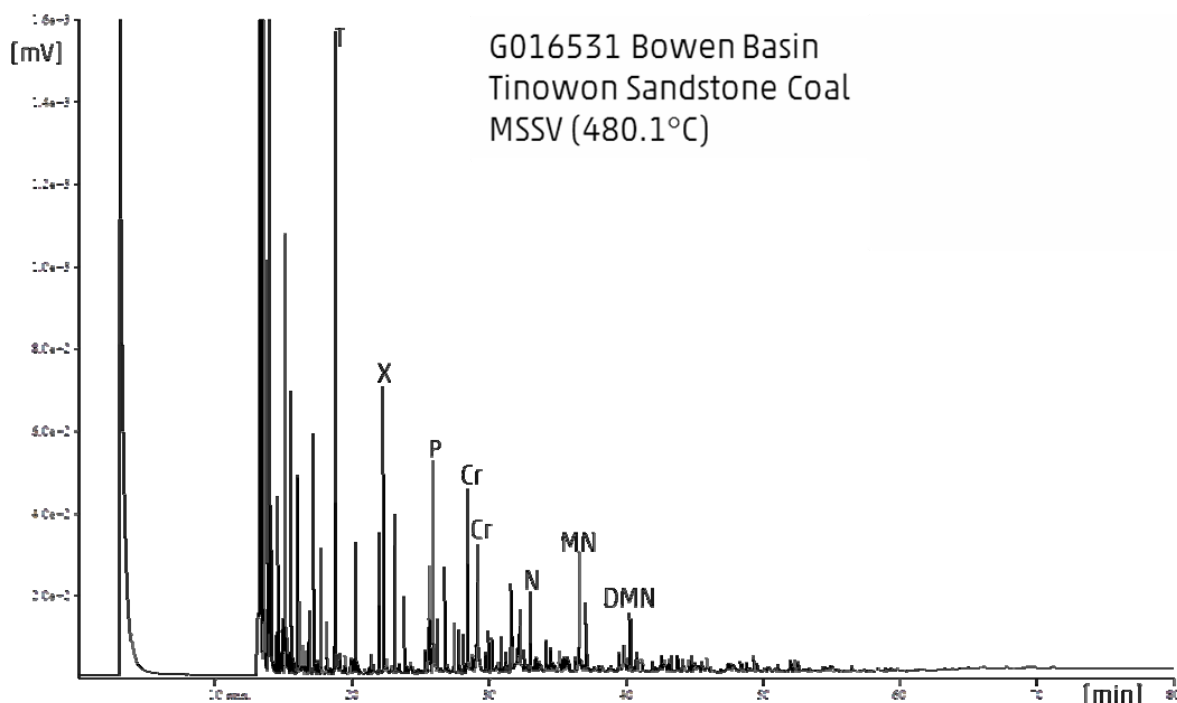


Figure 6-A1: MSSV chromatograms

e) sample G016531: Transformation ratio (TR) of 90 % (top).

For reference, selected peaks are marked: numbers= n-alkanes, T = toluene, X = meta/para-xylene, P = phenol, Cr = cresol, TMB = trimethylbenzene, N = naphthalene, MN = methylnaphthalene, DMN = dimethylnaphthalene.

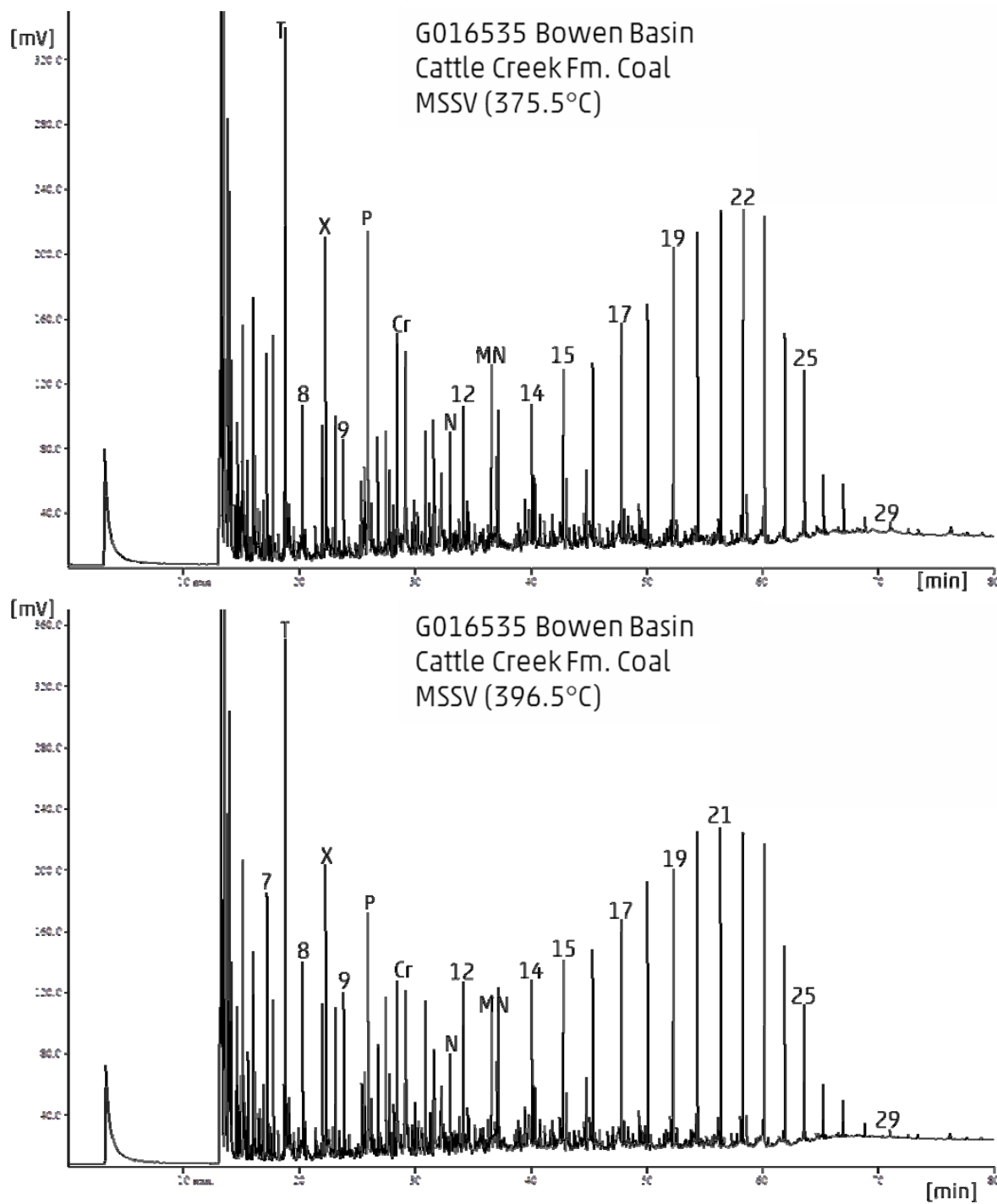


Figure 6-A1: MSSV chromatograms

f) sample G016535: Transformation ratio (TR) of 10 % (top) and 30% (bottom).

For reference, selected peaks are marked: numbers= n-alkanes, T = toluene, X = meta/para-xylene, P = phenol, Cr = cresol, TMB = trimethylbenzene, N = naphthalene, MN = methylnaphthalene, DMN = dimethylnaphthalene.

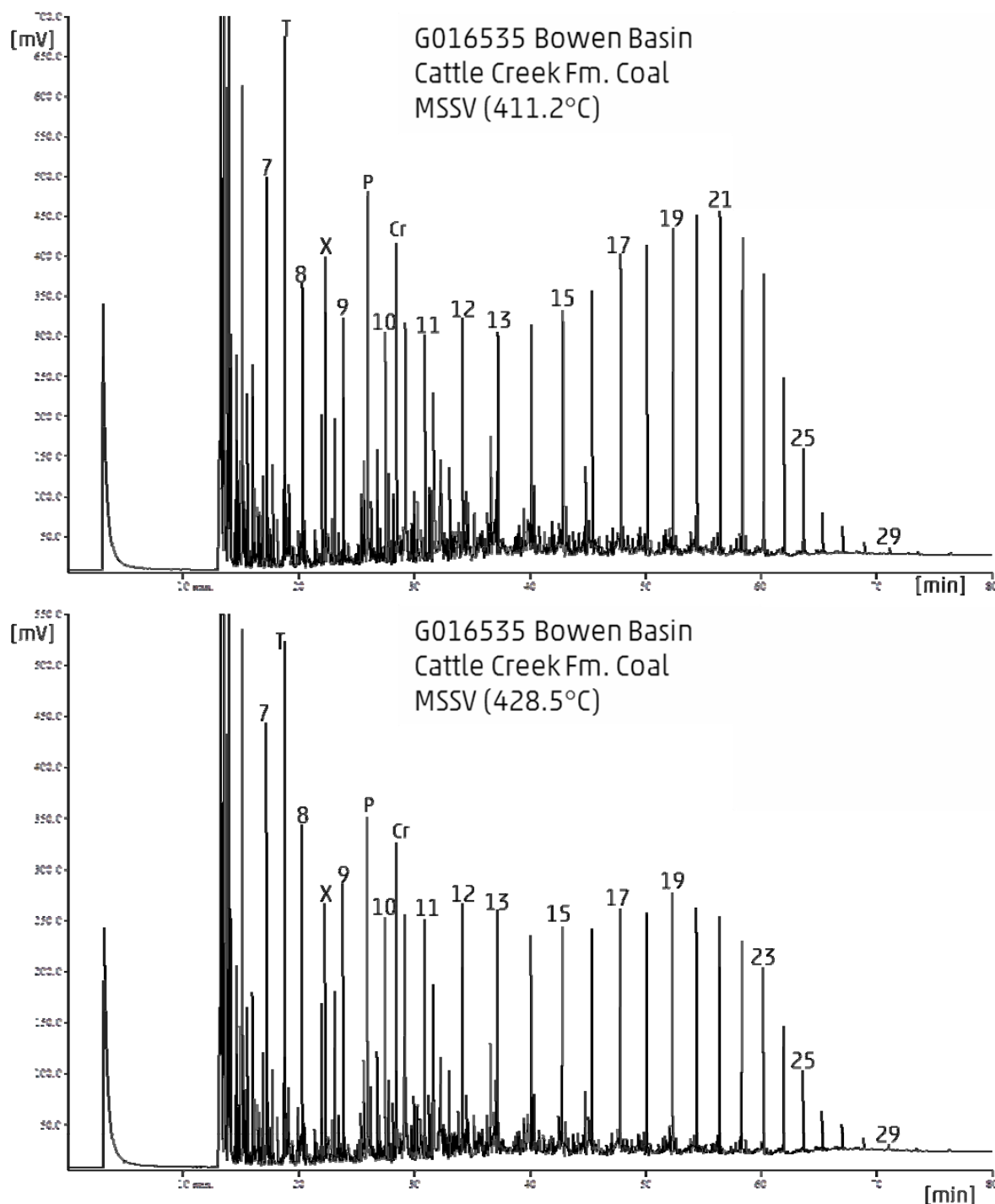


Figure 6-A1: MSSV chromatograms

f) sample G016535: Transformation ratio (TR) of 50 % (top) and 70% (bottom).

For reference, selected peaks are marked: numbers= n-alkanes, T = toluene, X = meta/para-xylene, P = phenol, Cr = cresol, TMB = trimethylbenzene, N = naphthalene, MN = methylnaphthalene, DMN = dimethylnaphthalene.

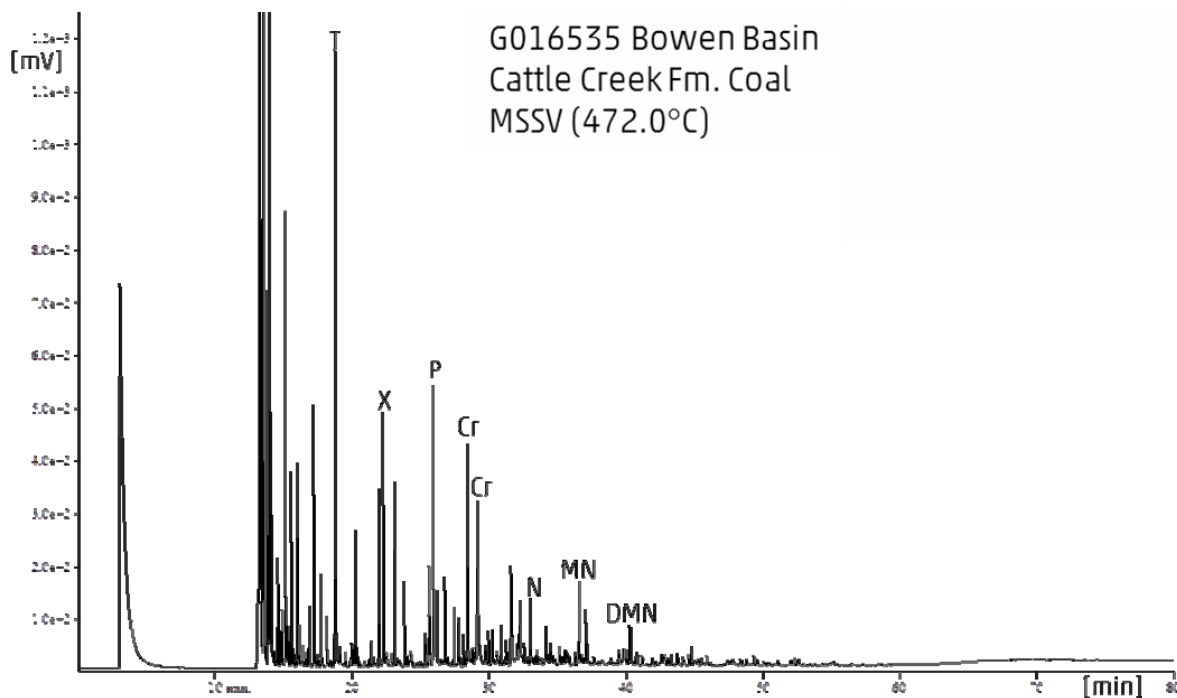


Figure 6-A1: MSSV chromatograms

f) sample G016535: Transformation ratio (TR) of 90 % (top).

For reference, selected peaks are marked: numbers= n-alkanes, T = toluene, X = meta/para-xylene, P = phenol, Cr = cresol, TMB = trimethylbenzene, N = naphthalene, MN = methylnaphthalene, DMN = dimethylnaphthalene.

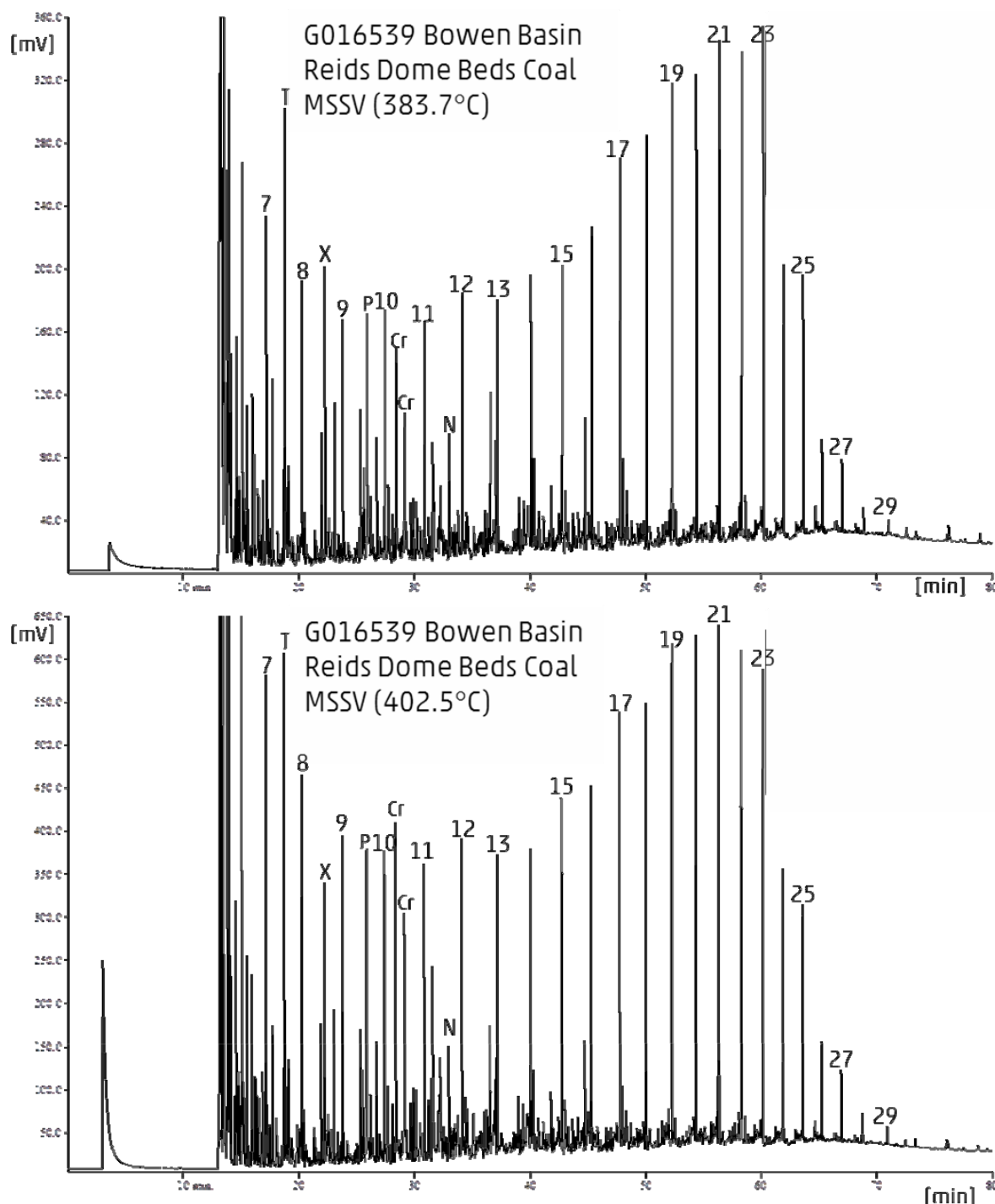


Figure 6-A1: MSSV chromatograms

g) sample G016539: Transformation ratio (TR) of 10 % (top) and 30% (bottom).

For reference, selected peaks are marked: numbers= n-alkanes, T = toluene, X = meta/para-xylene, P = phenol, Cr = cresol, TMB = trimethylbenzene, N = naphthalene, MN = methylnaphthalene, DMN = dimethylnaphthalene.

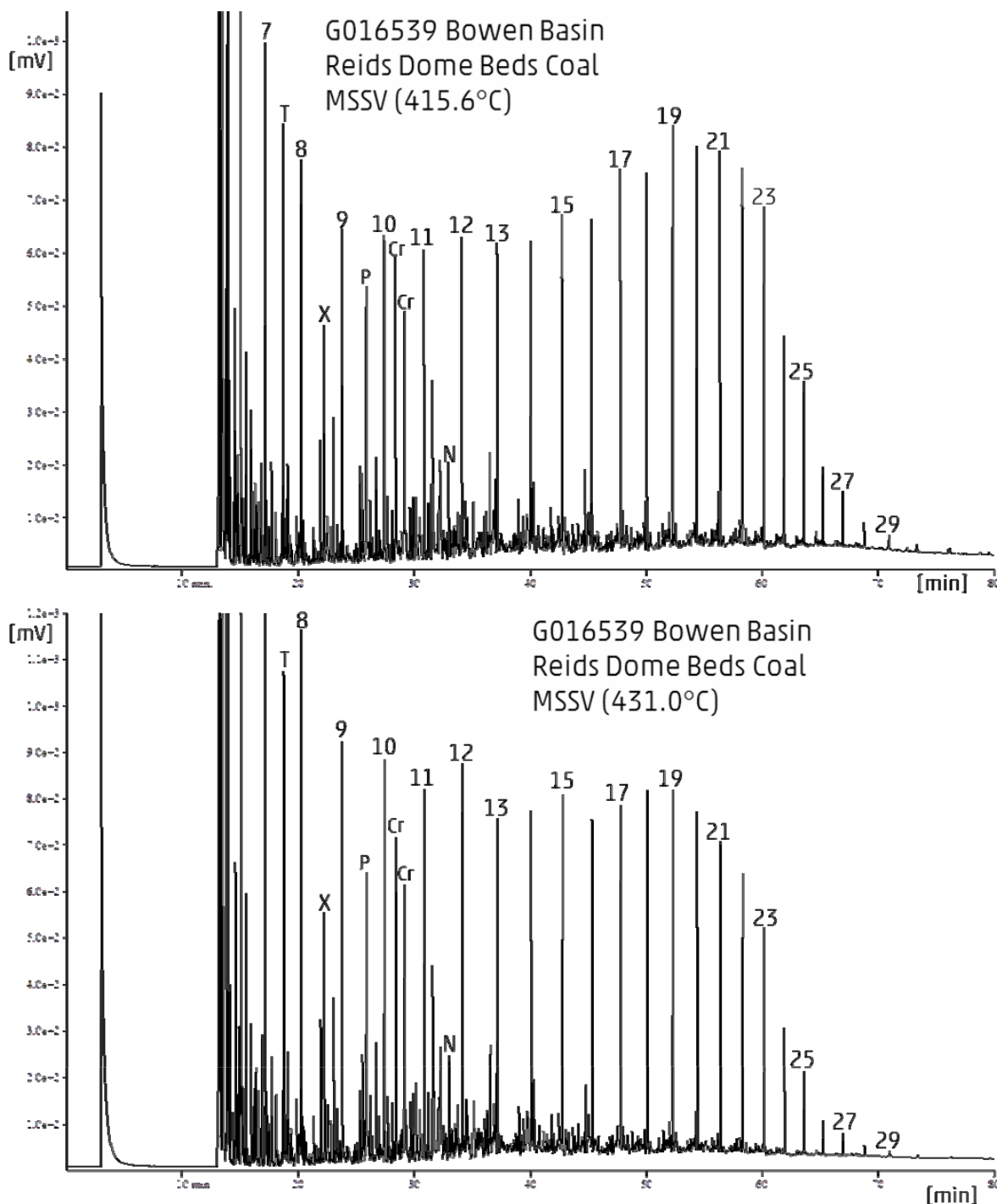


Figure 6-A1: MSSV chromatograms

g) sample G016539: Transformation ratio (TR) of 50 % (top) and 70% (bottom).

For reference, selected peaks are marked: numbers= n-alkanes, T = toluene, X = meta/para-xylene, P = phenol, Cr = cresol, TMB = trimethylbenzene, N = naphthalene, MN = methylnaphthalene, DMN = dimethylnaphthalene.

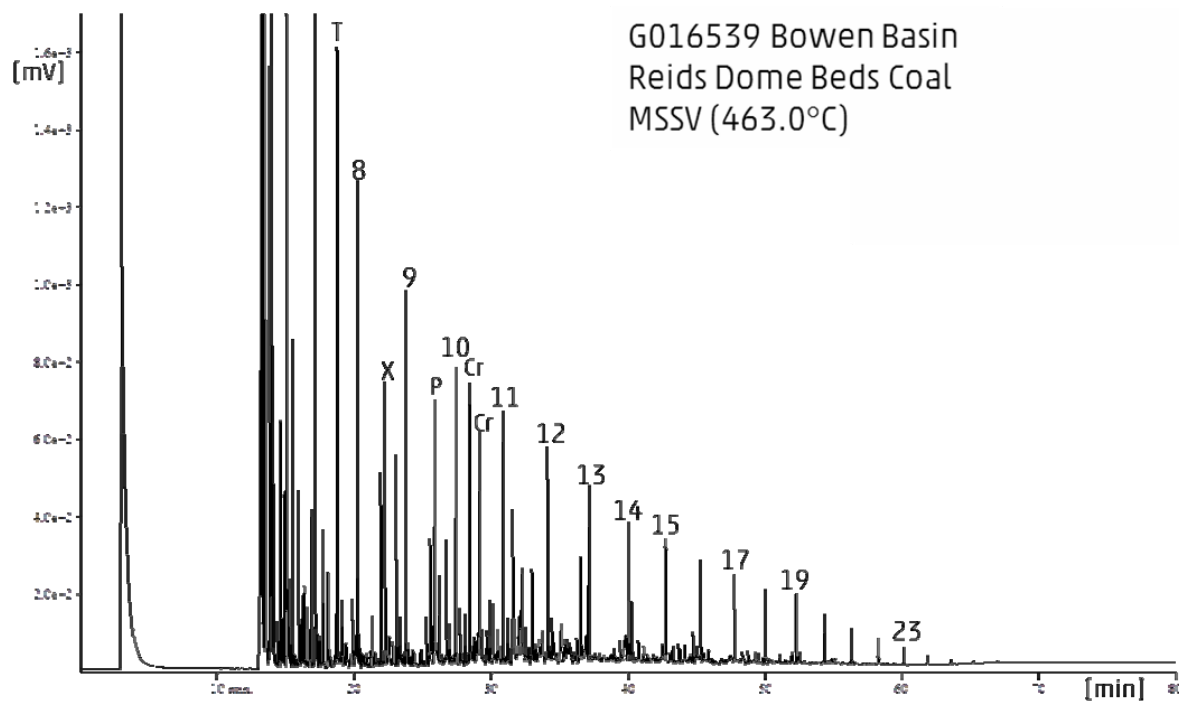


Figure 6-A1: MSSV chromatograms

g) sample G016539: Transformation ratio (TR) of 90 % (top).

For reference, selected peaks are marked: numbers = n-alkanes, T = toluene, X = meta/para-xylene, P = phenol, Cr = cresol, TMB = trimethylbenzene, N = naphthalene, MN = methylnaphthalene, DMN = dimethylnaphthalene.